

UNIVERSITY OF OKLAHOMA

A COMPARISON OF SOIL STABILIZATION ADDITIVES TO DETERMINE  
PARAMETERS AFFECTING SOIL STRENGTH VALUES

GRADUATE COLLEGE

A THESIS APPROVED BY THE  
SCHOOL OF CIVIL ENGINEERING

A COMPARISON OF SOIL STABILIZATION ADDITIVES TO DETERMINE  
PARAMETERS AFFECTING SOIL STRENGTH VALUES

A THESIS

SUBMITTED TO THE GRADUATE FACULTY

in partial fulfillment of the requirements for the

Degree of

MASTER OF SCIENCE

By

NICHOLAS LAWRENCE HUSSEY

Norman, Oklahoma

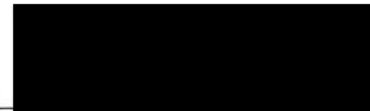
2010

OU  
THESIS  
HUS  
cop.2

A COMPARISON OF SOIL STABILIZATION ADDITIVES TO DETERMINE  
PARAMETERS AFFECTING SOIL STRENGTH VALUES

A THESIS APPROVED FOR THE  
SCHOOL OF CIVIL ENGINEERING AND ENVIRONMENTAL SCIENCE

BY



*l* Dr. Amy Cerato, Chair



Dr. Gerald Miller



Dr. Kanthasamy K. Muraleetharan



To Mum and Dad

for their love, support and encouragement to write

To Dr. John

for giving me the chance and further support to write

To David

for always being there and supporting me when you were there

To Wesley, Peter, John, Lisa, Dr. Hastings, Michael, Angela,

Karin, Sue, Anne, Yvonne, David, and Dr. Thompson

for being my friends - especially Caroline

To Ollie

for that precious companionship of this journey

# TABLE OF CONTENTS ACKNOWLEDGEMENTS

## CHAPTER 1: INTRODUCTION

1.1	General	1
1.2	Hypotheses and Objectives	2
1.2.1	Main Hypotheses of this Study	2
1.2.2	Primary Objectives of this Study	3
1.3	Thesis Layout	3

## CHAPTER 2: To Mom and Dad,

2.1	Introduction	4
2.2	Reasons for their support and for convincing me to stay.	4
2.2.1	Law	4
2.2.2	Career NP	4
2.2.3	Ph.D.	4
2.2.4	To Dr. Amy Cerato,	12
2.3	Project Motivation	12
2.3.1	for giving me the chance, and for her expert guidance.	14
2.3.2	Conduct	14
2.3.3	Control Changes	14
2.3.4	Project Cost Analysis	14

## CHAPTER 3: To Jacob Grasmick,

3.1	Introduction	16
3.2	Year	16
3.3	Classification and Physical Property Tests	18
3.3.1	Grain Size Distribution	18
3.3.2	To Wassim Tabet, Botao Lin, Eric Holderby, Michaela Campbell,	20
3.3.3	Karim Saadeddine, Parnaz Boodagh, and Zac Thompson,	21
3.3.4	for help on this project – including comic relief.	21
3.3.5		21
3.3.6		21
3.3.7		21
3.3.7.1	Linear Shrinkage	21
3.3.7.2	Shrinkage Limit	21
3.4	Mix	22
3.4.1	To ODOT,	24
3.4.1.1	for their generous sponsorship of this project.	24
3.4.2	Carbonic Content	25
3.4.3	Sulfate Content	26
3.4.4	Soil pH	29
3.4.5	Direct Current Electrical Conductivity	31
3.4.6	Castor Chloride Content	31

## CHAPTER 4: RESULTS OF CLASSIFICATION, PHYSICAL, AND MINERALOGICAL PROPERTIES TESTS

4.1	Introduction	34
-----	--------------	----

## TABLE OF CONTENTS

CHAPTER 1: INTRODUCTION .....	1
1.1 General .....	1
1.2 Hypotheses and Objectives .....	2
1.2.1 Main Hypotheses of this Study .....	2
1.2.2 Primary Objectives of this Study .....	3
1.3 Thesis Layout .....	3
CHAPTER 2: LITERATURE REVIEW .....	4
2.1 Introduction .....	4
2.2 Research into Effective Stabilizer Percentages .....	5
2.2.1 Lime .....	5
2.2.2 Cement Kiln Dust .....	7
2.2.3 Fly Ash .....	9
2.2.4 Alternative Stabilizers .....	12
2.3 Properties of Interest .....	13
2.3.1 Soil pH .....	14
2.3.2 Abrasion .....	15
2.3.3 Cation Exchange Capacity .....	15
2.3.4 Specific Surface Area .....	15
CHAPTER 3: MATERIALS AND TEST PROCEDURES .....	16
3.1 Introduction .....	16
3.2 Test Soils .....	17
3.3 Classification and Physical Property Tests .....	19
3.3.1 Grain Size Distribution .....	19
3.3.2 Sieve Analysis .....	20
3.3.3 Specific Gravity .....	20
3.3.4 Harvard Miniature Compaction .....	21
3.3.5 Unconfined Compression Strength .....	22
3.3.6 Atterberg Limits .....	23
3.3.7 Shrinkage .....	24
3.3.7.1 Linear Shrinkage .....	24
3.3.7.2 Shrinkage Limit .....	25
3.4 Mineralogical Property Tests .....	26
3.4.1 Specific Surface Area .....	26
3.4.1.1 Ethylene Glycol Monoethyl Ether (EGME) Method .....	26
3.4.1.2 BET Method .....	27
3.4.2 Carbonate Content .....	28
3.4.3 Sulfate Content .....	29
3.4.4 Soil pH .....	30
3.4.5 Direct Current Electrical Conductivity .....	31
3.4.6 Cation Exchange Capacity .....	31
CHAPTER 4: RESULTS OF CLASSIFICATION, PHYSICAL, AND MINERALOGICAL PROPERTY TESTS .....	31
4.1 Introduction .....	31



4.2	Soil Sources.....	31
4.3	Physical and Mineralogical Test Results .....	32
4.3.1	Harvard Miniature Compaction Results .....	32
4.3.2	Unconfined Compression Test Results.....	33
CHAPTER 5: THE EFFECTS OF CHEMICAL STABILIZERS ON SOIL		
PARAMETERS AND SOIL STRENGTH.....		
5.1	Introduction to Atterberg Limits Testing .....	37
5.2	Atterberg Limit Results.....	39
5.2.1	Introduction to Atterberg Results.....	39
5.2.2	Liquid Limit Cured 0 Days.....	40
5.2.2.1	Liquid Limit with CKD.....	40
5.2.2.2	Liquid Limit with Fly Ash .....	41
5.2.2.3	Liquid Limit with Lime.....	42
5.2.3	Plastic Limit Cured 0 Days.....	43
5.2.3.1	Plastic Limit with CKD.....	43
5.2.3.2	Plastic Limit with Fly Ash .....	44
5.2.3.3	Plastic Limit with Lime.....	44
5.2.4	Plasticity Index Cured 0 Days.....	45
5.2.4.1	Plasticity Index with CKD .....	45
5.2.4.2	Plasticity Index with Fly Ash.....	46
5.2.4.3	Plasticity Index with Lime .....	47
5.2.5	Liquid Limit Cured 14 Days.....	47
5.2.5.1	Liquid Limit with CKD.....	47
5.2.5.2	Liquid Limit with Fly Ash .....	48
5.2.5.3	Liquid Limit with Lime.....	49
5.2.6	Plastic Limit Cured 14 Days.....	50
5.2.6.1	Plastic Limit with CKD.....	50
5.2.6.2	Plastic Limit with Fly Ash .....	51
5.2.6.3	Plastic Limit with Lime.....	52
5.2.7	Plasticity Index Cured 14 Days.....	53
5.2.7.1	Plasticity Index with CKD .....	53
5.2.7.2	Plasticity Index with Fly Ash.....	53
5.2.7.3	Plasticity Index with Lime .....	54
5.2.8	Summary of Atterberg Limits.....	55
5.3	Shrinkage Results.....	56
5.3.1	Introduction to Shrinkage Testing .....	56
5.3.2	Linear Shrinkage Cured 0 Days.....	57
5.3.2.1	Linear Shrinkage with CKD.....	57
5.3.2.2	Linear Shrinkage with Fly Ash .....	58
5.3.2.3	Linear Shrinkage with Lime.....	58
5.3.3	Shrinkage Limit Cured 0 Days .....	59
5.3.3.1	Shrinkage Limit with CKD .....	59
5.3.3.2	Shrinkage Limit with Fly Ash.....	60
5.3.3.3	Shrinkage Limit with Lime .....	60
5.3.4	Linear Shrinkage Cured 14 Days.....	61
5.3.4.1	Linear Shrinkage with CKD.....	61

5.3.4.2	Linear Shrinkage with Fly Ash .....	62
5.3.4.3	Linear Shrinkage with Lime.....	63
5.3.5	Shrinkage Limit Cured 14 Days .....	63
5.3.5.1	Shrinkage Limit with CKD .....	63
5.3.5.2	Shrinkage Limit with Fly Ash.....	64
5.3.5.3	Shrinkage Limit with Lime .....	65
5.3.6	Summary of Shrinkage .....	65
5.4	pH Results .....	66
5.4.1	Introduction to pH Testing.....	66
5.4.2	pH with CKD .....	67
5.4.3	pH with Fly Ash.....	68
5.4.4	pH with Lime .....	68
5.4.5	Summary of pH.....	69
5.5	Conductivity Results .....	70
5.5.1	Introduction to Conductivity Testing.....	70
5.5.2	Conductivity with CKD .....	71
5.5.3	Conductivity with Fly Ash.....	71
5.5.4	Conductivity with Lime .....	72
5.5.5	Summary of Conductivity .....	73
5.6	Cation Exchange Capacity Results .....	73
5.6.1	Introduction to Cation Exchange Capacity Testing.....	73
5.6.2	Uncured CEC.....	74
5.6.2.1	CEC with CKD.....	74
5.6.2.2	CEC with Fly Ash .....	75
5.6.2.3	CEC with Lime.....	75
5.6.3	Cured CEC .....	76
5.6.3.1	CEC with CKD.....	76
5.6.3.2	CEC with Fly Ash .....	77
5.6.3.3	CEC with Lime.....	77
5.6.4	Summary of CEC.....	78
5.7	Specific Surface Area Results .....	79
5.7.1	Introduction to Specific Surface Area Testing.....	79
5.7.2	Total Specific Surface Area Cured 0 Days .....	80
5.7.2.1	Total SSA with CKD.....	80
5.7.2.2	Total SSA with Fly Ash .....	81
5.7.2.3	Total SSA with Lime.....	82
5.7.3	External Specific Surface Area Cured 0 Days .....	82
5.7.3.1	External SSA with CKD .....	82
5.7.3.2	External SSA with Fly Ash .....	83
5.7.3.3	External SSA with Lime .....	83
5.7.4	Internal Specific Surface Area Cured 0 Days .....	84
5.7.4.1	Internal SSA with CKD.....	84
5.7.4.2	Internal SSA with Fly Ash .....	85
5.7.4.3	Internal SSA with Lime.....	85
5.7.5	Total Specific Surface Area Cured 14 Days .....	86
5.7.5.1	Total SSA with CKD.....	86



5.7.5.2	Total SSA with Fly Ash .....	87
5.7.5.3	Total SSA with Lime.....	88
5.7.6	External Specific Surface Area Cured 14 Days.....	88
5.7.6.1	External SSA with CKD .....	88
5.7.6.2	External SSA with Fly Ash .....	89
5.7.6.3	External SSA with Lime .....	90
5.7.7	Internal Specific Surface Area Cured 14 Days.....	90
5.7.7.1	Internal SSA with CKD.....	90
5.7.7.2	Internal SSA with Fly Ash .....	91
5.7.7.3	Internal SSA with Lime.....	92
5.7.8	Summary of Specific Surface Area.....	92
5.8	Chapter Summary .....	93
CHAPTER 6: ANALYSIS OF SOIL PARAMETERS FOR PREDICTING SOIL STRENGTH .....		93
6.1	Introduction .....	93
6.2	Results for A-4 Soils .....	96
6.2.1	Introduction.....	96
6.2.2	Uncured Atterberg Limits Model.....	97
6.2.3	Cured Atterberg Limits Model.....	98
6.2.4	Combined Atterberg Limits Model.....	99
6.2.5	Full Analysis Model.....	101
6.2.6	Practical Analysis Model .....	102
6.2.7	Summary of A-4 Soil Models.....	104
6.3	Results for A-6 Soils .....	105
6.3.1	Introduction.....	105
6.3.2	Uncured Atterberg Limits Model.....	105
6.3.3	Cured Atterberg Limits Model.....	107
6.3.4	Combined Atterberg Limits Model.....	108
6.3.5	Full Analysis Model.....	110
6.3.6	Practical Analysis Model .....	112
6.3.7	Summary of A-6 Soil Models.....	115
6.4	A-7-6 Soils .....	116
6.4.1	Introduction.....	116
6.4.2	Uncured Atterberg Limits Model.....	116
6.4.3	Cured Atterberg Limits Model.....	118
6.4.4	Combined Atterberg Limits Model.....	120
6.4.5	Full Analysis Model.....	122
6.4.6	Practical Analysis Model .....	124
6.4.7	Summary of A-7-6 Soil Models.....	125
6.5	All Soils.....	127
6.5.1	Introduction.....	127
6.5.2	Uncured Atterberg Limits Model.....	127
6.5.3	Cured Atterberg Limits Model.....	129
6.5.4	Combined Atterberg Limits Model.....	130
6.5.5	Full Analysis Model.....	132
6.5.6	Practical Analysis Model .....	135

6.5.7	Summary of Combined Soil Models.....	137
6.6	Optimum Additive Percentage Prediction Using Raw Soils.....	138
6.6.1	Introduction.....	138
6.6.2	Atterberg Limits Model .....	138
6.6.3	Full Analysis Model.....	140
6.6.4	Atterberg Limits, Average pH, and Clay Fraction Model .....	142
6.6.5	Summary of Optimum Additive Percentage Prediction Models .....	144
CHAPTER 7: CONCLUSIONS AND RECOMMENDATIONS.....		145
7.1	Introduction .....	145
7.2	Conclusions .....	146
7.3	Recommendations .....	149
REFERENCES .....		150
APPENDIX A .....		153

Table 6-4	.....	138
Table 6-5	.....	142
Table 7-1	.....	149



## LIST OF TABLES

Table 1-1: OHD L-50 Soil Stabilization Table (ODOT, 2006).....	1
Table 3-1 - List of Soil Locations and Classifications.....	18
Table 3-2 - Additive Testing Percentages for pH and Conductivity Tests.....	30
Table 4-1 - General Raw Soil Descriptions and Locations.....	33
Table 4-2 - Physical Properties of the Raw Test Soils.....	34
Table 4-3 - Mineralogical Properties of the Raw Test Soils.....	35
Table 4-4 - Compaction Properties of the Raw Test Soils.....	36
Table 4-5 - Unconfined Compression Strengths of the Raw Test Soils .....	36
Table 5-1 - Table of Linear Shrinkage Decreases over 345 kPa Strength Gain .....	66
Table 6-1 - Coefficients of Best A-4 Soil Models .....	104
Table 6-2 - Coefficients of Best A-6 Soil Models .....	115
Table 6-3 - Coefficient of Best A-7-6 Soil Models .....	126
Table 6-4 - Coefficients of Best Combined Soil Models.....	137
Table 6-5 - Coefficients of Best Raw Soil Models.....	144
Table 7-1 - OHD L-50 Soil Stabilization Table (ODOT, 2006).....	148

## LIST OF FIGURES

Figure 2.1 - Map of Swelling Soils in United States (Olive, et al, 1989).....	5
Figure 3.1 - Locations of Test Soils in Oklahoma.....	17
Figure 3.2- Pictures of Test Soils.....	18
Figure 3.3 - Determination of the Shrinkage Limit .....	26
Figure 5.1 - Liquid Limits (0-day) with CKD for A-4 (Left), A-6 (Center), and A-7-6 (Right) Soils .....	40
Figure 5.2 - Liquid Limits (0-day) with Fly Ash for A-4 (Left), A-6 (Center), and A-7-6 (Right) Soils .....	41
Figure 5.3 - Liquid Limits (0-day) with Lime for A-6 (Left) and A-7-6 (Right) Soils ....	42
Figure 5.4 - Plastic Limit (0-day) with CKD for A-4 (Left), A-6 (Center), and A-7-6 (Right) Soils.....	43
Figure 5.5 - Plastic Limits (0-day) with Fly Ash for A-4 (Left), A-6 (Center), and A-7-6 Soils .....	44
Figure 5.6 - Plastic Limit (0-day) with Lime for A-6 (Left) and A-7-6 (Right) Soils.....	45
Figure 5.7 - Plasticity Index (0-day) with CKD for A-4 (Left), A-6 (Center), and A-7-6 (Right) Soils.....	45
Figure 5.8 - Plasticity Index (0-day) with Fly Ash for A-4 (Left), A-6 (Center), and A-7-6 Soils .....	46
Figure 5.9 - Plasticity Index (0-day) with Lime for A-6 (Left) and A-7-6 (Right) Soils .	47
Figure 5.10 - Liquid Limit (14-day) with CKD for A-4 (Left), A-6 (Center), and A-7-6 Soils.....	48
Figure 5.11 - Liquid Limit (14-day) with Fly Ash for A-4 (Left), A-6 (Center), and A-7-6 (Right) Soils .....	49
Figure 5.12 - Liquid Limit (14-day) with Lime for A-6 (Left) and A-7-6 (Right) Soils..	50
Figure 5.13 - Plastic Limit (14-day) with CKD for A-4 (Left), A-6 (Center), and A-7-6 (Right) Soils .....	50
Figure 5.14 - Plastic Limit (14-day) with Fly Ash for A-4 (Left), A-6 (Center), and A-7-6 (Right) Soils .....	51
Figure 5.15 - Plastic Limit (14-day) with Lime for A-6 (Left) and A-7-6 (Right) Soils..	52
Figure 5.16 - Plasticity Index (14-day) with CKD for A-4 (Left), A-6 (Center), and A-7-6 (Right) Soils .....	53
Figure 5.17 - Plasticity Index (14-day) with Fly Ash for A-4 (Left), A-6 (Center), and A-7-6 (Right) Soils .....	54
Figure 5.18 - Plasticity Index (14-day) with Lime for A-6 (Left) and A-7-6 (Right) Soils.....	55
Figure 5.19 - Linear Shrinkage (0-day) with CKD for A-4 (Left), A-6 (Center), and A-7-6 (Right) Soils .....	57
Figure 5.20 - Linear Shrinkage (0-day) with Fly Ash for A-4 (Left), A-6 (Center), and A-7-6 (Right) Soils .....	58
Figure 5.21 - Linear Shrinkage (0-day) with Lime for A-6 (Left) and A-7-6 (Right) Soils.....	59
Figure 5.22 - Shrinkage Limit (0-day) with CKD for A-4 (Left), A-6 (Center), and A-7-6 (Right) Soils .....	59
Figure 5.23 - Shrinkage Limit (0-day) with Fly Ash for A-4 (Left), A-6 (Center), and A-7-6 (Right) Soils .....	60



Figure 5.24 - Shrinkage Limit (0-day) with Lime for A-6 (Left) and A-7-6 (Right) Soils.....	61
Figure 5.25 - Linear Shrinkage (14-day) with CKD for A-4 (Left), A-6 (Center), and A-7-6 (Right) Soils.....	61
Figure 5.26 - Linear Shrinkage (14-day) with Fly Ash for A-4 (Left), A-6 (Center), and A-7-6 (Right) Soils.....	62
Figure 5.27 - Linear Shrinkage (14-day) with Lime for A-6 (Left) and A-7-6 (Right) Soils.....	63
Figure 5.28 - Shrinkage Limit (14-day) with CKD for A-4 (Left), A-6 (Center), and A-7-6 (Right) Soils.....	64
Figure 5.29 - Shrinkage Limit (14-day) with Fly Ash for A-4 (Left), A-6 (Center), and A-7-6 (Right) Soils.....	64
Figure 5.30 - Shrinkage Limit (14-day) with Lime for A-6 (Left) and A-7-6 (Right) Soils.....	65
Figure 5.31 - pH Results with CKD for A-4 (Left), A-6 (Center), and A-7-6 (Right) Soils.....	67
Figure 5.32 - pH Results with Fly Ash for A-4 (Left), A-6 (Center), and A-7-6 (Right) Soils.....	68
Figure 5.33 - pH Results with Lime for A-6 (Left) and A-7-6 (Right) Soils.....	69
Figure 5.34 - Combined pH Curves for Different Additives.....	70
Figure 5.35 - Conductivity with CKD for A-4 (Left), A-6 (Center), and A-7-6 (Right) Soils.....	71
Figure 5.36 - Conductivity with Fly Ash for A-4 (Left), A-6 (Center), and A-7-6 (Right) Soils.....	71
Figure 5.37 - Conductivity with Lime for A-6 (Left) and A-7-6 (Right) Soils.....	72
Figure 5.38 - CEC (Uncured) with CKD for A-4 (Left), A-6 (Center), and A-7-6 (Right) Soils.....	74
Figure 5.39 - CEC (Uncured) with Fly Ash for A-4 (Left), A-6 (Center), and A-7-6 (Right) Soils.....	75
Figure 5.40 - CEC (Uncured) with Lime for A-6 (Left) and A-7-6 (Right) Soils.....	76
Figure 5.41 - CEC (Cured) with CKD for A-4 (Left), A-6 (Center), and A-7-6 (Right) Soils.....	76
Figure 5.42 - CEC (Cured) with Fly Ash for A-4 (Left), A-6 (Center), and A-7-6 (Right) Soils.....	77
Figure 5.43 - CEC (Cured) with Lime for A-6 (Left) and A-7-6 (Right) Soils.....	78
Figure 5.44 - Total SSA (0-day) with CKD for A-4 (Left), A-6 (Center), and A-7-6 (Right) Soils.....	80
Figure 5.45 - Total SSA (0-day) with Fly Ash for A-4 (Left), A-6 (Center), and A-7-6 (Right) Soils.....	81
Figure 5.46 - Total SSA (0-day) with Lime for A-6 (Left) and A-7-6 (Right) Soils.....	82
Figure 5.47 - External SSA (0-day) with CKD for A-4 (Left), A-6 (Center), and A-7-6 (Right) Soils.....	83
Figure 5.48 - External SSA (0-day) with Fly Ash for A-4 (Left), A-6 (Center), and A-7-6 (Right) Soils.....	83
Figure 5.49 - External SSA (0-day) with Lime for A-6 (Left) and A-7-6 (Right) Soils ..	84



Figure 5.50 - Internal SSA (0-day) with CKD for A-4 (Left), A-6 (Center), and A-7-6 (Right) Soils .....	84
Figure 5.51 - Internal SSA (0-day) with Fly Ash for A-4 (Left), A-6 (Center), and A-7-6 (Right) Soils .....	85
Figure 5.52 - Internal SSA (0-day) with Lime for A-6 (Left) and A-7-6 (Right) Soils....	86
Figure 5.53 - Total SSA (14-day) with CKD for A-4 (Left), A-6 (Center), and A-7-6 (Right) Soils .....	86
Figure 5.54 - Total SSA (14-day) with Fly Ash for A-4 (Left), A-6 (Center), and A-7-6 (Right) Soils .....	87
Figure 5.55 - Total SSA (14-day) with Lime for A-6 (Left) and A-7-6 (Right) Soils.....	88
Figure 5.56 - External SSA (14-day) with CKD for A-4 (Left), A-6 (Center), and A-7-6 (Right) Soils .....	89
Figure 5.57 - External SSA (14-day) with Fly Ash for A-4 (Left), A-6 (Center), and A-7-6 (Right) Soils .....	89
Figure 5.58 - External SSA (14-day) with Lime for A-6 (Left) and A-7-6 (Right) Soils	90
Figure 5.59 - Internal SSA (14-day) with CKD for A-4 (Left), A-6 (Center), and A-7-6 (Right) Soils .....	91
Figure 5.60 - Internal SSA (14-day) with Fly Ash for A-4 (Left), A-6 (Center), and A-7-6 (Right) Soils .....	91
Figure 5.61 - Internal SSA (14-day) with Lime for A-6 (Left) and A-7-6 (Right) Soils..	92
Figure 6.1 - Uncured Atterberg Limits Model for A-4 Soils.....	97
Figure 6.2 - Cured Atterberg Limits Model for A-4 Soils.....	98
Figure 6.3 - Combined Atterberg Limits Model for A-4 Soils.....	100
Figure 6.4 - Full Analysis Model for A-4 Soils.....	101
Figure 6.5 - Practical Analysis Model for A-4 Soils .....	103
Figure 6.6 - Uncured Atterberg Limits Model for A-6 Soils.....	106
Figure 6.7 - Cured Atterberg Limits Model for A-6 Soils.....	107
Figure 6.8 - Combined Atterberg Limits Model for A-6 Soils.....	109
Figure 6.9 - Full Analysis Model for A-6 Soils.....	111
Figure 6.10 - Practical Analysis Model for A-6 Soils .....	113
Figure 6.11 - Uncured Atterberg Limits Model for A-7-6 Soils.....	117
Figure 6.12 - Cured Atterberg Limits Model for A-7-6 Soils.....	119
Figure 6.13 - Combined Atterberg Limits Model for A-7-6 Soils.....	120
Figure 6.14 - Full Analysis Model for A-7-6 Soils.....	122
Figure 6.15 - Practical Analysis Model for A-7-6 Soils .....	124
Figure 6.16 - Uncured Atterberg Limits Model for All Soils.....	128
Figure 6.17 - Cured Atterberg Limits Model for All Soils.....	129
Figure 6.18 - Combined Atterberg Limits Model for All Soils .....	131
Figure 6.19 - Full Analysis Model for All Soils.....	133
Figure 6.20 - Practical Analysis Model for All Soils.....	135
Figure 6.21 - Atterberg Limits Model for Raw Soils.....	139
Figure 6.22 - Full Analysis Model for Raw Soils.....	141
Figure 6.23 - Atterberg Limits, Average pH, and Clay Fraction Model for Raw Soils .	143

# CHAPTER 1: INTRODUCTION

## 1.1 General

Stabilization of fine-grained soils is an alternative for geotechnical engineers considering the economics of construction with silt or clay soils. Mechanical stabilization, such as compaction, is an option; however many engineers have found it necessary to alter the physicochemical properties of clay soils in order to permanently stabilize them. The results presented in this thesis are part of a larger study that seeks to validate and/or refine the Oklahoma Department of Transportation's (ODOT) recommended additive contents for stabilizing fine-grained soils in Oklahoma. ODOT recently published their OHD L-50 Standard "Soil Stabilization Mix Design Procedure" which gives guidelines on additive percentages to be used with soils classified by AASHTO M145 (AASHTO 2002). Table 1.1 below shows the design table from the OHD L-50.

**Table 1-1: OHD L-50 Soil Stabilization Table (ODOT, 2006)**

ADDITIVE (Expressed as a percentage added on dry over basis)	SOIL STABILIZATION TABLE											
	SOIL GROUP CLASSIFICATION – AASHTO M145											
	A-1		A-2					A-3	A-4	A-5	A-6	A-7
	A-1-a	A-1-b	A-2-4	A-2-5	A-2-6	A-2-7	A-3	A-4	A-5	A-6	A-7-5	A-7-6
<b>PORTLAND CEMENT</b>	4	4	4	4	4	4	5	√	√	√		
<b>FLY ASH</b>					10	10	11	12	12	12		
<b>CEMENT KILN DUST (Pre-Claciner Plants)</b>	4	4	4	4	4	4	5	√	√			
<b>CEMENT KILN DUST (Other Type Plants)</b>	8	8	8	9	9	9	10	10	10			
<b>HYDRATED LIME*</b>										4	5**	5**

A blank in the table indicates the additive is not recommended for that soil group. Recommended amounts include a safety factor for loss due to wind, grading, and/or mixing. Pre-calciner plants are identified on the Materials Division approved list for cement kiln dust.

√ = Mix Design Required

\* = Reduce quantity by 20% when quick lime is used, i.e. 4% x 0.8 = 3.2%, 5% x 0.8 = 4.0%, 6% x 0.8 = 4.8%

\*\* = Use 6% when liquid limit is greater than 50.



One of the concerns with these guidelines is that soils which fall into the same AASHTO category (i.e., A-6, A-7) may react differently to the same type and amount of additive listed in the table because of variations in mineralogical, physical and chemical constituents of the soil. Another concern is the lengthiness of a traditional full mix design approach used to select appropriate additive contents. In order to refine and optimize the recommendations in OHD L-50, various simple and inexpensive laboratory methods are being investigated for selecting additive contents.

This thesis presents the results of multiple laboratory tests on soils falling within the A-4, A-6 and A-7-6 AASHTO classifications, stabilized with increasing hydrated lime, cement kiln dust (CKD) and two types of Class C fly ash (from Red Rock and Muskogee, OK). The research described in this paper focused primarily on investigating the effects, if any, that other soil properties beyond Atterberg Limits have on predictions of increases in a soil's unconfined compression strength at varying chemical additive contents. This research may have an important effect on making chemical mix designs for pavement subgrades more efficient, as well as providing a better understanding of properties that significantly affect strength gains in soils.

## **1.2 Hypotheses and Objectives**

### **1.2.1 Main Hypotheses of this Study**

It is likely that additional soil properties beyond the Atterberg Limits will contribute significantly to predicting the strength increase of a soil at a given additive percentage. It is hypothesized that the design equations will be strongly influenced by the soil's surface area and the linear shrinkage. However, it is also expected that Atterberg limits will still be important factors in any correlations.

### **1.2.2 Primary Objectives of this Study**

This research focused on performing various laboratory tests on eight different natural soils collected from sites across the state of Oklahoma.

The primary objectives of this research were:

1. To investigate the properties of AASHTO-classified fine-grained soils, with the eight soils falling into the A-4, A-6, or A-7-6 classifications. This was accomplished by testing several index, chemical, and strength properties of the aforementioned soils.
2. To determine if accurate predictions of stabilized soil strengths can be made using only Atterberg Limits.
3. To determine if soil strength predictions are only feasible when the soils are divided by AASHTO classifications, or if the soil classification is an unnecessary division.
4. To investigate if the pH response is as consistent for CKD and fly ash stabilization as it is for lime stabilization.
5. To validate and/or refine the recommendations presented in the OHD L-50 "Soil Stabilization Mix Design Procedure."
6. To recommend additional laboratory tests, if any, to augment the design recommendations given in the OHD L-50.

### **1.3 Thesis Layout**

This thesis is organized into seven chapters. Chapter 2 reviews published studies on chemical stabilization of soils and previous studies about soil properties that have significant effects on stabilizer effectiveness. Chapter 3 provides detailed descriptions of

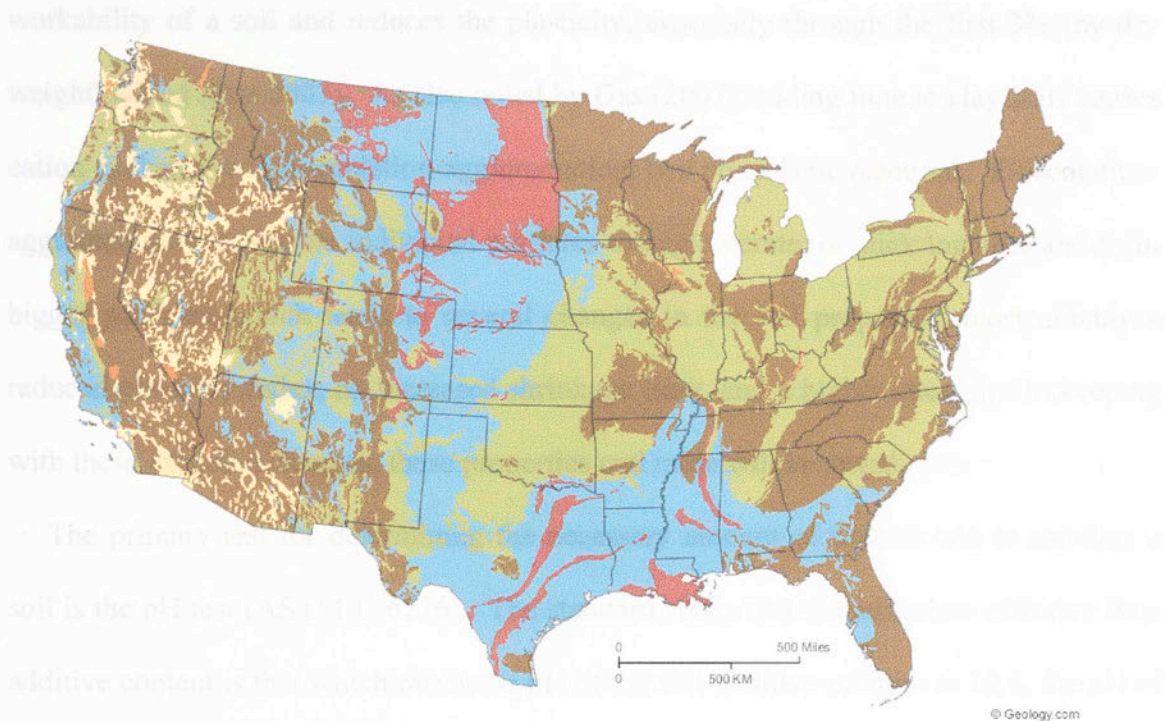


sample preparation, equipment, and testing used in this research study. Chapter 4 presents detailed descriptions of the soils used. Included in this chapter are the soil collection locations, the soil taxonomies, and soil properties that were found from the standard classification and physical property tests. Chapter 5 contains comparisons of the results of the statistical analyses performed on each soil. These results and the influences of the various tested properties on the prediction of soil strength gains with different additives are discussed in Chapter 6. Lastly, the summary and conclusions of this study are presented in Chapter 7. This chapter also provides recommendations for future studies on understanding the effects of different soil parameters for predicting the unconfined strength increase of a soil with chemical stabilization.

## **CHAPTER 2: LITERATURE REVIEW**

### **2.1 Introduction**

Many locations around the world, and especially many places in the United States, contain problematic soils such as expansive soils (Das 2007). Figure 2.1 below shows a map of swelling soil locations in the continental United States. It is an increasingly common practice worldwide to use chemical additives to stabilize these swelling soils before they are built upon. Highly plastic soils, including many soils found in Oklahoma, are stabilized using chemical additives. These additives used to stabilize soils include hydrated and quick lime, fly ash, cement kiln dust, and Portland cement. Table 1.1 shows the “Soil Stabilization Table” from OHD L – 50 that was developed to provide a quick guide to what additive to use for certain AASHTO M145 classified soils.



- Over 50 percent of these areas are underlain by soils with abundant clays of high swelling potential.
- Less than 50 percent of these areas are underlain by soils with clays of high swelling potential.
- Over 50 percent of these areas are underlain by soils with abundant clays of slight to moderate swelling potential.
- Less than 50 percent of these areas are underlain by soils with abundant clays of slight to moderate swelling potential.
- These areas are underlain by soils with little to no clays with swelling potential.
- Data insufficient to indicate the clay content or the swelling potential of soils.

**Figure 2.1 - Map of Swelling Soils in United States (Olive, et al, 1989)**

## **2.2 Research into Effective Stabilizer Percentages**

### **2.2.1 Lime**

For this study, hydrated lime was one of the three chemical stabilizers chosen. Of the three chemicals, it is the only one that is not a byproduct of an industrial process, which makes lime comparatively more expensive to use. As a stabilizer, lime increases the



workability of a soil and reduces the plasticity, especially through the first 3% (by dry weight) added (Das 2007). As also noted by Das (2007), adding lime to clay soils causes cation exchange and flocculation-agglomeration, two pozzolanic reactions. Flocculation-agglomeration causes the individual particles to agglomerate, or stick together and form bigger particles, which leads to several changes in the soil properties, most notably a reduced plasticity index, an increased shrinkage limit, and a higher strength. In keeping with these expected changes, these properties and more will be tested.

The primary test for determining the necessary amount of lime to add to stabilize a soil is the pH test (ASTM D 6276). The standard states that the minimum effective lime additive content is that which raises the pH of the soil-additive mixture to 12.4, the pH of lime itself. However, the standard also says that unconfined compression tests should be used to assure that the chosen lime percentage causes the desired strength gain. As lime is an extremely basic substance (calcium oxide, CaO, pH of 12.4) and most soils have pHs ranging from approximately 7 to 9, effective lime stabilization generally occurs with only 2% to 3% lime by dry weight. The Armed Forces of the United States use a very similar procedure for their pavement designs (U.S. Army, U.S. Air Force, and U.S. Navy 2005). The first step in their five step procedure is to mix several test batches of soil with increasing lime percentages to determine which percentage first causes a soil to reach a pH of 12.4. That percentage is then used to create UCT samples to evaluate if the percentage is sufficient in terms of the strength gained. If the strength is not acceptable, the next higher percentage is subjected to the same tests until the strength requirement is met.

Another important aspect of choosing the appropriate lime additive percentage is the degree of pulverization of the soil. According to Bozbey and Garaisayev (2009), the higher the percentage of soil particles that pass a #4 sieve, the more efficient lime stabilization treatments will be. Their study focused on the differences between high-quality pulverized samples (100% passing a #4 sieve) versus poor-quality pulverized samples representing common field conditions (40% passing a #4 sieve) (Bozbey and Garasayev 2009). In terms of the unconfined compression strength results, the study showed that non-mellowed, high-quality samples treated with 6% lime showed much higher strengths than poor-quality samples with the same conditions. Only at 9% lime did the soil have similar strength values, showing that samples tested at “ideal” laboratory conditions may under-predict the actual additive amount needed to achieve the same desired results in field applications.

Lime is also a popular stabilizer choice among international engineers. In Botswana, for example, hydrated lime is used to stabilize naturally-occurring calcium carbonate deposits, known as calcretes, commonly used as roadway base materials. The lime “is usually added to reduce the plasticity of a material by initiating a flocculation reaction with any clay minerals present” (Lionjanga, et al 1987).

### **2.2.2 Cement Kiln Dust**

Cement kiln dust (CKD) is a byproduct from the creation of Portland cement. As it is a byproduct from an industrial process and each cement plant is different than the next, the properties of CKD can vary widely from one source to another. This makes it somewhat difficult to standardize the effects of soil stabilization with CKD. According to Miller and Zaman (2000), CKD is an effective soil stabilizer for both cohesive (clays



and some silts) and non-cohesive soils (some silts and sands). This fact will be tested in this study as both expansive clays and silts will be tested with cement kiln dust. Their study also compared the effectiveness of CKD from three different sources. They ultimately determined that CKD from different sources results in different strength gains. This fact will not be examined in this study, but a future study on the properties governing the different strength characteristics could be beneficial.

Unlike lime treatments which primarily base a stabilizer's effectiveness on pH, soils treated with CKD are best judged by the UCS changes after stabilization (Si and Herrera 2007), although other methods are also used. Their study investigated the strength properties of a medium-PI soil classified as A-6 (16) treated with CKD from 2% up to 10% of the dry weight of the soil. They also investigated the effects of curing times on the compression strength of the stabilized soil. They determined that not only did the higher percentages of CKD yield higher unconfined strengths, a longer curing time also resulted in higher strengths. This has significant implications for the pavement design industry as the longer a construction company can wait after the initial soil treatment, the higher the compressive strength will be.

While the Si and Herrera study found 10% CKD was the optimum additive content for their clay sample, a separate study by Mohamed (2002) on a non-plastic silty sand determined that 6% CKD is effective for stabilization based on a peak shear strength at 6% CKD followed by a reduction in strength at higher additive contents. An alternate method to choosing the correct CKD percentage to treat a soil is to base the calculations on the recommendations for treating a soil with Portland cement. Miller, et al (1997) pointed out that since CKD reacts with soil in a similar manner as Portland cement but

contains about 50% less cement oxides, a reasonable method to choose a CKD content is to find the appropriate Portland cement content and double it to find the CKD content.

Another aspect of soil stabilization treatment that affects the percentage of CKD required to achieve a necessary strength gain is the compaction delay time. This was tested in a study by Brooks, et al (2009). Using a medium-PI (18%) clay, the researchers tested the effects of compaction delays on different soil parameters including the UCS and the California Bearing Ratio (CBR). They determined that as long as the compaction occurred within three hours of mixing, strength changes were negligible; but as the delay increased beyond three hours, the soil showed considerable UCS and CBR value reductions. This implies that for field applications, it seems to be very important for contractors to be ready to compact a site shortly after mixing in the desired chemical additive.

Cement kiln dust is also being increasingly used around the world. It is growing in popularity due to its ease of acquisition as it is a waste product of concrete production, one of the most common building materials today. In the United Arab Emirates, Mohamed (2002) performed a study on the use of CKD on soils in arid areas. The results indicate that these silts and sands have increased shear strengths and lower hydraulic conductivities when CKD is added as a stabilizer, making these soils usable for roadway design and as barrier materials for waste containment.

### **2.2.3 Fly Ash**

Fly ash is a byproduct of the combustion of lignite coal in coal-fired power plants. When used as a soil stabilizer, fly ash is divided into two categories based on the calcium content. Ashes with high calcium contents are labeled as Class C fly ash, and ashes with



low calcium contents and higher amounts of silica and/or alumina are called Class F fly ash (Turner 1997). In his study, Turner compared the effectiveness of the two types of fly ash on several different Wyoming soils. He ultimately found that the compression strengths of the Class C fly ash stabilized soils were higher than those soils stabilized with Class F fly ash.

In this study, Class C fly ash will be used. It is a self-cementing fly ash material, meaning that it contains some amount of free lime. This gives Class C fly ash an added benefit of essentially using two stabilizers. Fly ash also has the ability to be used with sandy and silty soils due to its cementitious properties, unlike lime which typically does not react well with those types of soils (IDOT 2005). Unfortunately, the proportion of free lime in fly ash can vary from source to source. The percentage of lime can be as low as 0 to 7% (ASTM D 5239) or up to 25% and higher (Das 2007). Despite the presence of this extra lime, soil stabilization applications that call for fly ash generally use relatively higher percentages by dry weight than applications with lime or CKD, with percentages ranging up to 12% or 15% or higher (Mackiewicz and Ferguson 2005).

As with CKD stabilization, fly ash stabilization does not have any specific methods for choosing the correct additive percentage. Laboratory testing of the unconfined compression strength after stabilization is still the safest method of choosing the fly ash content. However, several different methods are commonly used to choose the additive percentage when fly ash is the recommended additive. One of these methods is to base the fly ash percentage from the amount of lime that would be used for the particular soil. In the *Design, Construction, and Materials* manual, the Illinois Department of Transportation (IDOT) recommends as the fly ash content to use two to three times the



percentage of lime (IDOT 2005). A separate study investigated the optimum fly ash content using a free swell oedometer. Çokça (2001) tested fly ash percentages up to 25% on an expansive soil and found that the swell potential was barely reduced from 20 to 25% fly ash, implying that 20% fly ash is the optimum additive content, at least for that soil.

When fly ash is used in field applications, there are two major aspects of construction that do have specific guidelines. One aspect is the maximum compaction delay from the time of initial soil mixing (Little, et al 2000). As the hydration reactions begin as soon as the fly ash is added to soil, it is imperative that compaction begins within one to two hours to take full advantage of the cementing abilities of the fly ash. The cementitious materials bond the soil particles rapidly upon mixing, so any compaction delays can potentially disrupt these bonds and cause the final soil strength to be less than expected. The other important construction aspect is moisture control. If the moisture content of the soil at mixing is higher than the optimum moisture content, “the strength of the stabilized material can be reduced by 50 percent or more if the moisture content exceeds the optimum for maximum strength by 4 to 6 percent” (Little, et al 2000).

As with lime, fly ash is used internationally for stabilization projects. Research into the use of fly ash as a stabilizer has shown that the California Bearing Ratio increases when fly ash is added (Singh et al., 2008). Their research in India has shown that increasing the amount of cement in cement-stabilized fly ash mixed with soil increases the unconfined compression strength in a linear pattern. The strength also increased with increasing the curing time of the mixture.

#### 2.2.4 Alternative Stabilizers

In Southeast Asia, engineers in Papua New Guinea have treated soft clay subgrade soils with lime and Portland cement mixed with local natural resources (Hossain, et al. 2007). One of the more common of these natural resources is volcanic ash. When tested with A-6 and A-7-6 clayey soils, the combination of 4% cement and 10% volcanic ash provided the biggest strength increase, increasing the 90-day compression strength of the A-6 soil to 25 times its unstabilized strength and the A-7-6 soil to 10 times its original strength. Further research into the properties and usefulness of volcanic ash as a soil stabilizer could result in a potentially more economical stabilizer option in some areas.

Another alternative stabilizer is rice husk ash. This is formed by burning rice husks in the open air and then sieving the remains over a 75 micron sieve. A combination of rice husk ash and lime was tested in Northeastern India by Roy (1988). He tested five medium plasticity soils commonly found in India with a combination of 2% lime and 4% rice husk ash. The ash was used in this experimental study because some local soils have been found to not achieve a sufficient strength when treated with lime alone, and the ash might become a new economical stabilizer source. The research determined that the lime and rice husk ash combination increased both the compression and tensile strengths of the soils due to a pozzolanic reaction initiated by the addition of the rice husk ash to the soil (Roy 1988). This may signal that rice husk ash can be an effective soil stabilizer in the future.

A third stabilizer that is gaining popularity is recycled rubber tire scraps. Tires are a very common waste product and do not degrade easily, making them an ideal option for a recycling project such as this. In a 2007 study, Akbulut et al (2007) took tire shreds from



a tire repair company in Erzurum, Turkey and tested their effectiveness at stabilizing local expansive clays. The authors tested tire shreds in three groups: under 5 mm threads, under 10mm threads, and under 15mm threads. The tire fibers were mixed into the soil samples at percentages ranging from 1 to 5% of the dry soil weight and the unconfined compressive strength was tested for each soil and tire fiber mix. Their results showed that all three tire fiber lengths increased the unconfined strength of the test soils, but the 10mm fiber length group consistently yielded higher peak strengths. The optimum additive content was found to be 2% with a lower residual strength at increasing additive contents. Additional research into the use of recycling tires as soil stabilizers could prove highly beneficial to the environment and to future generations.

Chemical stabilizers have also been applied to granular soils. In Saudi Arabia, cement is being tested for its efficiency in stabilizing the sabkha soils, very low-density sands mixed with saltwater and salt brine (Al-Amoudi, 1994). While not a fine-grained expansive soil, the problem with these soils is that their low densities and strengths make them unusable for construction until chemical stabilizers or other methods are used. Using a cementitious material is a proven technique for strengthening granular-type materials because the cement actually causes the particles to become cemented together. The cement used in the Al-Amoudi study was found to increase both the density of the sand and its unconfined compression strength.

### **2.3 Properties of Interest**

It is expected that several different soil factors will have an effect on the efficiency of chemical stabilizers used in fine-grained Oklahoma soils. Many studies have already been performed on stabilizers and researchers have found many factors that influence the

compressive strength of the soil. The Oklahoma Department of Transportation (ODOT), for example, uses the Atterberg Limits to determine the stabilizer amount to use in their mix designs; however, they have found instances where this does not accurately predict the stabilized strength even though the soils may be classified identically by AASHTO classifications. In other words, while convenient for classification, Atterberg Limits are not adequate in all cases for determining the amount of stabilizer to use for road-way sub base design because they alone do not always explain soil behavior. It is likely that other properties may have significant effects as well.

### **2.3.1 Soil pH**

Miller and Azad (2000) performed a study on the influence of a soil's type on stabilization attained using cement kiln dust. Their study investigated several parameters, including the pH of the soil. Using data gathered from pH tests performed one hour after mixing a soil with cement kiln dust, they found that "Results of unconfined compression tests...indicate that the pH response can be used to predict relative performance of CKD-treated soils" (Miller and Azad 2000). Enough research has also been done on the subject of the pH response of soils mixed with lime that the ASTM Standards Manual contains a specific test procedure (ASTM D 4609) on how to determine the optimum lime additive content based on the pH (ASTM 2005). The standard states that once the recorded pH of the soil-additive mixture reaches 12.4, the additive content at which this occurs is the optimum content. While the pH may ultimately be a contributing factor in more accurately predicting the soil strength gain, the ASTM standard recommends testing the unconfined strength of the optimum additive content to ensure the strength reaches the minimum threshold.



### **2.3.2 Abrasion**

Arabi, et al. (1988), investigated the effectiveness of stabilizers by performing abrasion tests. Their study used a ball mill to examine the degree of bonding and compared the abrasion results to the increases in strength. Their study noted, "Clearly, as the degree of interlocking of soil particles increases during curing, larger forces are required to overcome this bonding and to break up the particles." While they only tested one soil with lime as a stabilizer, they developed an empirical relationship between their measured abrasion factor and the corresponding increase in compression strength. The abrasion factor will not be tested during the course of this study, but the concept has the potential to become an important test parameter influencing the strength increases.

### **2.3.3 Cation Exchange Capacity**

The cation exchange capacity (CEC) may also prove to be a useful parameter for predicting the soil strength gains with different additives. A study by Yukselen and Kaya (2006) investigated the interrelatedness of the cation exchange capacity with various other soil properties. Their study found strong relationships between the CEC and the EGME surface area values, the Liquid Limit, and the Plastic Limit. As soil stabilization already relies heavily on the data provided through Atterberg Limits, and this study showed that Atterberg Limits are related to the CEC, it stands to reason that the CEC may be another soil property that helps in the prediction of the soil strength gain.

### **2.3.4 Specific Surface Area**

The specific surface area of clay can tell a great deal about the expansion potential of the soil. "There is strong evidence in the literature that indicates that specific surface area may be the single most important contributing factor that controls the engineering

behavior of fine-grained soils” (Cerato and Lutenegeger 2002). In a separate study by Buhler and Cerato (2007), it was determined that for highly plastic soils treated with lime and Class C fly ash, higher specific surface areas coincided with higher amounts of shrinkage as determined with linear shrinkage tests. When treated with chemical stabilizers, higher stabilizer contents result in lower specific surface areas. This study only involved testing with one natural soil, but it is anticipated that the trend discovered through that research will apply to all soil types. The specific surface area is one of the properties that will be tested during the course of this research study.

## **CHAPTER 3: MATERIALS AND TEST PROCEDURES**

### **3.1 Introduction**

This chapter details the soils chosen for the study, as well as the methods of investigation used to determine properties of the various soil samples. The laboratory test program consisted of general classification tests, Harvard Miniature compaction tests, and chemical property tests. The test soils selected for this study were subjected to standard classification, physical property, and chemical property tests, including tests of: grain size distribution (ASTM 422-00), sieve analysis, specific gravity (ASTM D 845-00), Harvard Miniature compaction (ASTM D 4609-01), unconfined compression strength (ASTM D 2166-06), Atterberg Limits (ASTM D 4318-00), linear shrinkage (Heidema 1957), shrinkage limit (BS 1377: 1990, Test 5), specific surface area (Cerato and Lutenegeger 2002), carbonate content (Dreimanis 1962), sulfate content (ODOT 2005), pH (ASTM D 4972-01), direct current electrical conductivity, and cation exchange capacity (Rhoades 1982) tests. These tests were performed to classify the soil based on



USCS and AASHTO classifications, to characterize the compaction properties, and gather input parameters for the statistical analysis.

### 3.2 Test Soils

The soil samples for this study were taken from different sites across Oklahoma and were chosen to represent the AASHTO-classified A-4, A-6, and A-7-6 soils. A total of eight soils were used in the study: three silts (A-4, ML or CL), three lean clays (A-6, CL), and two fat clays (A-7-6, CH). Once removed from the field, the soils were sealed in plastic buckets and kept in a humidity-controlled room to maintain the natural water contents. Figure 3.1 below shows the locations of each soil and Table 3.1 provides a legend for Figure 3.1. As seen below, Figure 3.2 provides images of each soil.

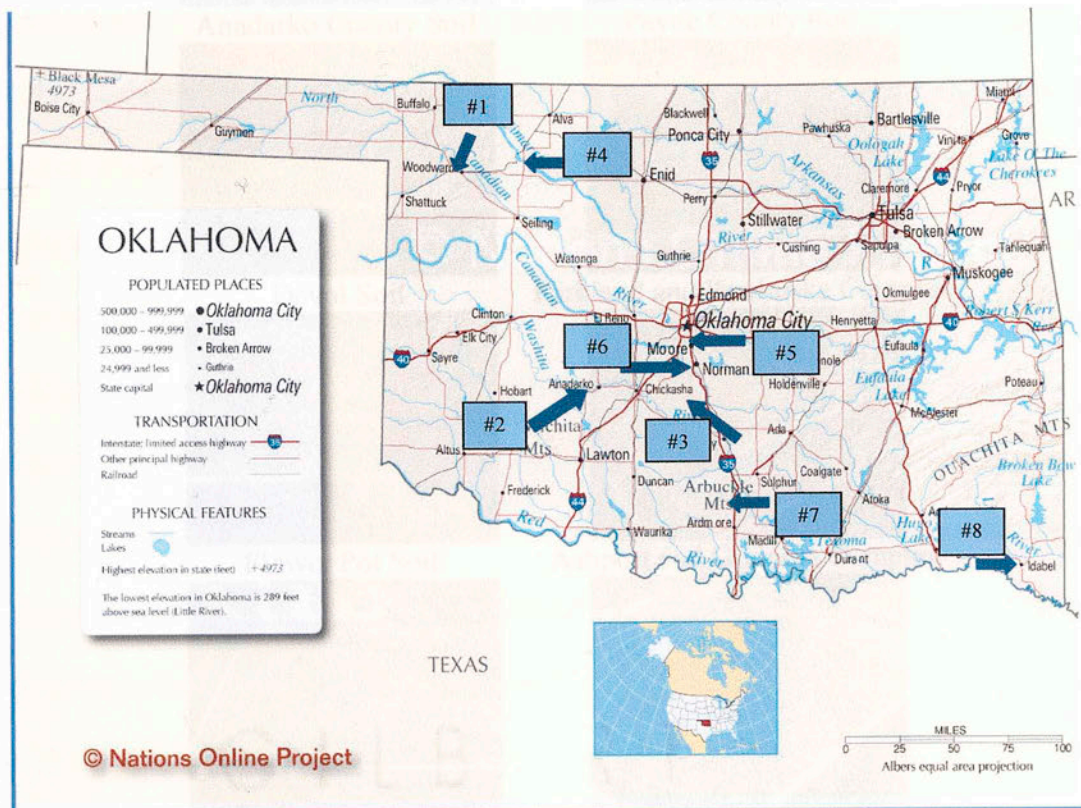


Figure 3.1 - Locations of Test Soils in Oklahoma

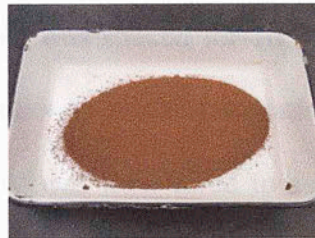


**Table 3-1 - List of Soil Locations and Classifications**

Soil No.	Soil Name	AASHTO Class.	USCS Class.	Location
1	Devol	A-4 (0)	ML	US 183, Woodward, OK
2	Anadarko	A-4 (0)	ML	US 62, East of Anadarko, OK
3	Payne	A-4 (2)	CL	Country Club Road, Payne Co., OK
4	Flower Pot	A-6 (18)	CL	Cimmaron River, East of Woodward, OK
5	Kirkland/Pawhuska Complex	A-6 (13)	CL	Sante Fe & South of 19th Moore, OK
6	Ashport/Grainola Complex	A-6 (9)	CL	24th E Robinson St., Norman, OK
7	Heiden Clay	A-7-6 (39)	CH	I-35 and Ardmore, OK, near Turner Falls
8	Hollywood	A-7-6 (45)	CH	Route US 70 & St. Rt. 7., Idabel, OK



Anadarko County Soil



Payne County Soil



Devol Soil



Kirkland and Pawhuska Complex



Flower Pot Soil



Ashport and Grainola Complex



Hollywood Soil



Heiden Clay

**Figure 3.2- Pictures of Test Soils**

### 3.3 Classification and Physical Property Tests

#### 3.3.1 Grain Size Distribution

The clay and silt fraction ( $< 75\mu\text{m}$ ) of the soils was determined by a sedimentation process, using a hydrometer to take the necessary data. This test procedure was performed in accordance with the American Society for Testing and Materials (ASTM 2005) D 422-00 "Standard Test Method for Particle-Size Analysis of Soils." An air-dried soil sample weighing approximately 50 g and passing a #10 sieve was required to perform the hydrometer test. The soil sample was soaked for 16 hours in a dispersing agent bath of sodium hexametaphosphate solution with a concentration of 40 g per 1 liter of distilled water. Then the soil-water slurry was transferred to a glass sedimentation cylinder and distilled water was added until the total volume reached 1000 ml. After a rubber stopper was placed over the open end, the cylinder was manually shaken end-over-end for 1 minute to achieve a completely homogenous mixed soil slurry. The cylinder was placed on a lab bench and a 152 H hydrometer was placed in the slurry and readings were taken at the following times; 0, 1, 2, 4, 8, 16, 30, 60, 120, 240, 1080, and 1440 minutes. Between readings, the hydrometer was removed from the soil suspension, rinsed and placed in a reference solution containing the same concentration of sodium hexametaphosphate. At each time interval, the temperature of the control fluid and the hydrometer control reading was recorded. After the hydrometer readings were completed, the soil suspension was passed over a #200 sieve. The soil retained on the #200 sieve was then oven dried, and then passed over a #40 sieve. The percentages of soil that passed # 200 and #40 were then determined.



### 3.3.2 Sieve Analysis

Approximately 500 grams of air-dried soil was required to perform this test method. The soil was first oven-dried at  $110 \pm 5^{\circ}\text{C}$  for 24 hours. The mass of the soil was determined after the drying. Then the soil was soaked at least 16 hours with the dispersing agent as a sodium hexametaphosphate solution with concentration of 40 g per 1 liter of distilled water. The soil–water slurry was transferred to a #200 sieve and then rinsed with tap water. The soil retained on the #200 sieve was then oven-dried again at  $110 \pm 5^{\circ}\text{C}$  for 24 hours. The mass of the dry soil was recorded. #4, #10 and #40 sieves were stacked together and a catch pan was placed in the bottom of the stack. The soil previously retained on the #200 sieve was placed on the top of stacked sieves. A shaker machine was used to shake the soil for 10 minutes. Then the soil retained on each of the three sieves was determined. The percentages of soil passing the #4, #10 and #40 sieves were calculated.

### 3.3.3 Specific Gravity

This test procedure was performed in general accordance with American Society for Testing and Materials (ASTM) D 854-00 “Standard Test Method for Specific Gravity of Soils” (ASTM 2005). The mass of an empty pycnometer was determined and the same pycnometer was filled with distilled water to the calibration mark, re-weighed, and the temperature was measured. The distilled water was then removed. Approximately 40 g of oven-dried soil passing the standard U. S. #10 sieve was placed in the pycnometer. Distilled water was added to the soil in the pycnometer and allowed to soak at least 16 hours. After 16 hours, the trapped air was removed from the slurry by using a vacuum pump for at least 2 hours while agitating the slurry. After removing the air, distilled water

was added to the slurry to raise the contents to the calibration mark. The mass of the pycnometer, soil, and water was obtained, and the temperature was determined. The specific gravity was determined by the following equation:

$$G \text{ at } 20^{\circ}\text{C} = K * G \text{ at } T_b \quad [3.1]$$

Where:

G: Specific Gravity,

K: A number found by dividing the density of water at temperature  $T_b$  by the density of water at  $20^{\circ}\text{C}$ . K values are given in a table in ASTM D 854-98.

$$G \text{ at } T_b = \frac{M_o}{[M_o + (M_a - M_b)]} \quad [3.2]$$

Where:

$M_o$  = Mass of sample of oven-dry soil (g)

$M_a$  = Mass of pycnometer filled with water at temperature  $T_b$  (g)

$M_b$  = Mass of pycnometer filled with water and soil at temperature  $T_b$  (g)

$T_b$  = Temperature ( $^{\circ}\text{C}$ ) of the contents of the pycnometer when mass  $M_b$  was determined

### 3.3.4 Harvard Miniature Compaction

Compaction tests were performed according to the American Society for Testing and Materials (ASTM) D 4609-01 "Evaluating Effectiveness of Chemicals for Soil Stabilization" (ASTM 2005). The Harvard Miniature compaction apparatus was used to create moisture-density curves for each soil at each additive percentage. To create each sample, 140 g of air-dried soil was measured into a mixing bowl. The appropriate additive mass was calculated based on the dry mass of the soil and was then mixed into the air-dried soil. Once the soil and additive were mixed, deionized water was added to the bowl to raise the moisture content to the desired level. The soil was then carefully



placed in the Harvard Miniature mold and compacted using a 12” drop hammer. The soil was compacted in five layers with 10 blows from the hammer used for each layer. This compaction process was designed and calibrated by Khoury and Khoury (2005) to closely match the compaction characteristics of a Standard Proctor test. They performed tests on 4 different soils and determined the best match to the Standard Proctor was with five compacted layers with the specially-calibrated drop hammer. Once the fifth layer was compacted, extra soil was trimmed from the top and bottom of the mold and used to determine the moisture content of the sample as a whole. The soil was then removed from the mold with a mechanical extractor. This process was repeated to create multiple-point moisture-density curves used to determine the optimum moisture content (OMC) of each soil-additive mixture.

### **3.3.5 Unconfined Compression Strength**

Unconfined compression strength (UCS) testing followed the guidelines laid out by the American Society for Testing and Materials (ASTM) D 2166-06 “Standard Test Method for Unconfined Compressive Strength of Cohesive Soil” (ASTM 2005). Based on the OMC curves determined through the Harvard Miniature compaction tests, samples for UCS testing were made at the OMC of each soil-additive combination. The samples were made with the Harvard Miniature apparatus following the procedure outlined above. Once the sample was removed from the mold, it was wrapped with plastic wrap and sealed in a plastic bag and was placed in a 100% humidity room to cure for 14 days. Three samples were molded at each additive percentage for each soil. To be considered eligible for UCS testing, samples were required to be within 0.5% of the target moisture

content and the range of moisture contents of the three samples could be no greater than 0.75%.

After curing, samples were unwrapped and placed on the uniaxial testing frame. The tests were strain-controlled and the testing rate was set to 2% strain per minute. The strain was measured using a standard deflection gage and the load was measured with a digital load cell. The values of load and strain were analyzed to create stress-strain curves. After the samples failed in compression, they were air-dried and saved for testing the Atterberg Limits.

### **3.3.6 Atterberg Limits**

The Atterberg Limits determination was done according to the American Society for Testing and Materials (ASTM) D 4318-00 “Standard Test Method for Liquid Limit, Plastic Limit, and Plasticity Index of Soils” (ASTM 2005). This test method was performed only on the portion of a soil that passed the 425- $\mu\text{m}$  (No. 40) sieve. Approximately 150-200 grams of soil were needed to perform the Atterberg Limits tests. The soil sample was mixed with distilled water to bring the water content to a point where the blow count equaled 15 or less. Then the soil sample was kept in a plastic bag and placed in a humid chamber for at least 16 hours to temper. Once the soil tempered, the soil sample was divided into two parts. Approximately 20 grams of soil was required to perform the Plastic Limit test and the rest was saved for the Liquid Limit test.

The liquid limit was determined by performing trials in which a portion of the specimen was spread in a brass cup called a Casagrande cup. The soil in the cup was divided half using a grooving tool, and then allowed to flow together by repeatedly dropping the cup at a standard rate of two blows per second. When the soil flowed



together to a length of a half inch, a sample was taken from the soil across the closed gap. At least four separate water content determinations were taken; two were taken at blow counts less than 25 blows and two were taken at blow counts more than 25 blows. The water contents were plotted versus the number of blows in logarithmic scale. The Liquid Limit was determined as the water content of the soil sample at 25 blows. The Plastic Limit was determined by rolling the soil into a thread on a standard glass plate to a diameter of 3.18 mm (1/8 in) until the soil specimen crumbled and could not be rolled any further. At least three threads were rolled and the average of the water contents was taken as the Plastic Limit of the soil.

### **3.3.7 Shrinkage**

#### **3.3.7.1 Linear Shrinkage**

This test method was first introduced by the Texas Highway Department in 1932 (Heidema 1957) and currently appears as a standard test procedure in the British Standard BS 1377: (1990). Approximately 150 grams of soil passing a #40 sieve were required to perform the test procedure. First, the soil sample was mixed with tap water to approximately the Liquid Limit, a consistency of 25 blows in the Casagrande cup. A portion of the soil was placed in a linear bar mold approximately 140 mm long and 25 mm in diameter. The soil was placed in three layers and tapped against a flat surface in between the layering to remove air bubbles from the soil sample. The mold was then allowed to air dry. Mass and length measurements were taken several times a day until the length did not change measurably. At that point, the mold was oven-dried for 24 hours at  $110 \pm 5^{\circ}\text{C}$ . After drying, the mass and length measurements were taken once more. The length of the soil sample was measured three times by using a digital caliper.

The average length was used to calculate the linear shrinkage. The linear shrinkage was calculated by the following equation:

$$LS = 100 * \left(1 - \frac{L_{avg}}{L_o}\right) \quad [3.3]$$

Where:

LS = Linear shrinkage (%),

$L_{avg}$  = Average final length of the soil inside the linear bar mold (mm),

$L_o$  = Original length of the linear bar mold (mm).

### 3.3.7.2 Shrinkage Limit

The linear shrinkage measurement of soil was used to determine the shrinkage limit. This test method was performed in general accordance with the British Standard (BS 1377: 1990, Test 5) and it is an alternative to the Mercury Method (ASTM D 427- 00) “Standard Test Method for Shrinkage Factors of Soils by the Mercury Method.” This test was also performed in conjunction with the Linear Shrinkage test detailed previously. The changes in length measured during the air-drying period were plotted versus the water content, where the shrinkage limit was described as the first water content at which no variation in the length of the soil sample was observed. The determination of the shrinkage limit from the linear shrinkage is presented in Figure 3.3.



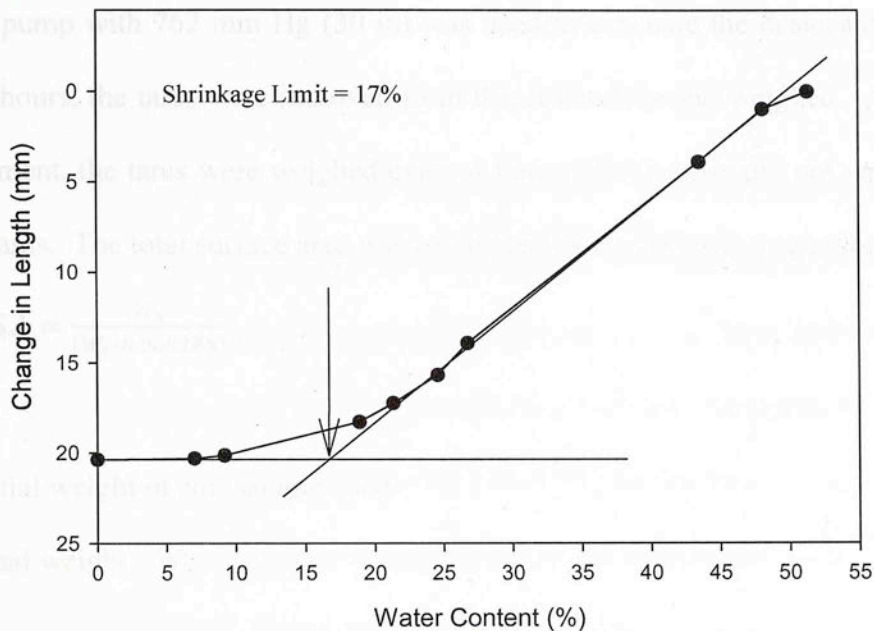


Figure 3.3 - Determination of the Shrinkage Limit

### 3.4 Mineralogical Property Tests

#### 3.4.1 Specific Surface Area

##### 3.4.1.1 Ethylene Glycol Monoethyl Ether (EGME) Method

This test method for the total surface area follows the methodology presented by Cerato and Lutenege (2002) in their study "Surface Area and Engineering Properties of Fine-Grained Soils." This test method was conducted on oven-dried soil. All soils were pulverized and then processed over a standard #40 sieve. Approximately one gram of oven-dried soil was spread on the bottom of an aluminum tare with 76 mm diameter and 25 mm height. Two aluminum tares were used for each soil sample. The mass of the soil was determined by using an electronic analytical balance with an accuracy of 0.0001 grams. Approximately 3 ml of Ethylene Glycol Monoethyl Ether (EGME) was added to the soil and gently mixed by hand to create a homogenous slurry. The slurry was allowed

to equilibrate for 20 minutes and then the tares were placed in vacuum desiccators. A vacuum pump with 762 mm Hg (30 in) was used to evacuate the desiccators. Initially, after 18 hours, the tares were removed from the desiccators and weighed. After the first measurement, the tares were weighed every 4 hours till the mass did not vary more than 0.001 grams. The total surface area was calculated by the following equation:

$$Total\ SSA = \frac{W_a}{(W_s * 0.000286)} \quad [3.4]$$

Where:

$W_s$  = Initial weight of soil sample used

$W_a$  = Final weight -  $W_s$

#### **3.4.1.2 BET Method**

This test procedure is used to determine the external specific surface area of soils (Brunauer et al. 1938). The Quantachrome Corporation's MONOSORB, a direct reading dynamic flow surface area analyzer, was used for this test. The principle of this test method is to measure the amount of adsorbate gas adsorbed on a solid surface by sensing the change in the thermal conductivity of a flowing mixture of adsorbate and an inert carrier gas. The adsorbate is nitrogen and the inert gas is helium. All soils were pulverized and processed over a standard #40 sieve, and then oven-dried at  $110 \pm 5^\circ\text{C}$  for 24 hours. Approximately 0.1 grams of oven dried soil was placed in a sample tube and then put in the cell holder. A Dewar flask was filled with liquid nitrogen and brought up until the liquid nitrogen covered the top of the cell by 0.5 inches. Nitrogen then begins to flow and the soil adsorbs the gas. The Dewar flask lowered when the nitrogen flow stops and the gas adsorption begins on the soil. When the adsorption was complete, the integrator displayed a number which represented the sample surface area in square



meters. The external surface area was determined by dividing that number by the mass of the soil.

### 3.4.2 Carbonate Content

This test method was performed by using the Chittick Apparatus which was presented by Dreimanis (1962). The Chittick Apparatus measures the amount of carbonates in the soil by measuring the amount of carbon dioxide that evolves from carbonates reacting with dilute hydrochloric acid. The soil sample was crushed and passed over a standard #40 sieve. The soil was then oven-dried at  $110 \pm 5^{\circ}\text{C}$  for 24 hours. Approximately 1.7 grams of the oven-dried soil was placed in a 250-ml Erlenmeyer flask with a plastic coated stirring magnet and fitted onto the apparatus. The hydrochloric acid solution was made by mixing 109.4 mL of concentrated hydrochloric acid in 1000 mL of distilled water. A pipette was filled with 20 ml of the 6N hydrochloric acid solution. Initially, the reservoir was raised to be in the same level of the annulus and this initial reading was recorded. Then a stop watch was started and the acid pipette valve was opened to allow 20 mL of acid to flow into the Erlenmeyer flask within a period of approximately 45 seconds. After one minute, the reservoir level was adjusted to be even with the level of the annulus and the first reading was taken,  $R_1$ . The temperature in the beaker and the barometric pressure were recorded. The second reading was taken after twenty minutes, where the reservoir was again raised and leveled with the annulus and a second reading,  $R_2$ , was taken. The temperature and barometric pressure were also recorded again. Using these readings and a table of correction factors, the calcite and dolomite percentages were determined using the calculation procedure described in Dreimanis (1962). The calcite digests in about 30 seconds and the dolomite digests in about 20

minutes. The total amount of calcite and dolomite was described as the total amount of carbonate content.

### 3.4.3 Sulfate Content

The sulfate content of the eight natural soil samples was determined according to the procedure established by the Oklahoma Department of Transportation (ODOT) OHD L-49 “Method of Test for Determining Soluble Sulfate Content of Soil” (ODOT 2005). Air-dried soil was crushed and sieved over a standard #10 sieve to collect a mass of at least 30 grams. This sample was then oven-dried for 24 hours at  $110 \pm 5^\circ\text{C}$ . Five grams of oven-dried soil was added to a plastic bottle with 200 g of deionized water and the slurry was shaken with a mechanical shake table for 15 minutes and then allowed to soak for at least 16 hours. The liquid in the bottle is then poured over a filter paper cone into a beaker. A 10 mL sample is extracted with a pipette from the filtered liquid and placed into a small glass vial. The vial is placed into a digital colorimeter and three sulfate content readings (ppm) are recorded. The sulfate content is determined using the following equations:

$$D = W_w / W_s \quad [3.5]$$

Where:

D = Dilution ratio of soil slurry

$W_w$  = Mass of water added to slurry

$W_s$  = Mass of oven-dried soil in slurry

$$C = RD \quad [3.6]$$

Where:

C = Sulfate concentration in ppm



R = Colorimeter reading in ppm

D = Dilution ratio

### 3.4.4 Soil pH

The pH curve of the eight soil samples with each desired chemical additive was determined using a test procedure based on the American Society for Testing and Materials (ASTM) D 4972-01 “Standard Test Method for pH of Soils” (ASTM 2005). Enough soil was crushed from each sample to test ten additive percentages to construct a pH curve. Table 3.2 shows the tested additive percentages based on the additive type being used. The testing percentages for lime were weighted slightly more toward the early percentages because the lime pH curve develops rapidly at low contents.

**Table 3-2 - Additive Testing Percentages for pH and Conductivity Tests**

Additive Type	Percentages Tested to Create Curves
Lime	0, 0.5, 1, 2, 3, 5, 10, 15, 25, 100
CKD	0, 1, 2, 3, 5, 7, 10, 15, 25, 100
Red Rock Fly Ash	0, 1, 2, 3, 5, 7, 10, 15, 25, 100
Muskogee Fly Ash	0, 1, 2, 3, 5, 7, 10, 15, 25, 100

First, enough air-dried soil was measured out to have a mass of 25 g if oven-dried. The desired additive amount was added based on the 25 g dry mass and was thoroughly mixed in a clean plastic bottle. 100 mL of deionized water was added to the bottle and the bottle was placed on a mechanical shaker to shake for 30 seconds. The shaking was repeated every 10 minutes for one hour to ensure a well-mixed sample for testing. After

the shaking was completed, a calibrated digital pH meter was used to determine the pH of the sample. Each additive percentage was tested three times to ensure accurate results.

### **3.4.5 Direct Current Electrical Conductivity**

The conductivity of the soil-additive combinations was determined following the same basic procedures outlined in the pH testing section above. The tests were also performed in conjunction with the pH tests. Table 3.2 above shows the testing percentages. After testing the pH of the soil-additive slurry in a bottle, a calibrated digital conductivity meter was used to measure the electrical conductivity of the slurry. As with the pH tests, three tests were done at each additive percentage for accuracy purposes.

### **3.4.6 Cation Exchange Capacity**

The cation exchange capacity of each soil and additive combination was determined by Harris Laboratory, Inc., Lincoln, Nebraska using a 1N ammonium acetate extraction method (Rhoades 1982).

## **CHAPTER 4: RESULTS OF CLASSIFICATION, PHYSICAL, AND MINERALOGICAL PROPERTY TESTS**

### **4.1 Introduction**

Eight natural soils were collected from various locations around Oklahoma for this research study. All eight soils were classified and tested with the different tests presented in Chapter 3. This chapter contains the results of these different property tests.

### **4.2 Soil Sources**

As noted above, a total of eight Oklahoma soils were chosen for this project. A description of the chosen soils, as well as their locations and classifications, is presented



in Table 4.1. The study contains three AASHTO classifications; A-4, A-6, and A-7-6, and three USCS classifications; ML, CL, and CH. Representing the A-4 classification were three low plasticity or non-plastic soils: Devol, a soil from Anadarko, OK, and a soil from Payne, OK. The three A-6 soils were Flower Pot clay, an Ashport and Grainola complex, and a Kirkland and Pawhuska complex. The last two soils were from the A-7-6 classification: a Hollywood soil and a Heiden clay.

### **4.3 Physical and Mineralogical Test Results**

The soils chosen for this study were tested with various different procedures designed to provide important properties to be used later in the analysis of the chemical stabilizer effectiveness. The testing regimen included tests of: specific gravity (ASTM D 845-00), Harvard Miniature compaction (ASTM D 4609-01), unconfined compression strength (ASTM D 2166-06), Atterberg Limits (ASTM D 4318-00), linear shrinkage (Heidema 1957), shrinkage limit (BS 1377: 1990, Test 5), specific surface area (Carter et al. 1986), carbonate content (Dreimanis 1962), sulfate content (ODOT 2005), pH (ASTM D 4972-01), direct current electrical conductivity, and cation exchange capacity (Rhoades 1982). Physical property test results are shown in Table 4.2 and mineralogical test results are shown in Table 4.3. Curves and results of individual tests such as Liquid Limit curves and Shrinkage Limit curves can be found in Appendix A.

#### **4.3.1 Harvard Miniature Compaction Results**

The Harvard Miniature compaction apparatus was used to determine the optimum moisture content (OMC) of each raw soil and, later, of each soil and additive combination. The OMCs were needed to prepare the UCT samples for strength testing. A summary of the compaction results appears in Table 4.4. The OMC curves for each

soil-additive combination can be seen in Appendix A in Figure A-1 through Figure A-22 and Table A-1 through Table A-8.

### 4.3.2 Unconfined Compression Test Results

Using a triaxial testing frame for uniaxial compression loading allowed the soils to be tested in unconfined compression to determine the maximum unconfined compression strength (UCS). Each sample was molded in a Harvard Miniature mold at the OMC for UCS testing. While the average UCS was determined for each soil and additive combination, Table 4.5 shows the results of the UCS tests for only the raw soils and the rest of the tests performed with varying additive type and amount are presented in Appendix A, Figure A-23 to Figure A-32.

**Table 4-1 - General Raw Soil Descriptions and Locations**

Soil Name	Description	Location
Devol	Tan	US 183, Woodward, OK
Anadarko	Red	US 62, East of Anadarko, OK
Payne	Reddish brown	Country Club Road, Payne Co., OK
Flower Pot	Light reddish brown	Cimmaron River, East of Woodward, OK
Kirkland/Pawhuska Complex	Red and brown	Sante Fe & South of 19th Moore, OK
Ashport/Grainola Complex	Light brown	24th E Robinson St., Norman, OK
Heiden Clay	Greenish gray	I-35 and Ardmore, OK, near Turner Falls
Hollywood	Yellowish green	Route US 70 & St. Rt. 7., Idabel, OK



**Table 4-2 - Physical Properties of the Raw Test Soils**

Soil Name	Specific Gravity	Liquid Limit (%)	Plastic Limit (%)	Plasticity Index (%)	Linear Shrinkage (%)	Shrinkage Limit (%)	Clay Fraction (%)	Activity (A)
Devol	2.72	26.0	NP	NP	3.0	2.5	7.1	n/a
Anadarko	2.70	NP	NP	NP	2.0	4.5	14.9	n/a
Payne	2.70	24.0	14.0	10.0	9.0	9.5	31.4	0.32
Flower Pot	2.80	36.7	17.3	19.4	10.7	15.0	62.1	0.31
Kirkland / Pawhuska	2.74	38.8	16.3	22.5	12.3	15.0	28.6	0.79
Ashport / Grainola	2.77	36.8	17.7	19.1	11.8	12.0	27.5	0.70
Heiden	2.77	66.9	22.8	44.1	19.4	17.0	50.1	0.88
Hollywood	2.78	54.0	19.6	34.4	16.4	11.0	61.5	0.56

**Table 4-3 - Mineralogical Properties of the Raw Test Soils**

Soil Name	Cation Exchange Capacity (meq/100g)	Total SSA (m <sup>2</sup> /g)	External SSA (m <sup>2</sup> /g)	Internal SSA (m <sup>2</sup> /g)	Sulfate Content (ppm)	Calcite Content (%)	Dolomite Content (%)	Carbonate Content (%)	pH	Conductivity (mS)
Devol	5.5	30.0	8.4	21.6	213	3.6	1.6	5.2	9.08	37.81
Anadarko	8.2	40.5	1.5	39.0	230	2.3	1.6	3.9	7.50	262.20
Payne	14.0	50.0	18.8	31.2	1013	1.4	1.5	2.9	7.80	358.00
Flower Pot	44.1	85.5	50.6	34.9	4133	4.3	2.3	6.6	8.41	546.00
Kirkland / Pawhuska	37.7	120.5	47.9	72.6	4118	5.6	3	8.6	8.65	1205.33
Ashport / Grainola	21.9	90.5	34.2	56.3	223	2.7	6.6	8.2	9.30	265.67
Heiden	50.7	229.0	51.5	177.5	335	12.1	2.3	14.4	8.93	300.00
Hollywood	26.4	145.5	40.3	105.2	247	3.1	0.9	4	7.65	190.67



**Table 4-4 - Compaction Properties of the Raw Test Soils**

Soil Name	Maximum Dry Unit Weight $\gamma_d$ (kN/m <sup>3</sup> )	OMC (%)
Devol	17.24	12.30
Anadarko	17.65	13.30
Payne	18.27	13.60
Flower Pot	16.73	20.90
Kirkland / Pawhuska	17.06	17.30
Ashport / Grainola	17.98	15.54
Heiden	15.50	24.20
Hollywood	16.73	20.60

**Table 4-5 - Unconfined Compression Strengths of the Raw Test Soils**

Soil Name	Average Maximum UCS (kPa)	Standard Deviation (kPa)
Devol	128.72	14.70
Anadarko	107.56	3.10
Payne	226.84	23.57
Flower Pot	291.00	24.63
Kirkland / Pawhuska	249.36	25.89
Ashport / Grainola	217.00	8.89
Heiden	312.52	25.62
Hollywood	365.25	9.25

## CHAPTER 5: THE EFFECTS OF CHEMICAL STABILIZERS ON SOIL PARAMETERS AND SOIL STRENGTH

### 5.1 Introduction to Atterberg Limits Testing

The minimum strength gain for a soil to be considered effectively stabilized, as specified in ASTM D 4609, is 345 kPa above the raw soil strength. However, it has been found that soils classified by Atterberg Limits in the same AASHTO classification group reached this minimum strength increase at varying additive stabilizer percentages, which makes design extremely difficult. As a result, it is necessary to attempt to find alternative soil parameters to the Atterberg Limits that may more accurately predict the stabilizer amount that would provide the adequate soil strength gain. Therefore, a number of different mineralogical and physico-chemical tests were performed on soil-additive mixtures and the results are presented in this chapter.

These tests were performed on soils with additive amounts that bracketed the estimated optimum additive amounts determined from UCS testing (results shown in Appendix A, Figure A-23 to Figure A-32 and Table A-9). The majority of the tests were performed at two curing times; 0 and 14 days. The 0-day samples were created by measuring an amount of soil and the appropriate additive amount based on the dry weight of soil and mixing the two immediately and adding water as needed for the particular test. The 14-day samples were obtained by air-drying and crushing the 14-day cured UCS samples over a #40 sieve and performing the various tests on the crushed soil. The two curing times were chosen to see if any significant changes in the soil properties occurred between 0 and 14 days of curing. From that study and a comparison to the recommendations in the Atterberg Limit-based OHD L-50 table (Table 1.1), it can be

seen that Atterberg Limits alone do not explain the optimum additive content. The following sections contain discussions on each of the different properties tested and their relation to the unconfined compression strengths.

The results that will be shown hereafter are all plotted with respect to the ordinate axis and the unconfined compression strength values are plotted with respect to the abscissa axis. The open-shape points in each plot are the raw soil values and the solid-shape points are the treated sample values. With all tested percentages for CKD and both fly ash stabilizers, the UCS increased linearly for the Devol A-4 soil, the A-6 soils, and the A-7-6 soils. The strengths of the remaining two A-4 soils peaked at the second-to-last percentage and decreased for the last percentage. With lime as the stabilizer for A-6 soils, Flower Pot strengths increased at each percentage, but the Ashport-Grainola strengths peaked with one percentage remaining and the Kirkland-Pawhuska strengths peaked with two percentages remaining and the strengths decreased after. Of the two A-7-6 soils, the Hollywood soil strengths peaked with one test percentage left and the Heiden soil peaked with two percentages left and their strengths decreased in each of the next percentages. These trends can all be seen in Figure A.23 to Figure A.32 in Appendix A. This relationship between increasing additive content and strength is important to keep in mind because the figures that follow only show the relationship between the soil parameter and the strength without distinguishing the actual additive content. However, as mentioned in most cases, an increase in the strength denotes an increase in the additive content. Also, there are only two plots in each figure with lime stabilization as the A-4 soils were not tested with lime.



The raw data values and the original plots of each property versus the specific additive percentages are shown in Appendix A: Atterberg Limits in Figure A.33 through Figure A.55 and Table A-10 to Table A-17, shrinkage results in Figure A.56 through Figure A.77 and Table A-18 to Table A-25, pH and conductivity data in Figure A.78 through Figure A.97 and Table A-26 to Table A-28, cation exchange capacity results in Figure A.98 through Figure A.107 and Table A-29 to Table A-31, and specific surface area data in Figure A.108 through Figure A.137 and Table A-32 to Table A-39.

In the following sections, each figure depicts A-4, A-6, and A-7-6 soils as three plots side by side from left to right, respectively. The empty shapes are the raw, untreated soil values and the black shapes are the treated soil values.

## **5.2 Atterberg Limit Results**

### **5.2.1 Introduction to Atterberg Results**

It has already been stated that Atterberg Limits alone do not explain the differences in strength gain of soils with identical AASHTO classifications. However, it is important to understand how these Atterberg Limits change with additive type and amount because it is quite likely that the Atterberg Limits will still play a role, along with other fundamental soil properties, in predicting the strength of stabilized soils.

Samples cured for 0 days were created by taking air-dried soil and mixing the stabilizer directly and then mixing in water and waiting two hours for the samples to mellow before testing. As described in the chapter introduction, tests labeled as 14-day cured were performed using the crushed soil from the UCT samples that cured for 14 days. After crushing past a #40 sieve, water was added to the soil and allowed to cure for two hours prior to testing the Atterberg Limits. The majority of samples were tested

promptly after 14 days, but due to schedule issues, some testing was delayed up to two days. In those instances, water was not added days earlier, but rather was added two hours prior to testing as with the other samples.

## 5.2.2 Liquid Limit Cured 0 Days

### 5.2.2.1 Liquid Limit with CKD

When plotted against the UCS, the CKD liquid limit failed to show consistent trends within a given soil group as shown in Figure 5.1.

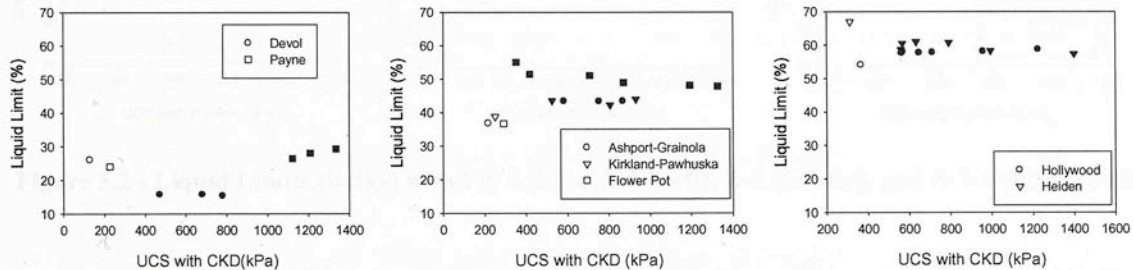


**Figure 5.1 - Liquid Limits (0-day) with CKD for A-4 (Left), A-6 (Center), and A-7-6 (Right) Soils**

In the A-4 soil group, the Anadarko soil was non-plastic and had no liquid limit, the Devol soil showed a decrease in the liquid limit with increasing strengths, and the Payne soil showed an increase in the liquid limit with increasing strengths. In the A-6 soil group, all three soils showed an initial jump in the liquid limit between the raw soil and the first tested CKD percentage. After that jump, the liquid limits for the Kirkland-Pawhuska and Ashport-Grainola Complexes decreased, but were nearly constant at increasing strengths. The Flower Pot soil showed a steady decrease in the liquid limit with increasing strengths. In the A-7-6 soil group, the liquid limit of the Hollywood soil showed a slight increase in the liquid limit as the strength increased, and the results from

the Heiden soil liquid limits steadily decreased and followed along the same trend line as the Hollywood soil liquid limits.

### 5.2.2.2 Liquid Limit with Fly Ash

The following figure shows the liquid limit trends found when the three soil classifications were treated with fly ash (Figure 5.2).

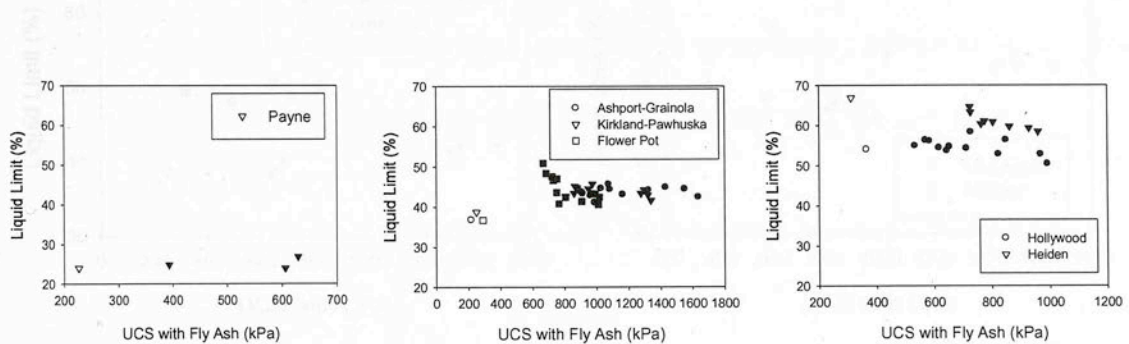


**Figure 5.2 - Liquid Limits (0-day) with Fly Ash for A-4 (Left), A-6 (Center), and A-7-6 (Right) Soils**

As seen in the A-4 soil plot, both the Devol and Anadarko soils became non-plastic when treated with fly ash stabilizers. The Payne soil showed a slight increase in the liquid limit with increasing strengths. In terms of the A-6 soils, all three showed the same trend, as with CKD stabilization, of an immediate jump in the liquid limit from the raw soil to the first additive percentage. All three soils then showed decreases in the liquid limit as the strength increased, signifying that perhaps this property may be of statistical importance for correlations predicting the strength gain. Along this line of thought, it is interesting to note that the Flower Pot soil only reaches about 60% of the strength of the Ashport-Grainola and Kirkland-Pawhuska soils with the same amount of additive. With the A-7-6 soils, both Hollywood and Heiden showed liquid limit decreases with increasing strengths, but along different parallel trend lines.



### 5.2.2.3 Liquid Limit with Lime

As shown in Figure 5.3, the liquid limit trends for stabilization with lime are not as well-defined as those from CKD and fly ash stabilization.

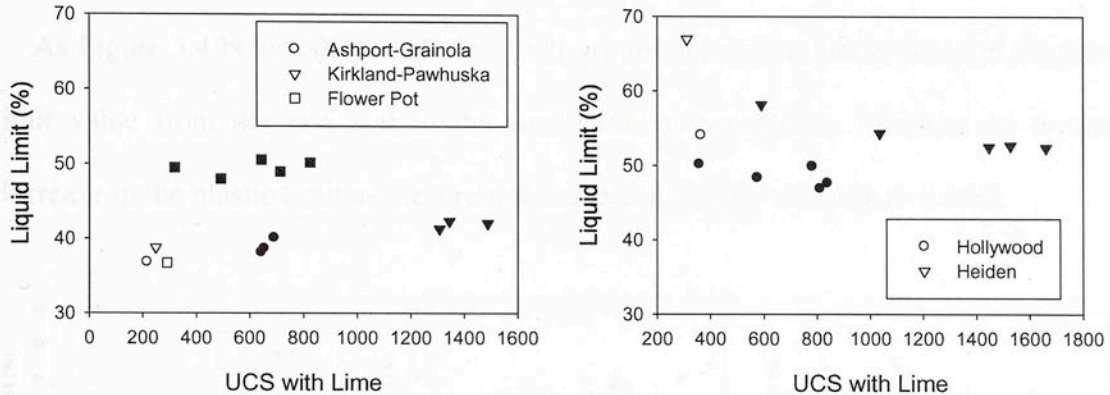


Figure 5.3 - Liquid Limits (0-day) with Lime for A-6 (Left) and A-7-6 (Right) Soils

As seen in the left plot, all three soils show an initial increase in the liquid limit upon adding lime. The Kirkland-Pawhuska Complex and the Flower Pot soil liquid limits remain fairly constant with increasing strengths, but the Ashport-Grainola Complex shows an increase in the liquid limit as the strength increases. The Kirkland-Pawhuska soil reaches more than double the strength of the Ashport-Grainola soil with the same amount of lime, yet while treated with CKD and fly ash their strengths are similar. With respect to the A-7-6 soils, both soils showed a decrease in the liquid limit as the strength increased, but as with the fly ash curves, the Heiden and Hollywood trend lines did not overlap and instead are close to parallel. It should also be noted that the Heiden clay achieved much higher strengths than the Hollywood soil with the same amount of lime stabilizer. When these two soils were stabilized with CKD and fly ash, they achieved

relatively similar strengths with the same additive amounts. This indicates that lime is more reactive with Heiden and the interaction should be investigated further.

### 5.2.3 Plastic Limit Cured 0 Days

#### 5.2.3.1 Plastic Limit with CKD

As Figure 5.4 below shows, all three soil groups showed an initial jump in the plastic limit value from the raw soil to the first additive percentage, followed by a steady decrease in the plastic limit as the strength increased, except with the A-4 soils.

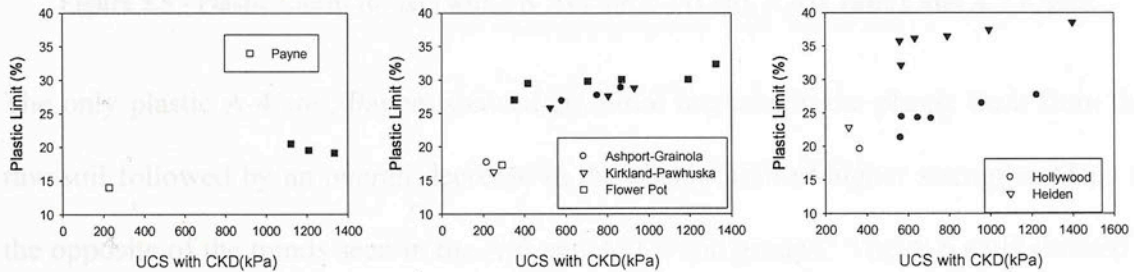


Figure 5.4 - Plastic Limit (0-day) with CKD for A-4 (Left), A-6 (Center), and A-7-6 (Right) Soils

In the A-4 group, both Devol and Anadarko were non-plastic soils and do not appear in the plot. However, the Payne soil plastic limit actually decreased as the strength increased. Both the A-6 and A-7-6 soils groups showed a consistent increase in the plastic limit as the strength increased. The values from the A-6 group seemed to fall along one trend line, but the A-7-6 soils seemed to have two separate trend lines. Also, in the A-7-6 group, both soils appeared to have samples with identical strengths and different plastic limit values. The data points in question had very similar strengths with the lower point in each instance being the result from the 6% CKD content and the point above the 7% CKD content. In this case, while the strength of the sample was not affected by increasing the additive content, the plastic limit was.

### 5.2.3.2 Plastic Limit with Fly Ash

Figure 5.5 presents the plastic limit after 0 days of curing plotted against the unconfined compression strength of the soil-additive mixture.

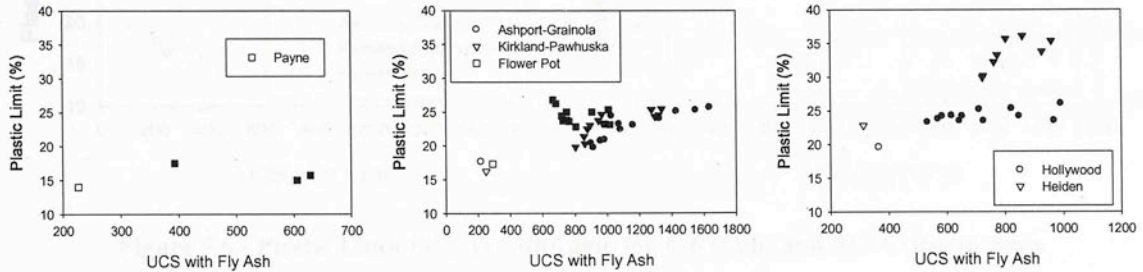


Figure 5.5 - Plastic Limits (0-day) with Fly Ash for A-4 (Left), A-6 (Center), and A-7-6 Soils

The only plastic A-4 soil, Payne, showed an initial increase in the plastic limit from the raw soil followed by an overall decrease in the plastic limit at higher strengths. This is the opposite of the trends seen in the A-6 and A-7-6 soil groups. The A-6 soils showed a steady increase in the plastic limit with the strength increase in a linear fashion. The A-7-6 soils also had steady increases in the plastic limit, but not along a single trend line. The Hollywood soil plastic limit increased along a relatively constant path while the Heiden clay plastic limit increased very quickly and then seemed to level off at higher stabilizer contents. While the strengths were very similar with the same additive content, the different material property behavior is interesting and merits further investigation.

### 5.2.3.3 Plastic Limit with Lime

As seen in Figure 5.6, both the A-6 and A-7-6 soils showed increased plastic limit values with increases in the unconfined strength, with the A-7-6 soils having a more consistent group trend response.



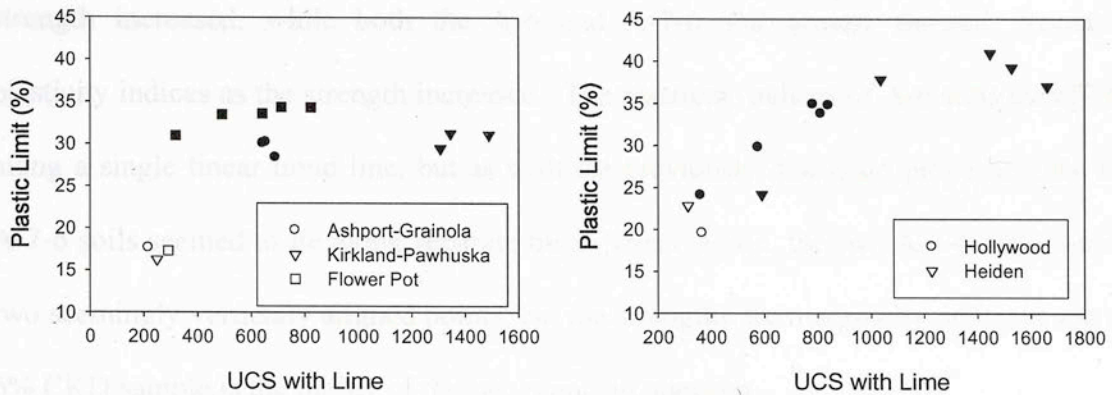


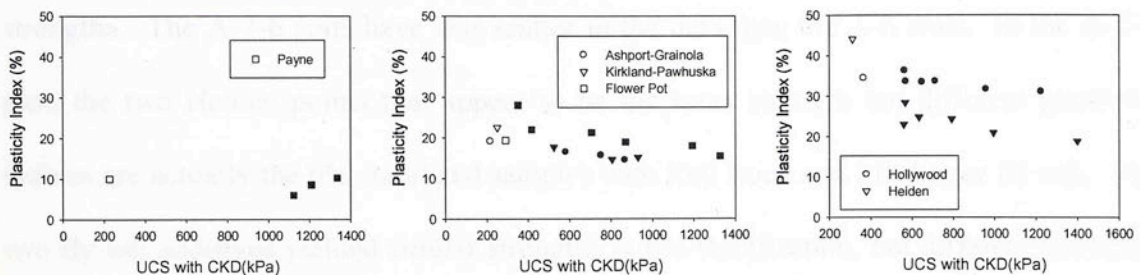
Figure 5.6 - Plastic Limit (0-day) with Lime for A-6 (Left) and A-7-6 (Right) Soils

The plastic limit of the raw A-6 soils increased rapidly with the addition of the lime, but then increased slowly with increasing strengths. The A-7-6 soils showed a more rapid increase in the plastic limit, and a greater range of increase than the A-6 soils (20% increase vs. 15% increase range). They also showed a more consistent increase, independent of the soil type, with increasing strengths.

## 5.2.4 Plasticity Index Cured 0 Days

### 5.2.4.1 Plasticity Index with CKD

The following figure shows the trends of the plasticity index vs. the unconfined strength after determining the plasticity index without curing the sample (Figure 5.7).



Payne, the only plastic A-4 soil tested, had an increase in the plasticity index as the strength increased, while both the A-6 and A-7-6 soil groups showed decreasing plasticity indices as the strength increased. The plasticity indices of A-6 soils mostly fell along a single linear trend line, but as with the previously discussed properties, the two A-7-6 soils seemed to lie along separate trend lines. Again, the two A-7-6 soils showed two seemingly vertically aligned points, but the strengths are marginally different and the 6% CKD sample is the higher of the two points in question.

#### 5.2.4.2 Plasticity Index with Fly Ash

As seen in Figure 5.8, all three soil groups show fairly linear trend lines in the plasticity index with increasing unconfined strengths.

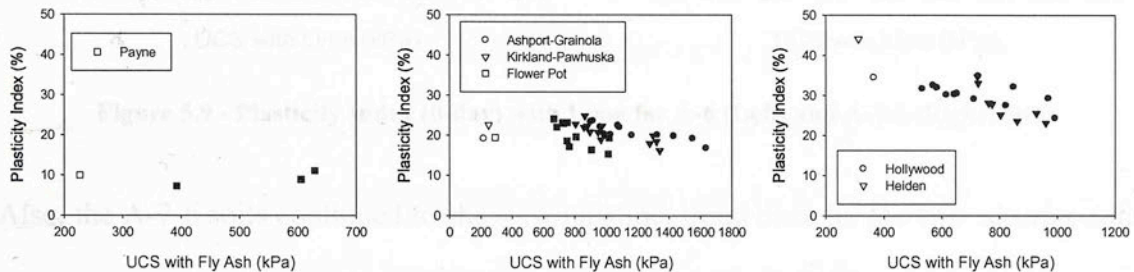


**Figure 5.8 - Plasticity Index (0-day) with Fly Ash for A-4 (Left), A-6 (Center), and A-7-6 Soils**

The Payne soil showed a slight increase in the plasticity index, but the general trends in both the A-6 and A-7-6 soil groups showed decreasing plasticity indices with increasing strengths. The A-7-6 soils have less scatter in the data than the A-6 soils. In the A-7-6 plot, the two Heiden points that appear to be the same strength but different plasticity indices are actually the 6% stabilized samples with Red Rock and Muskogee fly ash. The two fly ash additives yielded similar strengths at 6% stabilization, but different plasticity indices. This could be due to slight chemical differences between the two stabilizers.

### 5.2.4.3 Plasticity Index with Lime

Both the A-6 soils and the A-7-6 soils showed steady decreases in the plasticity index as the unconfined compression strength increased. Figure 5.9 shows that the A-7-6 soils reacted much stronger with the lime additive as seen by the steeper reduction in the plasticity index from the raw soil as compared to the reduction seen in the A-6 soils.

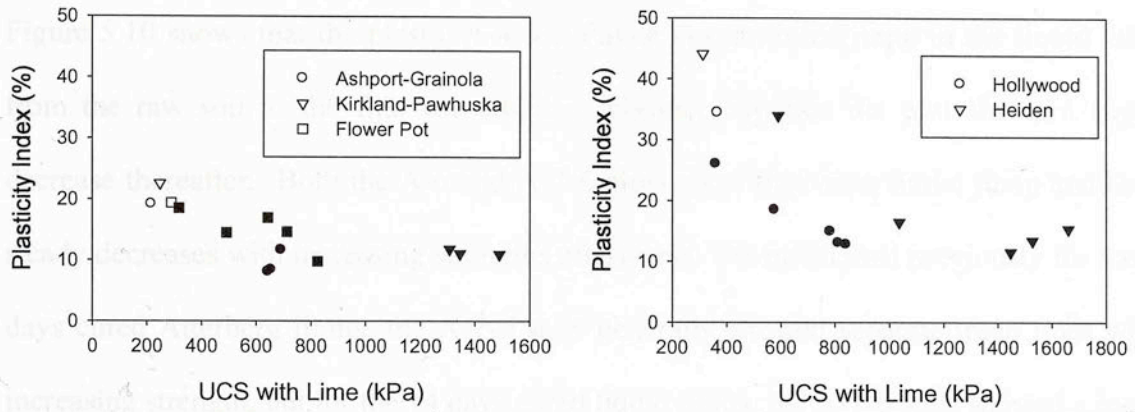


Figure 5.9 - Plasticity Index (0-day) with Lime for A-6 (Left) and A-7-6 (Right) Soils

Also, the A-7-6 soils continued to show two distinct trend lines for the two separate soils, as opposed to the fairly uniform response seen for the three A-6 soils.

### 5.2.5 Liquid Limit Cured 14 Days

#### 5.2.5.1 Liquid Limit with CKD

Figure 5.10 shows the results of the liquid limit tests performed after allowing the soil-additive mixtures to cure for 14 days.



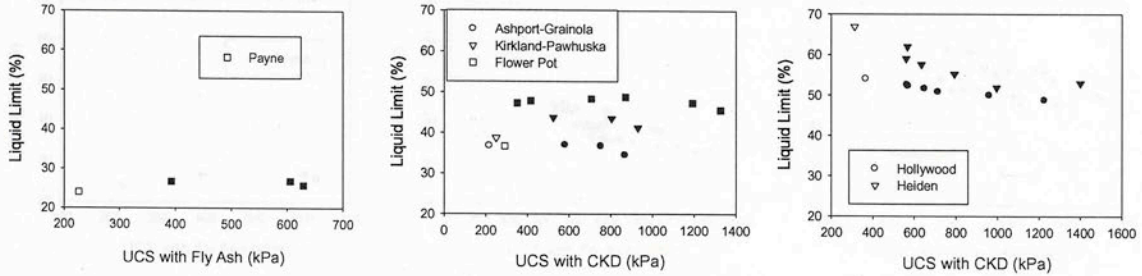


**Figure 5.10 - Liquid Limit (14-day) with CKD for A-4 (Left), A-6 (Center), and A-7-6 Soils**

Figure 5.10 shows that the plastic A-4 soil Payne has an initial jump in the liquid limit from the raw soil to the first soil-additive mixture, but then the plot shows a slight decrease thereafter. Both the A-6 and A-7-6 plots show that same initial jump and then steady decreases with increasing strengths afterwards. As mentioned previously for the 0 days cured Atterberg limits, the A-7-6 soils generally showed separate trend lines with increasing strength, but for the 14 days cured liquid limits, the A-7-6 soils showed a more consistent linear response and the A-6 soils appeared to have three distinct trend lines. In the A-7-6 plot, the two vertical points in the Heiden data are not errors, but in fact are the 6% (top point) and 7% CKD samples that showed a 3% drop in the liquid limit but only a very small strength change.

### 5.2.5.2 Liquid Limit with Fly Ash

As seen in Figure 5.11, the A-4 soil again showed the opposite trend as the A-6 and A-7-6 soils. The A-4 soil had a slight increase in the liquid limit with increasing strengths while both the A-6 and A-7-6 soils showed decreases.

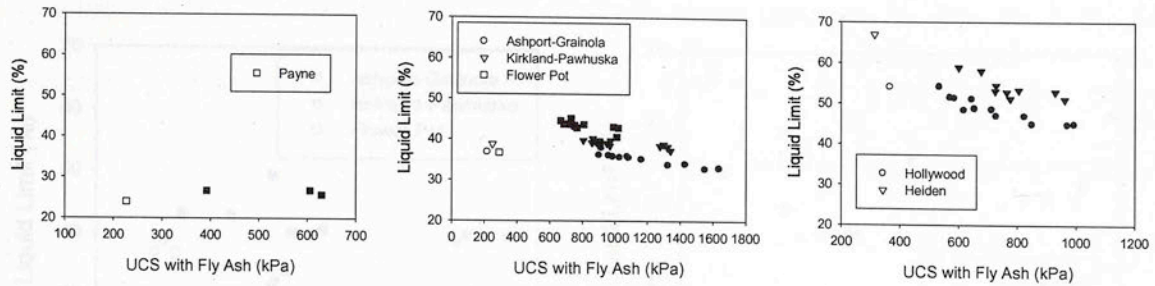


**Figure 5.11 - Liquid Limit (14-day) with Fly Ash for A-4 (Left), A-6 (Center), and A-7-6 (Right) Soils**

Both the A-6 soils and the three A-7-6 soils showed slightly separated linear trends with the respective soil groups, but they still showed general linear decreases as the unconfined compression strength increased. Also, the A-6 soils had an increase in the liquid limit once the first additive percentage was added, a trait not shared by the A-7-6 soils' liquid limits after 14 days of curing time. In the plots for the A-6 and A-7-6 soils, concerning the points that appear to have the same strengths but different liquid limits, it is important to remember that two fly ash stabilizers are combined in each curve and the resulting values may be similar.

### 5.2.5.3 Liquid Limit with Lime

Figure 5.12 shows the results of the 14 days cured liquid limit tests with lime plotted against the unconfined compression strengths. The left plot of the A-6 soils shows a fairly strong linear trend with the Flower Pot and Kirkland-Pawhuska soils. However, the results from the Ashport-Grainola soil fall slightly below this trend line.

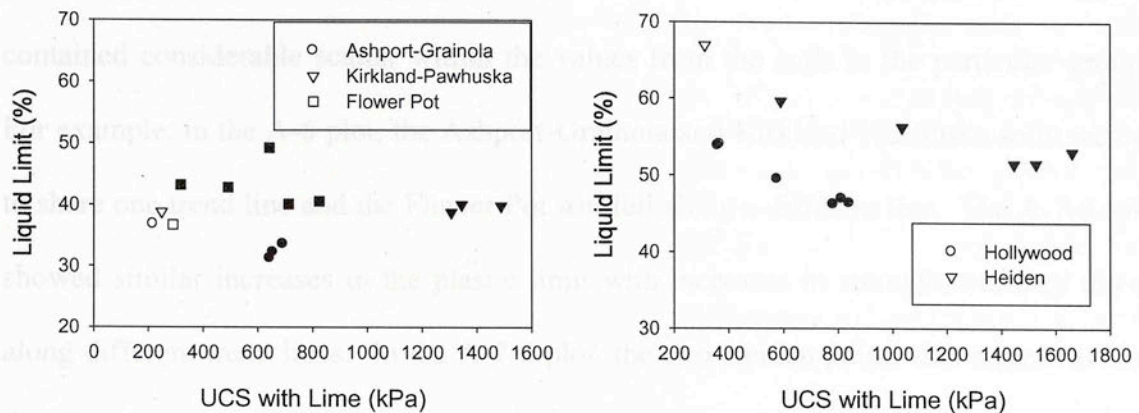


Figure 5.12 - Liquid Limit (14-day) with Lime for A-6 (Left) and A-7-6 (Right) Soils

The two A-7-6 soils show steady decreases in the liquid limit as the strength increases, but again these soils decrease along two parallel trends instead of generally along a single trend line.

## 5.2.6 Plastic Limit Cured 14 Days

### 5.2.6.1 Plastic Limit with CKD

As the following figure shows, all three soil groups had plastic limits that increased steadily from the values of the raw soils when CKD was used as the stabilizer (Figure 5.13). Again, only the Payne soil was plastic from the A-4 group and its plastic limit increased approximately 10% from the raw soil to the sample with the highest strength.

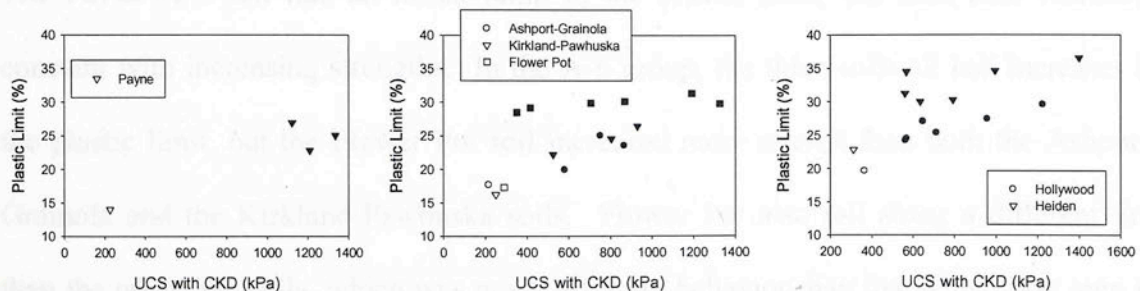


Figure 5.13 - Plastic Limit (14-day) with CKD for A-4 (Left), A-6 (Center), and A-7-6 (Right) Soils



Both the A-6 and A-7-6 soil groups had generally linear trends in the data, but both also contained considerable scatter within the values from the soils in the particular groups. For example, in the A-6 plot, the Ashport-Grainola and Kirkland-Pawhuska soils seemed to share one trend line and the Flower Pot soil fell along a different line. The A-7-6 soils showed similar increases in the plastic limit with increases in strength, but they did so along different trend lines. In the A-7-6 plot, the two Heiden points that appear to have the same strength are actually the 6% and 7% CKD samples where the 6% point has the higher plastic limit.

### 5.2.6.2 Plastic Limit with Fly Ash

All three soil groups showed increased plastic limits with increases in the strength due to the stabilizing effects of fly ash, as seen in Figure 5.14 below.

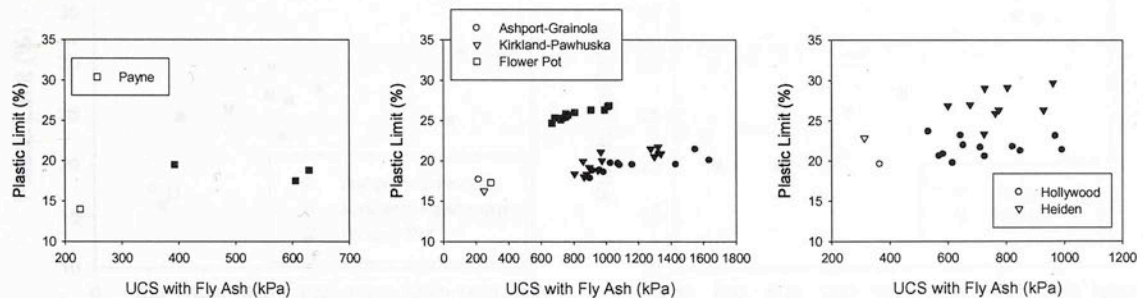


Figure 5.14 - Plastic Limit (14-day) with Fly Ash for A-4 (Left), A-6 (Center), and A-7-6 (Right) Soils

The Payne A-4 soil had an initial jump in the plastic limit, but then held relatively constant with increasing strengths. In the A-6 group, the three soils all had increases in the plastic limit, but the Flower Pot soil increased more overall than both the Ashport-Grainola and the Kirkland-Pawhuska soils. Flower Pot also fell along a different line than the other two soils, which was much different behavior than that which was seen in

the 0-day cured samples. It is unclear why the trends reversed after a 14-day curing period. Additionally, the A-6 soils achieved much higher strengths with the same additive and additive percentages than the A-7-6 soils. The A-7-6 soils had considerable scatter in the values from the two soils, with the Hollywood soil showing a more linear trend. Both, however, increased from the raw soil values. In the A-6 and A-7-6, there are two types of fly ash combined in the plot which accounts for points that may share similar strengths but different plastic limits.

### 5.2.6.3 Plastic Limit with Lime

Both soil groups showed consistent linear increases in the plastic limit when lime was added as a stabilizer, as seen in Figure 5.15.

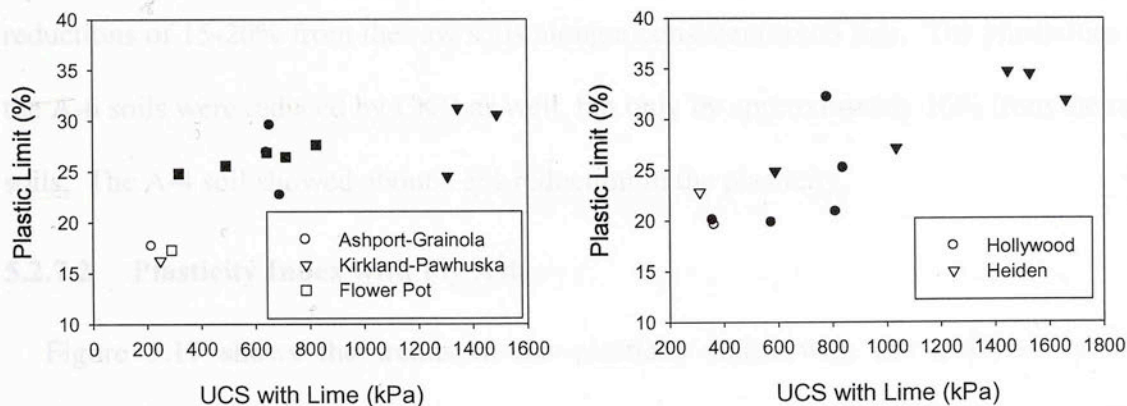


Figure 5.15 - Plastic Limit (14-day) with Lime for A-6 (Left) and A-7-6 (Right) Soils

While there is some scatter in the data in both plots, the A-6 group in the left plot showed more variability among the soils, especially with the Ashport-Grainola and Kirkland-Pawhuska soils. Concerning the Hollywood soil curve, the point with the highest plastic limit is the 5% lime sample, and the point with the next lower plastic limit and the highest strength is the 4% lime stabilized sample.

## 5.2.7 Plasticity Index Cured 14 Days

### 5.2.7.1 Plasticity Index with CKD

As Figure 5.16 shows, all three soil groups showed reduced plasticity indices due to the addition of CKD.

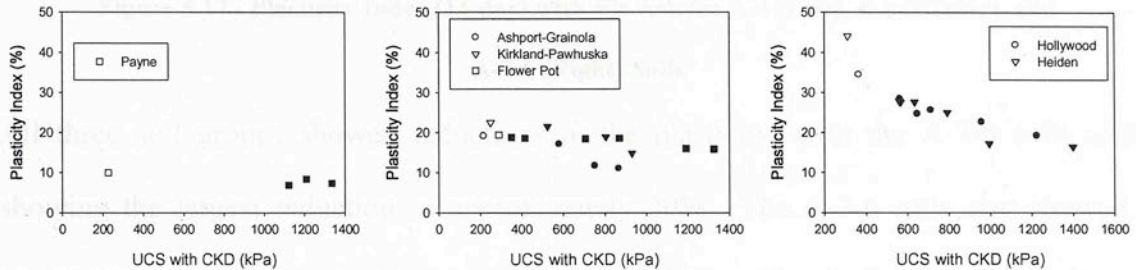


Figure 5.16 - Plasticity Index (14-day) with CKD for A-4 (Left), A-6 (Center), and A-7-6 (Right) Soils

The A-7-6 soils were the most responsive to the CKD stabilizer, showing plasticity reductions of 15-20% from the raw soils along a consistent trend line. The plasticities of the A-6 soils were reduced by CKD as well, but only by approximately 10% from the raw soils. The A-4 soil showed about a 3% reduction in the plasticity.

### 5.2.7.2 Plasticity Index with Fly Ash

Figure 5.17 shows the trends in the plasticity index with the additive fly ash, combining the two sources from Red Rock and Muskogee into the single plots. This creates the illusion that a soil may have multiple values of the plasticity index at one strength value, but that is not the case.



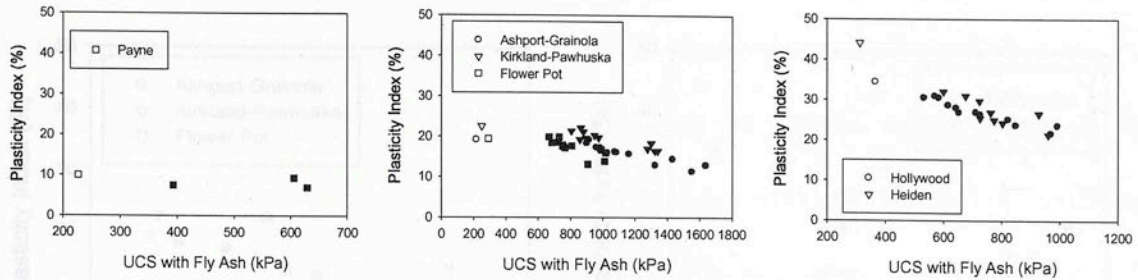


**Figure 5.17 - Plasticity Index (14-day) with Fly Ash for A-4 (Left), A-6 (Center), and A-7-6 (Right) Soils**

All three soil groups showed reductions in the plasticity, with the A-7-6 soils again showing the largest reduction of approximately 20%. The A-7-6 soils also showed a fairly consistent response along a single trend line. The A-6 soils again showed approximately a 10% overall reduction in the plasticity index from the raw soil and also had a consistent trend response from all three soils. The Payne (A-4) soil only showed a slight decrease in the plasticity index with increasing strengths.

### 5.2.7.3 Plasticity Index with Lime

All five soils tested with lime showed reduced plasticity indices as the unconfined compression strength increased (Figure 5.18). The Flower Pot and Kirkland-Pawhuska soils (A-6) fell along one trend line, but the Ashport-Grainola soil did not exhibit this same response. In the A-7-6 group, both soils initially showed the same linear response, but the Hollywood soil fell from the trend line as it reached its peak strength. The plasticity index continually decreases for the two A-7-6 soils, but the fact that the soils reach a peak strength and then have decreased strengths causes the curves to “bend” toward the left.

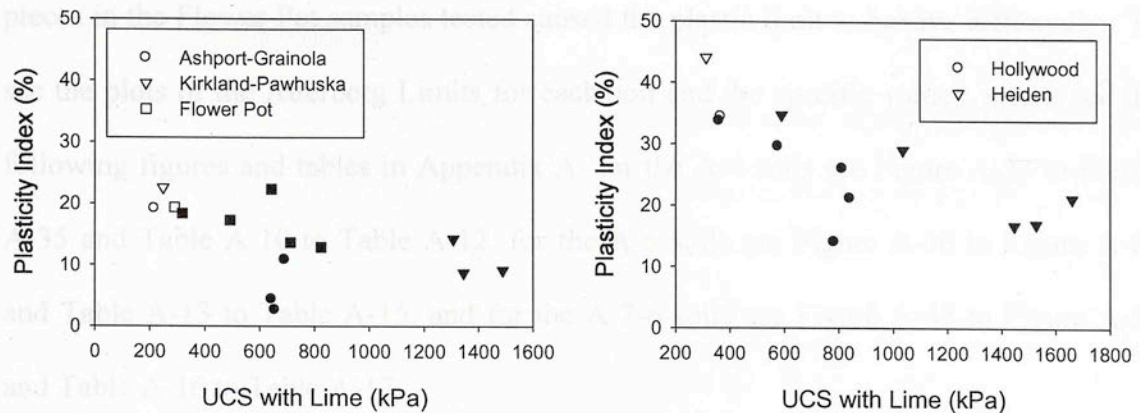


Figure 5.18 - Plasticity Index (14-day) with Lime for A-6 (Left) and A-7-6 (Right) Soils

### 5.2.8 Summary of Atterberg Limits

In general, adding additives to the different soils caused reductions in the liquid limits, increases in the plastic limits, and reductions in the plasticity indices. The additives caused approximately 5-10% changes in the three properties in the trends just mentioned. In terms of the soil groups, only the A-6 and A-7-6 groups can truly be compared as only one of the three A-4 soils (Payne) was consistently plastic and found to have any Atterberg Limits. Of the other two groups, the A-7-6 soils generally did not show a consistent linear trend whereas the three A-6 soils typically could be combined as a single line. The difference in curing time between 0 and 14 days did not change the general trends of the properties, but it did cause a slight reduction in the liquid limits and plasticity indices and a slight increase in the plastic limits. The only major difference between the cured and uncured results pertained to the Flower Pot soil when treated with fly ash. The 0-day plastic limit decreased as the strength increased (Figure 5.5), but the 14-day plastic limit values increased as the strength increased (Figure 5.14). As this was the only soil to exhibit this trend, it could be a result of human error in testing the plastic

limit. Another possible explanation could be the varying amount of gypsum (sulfate) pieces in the Flower Pot samples tested caused the plastic limit to behave differently. To see the plots of the Atterberg Limits for each soil and the specific values, please see the following figures and tables in Appendix A: for the A-4 soils see Figure A-33 to Figure A-35 and Table A-10 to Table A-12, for the A-6 soils see Figure A-36 to Figure A-47 and Table A-13 to Table A-15, and for the A-7-6 soils see Figure A-48 to Figure A-55 and Table A-16 to Table A-17.

### **5.3 Shrinkage Results**

#### **5.3.1 Introduction to Shrinkage Testing**

The linear shrinkage and shrinkage limit values are very easy to determine and may possibly give a better indication of a particular soil response to stabilizers and, therefore, were tested for each soil at each stabilization amount. The testing of the shrinkage properties took place simultaneously with the Atterberg Limit tests. The soil for Atterberg Limit testing was mixed to a blow count of approximately  $25 \pm 1$  blows and the soil was then placed in the linear shrinkage mold for testing. As such, the 0- and 14-day curing designations carry the same meaning here as with the Atterberg Limits.

For soils tested with CKD and fly ash, in the A-4 soil plot only a single point appears for each of the Anadarko and Payne soils and these points represent the raw soil shrinkage values. This is due to the fact that these soils were tested at Oklahoma State University and they were unable to supply additional test results or additional soil for testing at the University of Oklahoma.



### 5.3.2 Linear Shrinkage Cured 0 Days

#### 5.3.2.1 Linear Shrinkage with CKD

As seen in Figure 5.19 below, all three soil groups showed strong linear correlations between the percentage of linear shrinkage and the unconfined compression strengths.

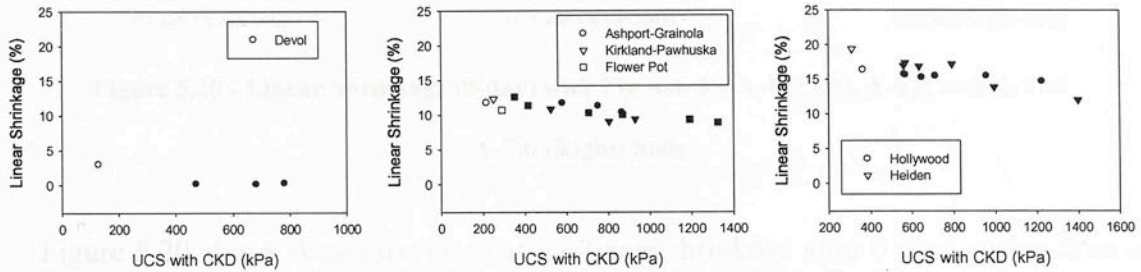


**Figure 5.19 - Linear Shrinkage (0-day) with CKD for A-4 (Left), A-6 (Center), and A-7-6 (Right) Soils**

In the A-4 soil group, only the Devol soil was tested for the linear shrinkage with CKD added. It had very small values for the linear shrinkage, but did show a decreasing trend in the shrinkage values. Both the A-6 and A-7-6 soils showed a consistent linear reduction in the linear shrinkage as the strength increased, with the A-6 soils showing an approximate maximum reduction of 5% and the A-7-6 soils being reduced about 5-10%.

### 5.3.2.2 Linear Shrinkage with Fly Ash

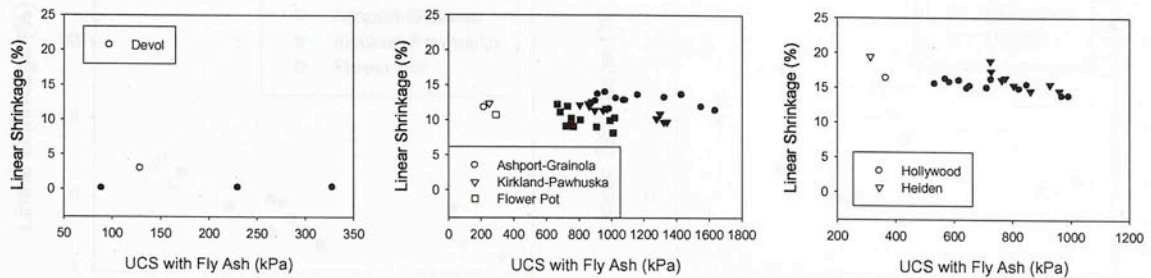


**Figure 5.20 - Linear Shrinkage (0-day) with Fly Ash for A-4 (Left), A-6 (Center), and A-7-6 (Right) Soils**

Figure 5.20 above shows the plots of the linear shrinkage after 0 days curing time vs. the unconfined strength. The Devol (A-4) soil had an initial jump in the shrinkage when fly ash was added, but the shrinkage was lessened as the strength increased. The three A-6 soils did not show a uniform trend across the group, but each soil exhibited a decrease in the linear shrinkage as the strength increased. In contrast, the A-7-6 soils showed a consistent decrease in the shrinkage amount with increasing strength values. The two points that seem vertical on the Heiden soil curve are the results of combining the data from the two sources of fly ash into one plot because the two additives yielded similar strengths and similar shrinkage values.

### 5.3.2.3 Linear Shrinkage with Lime

As seen in Figure 5.21, the linear shrinkage of the A-6 and A-7-6 soil groups decreased as the strength of the soil-additive mixtures increased.

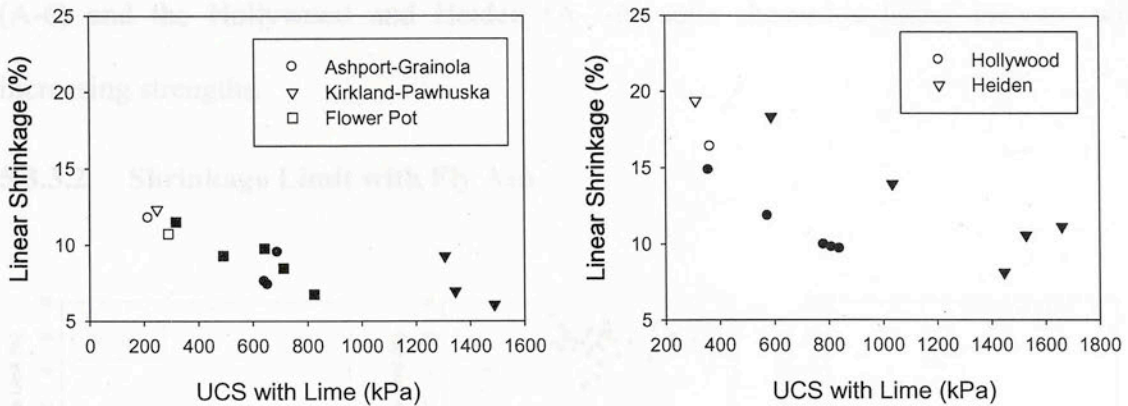


Figure 5.21 - Linear Shrinkage (0-day) with Lime for A-6 (Left) and A-7-6 (Right) Soils

In the A-6 soil group, the three soils decreased along a fairly uniform trend line, but the two A-7-6 soils did not share the same trend. The Hollywood soil seemed to show an exponential decrease as the strength increased, and the Heiden soil decreased linearly.

### 5.3.3 Shrinkage Limit Cured 0 Days

#### 5.3.3.1 Shrinkage Limit with CKD

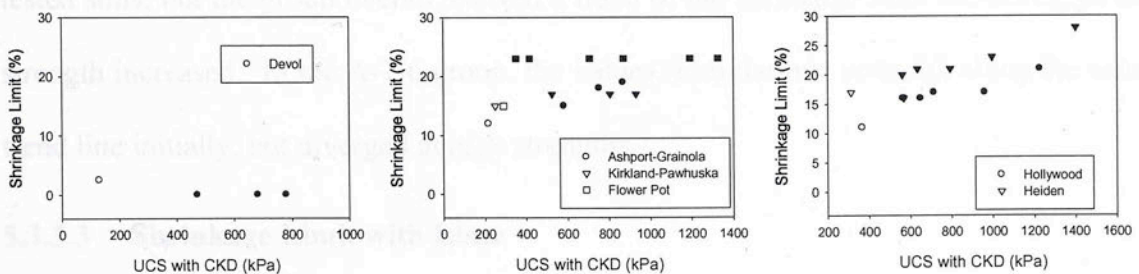


Figure 5.22 - Shrinkage Limit (0-day) with CKD for A-4 (Left), A-6 (Center), and A-7-6 (Right) Soils

As seen in Figure 5.22, the Devol (A-4) soil did not show a measurable shrinkage limit once CKD was added. In both the A-6 and A-7-6 soil groups, however, the shrinkage limit increased as the strength increased. The shrinkage limit of the Flower Pot



soil did not change with the strength, but the Ashport-Grainola and Kirkland-Pawhuska (A-6) and the Hollywood and Heiden (A-7-6) soils showed a linear increase with increasing strengths.

### 5.3.3.2 Shrinkage Limit with Fly Ash

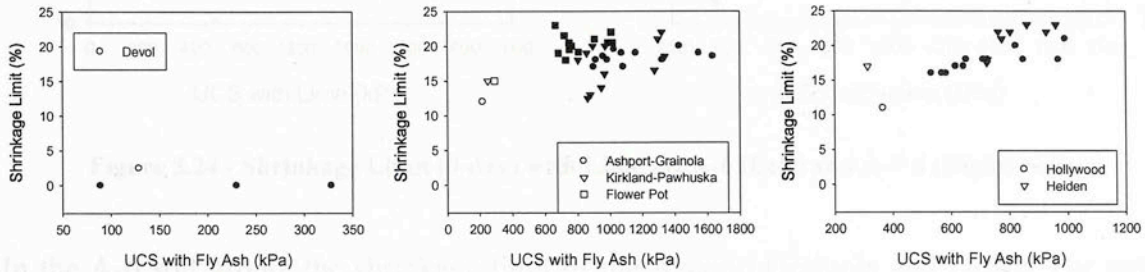


**Figure 5.23 - Shrinkage Limit (0-day) with Fly Ash for A-4 (Left), A-6 (Center), and A-7-6 (Right) Soils**

Figure 5.23 shows the shrinkage limit of the three soil groups treated with fly ash plotted vs. the unconfined compression strengths. The Devol soil again had no measureable shrinkage limit. The A-6 soils showed considerable scatter among the three tested soils, but the group overall showed a trend of the shrinkage limit increasing as the strength increased. In the A-7-6 group, the values from the two soils fell along the same trend line initially, but diverged at high strengths.

### 5.3.3.3 Shrinkage Limit with Lime

Figure 5.24 below shows that the shrinkage limit increases with the unconfined compression strength when the soils were treated with lime as an additive.

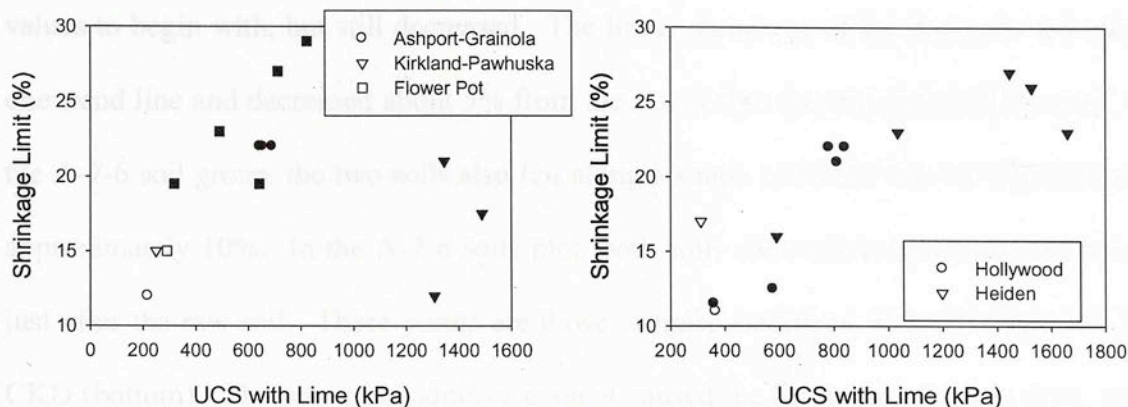


Figure 5.24 - Shrinkage Limit (0-day) with Lime for A-6 (Left) and A-7-6 (Right) Soils

In the A-6 soil group, the shrinkage limit of the Ashport-Grainola and Flower Pot soils increased rapidly as the strength increased, but the Kirkland-Pawhuska soil did not show any trend. The two A-7-6 soils showed shrinkage limits that increased linearly along the same trend line.

### 5.3.4 Linear Shrinkage Cured 14 Days

#### 5.3.4.1 Linear Shrinkage with CKD

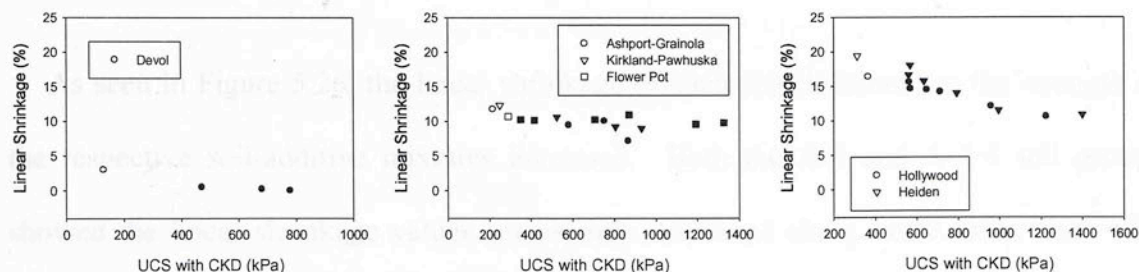
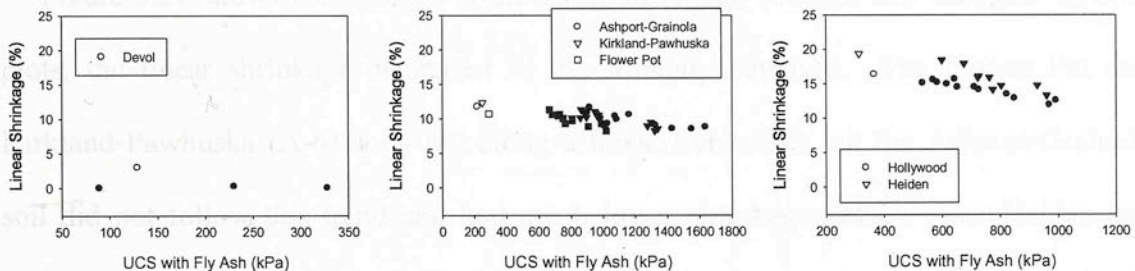


Figure 5.25 - Linear Shrinkage (14-day) with CKD for A-4 (Left), A-6 (Center), and A-7-6 (Right) Soils

As Figure 5.25 shows, the 14 days cured linear shrinkage of the three soil groups decreased as the strength values increased. This trend matches the trend seen from the 0-

day cured test results (Figure 5.19). The Devol (A-4) soil had very small shrinkage values to begin with, but still decreased. The linear shrinkage of the A-6 soils fell along one trend line and decreased about 5% from the raw soil to the strongest soil mixture. In the A-7-6 soil group, the two soils also fell along a single trend line but the decrease was approximately 10%. In the A-7-6 soils plot, both soils showed vertically aligned points just after the raw soil. These points are those samples stabilized with 6% (top) and 7% CKD (bottom). The increased additive content caused the linear shrinkage to drop, even though the samples had very similar strengths.

### 5.3.4.2 Linear Shrinkage with Fly Ash



**Figure 5.26 - Linear Shrinkage (14-day) with Fly Ash for A-4 (Left), A-6 (Center), and A-7-6 (Right) Soils**

As seen in Figure 5.26, the linear shrinkage of each soil decreased as the strength of the respective soil-additive mixtures increased. Both the A-6 and A-7-6 soil groups showed the linear shrinkage values consistently decreased along linear trend lines with the A-7-6 soils showing more shrinkage than the A-6 soils. Any points in the curves that may show different shrinkages at very close strengths can be attributed to the fact that data from the two sources of fly ash were combined to form these plots.



### 5.3.4.3 Linear Shrinkage with Lime

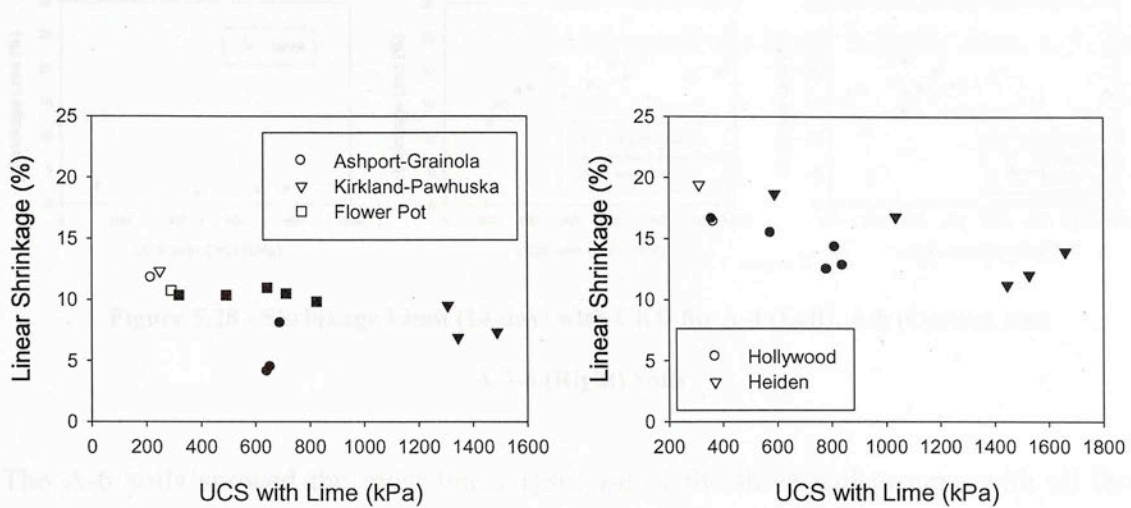


Figure 5.27 - Linear Shrinkage (14-day) with Lime for A-6 (Left) and A-7-6 (Right) Soils

Figure 5.27 shows the changes in the linear shrinkage with the soil strength. In both plots, the linear shrinkage decreased as the strength increased. The Flower Pot and Kirkland-Pawhuska (A-6) soils fell along a linear trend line, but the Ashport-Grainola soil did not follow this trend and had much lower shrinkage values. The Heiden and Hollywood (A-7-6) soils both decreased linearly, but seemed to have parallel trend lines. While the two A-7-6 soils show steadily decreasing linear shrinkages, the curves “bend” back to the left because the soils reached peak strengths before the final tested additive percentage and the strengths dropped after the peak.

### 5.3.5 Shrinkage Limit Cured 14 Days

#### 5.3.5.1 Shrinkage Limit with CKD

The shrinkage limit generally increases as the strength of the soil-additive mixtures increase (Figure 5.28).

### 5.3.5.3 Shrinkage Limit with Limer

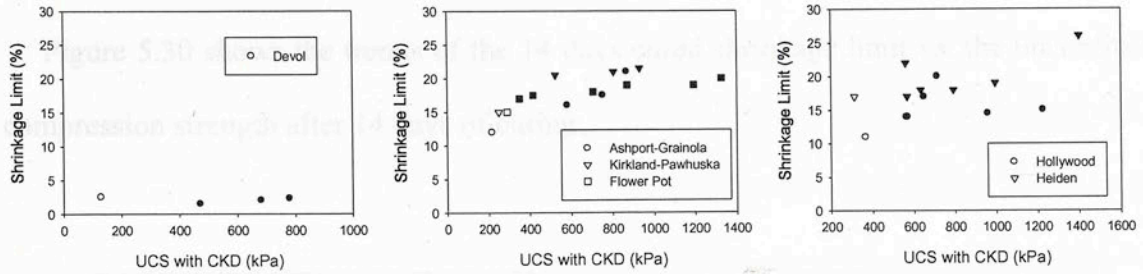


**Figure 5.28 - Shrinkage Limit (14-day) with CKD for A-4 (Left), A-6 (Center), and A-7-6 (Right) Soils**

The A-6 soils showed the most linear response of the three soil groups, with all three soils having similar shrinkage limit trends. The two A-7-6 soils increased, as well, but the data points were scattered and do not fit along any noticeable trend line.

### 5.3.5.2 Shrinkage Limit with Fly Ash

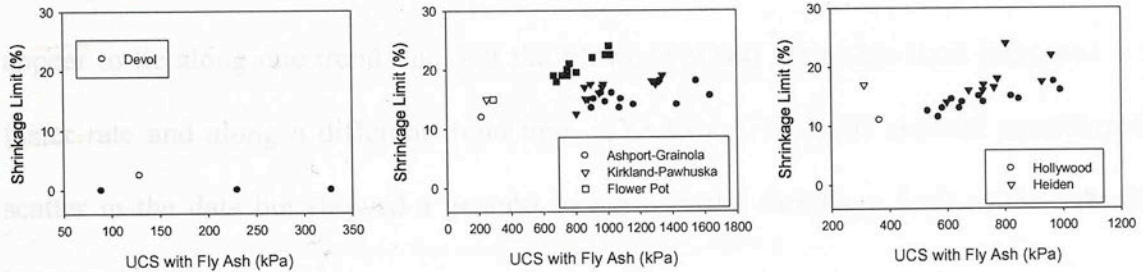


**Figure 5.29 - Shrinkage Limit (14-day) with Fly Ash for A-4 (Left), A-6 (Center), and A-7-6 (Right) Soils**

Figure 5.29 shows that the shrinkage limits of all three soil groups increased as the strength increased. The shrinkage limits of the three A-6 soils increased at three different rates, instead of a consistent linear response as seen with CKD stabilization. The A-7-6 soils did show a fairly uniform linear response between the two soils, with some scatter occurring at high strength values.

### 5.3.5.3 Shrinkage Limit with Lime

Figure 5.30 shows the trends of the 14 days cured shrinkage limit vs. the unconfined compression strength after 14 days of curing.

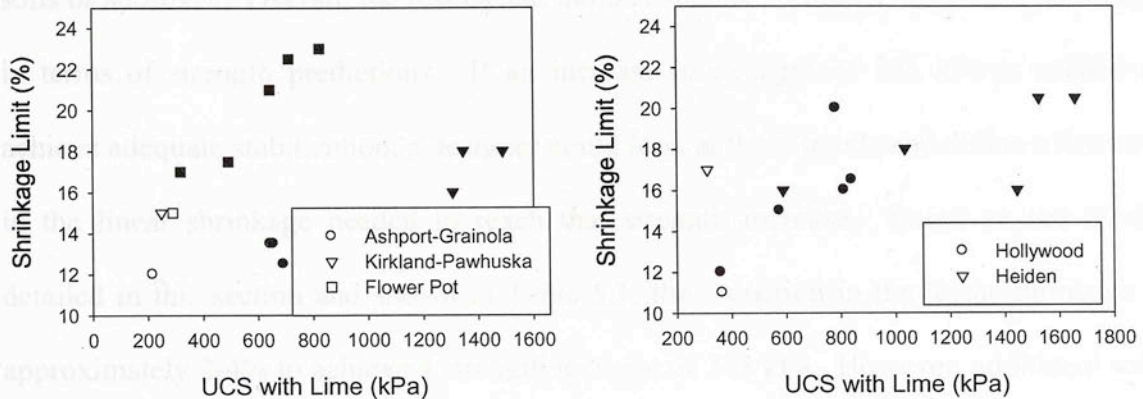


Figure 5.30 - Shrinkage Limit (14-day) with Lime for A-6 (Left) and A-7-6 (Right) Soils

In the plot of the three A-6 soils, the Ashport-Grainola and the Kirkland-Pawhuska soils appear to lie along one trend line, but the Flower Pot soil shrinkage limit increased at a faster rate and along a different trend line. The two A-7-6 soils showed considerable scatter in the data but showed a general increase in the shrinkage limit as the strength increased.

### 5.3.6 Summary of Shrinkage

Adding the different chemical stabilizers to the test soils caused the linear shrinkage to decrease and the shrinkage limit to increase. From the 0-day to the 14-day tests, the linear shrinkage was found to be approximately 2-3% lower and the shrinkage limit was typically 0-5% lower after 14 days of curing time. Lime was generally the most effective stabilizer in reducing the amount of shrinkage each soil experienced. Only the Devol soil was tested for the shrinkage properties from the A-4 group, so group comparisons were



not made. The linear shrinkage curves from both 0-day and 14-day curing times were the most consistent combined trends with CKD for the A-6 and A-7-6 soils, followed next by the fly ash trend. The lime results were rather scattered and did not show good combined trends. Also, the shrinkage limit results did not show good combined trends with any soils or additives. Overall, the results and trends from the shrinkage tests were promising in terms of strength predictions. If an increase in strength of 345 kPa is needed to achieve adequate stabilization, a designer could look at these trends and define a decrease in the linear shrinkage needed to reach that strength increase. Based on the results detailed in this section and shown in Table 5.1, the reduction in the linear shrinkage is approximately 2-4% to achieve a strength increase of 345 kPa. However, additional soils would need to be added to this database to further prove this conclusion.

**Table 5-1 - Table of Linear Shrinkage Decreases over 345 kPa Strength Gain**

	A-6 Soils				A-7-6 Soils		
Curing Time	CKD	Fly Ash	Lime	Curing Time	CKD	Fly Ash	Lime
0 days	3%	2%	4%	0 days	3%	3%	4%
14 days	3%	3%	2%	14 days	4%	4%	3%

To see the results of each shrinkage test plotted versus the additive content, please reference in Appendix A: Figure A-56 to Figure A-57 and Table A-18 to Table A-20 for the A-4 soils, Figure A-58 to Figure A-69 and Table A-21 to Table A-23 for the A-6 soils, and Figure A-70 to Figure A-77 and Table A-24 to Table A-25 for the A-7-6 soils.

## 5.4 pH Results

### 5.4.1 Introduction to pH Testing

As was mentioned in the literature review, pH-based stabilization is currently in use but only lime stabilization officially has an ASTM standard (ASTM D 6276). The

standard states that once the soil-additive pH reaches 12.4, the pH of pure lime, the mixture is adequately stabilized. Unfortunately, no such standard exists for stabilization with cement kiln dust or fly ash. Research has been done on these stabilizers to see if a similar threshold exists, but as these stabilizers are industrial byproducts, it is difficult to determine a consistent pH threshold level. One of the more notable studies was done by Miller and Azad (2000). In their study, they determined the pH of CKD was approximately 12.3 and their soil-additive mixture reached this pH at 15% CKD, which also corresponded to the additive percentage at which the soil was adequately stabilized. In this study, all soils were tested with each stabilizer to determine if similar trends exist across a wider soil database.

#### 5.4.2 pH with CKD

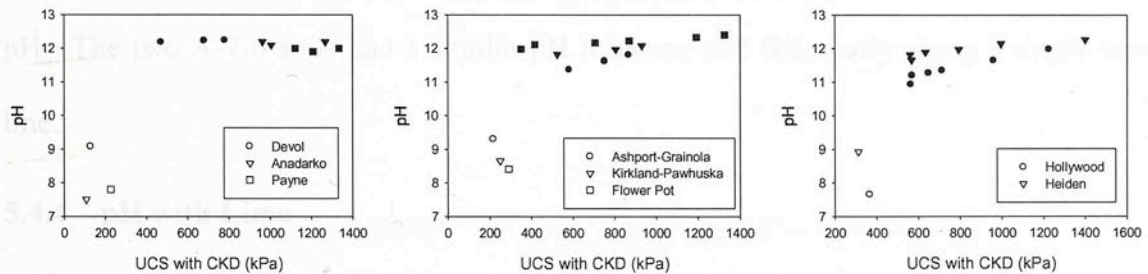


Figure 5.31 - pH Results with CKD for A-4 (Left), A-6 (Center), and A-7-6 (Right) Soils

All three soil groups showed bi-linear correlations between the strength and the pH, as seen in Figure 5.31. All eight soils showed an initial jump in the pH to the first soil-additive mixture. Each soil reached a plateau in the pH value at approximately 12.2 when plotted versus the available strength data.

### 5.4.3 pH with Fly Ash

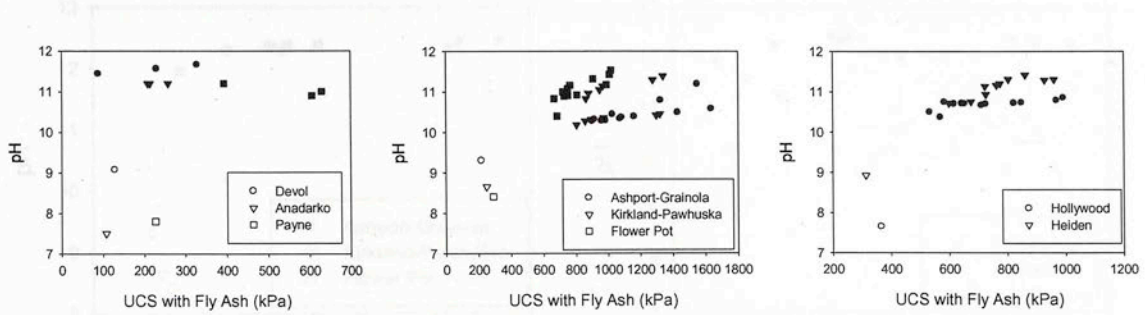


Figure 5.32 - pH Results with Fly Ash for A-4 (Left), A-6 (Center), and A-7-6 (Right) Soils

As shown in Figure 5.32, the pH response of the test soils was much more varied with fly ash than with CKD. The A-4 soils seemed to have a bi-linear response in the pH with a maximum value between 11.2 and 11.5. The three A-6 soils showed three different trend lines, with the Flower Pot reaching the highest pH after starting at the lowest pH and the Ashport-Grainola soil had the lowest stabilized pH after starting at the highest raw soil pH. The two A-7-6 soils had a similar pH response and fell nearly along a single trend line.

### 5.4.4 Summary of pH

#### 5.4.4 pH with Lime

Figure 5.33 shows the pH test results with lime as the stabilizing chemical.

When treated with the same additive, CKD for example, even the different soils within a single group reacted differently. The same was true for the fly ash series as there were clear differences between the Red Fork and Mustangs fly ash stabilized soils and the pH values with fly ash never exceeded 10.5. In fact, only the soils treated with fly ash reacted the same way. As a rule, the pH values for the soils treated with lime were higher than the soil and ash values. For example, Figure 5.34. For example, the A-6 soils stabilized with fly ash have a pH of 10.5 and 10.6 for the same additive percentage and



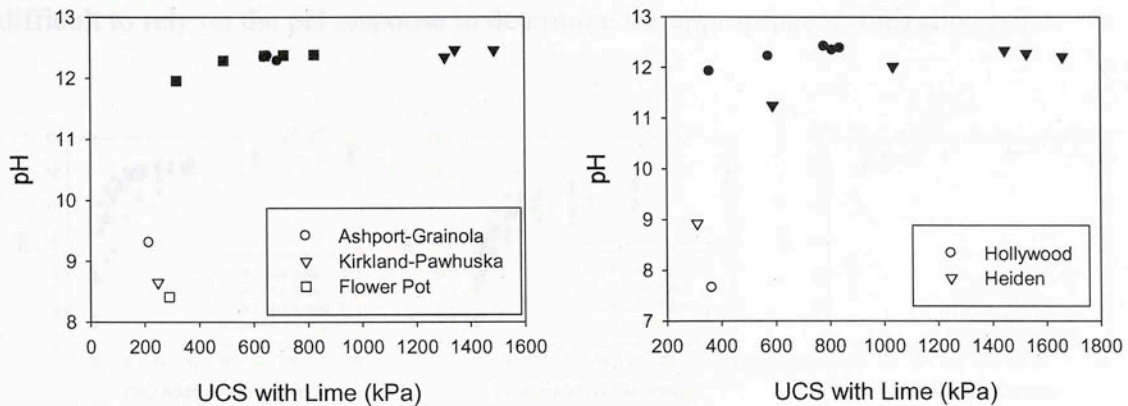


**Figure 5.33 - pH Results with Lime for A-6 (Left) and A-7-6 (Right) Soils**

Both soil groups show bi-linear trends in the pH response of the different soils with lime as the stabilizing additive. The soils reached a plateau in the pH values at approximately 12.4, the pH of raw lime, and the response with lime was much steeper than those from either CKD or fly ash. In the A-7-6 soil group, the Hollywood soil pH increased faster than that of the Heiden soil.

#### 5.4.5 Summary of pH

Each soil group reacted slightly differently with the addition of each stabilizer, but in general, the A-7-6 soils showed the most rapid increase in the pH to the maximum value. When treated with the same additive, CKD for example, even the different soils within a single group reacted differently. The same was true in the fly ash section as there were clear differences between the Red Rock and Muskogee fly ash stabilized soils and the pH values with fly ash never leveled out. In fact, only the soils treated with lime reacted the same way. Aside from lime stabilization, there is no consistent trend within a particular soil and additive type, as shown in Figure 5.34. For example, the A-6 soils stabilized with fly ash have a pH difference of nearly 1.0 for the same additive percentage and

never reach a consistent maximum value, as can be seen with lime. This would make it difficult to rely on the pH response to determine the appropriate stabilization point.

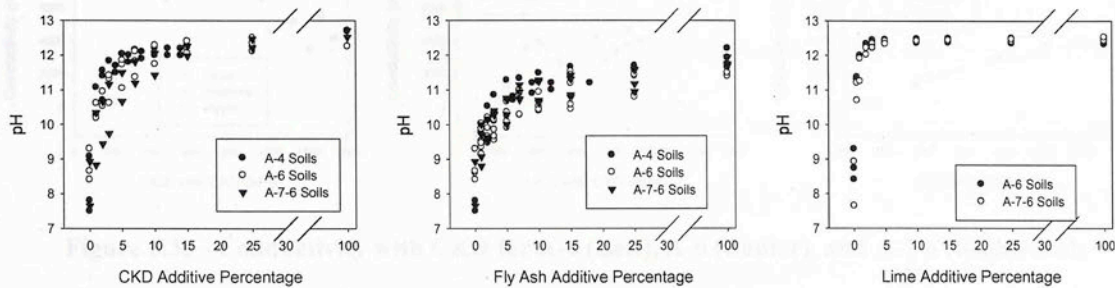


**Figure 5.34 - Combined pH Curves for Different Additives**

Please see the following figures and tables in Appendix A for the plots of pH versus the additive percentage and the actual pH values: Figure A-78 to Figure A-79 and Table A-26 for the A-4 soils, Figure A-82 to Figure A-85 and Table A-27 for the A-6 soils, and Figure A-90 to Figure A-93 and Table A-28 for the A-7-6 soils.

## 5.5 Conductivity Results

### 5.5.1 Introduction to Conductivity Testing

Unlike the Atterberg Limits or the shrinkage properties, it was unknown whether or not the electrical conductivity of the soil-additive mixtures would be relevant to predicting the strength gain of stabilized soils. The conductivity was tested with a digital measuring device very similar to the one used for determining the pH. The same samples used for the pH tests were reused for the conductivity tests as the digital meters did not alter the soils. Due to the ease of testing the conductivity, it was included in the parameter database.

### 5.5.2 Conductivity with CKD

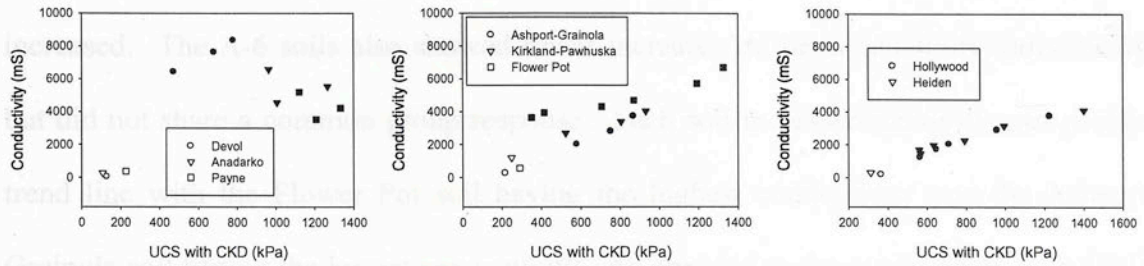


Figure 5.35 - Conductivity with CKD for A-4 (Left), A-6 (Center), and A-7-6 (Right) Soils

As seen in Figure 5.35, the A-7-6 soils showed the strongest linear correlation between the conductivity and the unconfined compression strength. The values from the two soils fell closely along one trend line. The A-6 soils also showed a solid linear correlation, with the Ashport-Grainola and Kirkland-Pawhuska soils having a near-identical response and the Flower Pot soil having a higher conductivity. The trend line from the three A-4 soils moved in the opposite direction as the two other soil groups. The correlation was also not as strong as the Devol soil conductivity actually increased while the general group results trended downward with increasing strengths.

### 5.5.3 Conductivity with Fly Ash

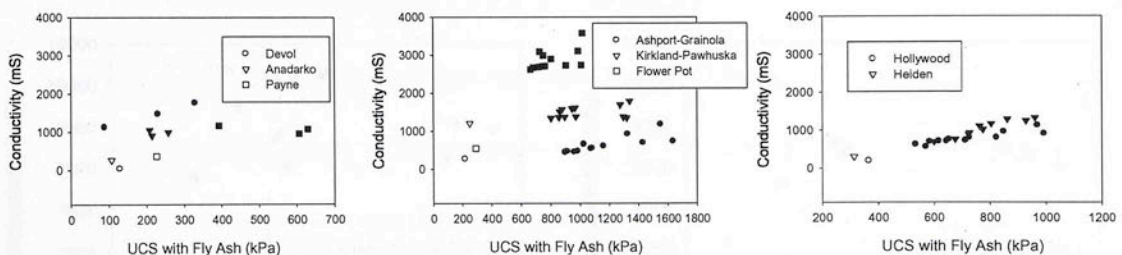


Figure 5.36 - Conductivity with Fly Ash for A-4 (Left), A-6 (Center), and A-7-6 (Right) Soils



As Figure 5.36 shows, the A-7-6 soil group again showed the most consistent conductivity response. Both soils increased linearly along one trend line as the strength increased. The A-6 soils also showed linear increases in the conductivity individually, but did not share a common group response. Each soil increased along its own parallel trend line with the Flower Pot soil having the highest conductivity and the Ashport-Grainola soil having the lowest conductivity. As opposed to the conductivity with CKD, the A-4 soils showed an increasing trend in the conductivity with fly ash as the unconfined compression strength increased. The plot contained considerable scatter in the data as the values from the three soils did not fall along a common trend line.

#### 5.5.4 Conductivity with Lime

The plots in Figure 5.37 show the conductivity responses of the five soils in the A-6 and A-7-6 soil groups. All five soils had linear increases in the conductivity of the soil-additive mixtures, but neither group showed a uniform group response. The A-6 soils had the highest conductivity values, but each soil conductivity increased at a different rate. In the A-7-6 soil group, the conductivities of the two soils increased seemingly in parallel.

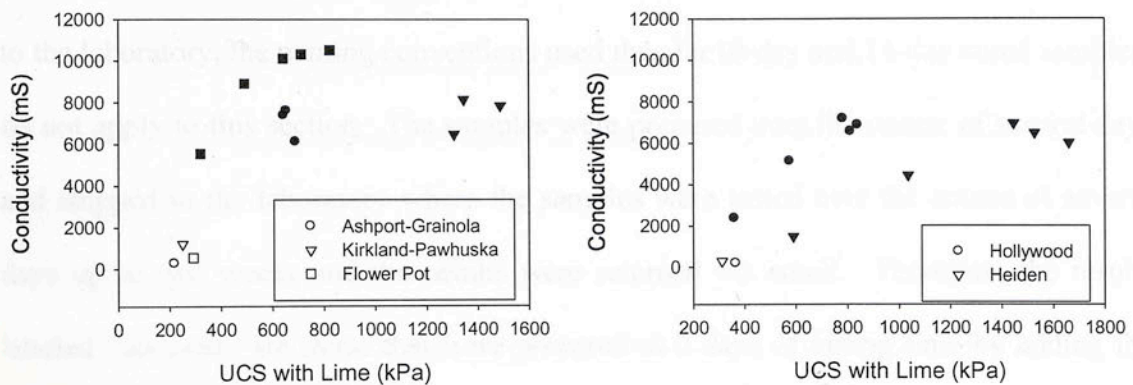


Figure 5.37 - Conductivity with Lime for A-6 (Left) and A-7-6 (Right) Soils

### **5.5.5 Summary of Conductivity**

The A-4 soils showed considerable scatter when treated with both CKD and fly ash. However, when the A-6 and A-7-6 soils were treated with fly ash, both groups showed fairly consistent linear trends. That carried over to the fly ash stabilized samples for the two A-7-6 soils, and to the lime stabilized samples at a lesser degree. The conductivities of the three A-6 soils when treated with fly ash were quite different, though. Each soil was essentially its own linear trend parallel to the other soils. When treated with lime, the A-6 soils did not even show a general trend and were quite scattered instead. The actual results and the plots of the conductivity versus the additive percentage for each soil group are contained in Appendix A in: Figure A-80 to Figure A-81 and Table A-26 for the A-4 soils, Figure A-86 to Figure A-89 and Table A-27 for the A-6 soils, and Figure A-94 to Figure A-97 and Table A-28 for the A-7-6 soils.

## **5.6 Cation Exchange Capacity Results**

### **5.6.1 Introduction to Cation Exchange Capacity Testing**

Unlike the other tests discussed in this chapter, the cation exchange capacity was the only one that required samples to be sent to an external testing facility. That facility was MDS Harris Laboratory located in Lincoln, Nebraska. As the samples had to be shipped to the laboratory, the naming conventions used thus far (0-day and 14-day cured samples) do not apply to this section. The samples were prepared over the course of several days and shipped to the laboratory where the samples were tested over the course of several days up to two weeks and the results were returned via email. Therefore, the results labeled “uncured” are those that were prepared at 0 days of curing time by adding the required amount of each additive to a standard amount of soil and then shipped to the

laboratory, and those labeled as “cured” are those samples that were shipped to the laboratory after testing the UCS and crushing the UCS samples at 14 days of curing time. The actual curing times of the samples are unknown, but likely range from one to six weeks based on delays at the laboratory.

## 5.6.2 Uncured CEC

### 5.6.2.1 CEC with CKD

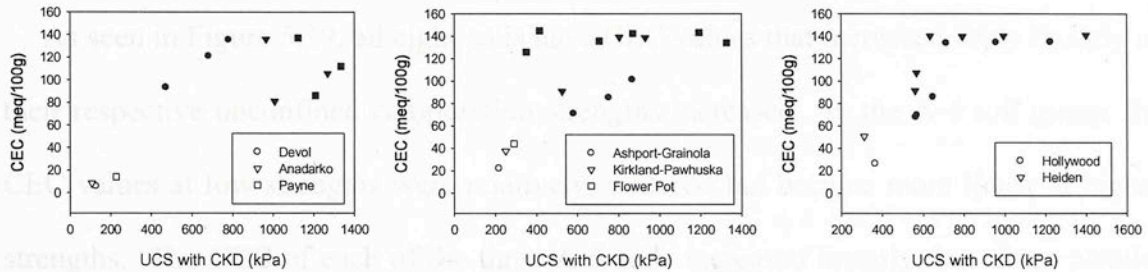


**Figure 5.38 - CEC (Uncured) with CKD for A-4 (Left), A-6 (Center), and A-7-6 (Right) Soils**

Figure 5.38 shows the cation exchange capacity values for the three soil groups. Each soil group had a different general response. In the A-4 group, the Devol soil CEC increased linearly with the strength, but the Payne and Anadarko soils did not have noticeable trends. The Ashport-Grainola and Kirkland-Pawhuska soils in the A-6 group increased linearly at similar rates, but the Flower Pot soil had an initial jump in the CEC from the raw soil and then remained nearly constant thereafter. In the A-7-6 soil group, both soils' CEC values increased rapidly at low strengths but then remained constant at higher strengths.



### 5.6.2.2 CEC with Fly Ash

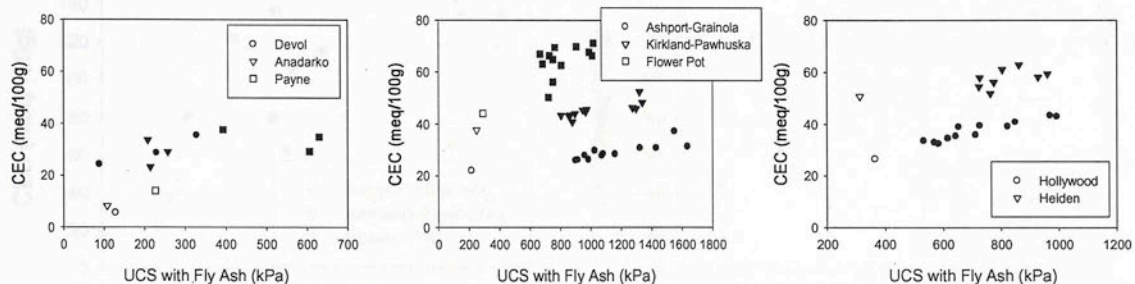


Figure 5.39 - CEC (Uncured) with Fly Ash for A-4 (Left), A-6 (Center), and A-7-6 (Right) Soils

As seen in Figure 5.39, all eight soils have CEC values that increased fairly linearly as their respective unconfined compression strengths increased. In the A-4 soil group, the CEC values at low strengths were relatively scattered but became more linear at higher strengths. The CEC of each of the three A-6 soils increased linearly, but along parallel trend lines for each soil, not a single response as a group. The same held true for the two A-7-6 soils, as both the Hollywood and Heiden soil CEC values increased with increasing strengths, but in parallel instead of together.

### 5.6.2.3 CEC with Lime

Figure 5.40 shows the results of cation exchange capacity tests performed on the five soils treated with lime from this study.

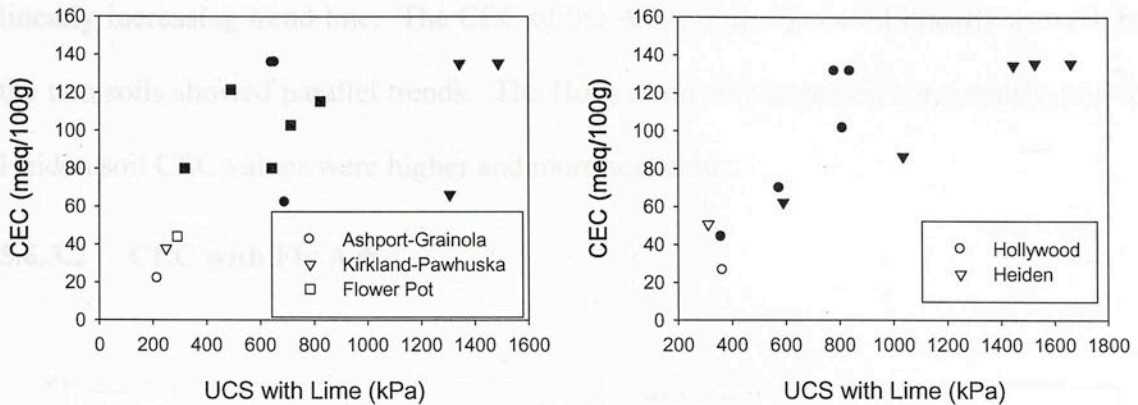


Figure 5.40 - CEC (Uncured) with Lime for A-6 (Left) and A-7-6 (Right) Soils

The three A-6 soils had significant scatter within the data, with all three soils having different CEC responses. The A-7-6 soils showed more consistent data, as the CEC values of both soils increased linearly at low strengths and the Hollywood soil CEC values deviated from the trend line at higher Hollywood soil strengths.

### 5.6.3 Cured CEC

#### 5.6.3.1 CEC with CKD

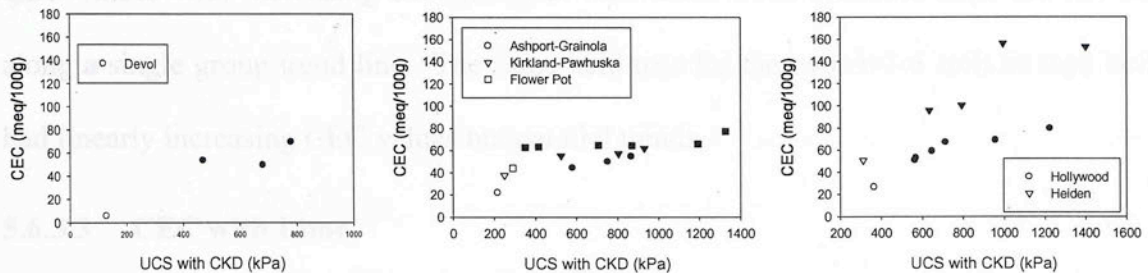
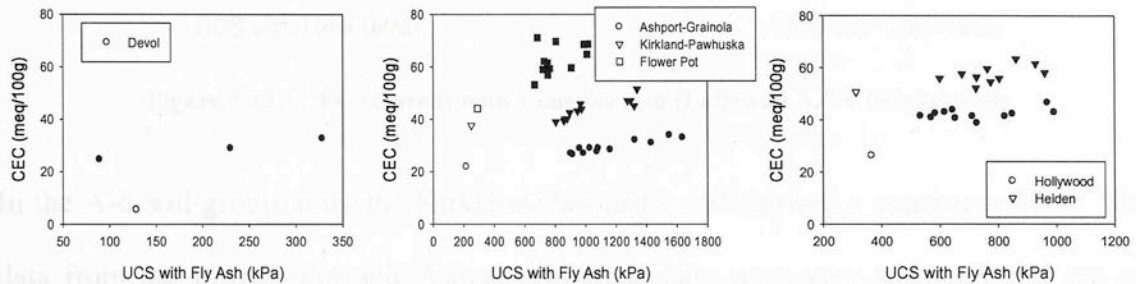


Figure 5.41 - CEC (Cured) with CKD for A-4 (Left), A-6 (Center), and A-7-6 (Right) Soils

Figure 5.41 contains the results of CEC tests performed after allowing the soil-additive mixtures to cure for at least 14 days. Only the Devol soil was tested after curing from the three A-4 soils, but it showed a distinct linearly increasing trend in the CEC as

the strength increased. The data from the three A-6 soils mostly fell along a single, linearly increasing trend line. The CEC of the A-7-6 soils increased linearly as well, but the two soils showed parallel trends. The Hollywood soil increased consistently, and the Heiden soil CEC values were higher and more scattered.

### 5.6.3.2 CEC with Fly Ash



**Figure 5.42 - CEC (Cured) with Fly Ash for A-4 (Left), A-6 (Center), and A-7-6 (Right) Soils**

As seen in Figure 5.42, when treated with fly ash, each soil in the three groups reacted differently. The Devol (A-4) soil CEC values increased linearly after the initial strength decrease from the raw soil. In the A-6 soil group, each soil showed linear increases in the CEC values with increasing strengths, but the values from the three soils did not fall along a single group trend line. The same held true for the two A-7-6 soils as they both had linearly increasing CEC values but parallel trends.

### 5.6.3.3 CEC with Lime

Figure 5.43 shows the results of CEC tests performed on A-6 and A-7-6 soils after allowing the soil-additive mixtures to cure.



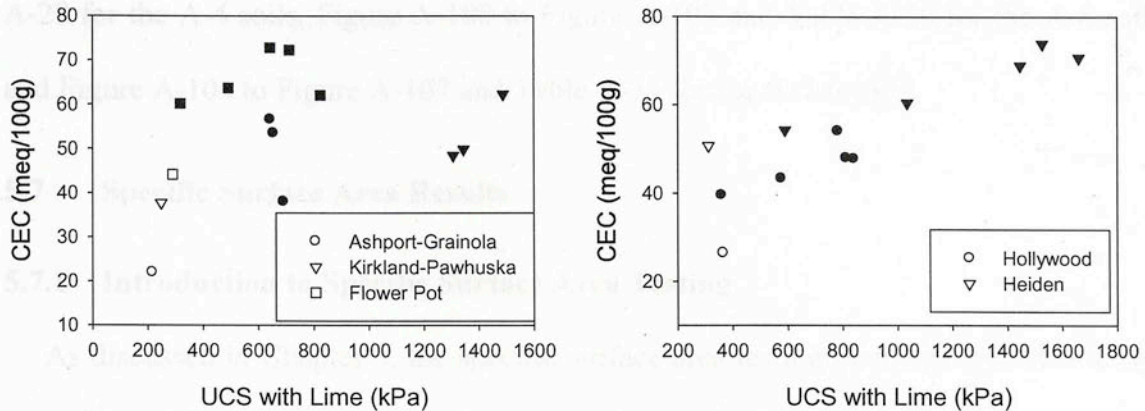


Figure 5.43 - CEC (Cured) with Lime for A-6 (Left) and A-7-6 (Right) Soils

In the A-6 soil group, only the Kirkland-Pawhuska soil showed a consistent trend. The data from the Flower Pot and Ashport-Grainola soils were very scattered and did not show noticeable trends. However, the CEC values from the A-7-6 soils increased linearly along a common trend line.

#### 5.6.4 Summary of CEC

When stabilized with fly ash, none of the test soils showed any appreciable differences between the uncured and the cured samples. However, there were noticeable differences in the soils stabilized with CKD and lime. In each soil treated with either CKD or lime, the cured CEC values were approximately half of the values of the uncured samples treated at the same percentage. The reactivity of CKD and lime are much higher due to the presence of higher amounts of calcium oxide (lime) in CKD and lime than in the two fly ash samples used here, but the cause of the CEC reduction is unknown. One potential explanation could be that the  $\text{Ca}^{+2}$  ions are initially reactive, but that reactivity (and the CEC) drops after curing because the  $\text{Ca}^{+2}$  ions have replaced all the lower valence cations by that point. The actual results for each soil are plotted versus the additive content in

Appendix A in the following figures and tables: Figure A-98 to Figure A-99 and Table A-29 for the A-4 soils, Figure A-100 to Figure A-103 and Table A-30 for the A-6 soils, and Figure A-104 to Figure A-107 and Table A-31 for the A-7-6 soils.

## **5.7 Specific Surface Area Results**

### **5.7.1 Introduction to Specific Surface Area Testing**

As discussed in Chapter 3, the specific surface area testing plan was split into testing the total and external specific surface areas of a single sample. The internal specific surface area was the difference between the two. On the whole, these tests followed the same 0-day and 14-day curing time regimen. The 0-day total specific surface area samples were mixed without curing and then placed in a 110°C oven to dry at least 16 hours prior to testing. This led the samples to be technically tested after one day of curing. Due to technical problems with the BET Monosorb machine, leaky gas tanks, and a lack of extra soil to test, many of the 0-day external specific surface area samples were not tested after one day of curing, but rather times ranging from one day to two weeks. The effect of these delays were not expected to be significant as the soils were never mixed with water which might facilitate the soil-additive reactions, and the oven-drying would have eliminated any water initially in the mixture.

## 5.7.2 Total Specific Surface Area Cured 0 Days

### 5.7.2.1 Total SSA with CKD

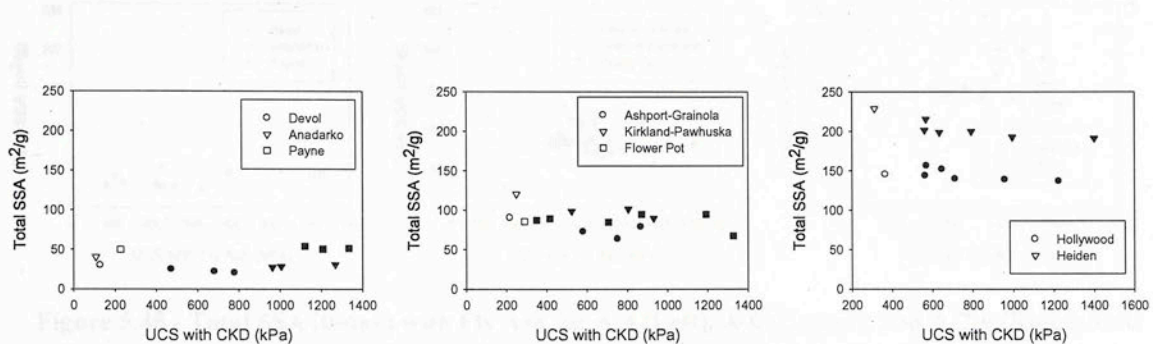
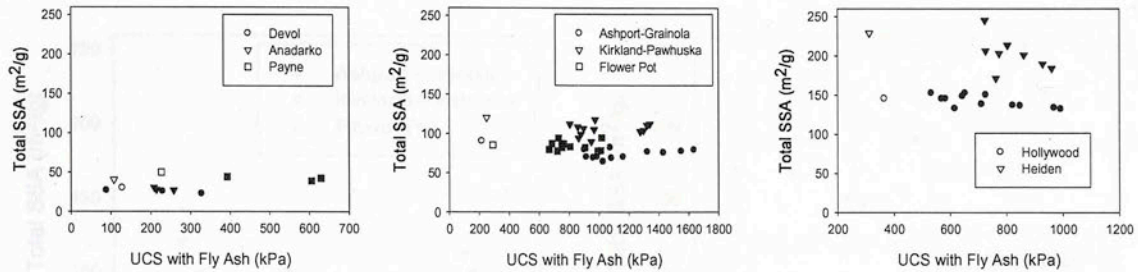


Figure 5.44 - Total SSA (0-day) with CKD for A-4 (Left), A-6 (Center), and A-7-6 (Right) Soils

As Figure 5.44 shows, only the A-7-6 soils showed consistent trends when treated with CKD, albeit in parallel lines instead of a single group line. The difference in SSA between two soils classified with very similar Atterberg Limits is important to note and helps explain the differences in behavior when stabilized with a particular type and amount of stabilizer. The SSA of the A-7-6 soils each decreased as the strength increased. The data from the A-6 soils was quite inconsistent, and the three A-4 soils each reacted differently. The Devol soil SSA values decreased, the Anadarko values decreased initially and then increased, and the Payne SSA values were relatively constant as the strength increased.



### 5.7.2.2 Total SSA with Fly Ash



**Figure 5.45 - Total SSA (0-day) with Fly Ash for A-4 (Left), A-6 (Center), and A-7-6 (Right) Soils**

Figure 5.45 contains the results of the total specific surface area tests performed on the eight study soils. In the left plot, the SSA of each A-4 soil remained fairly constant as the strength increased. The data in the A-6 soils plot shows generally constant trends in the SSA values with increasing unconfined strengths, but the combined data set is quite scattered. As seen in the right plot of the A-7-6 soils, the SSA values of the two soils fell slightly with increasing strengths, albeit at different rates. The Heiden soil SSA was initially higher and fell at a faster rate than the Hollywood soil, which only decreased slightly.

### 5.7.2.3 Total SSA with Lime

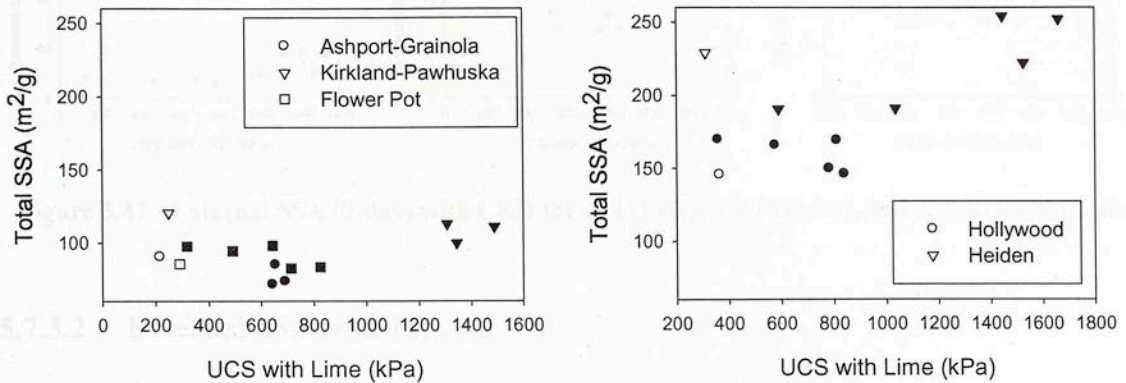


Figure 5.46 - Total SSA (0-day) with Lime for A-6 (Left) and A-7-6 (Right) Soils

Figure 5.46 shows two different trends. In the plot of the A-6 soils, a generally constant trend can be seen, despite the scatter in the individual soils. In the right plot, a different trend appeared. The Hollywood A-7-6 soil remained constant, but the Heiden soil SSA decreased initially and then increased as the strength increased.

## 5.7.3 External Specific Surface Area Cured 0 Days

### 5.7.3.1 External SSA with CKD

Figure 5.47 shows generally decreasing trends in the external specific surface area with increasing soil strengths. While none of the soil groups show consistent group trends, each individual soil seems to have its own decreasing trend relatively parallel to the other soils in its group. The plots also contain some scatter, with the Flower Pot soil appearing to suffer the worst, potentially due to the varying amounts of gypsum in the samples or due to the small sample sizes used in testing.

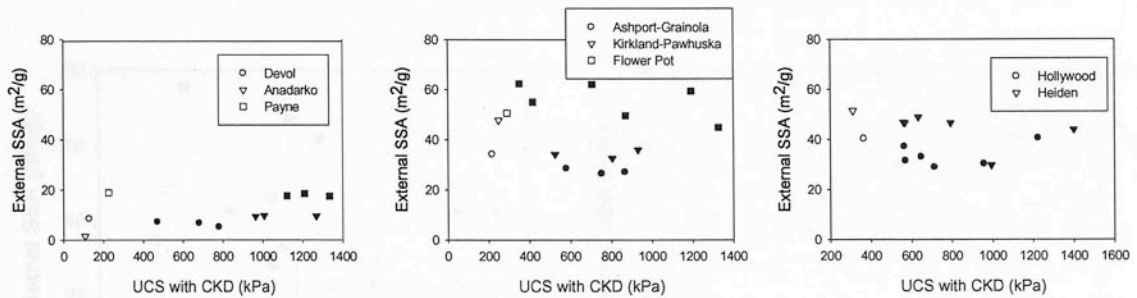


Figure 5.47 - External SSA (0-day) with CKD for A-4 (Left), A-6 (Center), and A-7-6 (Right) Soils

### 5.7.3.2 External SSA with Fly Ash

As seen in Figure 5.48, each soil generally shows a decrease in the external specific surface area when treated with fly ash. However, especially in the A-6 soil group, the data is quite scattered, making it difficult to determine an accurate trend line for the whole group. The only soil to show a consistent trend line was the Ashport-Grainola soil in the A-6 group.

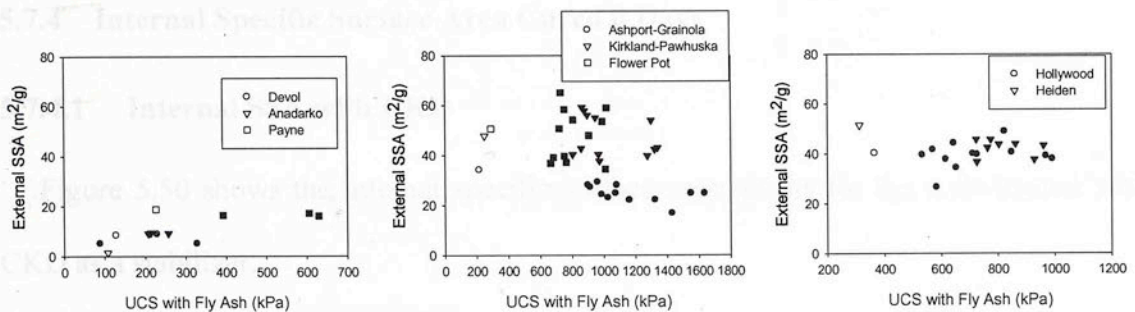


Figure 5.48 - External SSA (0-day) with Fly Ash for A-4 (Left), A-6 (Center), and A-7-6 (Right) Soils

### 5.7.3.3 External SSA with Lime

Figure 5.49 shows the results of the external specific surface area tests with soils stabilized with lime.



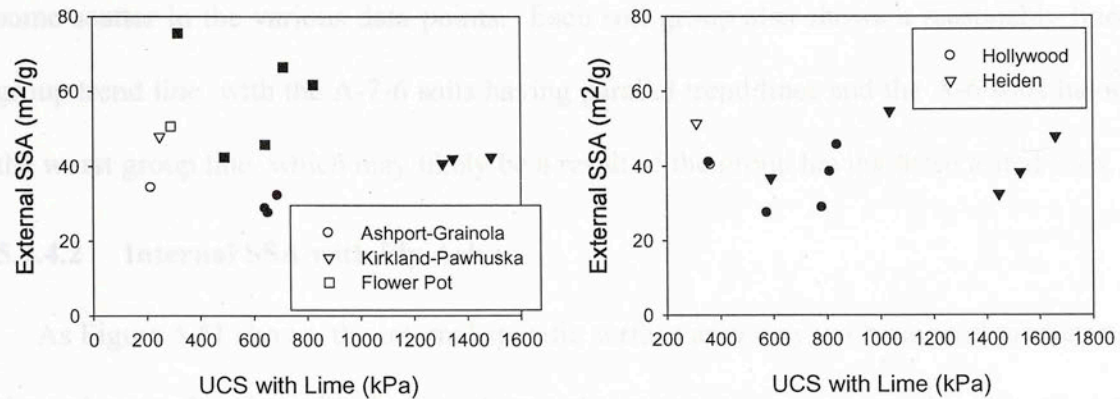


Figure 5.49 - External SSA (0-day) with Lime for A-6 (Left) and A-7-6 (Right) Soils

The values for each soil generally decrease with increasing strengths, but not along a single group trend line. In the A-6 group for example, the Ashport-Grainola and Kirkland-Pawhuska soils both show decreased external SSA values, but different parallel trend lines.

### 5.7.4 Internal Specific Surface Area Cured 0 Days

#### 5.7.4.1 Internal SSA with CKD

Figure 5.50 shows the internal specific surface area results for the soils treated with CKD as a stabilizer.

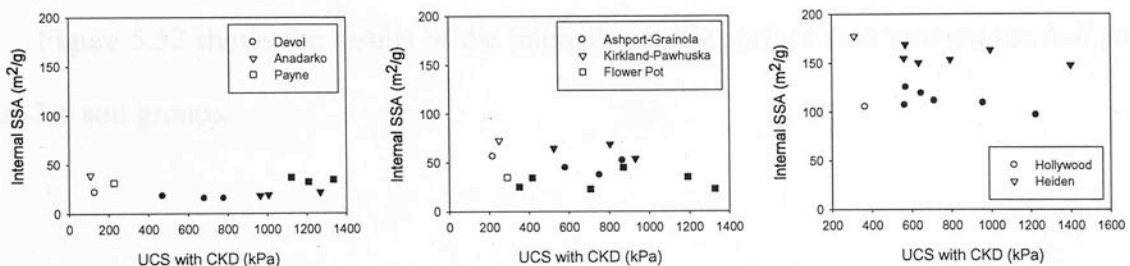


Figure 5.50 - Internal SSA (0-day) with CKD for A-4 (Left), A-6 (Center), and A-7-6 (Right) Soils

Each soil shows decreasing internal SSA values as the strength increases, albeit with some scatter in the various data points. Each soil group also shows a reasonably linear group trend line, with the A-7-6 soils having parallel trend lines and the A-6 soils having the worst group line, which may likely be a result of the group having three tested soils.

#### 5.7.4.2 Internal SSA with Fly Ash

As Figure 5.51 shows, the internal specific surface area may not be a good predictor of the soil strength gains with fly ash. Especially in the A-6 soil group, the soils all show considerable scatter within the results. The soils in the A-4 group showed a linearly decreasing trend that appears fairly constant in the figure due to the uniform SSA scale used in the three plots, but the actual values in the Appendix prove otherwise.

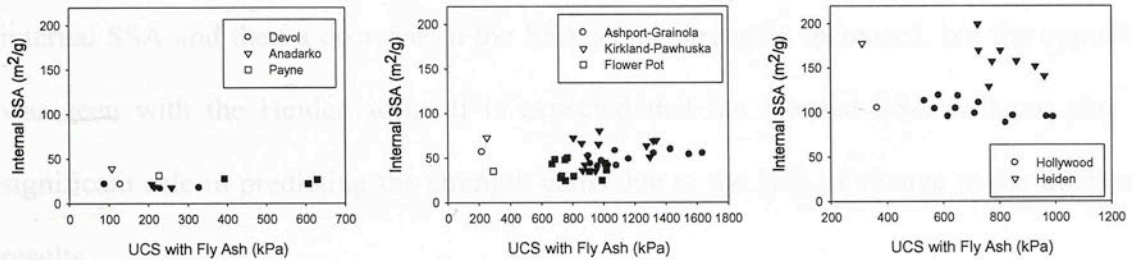


Figure 5.51 - Internal SSA (0-day) with Fly Ash for A-4 (Left), A-6 (Center), and A-7-6 (Right) Soils

#### 5.7.4.3 Internal SSA with Lime

Figure 5.52 shows the results of the internal specific surface area tests on the A-6 and A-7-6 soil groups.

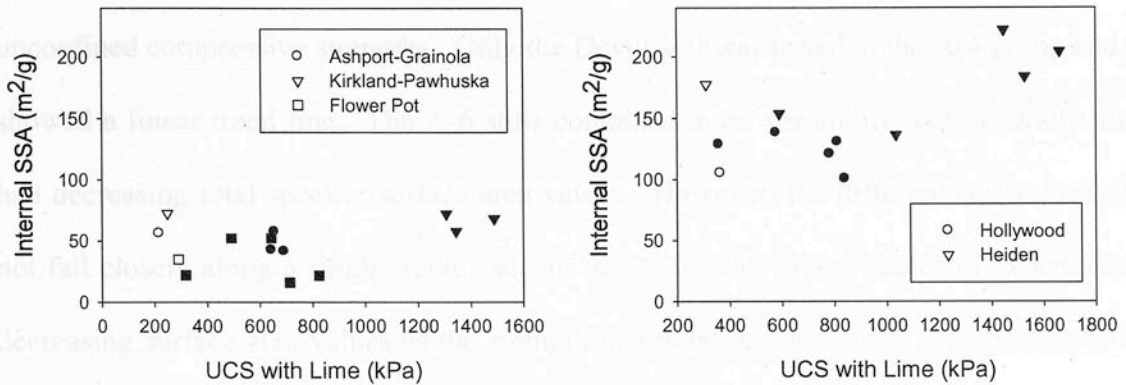


Figure 5.52 - Internal SSA (0-day) with Lime for A-6 (Left) and A-7-6 (Right) Soils

The results appear to show that the internal SSA remains fairly constant at increasing strengths for the A-6 soils. Although the results remained constant, they did so as a consistent group response. The Hollywood A-7-6 soil showed an initial increase in the internal SSA and then a decrease in the SSA as the strengths increased, but the opposite was seen with the Heiden soil. It is expected that the internal SSA will not play a significant role in predicting the strength gains due to the lack of change in the different results.

### 5.7.5 Total Specific Surface Area Cured 14 Days

#### 5.7.5.1 Total SSA with CKD

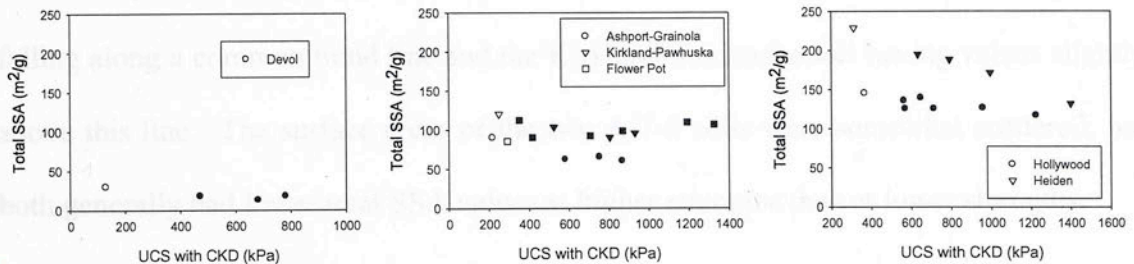


Figure 5.53 - Total SSA (14-day) with CKD for A-4 (Left), A-6 (Center), and A-7-6 (Right) Soils



Figure 5.53 shows decreasing total specific surface area values with increasing unconfined compressive strengths. Only the Devol soil was tested in the A-4 group and it showed a linear trend line. The A-6 soils contained more variability, but generally also had decreasing total specific surface area values. However, the different soil values did not fall closely along a single trend line. In the A-7-6 soil group, each soil experienced decreasing surface area values as the strength increased, but again the soils decreased in parallel instead of along a single group trend line.

### 5.7.5.2 Total SSA with Fly Ash

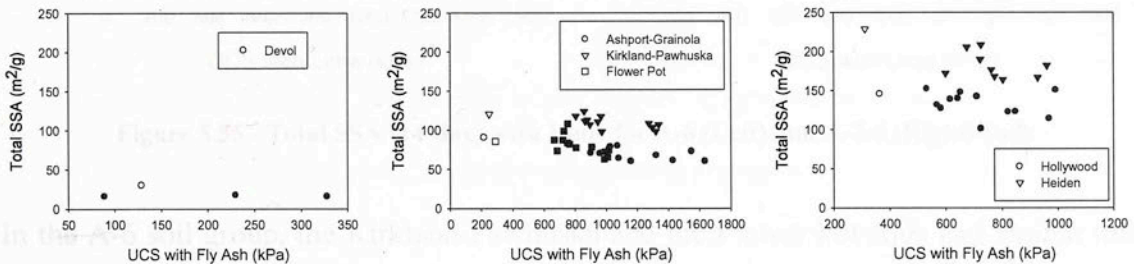


Figure 5.54 - Total SSA (14-day) with Fly Ash for A-4 (Left), A-6 (Center), and A-7-6 (Right) Soils

Figure 5.54 shows that as the unconfined strength rises, the total specific surface area of each soil-additive mixture falls. The total surface area of the Devol soil rose initially but then steadily decreased as the strength increased. The three A-6 soils also had consistently decreasing surface areas, with the Ashport-Grainola and Flower Pot soils falling along a common trend line and the Kirkland-Pawhuska soil having values slightly above this line. The surface areas of the two A-7-6 soils were somewhat scattered, but both generally had lower total SSA values at higher strengths than at lower strengths.

### 5.7.5.3 Total SSA with Lime

Figure 5.55 illustrates how the total specific surface area of a soil is affected to a greater degree with lime stabilization than with the other chemical stabilizers and generally decreases as the unconfined compression strength increases.

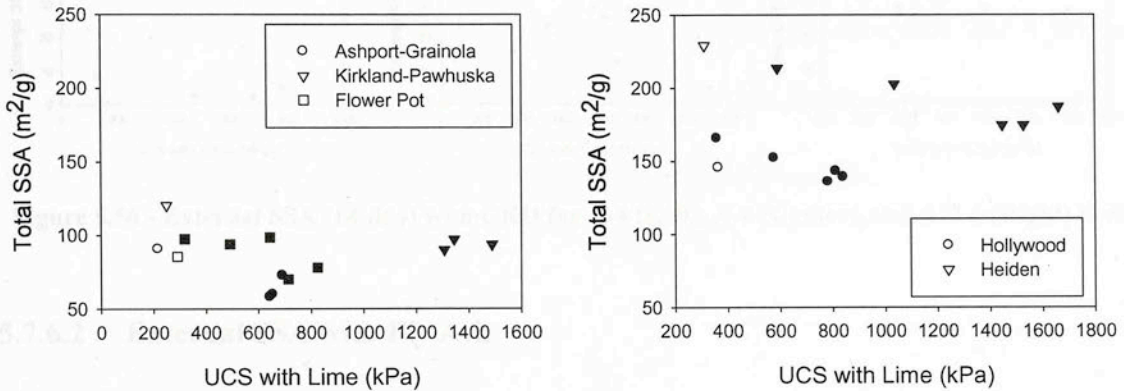


Figure 5.55 - Total SSA (14-day) with Lime for A-6 (Left) and A-7-6 (Right) Soils

In the A-6 soil group, the Kirkland-Pawhuska and the Flower Pot soils had similar total surface area responses that appeared to fall along a single trend line, but the Ashport-Grainola surface area values were lower than this line. In the A-7-6 soil group, the total specific surface areas of both the Hollywood and Heiden soils decreased, but in parallel and not along a common trend line.

## 5.7.6 External Specific Surface Area Cured 14 Days

### 5.7.6.1 External SSA with CKD

Figure 5.56 shows that with increasing strengths, the external specific surface area of the soils tends to decrease. However, the different plots each also show considerable scatter in the data. The A-7-6 soils responded in the most consistent linear fashion, although they had different parallel trend lines and not a single group line. In the A-6

group, the Flower Pot soil had a relatively linear trend line, but the other two soils were very scattered and did not share that trend. The Anadarko and Payne soils do not appear in the figure because those soils were not tested by the researchers at OSU.

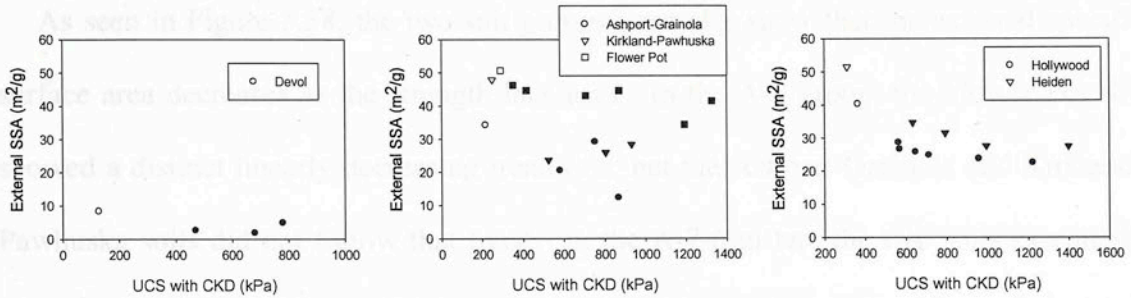


Figure 5.56 - External SSA (14-day) with CKD for A-4 (Left), A-6 (Center), and A-7-6 (Right) Soils

### 5.7.6.2 External SSA with Fly Ash

As seen in Figure 5.57, each soil group shows a general decrease in the external specific surface area with increases in the unconfined strengths.

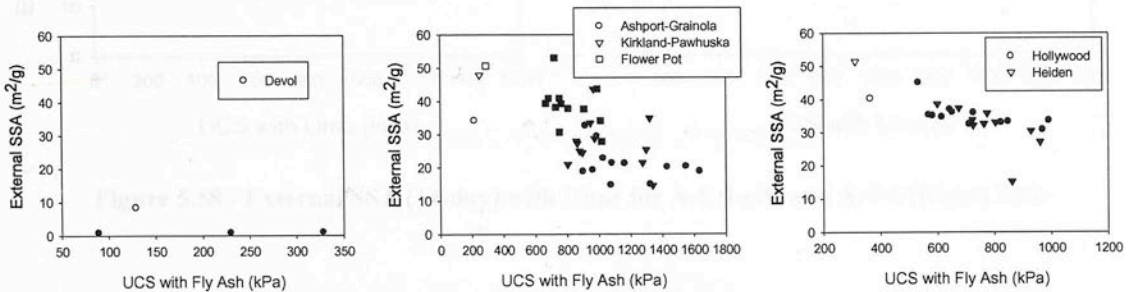


Figure 5.57 - External SSA (14-day) with Fly Ash for A-4 (Left), A-6 (Center), and A-7-6 (Right) Soils

While each soil group shows a decreasing linear trend line, the A-7-6 soils show the most consistent trend. The A-6 soils generally decrease, but the group data as a whole is widely scattered as the values decrease. The strong trend line for the A-7-6 soils may



mean that the 14-day external SSA is a parameter of interest for predicting the strength gains of stabilized soils.

### 5.7.6.3 External SSA with Lime

As seen in Figure 5.58, the two soil groups generally show that the external specific surface area decreases as the strength increases. In the A-6 group, the Flower Pot soil showed a distinct linearly decreasing trend line, but the Ashport-Grainola and Kirkland-Pawhuska soils did not follow that trend. In the A-7-6 group, the two soils essentially decreased linearly, but in parallel instead of as a single group response.

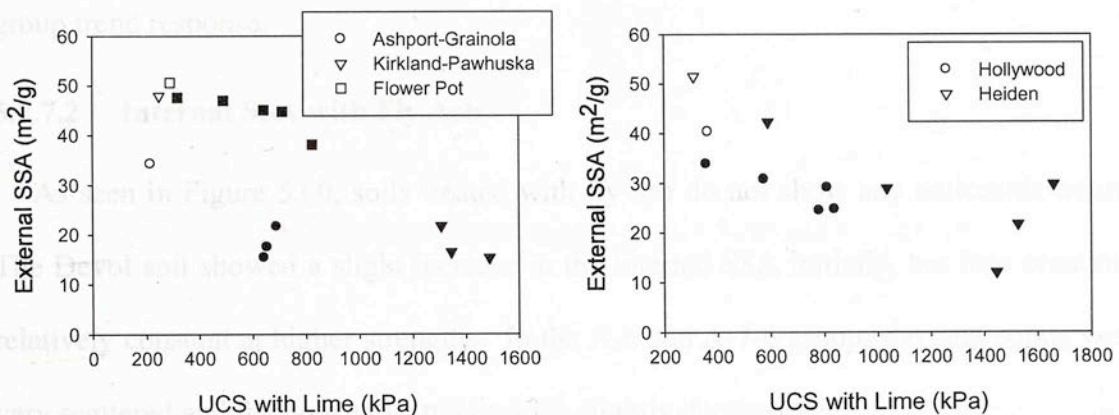


Figure 5.58 - External SSA (14-day) with Lime for A-6 (Left) and A-7-6 (Right) Soils

## 5.7.7 Internal Specific Surface Area Cured 14 Days

### 5.7.7.1 Internal SSA with CKD

Figure 5.59 shows the results from determining the internal specific surface area from the total and external SSA tests.

### 5.7.7.3 Internal SSA with Lime

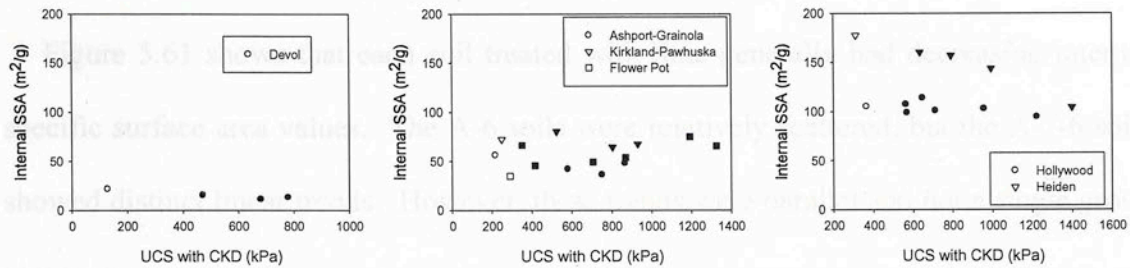


**Figure 5.59 - Internal SSA (14-day) with CKD for A-4 (Left), A-6 (Center), and A-7-6 (Right) Soils**

The A-4 and A-7-6 soil groups showed linear decreases in the internal SSA as the strength increased, with the two A-7-6 soils showing parallel lines instead of a single group line. The values from the A-6 soils were widely scattered and did not show a group trend response.

### 5.7.7.2 Internal SSA with Fly Ash

As seen in Figure 5.60, soils treated with fly ash do not show any noticeable trends. The Devol soil showed a slight increase in the internal SSA initially, but then remained relatively constant at higher strengths. In the A-6 and A-7-6 groups the data points were very scattered and the noticeable trends were slightly decreasing.

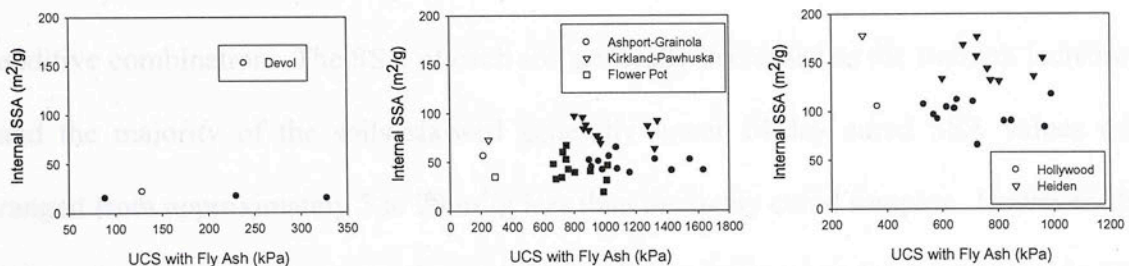


**Figure 5.60 - Internal SSA (14-day) with Fly Ash for A-4 (Left), A-6 (Center), and A-7-6 (Right) Soils**

### 5.7.7.3 Internal SSA with Lime

Figure 5.61 shows that each soil treated with lime generally had decreasing internal specific surface area values. The A-6 soils were relatively scattered, but the A-7-6 soils showed distinct linear trends. However, these trends were parallel and not a single group response.

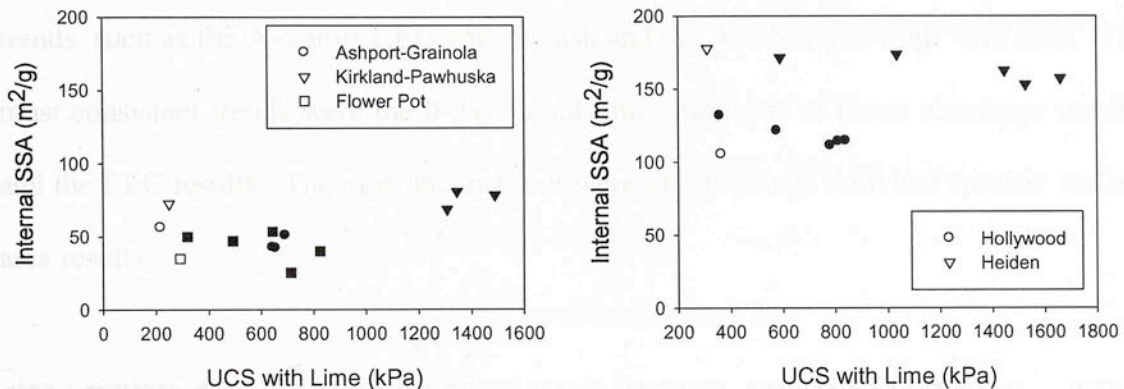


Figure 5.61 - Internal SSA (14-day) with Lime for A-6 (Left) and A-7-6 (Right) Soils

### 5.7.8 Summary of Specific Surface Area

After comparing the results from the 0 days cured and 14 days cured specific surface area tests, there were not many differences between the two values for a given soil and additive combination. The SSA of each soil generally decreased as the strength increased and the majority of the soils showed generally lower 14-day cured SSA values that ranged from approximately 5 to 20 m<sup>2</sup>/g less than the 0-day cured samples. However, the SSA values for the Heiden (A-7-6) soil showed changes ranging for 0 up to nearly 100 m<sup>2</sup>/g. To see the actual data values and the plots of the specific surface areas vs. the additive percentage, please refer to the following figures in Appendix A: Figure A.108 through Figure A.113 and Table A.32 to Table A.34 for the A-4 soils, Figure A.114



through Figure A.125 and Table A.35 to Table A.37 for the A-6 soils, and Figure A.126 to Figure A.137 and Table A.38 to Table A.39 for the A-7-6 soils.

## **5.8 Chapter Summary**

In many instances, the soils within a specific group showed linear correlations, such as the linear shrinkage with CKD and the A-6 soils CEC with CKD. At other times, the soils within a particular group did not show a group response and instead showed parallel trends, such as the A-6 soils CEC with fly ash and the A-7-6 liquid limit with lime. The most consistent trends were the 0-day liquid limit, both sets of linear shrinkage results, and the CEC results. The most inconsistent were the shrinkage limit and specific surface area results.

# **CHAPTER 6: ANALYSIS OF SOIL PARAMETERS FOR PREDICTING SOIL STRENGTH**

## **6.1 Introduction**

This chapter contains the results of the statistical analyses performed on the data collected from the different tests performed during the course of this study. The goal of the statistical analyses was to determine correlations among the different soils of a given AASHTO classification with a specific additive, such as the three A-6 soils with lime as the stabilizer. The actual measured unconfined compression strength was chosen as the dependent variable with each tested soil property input as an independent variable possibly to be used in predicting the strength. This process was repeated for each soil group and additive combination. Each correlation set contained five separate equations

where each equation only used the treated soil values and left out the untreated, raw soil values:

- An equation based on the additive percentage and the uncured Atterberg Limits
- An equation based on the additive percentage and the cured Atterberg Limits
- An equation containing the additive percentage, the uncured Atterberg Limits, and the 14 days cured Atterberg Limits
- An equation derived from all tested parameters, which may or may not contain all the different parameters
- A “practical” equation based solely on parameters with short testing durations, including the uncured Atterberg Limits, pH, conductivity, uncured shrinkage properties, and the uncured total specific surface area

Additionally, four different statistical analyses were performed beyond those just mentioned. Three analyses combined all eight soils into the three additive groups to determine if accurate models could be created to apply to all soils treated with a certain additive. The fourth tested all soils and all additives together.

The statistical analysis generated an  $R^2$  and a standard estimate error for each equation. The  $R^2$  value is the coefficient of determination, a parameter which provides a measure of how accurate the model predictions are. The closer the  $R^2$  value is to 1.0, the more accurate the model is. The standard estimate error is the standard deviation of the error from the estimate. Generally, the higher the standard estimate error, the less accurate the model is. In the equations presented in this chapter, the larger the coefficient before each parameter, the more weight that is placed on that particular parameter and the more important it is for the strength correlation. Also, each equation contains a constant

term. The lower this constant term is, the more weight was able to be given to the included soil parameters and the more reflective the model is to the actual data trends. If the constant is large, the model was not able to put appropriate weight on the different parameters and the large constant effectively becomes another source of error in the model.

In this chapter, various abbreviations for the tested parameters will be used in the different correlation equations. A description of each of these abbreviations follows.

UCS = Unconfined compression strength (kPa)

UCS<sup>+</sup> = Raw soil UCS + 345 kPa minimum strength gain (kPa)

Constant = Height of the linear model as it crosses the UCS axis

% = Additive percentage (2% = 2)

LL<sub>0</sub> = Liquid limit, cured 0 days (%)

PL<sub>0</sub> = Plastic limit, cured 0 days (%)

PI<sub>0</sub> = Plasticity index, cured 0 days (%)

LL<sub>14</sub> = Liquid limit, cured 14 days (%)

PL<sub>14</sub> = Plastic limit, cured 14 days (%)

PI<sub>14</sub> = Plasticity index, cured 14 days (%)

pH = pH of the soil-additive mixture

pH<sub>avg</sub> = Average pH at a specific additive percentage

C = Conductivity of the soil-additive mixture (mS)

LS<sub>0</sub> = Linear shrinkage, cured 0 days (%)

SL<sub>0</sub> = Shrinkage limit, cured 0 days (%)

LS<sub>14</sub> = Linear shrinkage, cured 14 days (%)



$SL_{14}$  = Shrinkage limit, cured 14 days (%)

$TS_0$  = Total specific surface area, cured 0 days ( $m^2/g$ )

$ES_0$  = External specific surface area, cured 0 days ( $m^2/g$ )

$IS_0$  = Internal specific surface area, cured 0 days ( $m^2/g$ )

$CEC_0$  = Cation exchange capacity, uncured (meq/100g)

$TS_{14}$  = Total specific surface area, cured 14 days ( $m^2/g$ )

$ES_{14}$  = External specific surface area, cured 14 days ( $m^2/g$ )

$IS_{14}$  = Internal specific surface area, cured 14 days ( $m^2/g$ )

$CEC_{14}$  = Cation exchange capacity, cured (meq/100g)

Adjusted  $R^2$  = Adjusted coefficient of determination

SE = Standard error of the estimate (kPa)

N = Number of data points analyzed in the model

Op% = Optimum additive percentage (%)

Sulf = Sulfate concentration, measured by the Colorimetry method (ppm)

Clay = Clay size fraction (%)

Carb = Carbonate content, measured by the Chittick Apparatus (%)

## 6.2 Results for A-4 Soils

### 6.2.1 Introduction

The fact that many A-4 classified soils are non-plastic makes the usage of Atterberg Limits as a determining factor in choosing stabilizer amounts an unreliable parameter. For the statistical analysis, all the tested parameters were available for the models. Many parameters were incomplete though, resulting in models with lower accuracies.

## 6.2.2 Uncured Atterberg Limits Model

Equations [6.1] and [6.2] are the results of the statistical analyses performed on the data from the Devol, Anadarko, and Payne soils after being treated with CKD and Fly Ash.

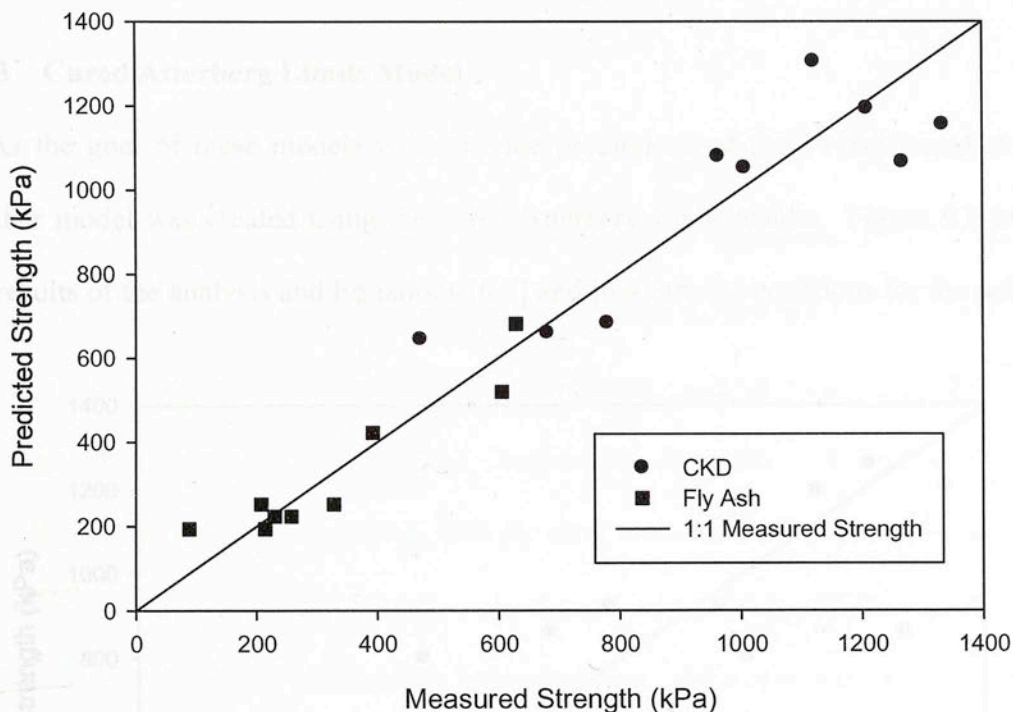


Figure 6.1 - Uncured Atterberg Limits Model for A-4 Soils

$$UCS_{CKD} = 6.904(\%) - 25.934(LL_0) + 44.42(PL_0) + 996.641$$

[6.1]

Adjusted  $R^2 = 0.612$ , SE = 180 kPa, and N = 9.

$$UCS_{FA} = 9.73(\%) + 67.08(LL_0) - 85.255(PL_0) + 105.753$$

[6.2]

Adjusted  $R^2 = 0.814$ , SE = 80 kPa, and N = 9.

An assessment of Figure 6.1 shows that prediction equations provide relatively close estimates of the unconfined strength compared to the measured strengths. The fly ash strength estimates were generally closer matches to the measured strengths than the CKD estimates. However, since most of the measured strength values were relatively small, the standard estimate errors are rather high in comparison.

### 6.2.3 Cured Atterberg Limits Model

As the goal of these models is to provide predictions of the 14-day cured strength, another model was created using the cured Atterberg Limit results. Figure 6.2 presents the results of the analysis and Equations [6.3] and [6.4] are the equations for the points.

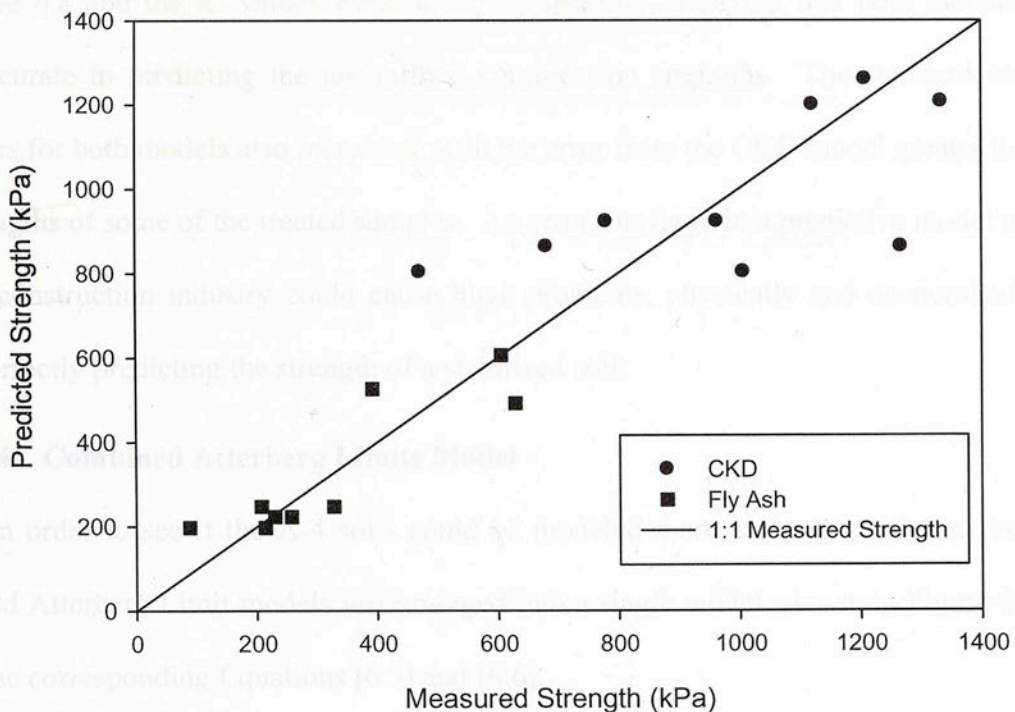


Figure 6.2 - Cured Atterberg Limits Model for A-4 Soils



$$UCS_{CKD} = 29.779(\%) + 85.689(LL_{14}) - 97.131(PL_{14}) + 564.232 \quad [6.3]$$

Adjusted  $R^2 = 0.056$ , SE = 281 kPa, and N = 9.

$$UCS_{FA} = 8.284(\%) + 55.78(LL_{14}) - 62.078(PL_{14}) + 122.707 \quad [6.4]$$

Adjusted  $R^2 = 0.656$ , SE = 108 kPa, and N = 9.

Compared to the uncured Atterberg Limits model, this model was a worse predictor. The fly ash model was again the better predictor, but neither model had an  $R^2$  value above 0.8 and the  $R^2$  values went down significantly, implying that both models were inaccurate in predicting the unconfined compression strengths. The standard estimate errors for both models also increased, with the error from the CKD model greater than the strengths of some of the treated samples. An error this large in a predictive model used in the construction industry could cause huge problems, physically and economically, by incorrectly predicting the strength of a stabilized soil.

#### 6.2.4 Combined Atterberg Limits Model

In order to see if the A-4 soils could be modeled more accurately, the uncured and cured Atterberg Limit models were merged into a single model, shown in Figure 6.3 and in the corresponding Equations [6.5] and [6.6].

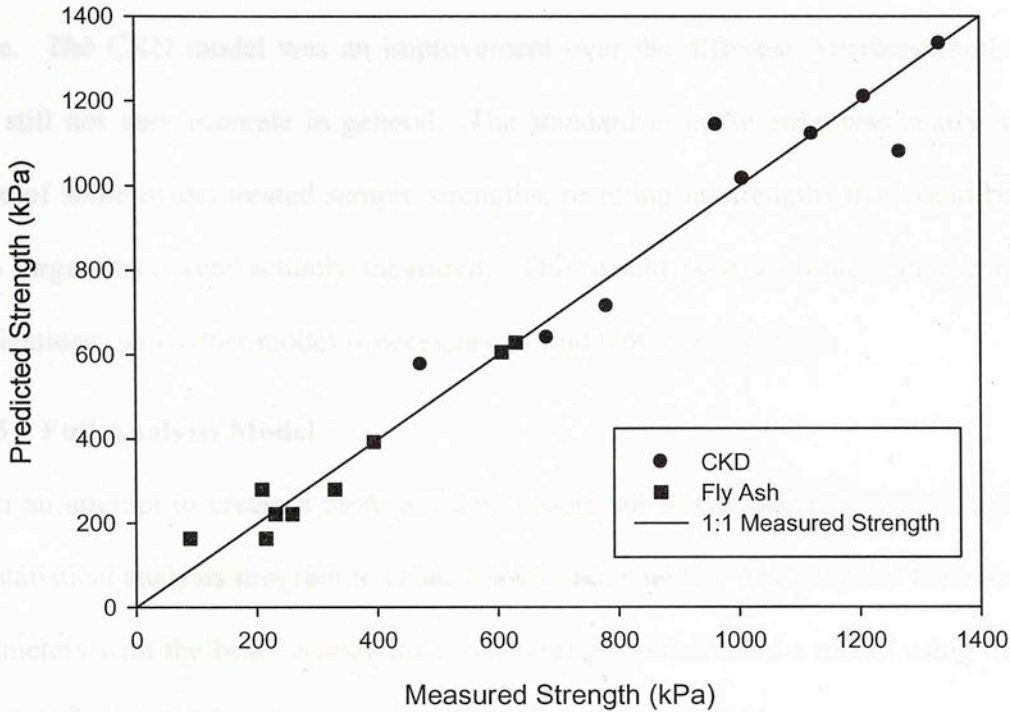


Figure 6.3 - Combined Atterberg Limits Model for A-4 Soils

$$\begin{aligned}
 UCS_{CKD} = & 31.676(\%) - 28.031(LL_0) - 341.7(PL_0) + 427.23(LL_{14}) \\
 & - 248.838(PL_{14}) + 763.111
 \end{aligned}$$

[6.5]

Adjusted  $R^2 = 0.663$ , SE = 168 kPa, and N = 9.

$$UCS_{FA} = 19.421(\%) + 103.564(LL_0) + 60.574(LL_{14}) - 208.889(PL_{14}) - 11.753$$

[6.6]

Adjusted  $R^2 = 0.875$ , SE = 65 kPa, and N = 9.

These models were improvements over the previous two model scenarios. The equations provided estimates that were much closer to the measured strengths, as seen in

Figure 6.3. The fly ash model was the more accurate of the two and had a very low  $R^2$  value. The CKD model was an improvement over the different Atterberg models, but was still not very accurate in general. The standard estimate error was nearly half the value of some of the treated sample strengths, resulting in strengths that could be up to 50% larger than were actually measured. This would pose a problem in construction applications, so another model is necessary to find better correlations.

### 6.2.5 Full Analysis Model

In an attempt to create a more accurate model, all tested parameters were input into the statistical analysis program to create another new model. The program then chose the parameters with the best correlations to the strength and created a model using those, as shown in Figure 6.4 and the respective Equations [6.7] and [6.8].

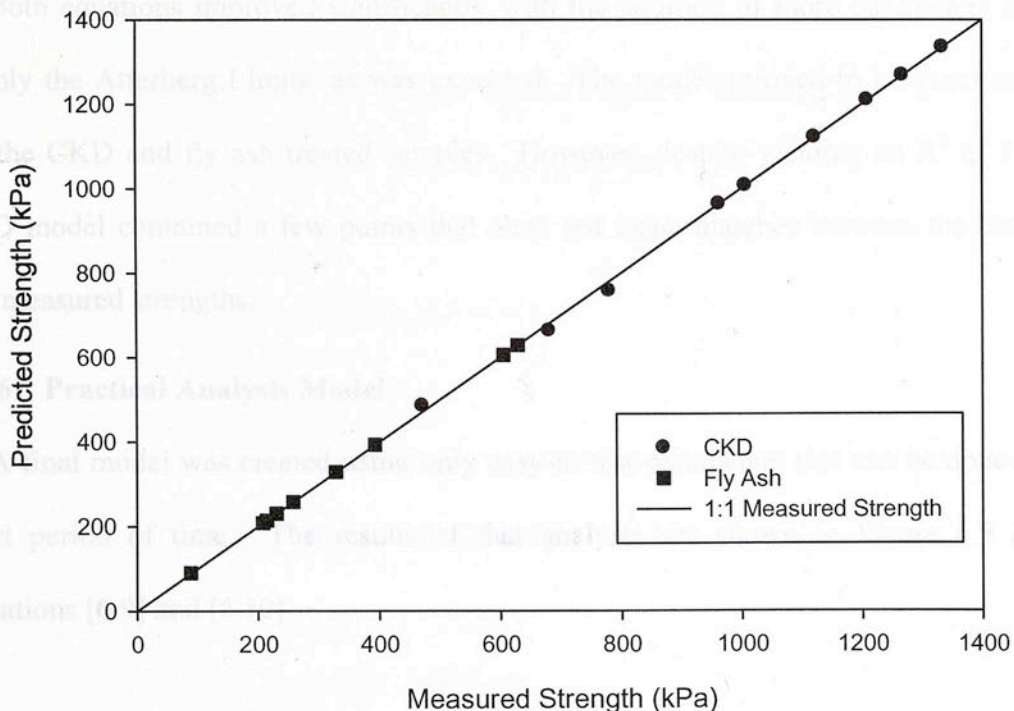


Figure 6.4 - Full Analysis Model for A-4 Soils



$$\begin{aligned}
 UCS_{CKD} = & -120.713(\%) - 7.698(PI_0) + 93.663(PI_0) + 4575.132(pH) \\
 & - 1071.027(LS_{14}) + 18.093(TS_0) + 63.891(ES_{14}) - 6.896(CEC_{14}) \\
 & - 53902.41
 \end{aligned}
 \tag{6.7}$$

Adjusted  $R^2 = 1.0$ , SE = 0 kPa, and N = 9.

$$\begin{aligned}
 UCS_{FA} = & 7.583(\%) + 52.706(PI_0) + 10.691(PI_{14}) - 166.955(pH) + 925.869(LS_0) \\
 & + 137.438(LS_{14}) - 20.682(TS_0) - 8.835(CEC_{14}) + 2595.188
 \end{aligned}
 \tag{6.8}$$

Adjusted  $R^2 = 1.0$ , SE = 0 kPa, and N = 9.

Both equations improved significantly with the addition of more parameters beyond simply the Atterberg Limits, as was expected. The models proved to be exact matches for the CKD and fly ash treated samples. However, despite yielding an  $R^2$  of 1.0, the CKD model contained a few points that were not exact matches between the predicted and measured strengths.

### 6.2.6 Practical Analysis Model

A final model was created using only easy-to-test parameters that can be done over a short period of time. The results of that analysis are shown in Figure 6.5 and in Equations [6.9] and [6.10].

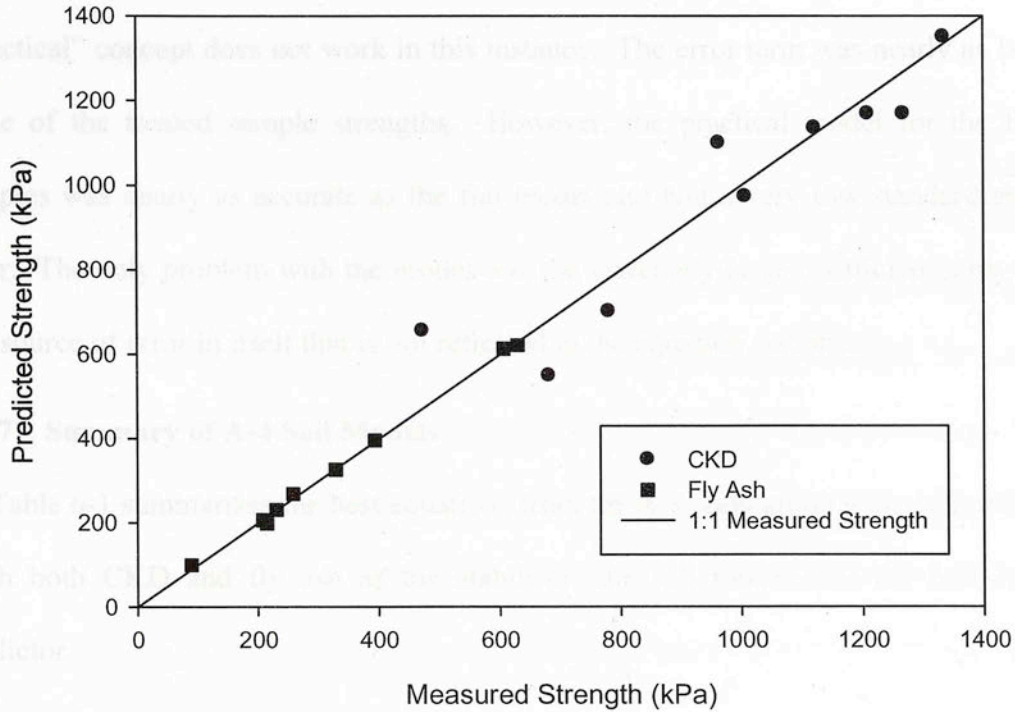


Figure 6.5 - Practical Analysis Model for A-4 Soils

$$\begin{aligned}
 UCS_{CKD} = & 119.26(\%) - 4.151(PI_0) + 4889.589(pH) - 0.401(C) + 2485.527(LS_0) \\
 & - 42.242(TS_0) + 196.123(ES_0) - 58018.04
 \end{aligned}$$

[6.9]

Adjusted  $R^2 = 0.095$ , SE = 276 kPa, and N = 9.

$$\begin{aligned}
 UCS_{FA} = & -34.712(\%) + 22.274(PI_0) - 852.563(pH) - 1.84(C) - 2649.241(LS_0) \\
 & - 19.227(TS_0) + 11.421(ES_0) + 8837.525
 \end{aligned}$$

[6.10]

Adjusted  $R^2 = 0.984$ , SE = 24 kPa, and N = 9.

The CKD model was a step backward from the full model, meaning that the “practical” concept does not work in this instance. The error term was nearly as large as some of the treated sample strengths. However, the practical model for the fly ash samples was nearly as accurate as the full model and had a very low standard estimate error. The only problem with the model was the extremely large coefficient term, which is a source of error in itself that is not reflected in the equation statistics.

### 6.2.7 Summary of A-4 Soil Models

Table 6-1 summarizes the best equations from the A-4 soils group with each stabilizer. With both CKD and fly ash as the stabilizer, the full model was the best strength predictor.

**Table 6-1 - Coefficients of Best A-4 Soil Models**

	CKD	Fly Ash
Model Type	Full	Full
Adjusted R <sup>2</sup> Value	1.0	1.0
Standard Estimate Error	0 kPa	0 kPa
Number of Points in Model	9	9
Constant	-53902.410	2595.188
Additive Percentage	-120.713	7.583
Plasticity Index (0-day)	-7.698	52.706
Plasticity Index (14-day)	93.663	10.691
pH	4575.132	-166.955
Linear Shrinkage (0-day)	0	925.869
Linear Shrinkage (14-day)	-1071.027	137.438
Total SSA (0-day)	18.093	-20.682
External SSA (14-day)	63.891	0
CEC (14-day)	-6.896	-8.835

The table shows that although the CKD model provides the better R<sup>2</sup> value, it provides a higher standard error than the fly ash model. The comparison also shows that besides the additive percentage, the pH, linear shrinkage, and CEC parameters are the main strength predictors for the A-4 soils tested in this study.



## 6.3 Results for A-6 Soils

### 6.3.1 Introduction

Unlike the analyses done on the three A-4 soils tested for this study, the A-6 soil database was fully complete and all tested properties were introduced into the statistical models. Not every input property was included in the output model, as the analysis program excluded those properties with weak correlations from the model. Five models will be presented in the following section: the first equation predicts the strength based solely on uncured Atterberg Limits, the second equation uses the cured Atterberg Limits, the third equation includes both the uncured and the 14 days cured Atterberg Limits, the fourth is the full model, and the final equation is the practical model for potential industry usage.

### 6.3.2 Uncured Atterberg Limits Model

Figure 6.6 is a statistical model representing a way soil stabilization is partially based upon uncured Atterberg Limits and the points are modeled using Equations [6.11], [6.12], and [6.13].

$$UCS_{FA} = 78.875(\%) + 23.215(LL) - 105.21(PI) + 189674$$

$$\text{Adjusted } R^2 = 0.37, SE = 161 \text{ kPa, and } N = 36$$

$$UCS_{14d} = 117.02(\%) - 2459(LL) - 52060(PI) + 1204000$$

$$\text{Adjusted } R^2 = 0.09, SE = 378 \text{ kPa, and } N = 31$$

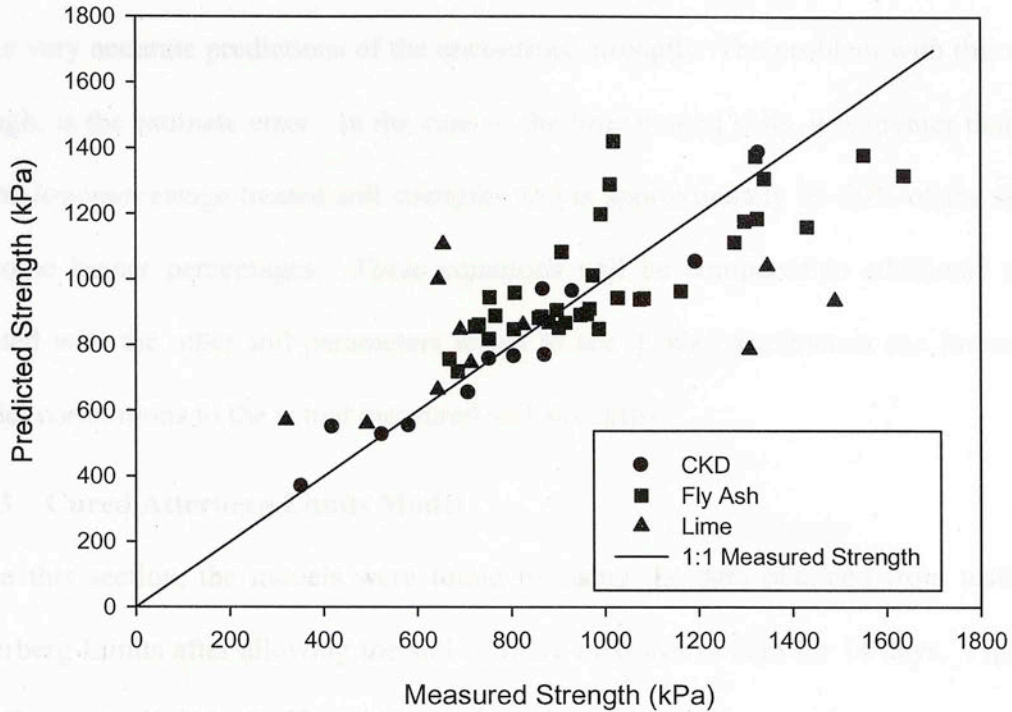


Figure 6.6 - Uncured Atterberg Limits Model for A-6 Soils

$$UCS_{CKD} = 91.906(\%) - 8.336(LL_o) + 24.768(PL_o) - 392.634$$

[6.11]

Adjusted  $R^2 = 0.900$ , SE = 93 kPa, and N = 12.

$$UCS_{FA} = 78.875(\%) + 23.215(LL_o) - 40.534(PL_o) + 189.873$$

[6.12]

Adjusted  $R^2 = 0.573$ , SE = 161 kPa, and N = 36.

$$UCS_{Lime} = 117.026(\%) - 2.839(LL_o) - 52.065(PL_o) + 2207.027$$

[6.13]

Adjusted  $R^2 = -0.091$ , SE = 396 kPa, and N = 11.

As shown by the scatter in Figure 6.6 fairly high SE error values, these models do not make very accurate predictions of the unconfined strength. The problem with this model, though, is the estimate error. In the case of the lime treated soils, it is greater than some of the low-percentage treated soil strengths and is approximately 25-50% of the strength of some higher percentages. These equations will be compared to additional models created with the other soil parameters tested to see if other parameters can improve the model correlations to the actual measured soil strengths.

### 6.3.3 Cured Atterberg Limits Model

In this section, the models were found by using the data obtained from testing the Atterberg Limits after allowing the soil-additive mixtures to cure for 14 days. Figure 6.7 and Equations [6.14], [6.15], and [6.16] show the results of those analyses.

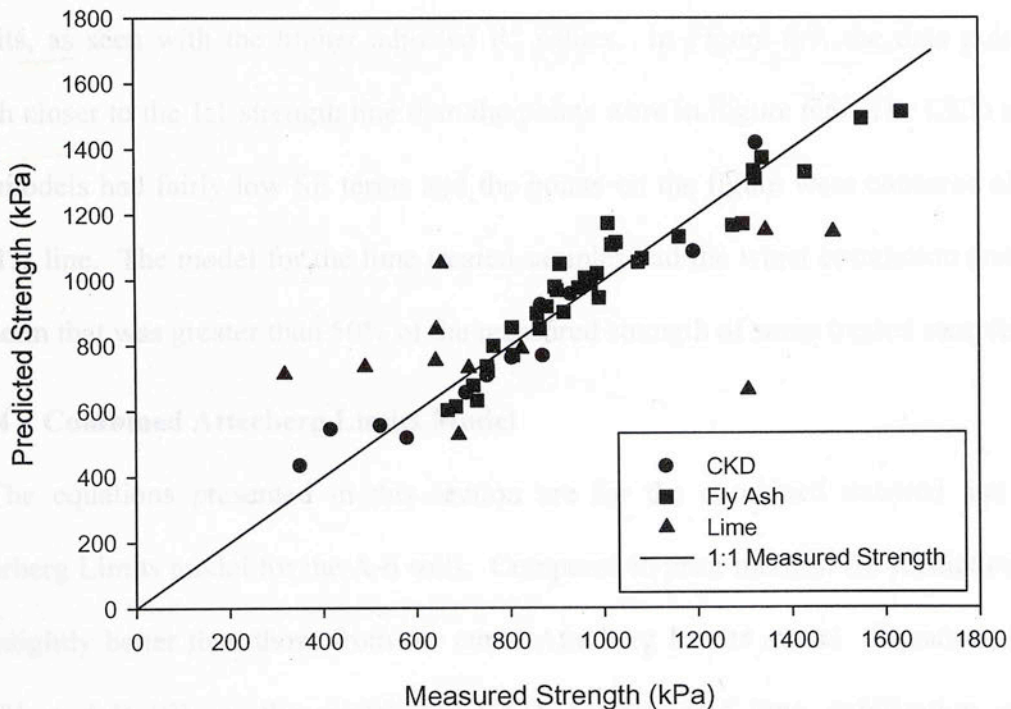


Figure 6.7 - Cured Atterberg Limits Model for A-6 Soils



$$UCS_{CKD} = 111.617(\%) + 7.593(LL_{14}) - 5.962(PL_{14}) - 426.002 \quad [6.14]$$

Adjusted  $R^2 = 0.900$ , SE = 93 kPa, and N = 12.

$$UCS_{FA} = 54.965(\%) - 28.426(LL_{14}) - 18.363(PL_{14}) + 1994.582 \quad [6.15]$$

Adjusted  $R^2 = 0.912$ , SE = 74 kPa, and N = 36.

$$UCS_{Lime} = -55.829(\%) - 8.521(LL_{14}) + 99.144(PL_{14}) + 890.623 \quad [6.16]$$

Adjusted  $R^2 = -0.020$ , SE = 383 kPa, and N = 11.

These models were significant improvements over using only the uncured Atterberg Limits, as seen with the higher adjusted  $R^2$  values. In Figure 6.7, the data points are much closer to the 1:1 strength line than the points were in Figure 6.6. The CKD and fly ash models had fairly low SE terms and the points on the figure were clustered close to the 1:1 line. The model for the lime treated samples had the worst correlation and had a SE term that was greater than 50% of the measured strength of some treated samples.

### 6.3.4 Combined Atterberg Limits Model

The equations presented in this section are for the combined uncured and cured Atterberg Limits model for the A-6 soils. Compared to prior models, the predictions here are slightly better than those from the cured Atterberg Limits model. Equations [6.17], [6.18], and [6.19] are the models for CKD, fly ash, and lime stabilization and the prediction results are plotted against the measured strengths in Figure 6.8.

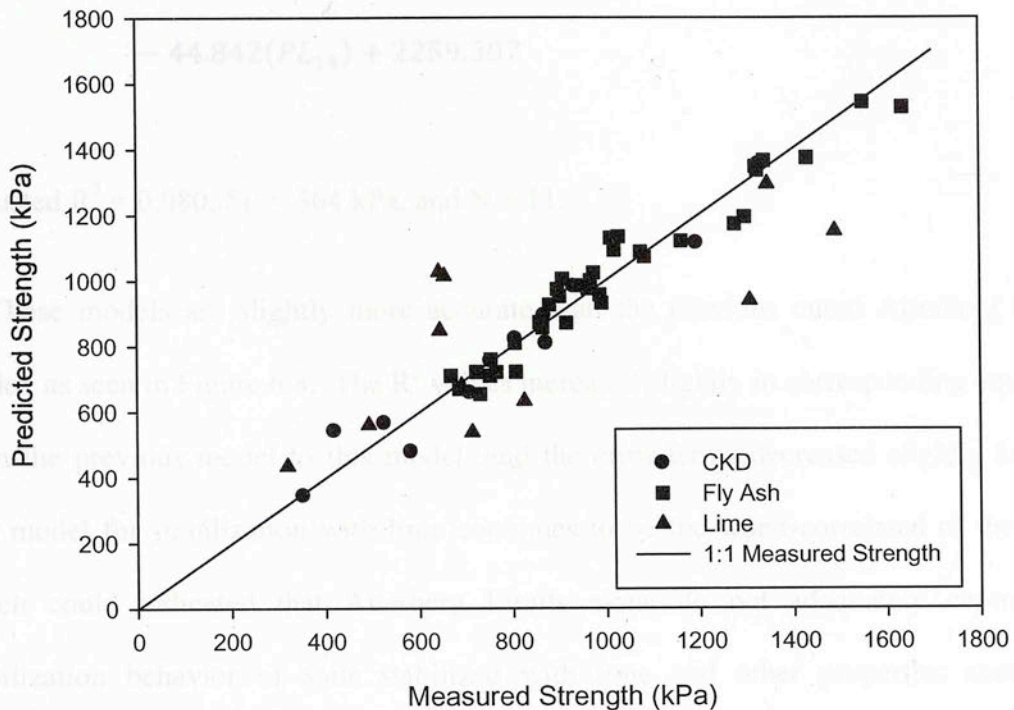


Figure 6.8 - Combined Atterberg Limits Model for A-6 Soils

$$\begin{aligned}
 UCS_{CKD} = & 90.145(\%) - 24.009(LL_o) + 1.763(PL_o) + 7.327(LL_{14}) + 18.734(PL_{14}) \\
 & + 198.821
 \end{aligned}$$

[6.17]

Adjusted  $R^2 = 0.912$ ,  $SE = 87$  kPa, and  $N = 12$ .

$$\begin{aligned}
 UCS_{FA} = & 60.751(\%) + 19.603(LL_o) + 1.426(PL_o) - 29.553(LL_{14}) - 20.553(PL_{14}) \\
 & + 1135.054
 \end{aligned}$$

[6.18]

Adjusted  $R^2 = 0.933$ ,  $SE = 64$  kPa, and  $N = 36$ .

$$\begin{aligned}
 UCS_{Lime} = & 162.188(\%) + 81.307(LL_o) - 10.831(PL_o) - 77.597(LL_{14}) \\
 & - 44.842(PL_{14}) + 2259.307
 \end{aligned}$$

[6.19]

Adjusted  $R^2 = 0.080$ , SE = 364 kPa, and N = 11.

These models are slightly more accurate than the previous cured Atterberg Limits model, as seen in Figure 6.8. The  $R^2$  values increased slightly in corresponding equations from the previous model to this model, and the error terms decreased slightly as well. The model for stabilization with lime continues to be the worst-correlated of the three, which could indicate that Atterberg Limits alone do not adequately capture the stabilization behavior of soils stabilized with lime and other properties should be introduced to the model to better predict the strength gains.

### 6.3.5 Full Analysis Model

To try to get the most complete and accurate models for predicting the strength of chemically stabilized soils, each tested soil parameter was input into the statistical analysis program for potential inclusion in a predictive model. Equations [6.20], [6.21], and [6.22] present the results from each of the analyses on the CKD, fly ash, and lime treated samples and the predicted strength values are plotted against the actual measured strength values in Figure 6.9.



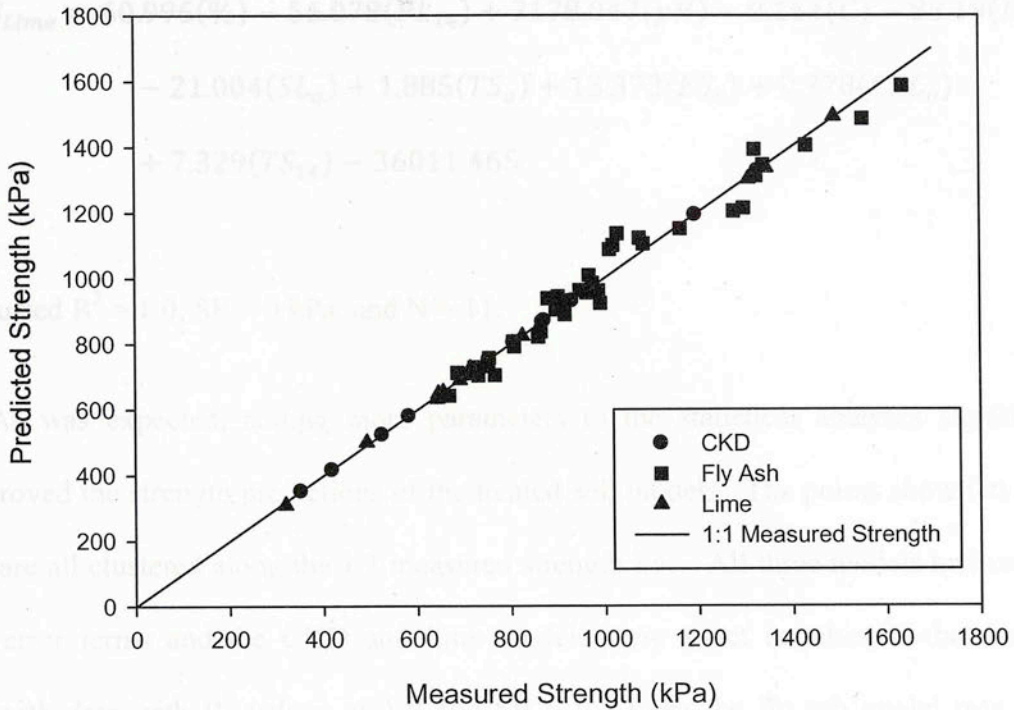


Figure 6.9 - Full Analysis Model for A-6 Soils

$$\begin{aligned}
 UCS_{CKD} = & 163.76(\%) + 79.588(LL_o) - 27.37(PL_{14}) - 200.927(LS_o) + 12.771(SL_o) \\
 & + 107.113(LS_{14}) + 29.21(SL_{14}) - 0.204(TS_o) + 0.033(CEC_o) \\
 & + 1.268(TS_{14}) - 46.532(CEC_{14}) - 799.887
 \end{aligned}$$

[6.20]

Adjusted  $R^2 = 1.0$ , SE = 0 kPa, and N = 12.

$$\begin{aligned}
 UCS_{FA} = & 73.703(\%) + 10.875(LL_o) + 12.769(PL_o) + 2.284(LL_{14}) + 10.19(PL_{14}) \\
 & - 21.329(pH) - 0.09(C) + 7.302(LS_o) - 12.859(SL_o) - 14.11(LS_{14}) \\
 & - 19.407(SL_{14}) + 0.339(TS_o) + 1.414(ES_o) - 3.471(CEC_o) \\
 & - 0.595(TS_{14}) + 0.171(ES_{14}) - 0.385(CEC_{14}) + 374.613
 \end{aligned}$$

[6.21]

Adjusted  $R^2 = 0.932$ , SE = 64 kPa, and N = 36.

$$\begin{aligned}
 UCS_{Lime} = & 60.996(\%) - 56.078(PL_{14}) + 3178.047(pH) - 0.164(C) - 88.19(LS_o) \\
 & - 21.004(SL_o) + 1.885(TS_o) + 13.373(ES_o) + 0.978(CEC_o) \\
 & + 7.329(TS_{14}) - 36011.465
 \end{aligned}$$

[6.22]

Adjusted  $R^2 = 1.0$ , SE = 0 kPa, and N = 11.

As was expected, adding more parameters to the statistical analyses significantly improved the strength predictions of the treated soil models. The points shown in Figure 6.9 are all clustered along the 1:1 measured strength line. All three models had very low SE error terms and the CKD and lime models were exact matches to the measured strength data with  $R^2$  values of 1.0 and SE = 0. Even the fly ash model was a very accurate predictor of the treated soil strength. The only real problems with the three models presented here are the constant terms at the end of each equation. The constants are quite large, especially in the lime model, and introduce errors to the models that are not reflected in the SE terms.

### 6.3.6 Practical Analysis Model

The final A-6 soil models presented here are the attempts to create practical equations for the construction industry and ones that can be done in a short amount of time. Figure 6.10 presents the measured strength values plotted against the predicted strength values from Equations [6.23], [6.24], and [6.25].

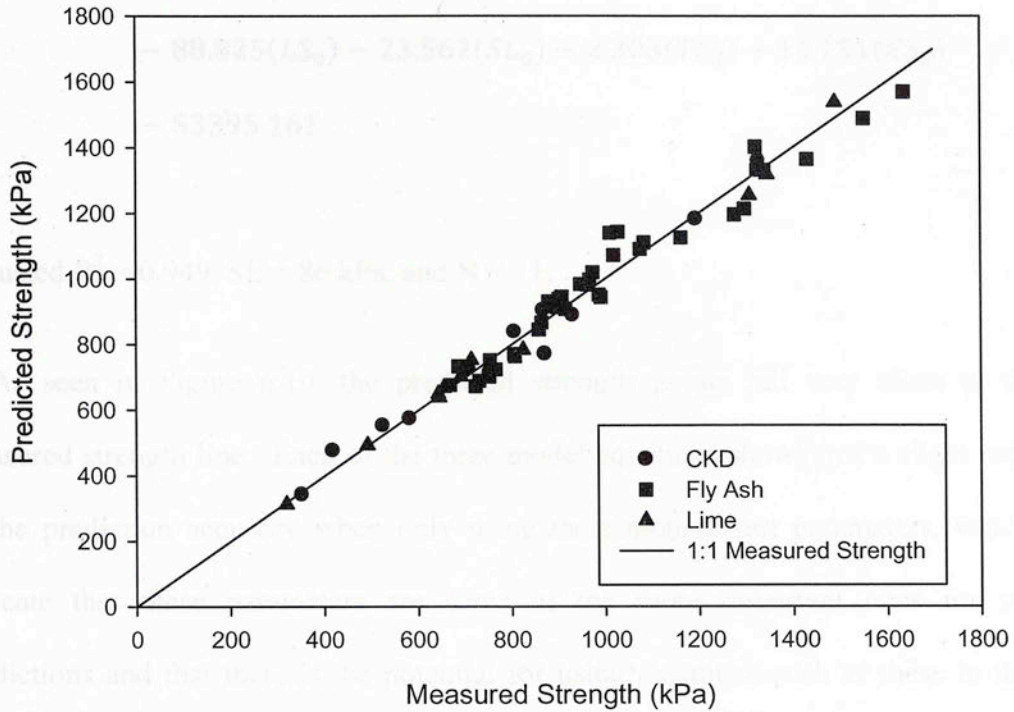


Figure 6.10 - Practical Analysis Model for A-6 Soils

$$\begin{aligned}
 UCS_{CKD} = & 44.269(\%) - 27.173(LL_0) - 22.846(PL_0) - 661.803(pH) + 0.166(C) \\
 & - 113.804(LS_0) + 16.975(SL_0) - 1.223(TS_0) + 7.501(ES_0) \\
 & + 10204.585
 \end{aligned}$$

[6.23]

Adjusted  $R^2 = 0.872$ , SE = 105 kPa, and N = 12.

$$\begin{aligned}
 UCS_{FA} = & 78.411(\%) + 16.527(LL_0) + 8.592(PL_0) - 82.071(pH) - 0.118(C) \\
 & + 5.002(LS_0) - 21.401(SL_0) - 0.598(TS_0) - 0.18(ES_0) + 817.848
 \end{aligned}$$

[6.24]

Adjusted  $R^2 = 0.940$ , SE = 61 kPa, and N = 36.



$$\begin{aligned}
 UCS_{Lime} = & -34.338(\%) + 42.108(LL_0) + 35.299(PL_0) + 4440.653(pH) - 0.301(C) \\
 & - 88.825(LS_0) - 23.562(SL_0) - 2.303(TS_0) + 11.151(ES_0) \\
 & - 53395.161
 \end{aligned}$$

[6.25]

Adjusted  $R^2 = 0.949$ , SE = 86 kPa, and N = 11.

As seen in Figure 6.10, the predicted strength points fall very close to the 1:1 measured strength line. Each of the three model equations shows just a slight reduction in the prediction accuracy when only using the simple-to-test parameters, which may indicate that these parameters are some of the more important ones for strength predictions and that there is the potential for using equations such as these in the road construction industry. The only real problem is that the constant term in each of the three equations is quite large, meaning the analysis program was unable to assign correctly weighted coefficients to each parameter.

### 6.3.7 Summary of A-6 Soil Models

The following table provides a concise summary and side-by-side comparison of the best equations found through the statistical analysis.

**Table 6-2 - Coefficients of Best A-6 Soil Models**

	CKD	Fly Ash	Lime
Model Type	Full	Practical	Full
Adjusted R <sup>2</sup> Value	1.0	0.940	1.0
Standard Estimate Error	0 kPa	61 kPa	0 kPa
Number of Points in Model	12	36	11
Constant	-799.887	817.848	-36011.465
Additive Percentage	163.760	78.411	60.996
Liquid Limit (0-day)	79.588	16.527	0
Plastic Limit (0-day)	0	8.592	0
Plastic Limit (14-day)	-27.370	0	-56.078
pH	0	-82.071	3178.047
Conductivity	0	-.118	-.164
Linear Shrinkage (0-day)	-200.927	5.002	-88.190
Shrinkage Limit (0-day)	12.771	-21.401	-21.004
Linear Shrinkage (14-day)	107.113	0	0
Shrinkage Limit (14-day)	29.210	0	0
Total SSA (0-day)	-0.204	-.598	1.885
External SSA (0-day)	0	-.180	13.373
CEC (0-day)	0.033	0	.978
Total SSA (14-day)	1.268	0	7.329
CEC (14-day)	-46.532	0	0

Within the A-6 soil group, for CKD and lime stabilized soils, the full-analysis model was shown to provide the best fit to the data. The practical analysis model was the most accurate for the fly ash stabilized samples. This table shows that not every parameter is of significance for modeling each stabilizer type. However, based on the repeated inclusion of the linear shrinkage properties and the total SSA (0-day), the conclusion can be drawn that those are important properties to consider when attempting to make predictions about soil strength increases, regardless of the additive type.

## 6.4 A-7-6 Soils

### 6.4.1 Introduction

As with the analyses performed on the three A-6 soils, the analyses of the two A-7-6 soils, Hollywood and Heiden, with the three additives had a full database of soil properties to use in creating the statistical models. The only drawback to the A-7-6 analyses was the small sample size of only two soils. Each additive subsection will contain four separate equations representing different strength modeling scenarios. The first equation will represent predictions based on uncured Atterberg Limits, the second will include 14 days cured Atterberg Limits, the third equation will combine both the uncured and cured Atterberg Limits, the fourth will be the equation derived from all available test data, and the fifth equation will predict the strength using the “practical” parameters.

### 6.4.2 Uncured Atterberg Limits Model

The first equation presented in this subsection is the model that attempts to predict the stabilized soil strength by using the additive percentage and the uncured Atterberg Limits as parameters. Figure 6.11 shows the plotted results of these analyses determined from comparing the measured strength values to the predicted values from Equations [6.26], [6.27], and [6.28].



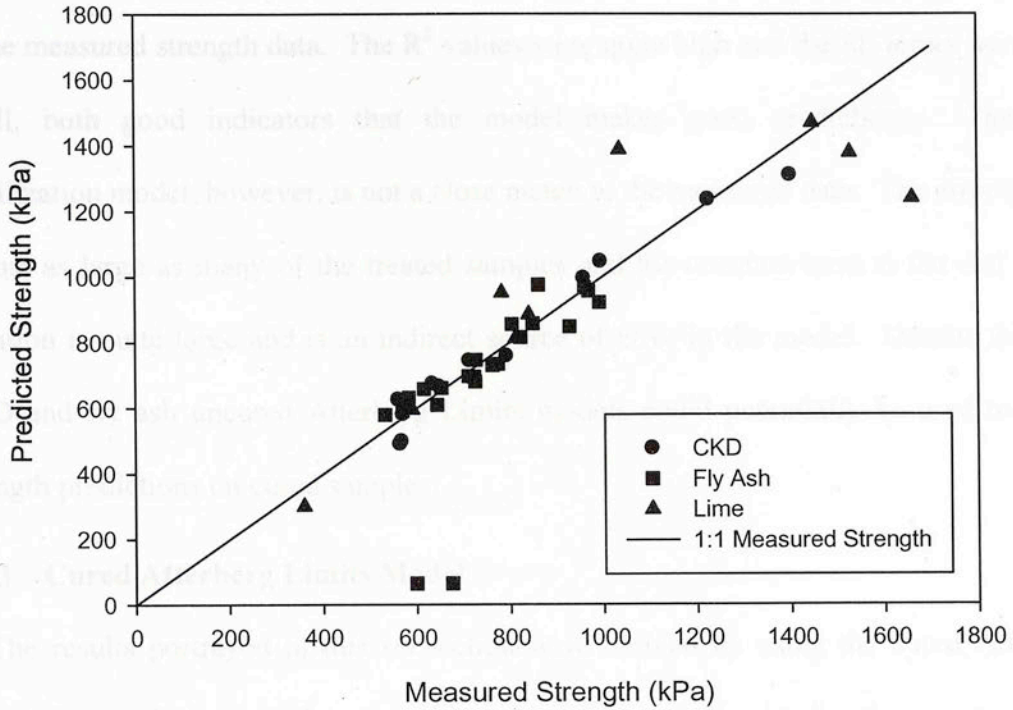


Figure 6.11 - Uncured Atterberg Limits Model for A-7-6 Soils

$$UCS_{CKD} = 81.186(\%) - 15.517(LL_o) + 4.96(PL_o) + 791.053 \quad [6.26]$$

Adjusted  $R^2 = 0.952$ , SE = 62 kPa, and N = 12.

$$UCS_{FA} = 44.563(\%) + 10.333(LL_o) - 4.191(PL_o) - 158.034 \quad [6.27]$$

Adjusted  $R^2 = 0.864$ , SE = 51 kPa, and N = 26.

$$UCS_{Lime} = 22.428(\%) + 35.939(LL_o) + 69.603(PL_o) - 3154.546 \quad [6.28]$$

Adjusted  $R^2 = 0.696$ , SE = 245 kPa, and N = 10.

The resulting equations for CKD and fly ash stabilization proved to be good matches to the measured strength data. The  $R^2$  values were quite high and the SE terms were very small, both good indicators that the model makes good predictions. The lime stabilization model, however, is not a close match to the measured data. The error term is almost as large as many of the treated samples and the constant term at the end of the equation is quite large and is an indirect source of error in the model. Despite this, the CKD and fly ash uncured Atterberg Limits models could potentially be used to make strength predictions on cured samples.

#### 6.4.3 Cured Atterberg Limits Model

The results portrayed in this subsection were derived by using the cured Atterberg Limits data to determine if used cured test results can better predict the cured strength than uncured test results can. Equations [6.29], [6.30], and [6.31] are the results of the statistical analysis and Figure 6.12 shows the predicted strength results plotted against the measured strength results.

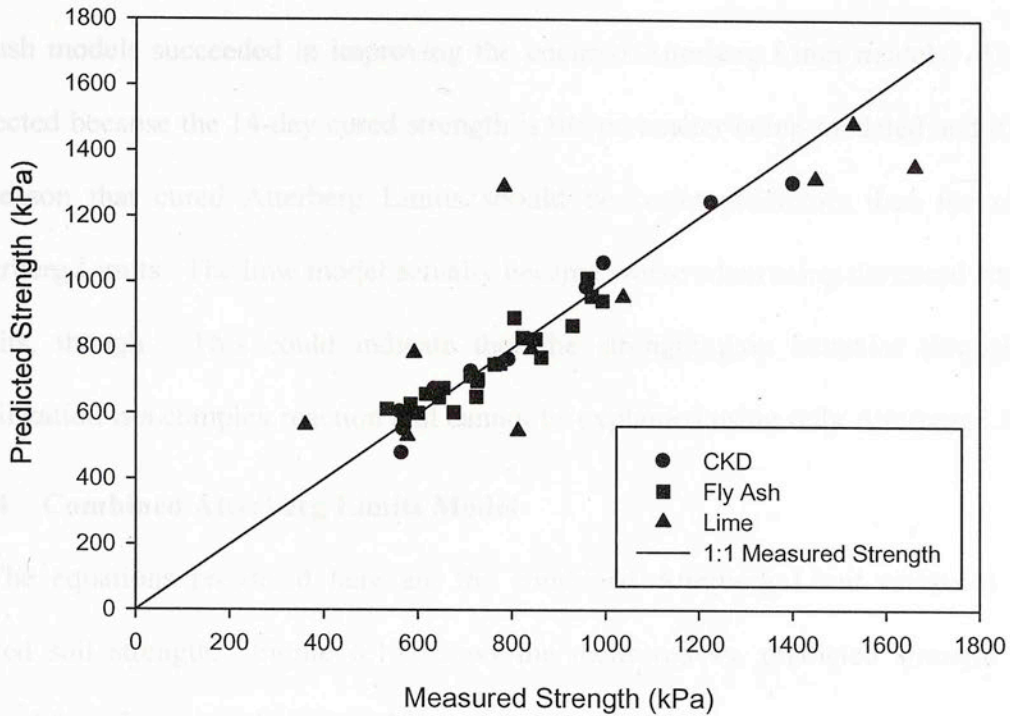


Figure 6.12 - Cured Atterberg Limits Model for A-7-6 Soils

$$UCS_{CKD} = 76.331(\%) - 4.68(LL_{14}) + 11.432(PL_{14}) - 9.255$$

[6.29]

Adjusted  $R^2 = 0.958$ , SE = 58 kPa, and N = 12.

$$UCS_{FA} = 38.499(\%) - 0.19(LL_{14}) + 8.442(PL_{14}) + 194.38$$

[6.30]

Adjusted  $R^2 = 0.872$ , SE = 50 kPa, and N = 26.

$$UCS_{Lime} = -193.747(\%) - 42.566(LL_{14}) + 97.632(PI_{14}) + 1089.221$$

[6.31]

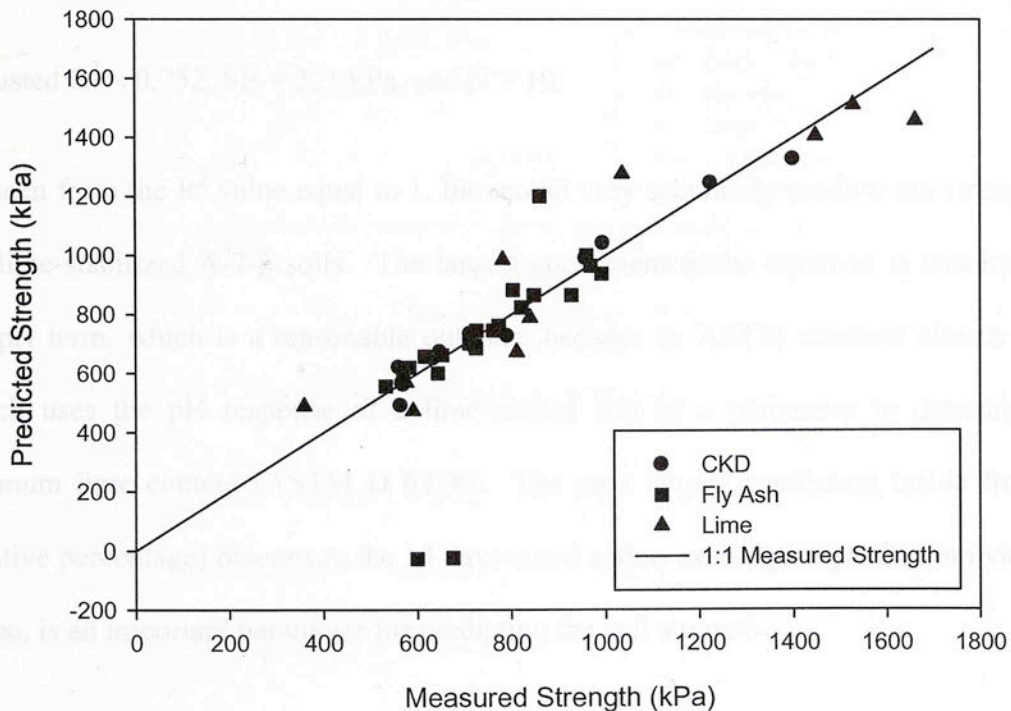
Adjusted  $R^2 = 0.551$ , SE = 298 kPa, and N = 10.



As seen by the slightly higher  $R^2$  values and the reduced SE error terms, the CKD and fly ash models succeeded in improving the uncured Atterberg Limit models. This was expected because the 14-day cured strength is the parameter being modeled and it serves to reason that cured Atterberg Limits should be better predictors than the uncured Atterberg Limits. The lime model actually became worse when using the cured Atterberg Limits, though. This could indicate that the strength gain behavior through lime stabilization is a complex reaction that cannot be explained using only Atterberg Limits.

#### 6.4.4 Combined Atterberg Limits Model

The equations presented here are the combined Atterberg Limit estimates of the treated soil strength. Figure 6.13 shows the measured vs. predicted strength results derived from Equations [6.32], [6.33], and [6.34].



#### 6.4.5 Full Analysis Model

$$UCS_{CKD} = 83.115(\%) - 14.879(LL_o) - 2.594(PL_o) + 4.309(LL_{14}) + 10.411(PL_{14}) + 425.401 \quad [6.32]$$

Adjusted  $R^2 = 0.951$ , SE = 63 kPa, and N = 12.

$$UCS_{FA} = 42.901(\%) + 9.566(LL_o) + 0.01(PL_o) - 4.603(LL_{14}) + 1.595(PL_{14}) - 14.803 \quad [6.33]$$

Adjusted  $R^2 = 0.906$ , SE = 43 kPa, and N = 26.

$$UCS_{Lime} = -218.964(\%) - 61.466(LL_o) + 48.235(PL_o) + 15.922(LL_{14}) + 79.24(PL_{14}) + 177.279 \quad [6.34]$$

Adjusted  $R^2 = 0.752$ , SE = 221 kPa, and N = 10.

As seen from the  $R^2$  value equal to 1, the model very accurately predicts the strengths of the lime-stabilized A-7-6 soils. The largest coefficient in the equation is matched with the pH term, which is a reasonable outcome because an ASTM standard already exists which uses the pH response of a lime-treated soil as a parameter to determine the optimum lime content (ASTM D 6276). The next largest coefficient (aside from the additive percentage) belongs to the 14 days cured cation exchange capacity, implying that it, too, is an important parameter for predicting the soil strength.

### 6.4.5 Full Analysis Model

Figure 6.14 shows the plotted results of the statistical analyses performed on the two A-7-6 soils. All tested parameters were available for inclusion in the different models, but only those with the strongest correlations were selected by the analysis program. Equations [6.35], [6.36], and [6.37] are the models used to determine the predicted strength points to compare against the measured strength values.

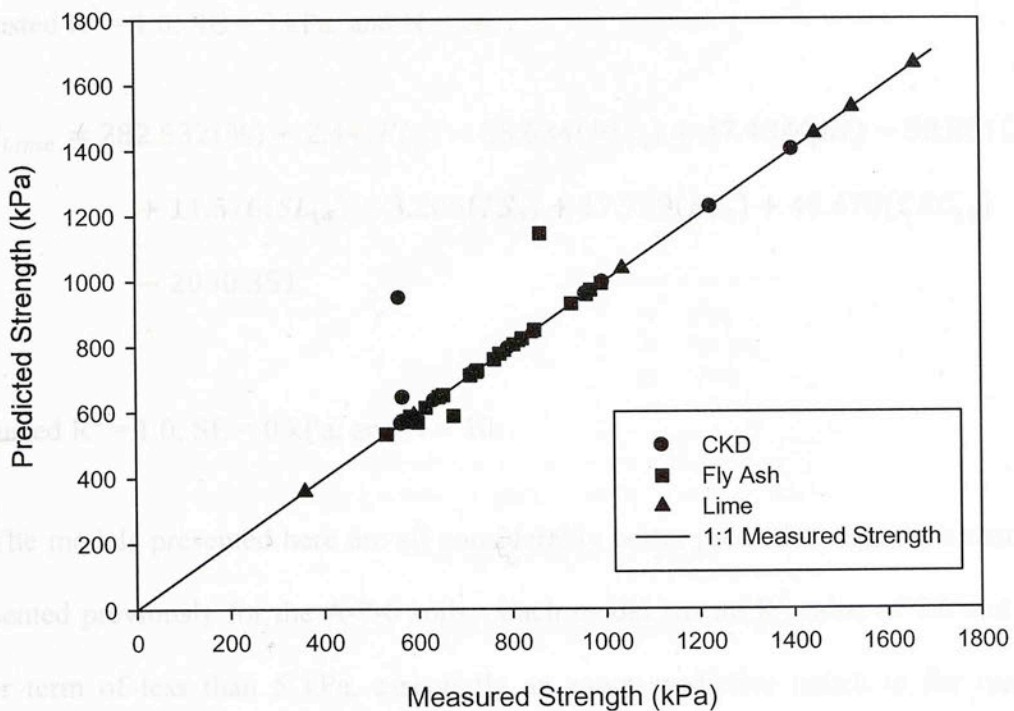


Figure 6.14 - Full Analysis Model for A-7-6 Soils

$$\begin{aligned}
 UCS_{CKD} = & 101.625(\%) - 122.813(LL_o) + 9.234(LL_{14}) + 149.607(LS_o) \\
 & + 6.394(SL_{14}) + 9.614(ES_o) - 1.885(CEC_o) - 2.194(TS_{14}) \\
 & + 4.357(CEC_{14}) + 3938.259
 \end{aligned}
 \tag{6.35}$$

Adjusted  $R^2 = 1.0$ ,  $SE = 0$  kPa, and  $N = 12$ .



$$\begin{aligned}
 UCS_{FA} = & 38.513(\%) + 62.875(LL_o) - 48.401(PL_o) + 55.367(LL_{14}) - 63.526(PL_{14}) \\
 & + 610.978(pH) - 0.846(C) - 178.195(LS_o) - 17.167(SL_o) \\
 & - 77.373(LS_{14}) - 10.118(SL_{14}) - 5.873(TS_o) + 9.738(ES_o) \\
 & + 33.874(CEC_o) + 2.314(TS_{14}) - 10.468(ES_{14}) + 0.506(CEC_{14}) \\
 & - 5595.353
 \end{aligned}
 \tag{6.36}$$

Adjusted  $R^2 = 1.0$ , SE = 3 kPa, and N = 26.

$$\begin{aligned}
 UCS_{Lime} = & 282.532(\%) - 2.44(PL_o) - 58.634(PL_{14}) + 47.434(pH) - 50.801(SL_o) \\
 & + 11.676(SL_{14}) + 3.206(TS_o) + 17.739(ES_o) + 49.478(CEC_{14}) \\
 & - 2030.351
 \end{aligned}
 \tag{6.37}$$

Adjusted  $R^2 = 1.0$ , SE = 0 kPa, and N = 10.

The models presented here are all considerably better predictive equations than those presented previously for the A-7-6 soils. Each model has an  $R^2$  value of 1.0 and an SE error term of less than 5 kPa, essentially an exact predictive match to the measured strength values. A few points strayed from the 1:1 measured strength line, but these instances were when the measured strength decreased from one point to another, but then continuously increased over the other tested percentages. These points were likely due to human errors such as improper sample preparation or incorrect testing methods. The only significant problems with these models are the very large constant terms which are indirect sources of error not reflected in the SE terms.

### 6.4.6 Practical Analysis Model

Figure 6.15 shows the plotted results of the statistical analyses using only the easy-to-test parameters. Equations [6.38], [6.39], and [6.40] are the statistical models that were used to determine the different points shown in Figure 6.15.

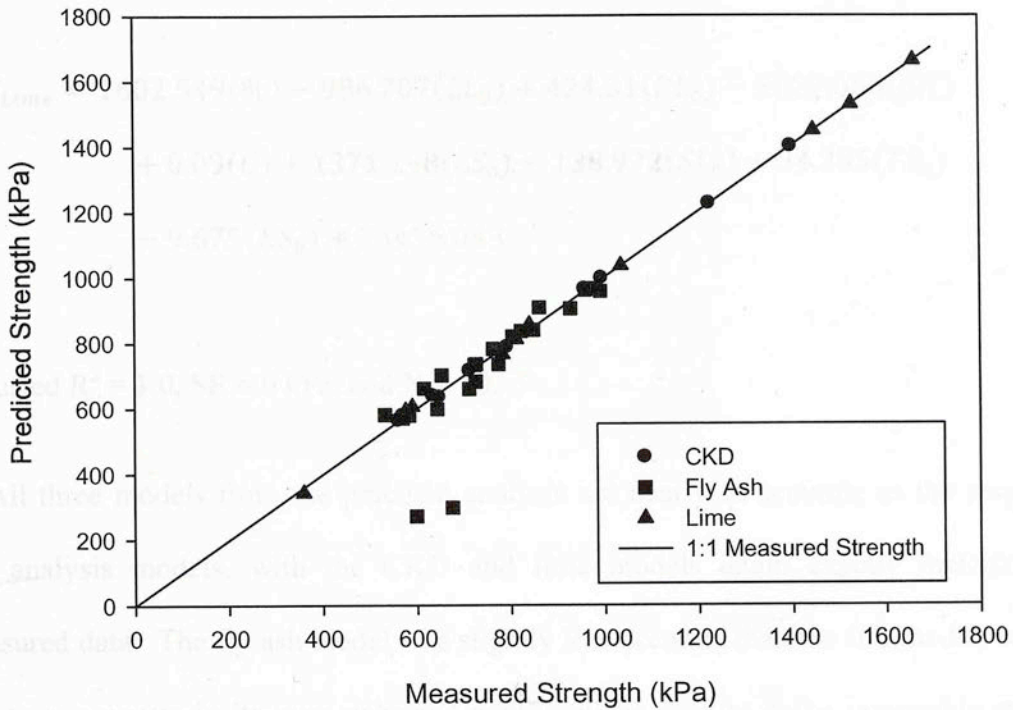


Figure 6.15 - Practical Analysis Model for A-7-6 Soils

$$\begin{aligned}
 UCS_{CKD} = & 120.715(\%) - 12.476(LL_o) - 14.084(PL_o) - 775.979(pH) + 0.188(C) \\
 & + 79.537(LS_o) + 33.108(SL_o) + 8.515(TS_o) - 2.698(ES_o) + 6201.41
 \end{aligned}
 \tag{6.38}$$

Adjusted  $R^2 = 0.998$ ,  $SE = 11$  kPa, and  $N = 12$ .

$$\begin{aligned}
 UCS_{FA} = & 26.165(\%) - 23.008(LL_o) - 14.897(PL_o) - 232.25(pH) + .0524(C) \\
 & + 71.391(LS_o) + 34.394(SL_o) + 2.005(TS_o) - 2.141(ES_o) \\
 & + 2268.966
 \end{aligned}
 \tag{6.39}$$

Adjusted  $R^2 = 0.896$ , SE = 45 kPa, and N = 26.

$$\begin{aligned}
 UCS_{Lime} = & 1602.549(\%) - 986.707(LL_o) + 424.31(PL_o) - 5027.083(pH) \\
 & + 0.09(C) + 1371.298(LS_o) - 138.972(SL_o) + 34.295(TS_o) \\
 & - 9.675(ES_o) + 73456.043
 \end{aligned}
 \tag{6.40}$$

Adjusted  $R^2 = 1.0$ , SE = 0 kPa, and N = 10.

All three models from the practical analysis are nearly as accurate as the respective full analysis models, with the CKD and lime models again exactly matching the measured data. The fly ash model was slightly less accurate than the full model, but was still very accurate in its own right and could still be used to make reasonable strength predictions. Based on the different coefficients in each model, it can be determined that the Atterberg Limits, pH, and shrinkage properties are the most important in these analyses. The only real issue with these models is the extremely large coefficient term at the end of each equation.

#### 6.4.7 Summary of A-7-6 Soil Models

Table 6-3 shows the coefficients of the best models found through the statistical analyses performed on the A-7-6 soils data.



**Table 6-3 - Coefficient of Best A-7-6 Soil Models**

	CKD	Fly Ash	Lime
Model Type	Full	Full	Practical
Adjusted R <sup>2</sup>	1.0	1.0	1.0
Standard Estimate Error	n/a	3 kPa	n/a
Number of Terms in Model	12	26	10
Constant	3938.259	-5595.353	73456.043
Additive Percentage	101.625	38.513	1602.549
Liquid Limit (0-day)	-122.813	62.875	-986.707
Plastic Limit (0-day)	0	-48.401	424.310
Liquid Limit (14-day)	9.234	55.367	0
Plastic Limit (14-day)	0	-63.526	0
pH	0	610.978	-5027.083
Conductivity	0	-.846	.090
Linear Shrinkage (0-day)	149.607	-178.195	1371.298
Shrinkage Limit (0-day)	0	-17.167	-138.972
Linear Shrinkage (14-day)	0	-77.373	0
Shrinkage Limit (14-day)	6.394	-10.118	0
Total SSA (0-day)	0	-5.873	34.295
External SSA (0-day)	9.614	9.738	-9.675
CEC (0-day)	-1.885	33.874	0
Total SSA (14-day)	-2.194	2.314	0
External SSA (14-day)	0	-10.468	0
CEC (14-day)	4.357	.506	0

For the A-7-6 soils, unlike the A-6 soils, the best prediction models are not all from the full analyses. The full analysis was the most accurate for CKD and fly ash stabilization, but the practical analysis was the best for lime stabilization. The practical model was actually as accurate as the full model, but the practical model was chosen as the best because the parameters involved are easier to determine. Based on these comparisons, it can be seen that the liquid limit (0-day), linear shrinkage (0-day), and the external SSA (0-day) parameters are the only recurring terms among the three models. However, it can also be seen that the most important equation parameters, based on the size of the leading coefficient, changes from equation to equation. This may mean that for A-7-6 soils, a set list of parameters cannot fully explain the strength gain behavior for different additives.

## **6.5 All Soils**

### **6.5.1 Introduction**

To test the limits of the statistical models discussed earlier, additional models were created. These extra models combined the data from the eight soils into their respective additive categories, resulting once again in models for CKD, fly ash, and lime. The goal of this exercise was to find out if the individual models created for each soil classification were unnecessary. Another model was run using the combined data from all eight soils with every additive, but the results were inconclusive and, as such, are not presented. The format of this subsection will follow that of the previous subsections: subsections divided up by additive with each containing five equations beginning with an uncured Atterberg Limit model and ending with a practical model.

### **6.5.2 Uncured Atterberg Limits Model**

The equations presented here tested the effectiveness of the uncured Atterberg Limits at predicting the 14 days cured strength of CKD-treated fine-grained soils ranging from A-4 to A-7-6. Equations [6.41], [6.42], and [6.43] are the statistical models for the different additives and the equations were used to determine the points in Figure 6.16 to compare the predicted strengths to the measured strengths.

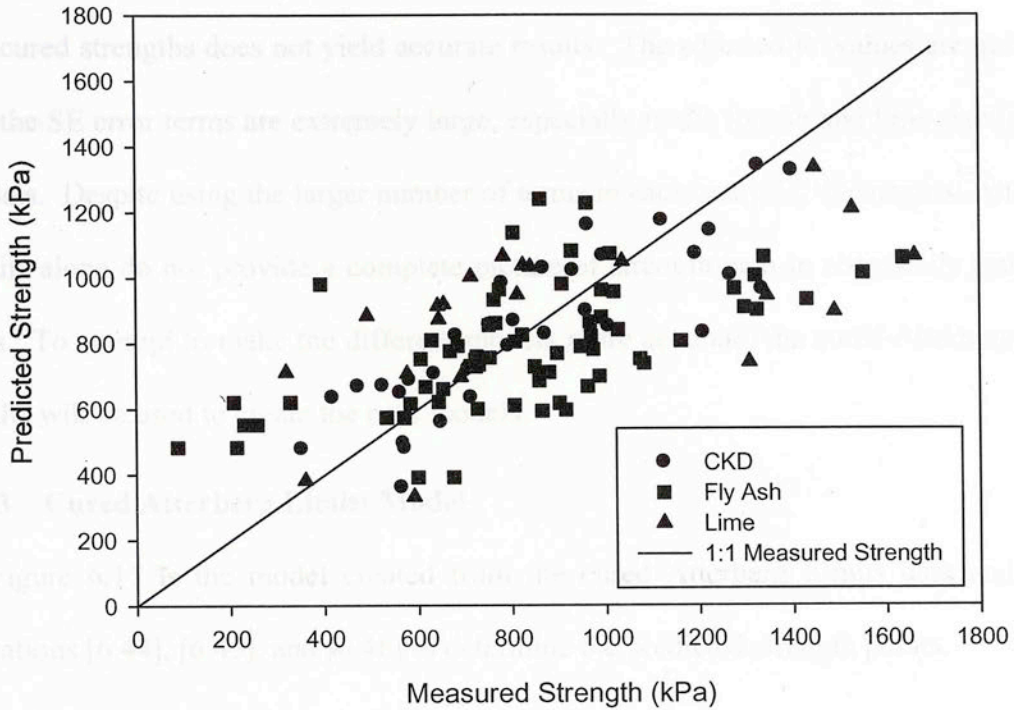


Figure 6.16 - Uncured Atterberg Limits Model for All Soils

$$UCS_{CKD} = 77.244(\%) - 11.57(LL_o) + 15.524(PL_o) + 233.418 \quad [6.41]$$

Adjusted  $R^2 = 0.684$ , SE = 165 kPa, and N = 33.

$$UCS_{FA} = 22.929(\%) - 14.649(LL_o) + 41.361(PL_o) + 277.072 \quad [6.42]$$

Adjusted  $R^2 = 0.230$ , SE = 314 kPa, and N = 71.

$$UCS_{Lime} = 42.239(\%) - 6.722(LL_o) + 47.446(PL_o) - 466.245 \quad [6.43]$$

Adjusted  $R^2 = 0.231$ , SE = 357 kPa, and N = 21.



Based on these equations, using solely the uncured Atterberg Limits to predict the 14-day cured strengths does not yield accurate results. The adjusted  $R^2$  values are quite low and the SE error terms are extremely large, especially in the fly ash and lime stabilization models. Despite using the larger number of terms in each analysis, the uncured Atterberg Limits alone do not provide a complete picture of strength gain in chemically stabilized soils. To attempt to make the different models more accurate, the cured Atterberg Limit results will be used to create the next models.

### 6.5.3 Cured Atterberg Limits Model

Figure 6.17 is the model created from the cured Atterberg Limits data and using Equations [6.44], [6.45], and [6.46] to determine the predicted strength points.

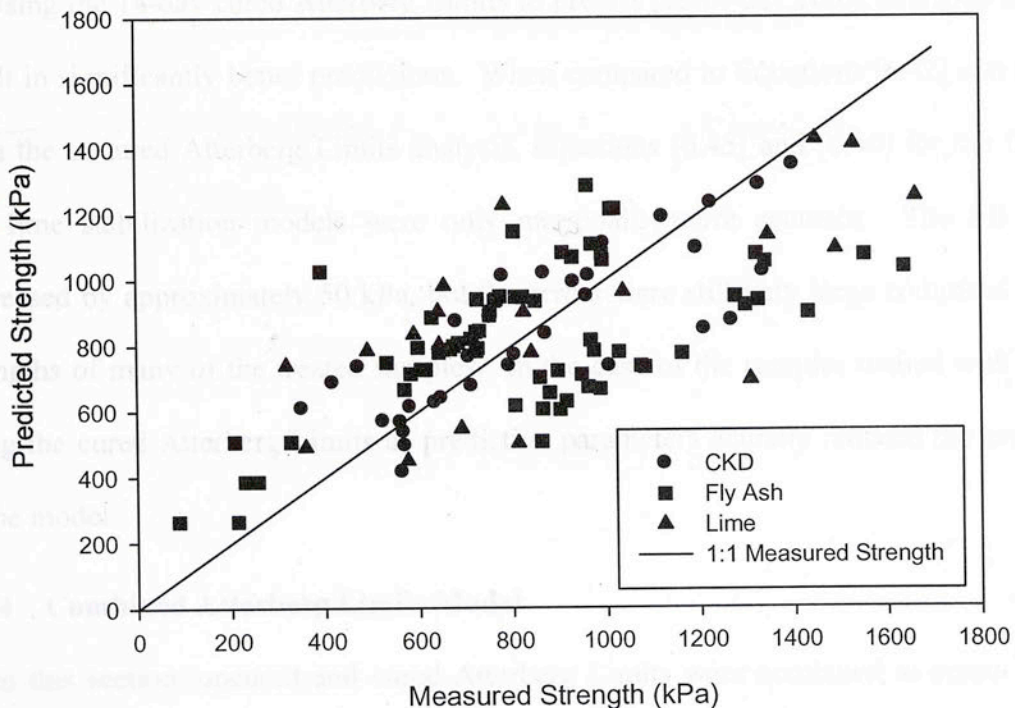


Figure 6.17 - Cured Atterberg Limits Model for All Soils

$$UCS_{CKD} = 68.681(\%) - 15.423(LL_{14}) + 25.939(PL_{14}) + 187.85 \quad [6.44]$$

Adjusted  $R^2 = 0.645$ , SE = 174 kPa, and N = 33.

$$UCS_{FA} = 40.531(\%) - 1.033(LL_{14}) + 28.071(PL_{14}) - 100.56 \quad [6.45]$$

Adjusted  $R^2 = 0.494$ , SE = 255 kPa, and N = 71.

$$UCS_{Lime} = -1.441(\%) + 5.463(LL_{14}) + 65.02(PL_{14}) - 1107.045 \quad [6.46]$$

Adjusted  $R^2 = 0.407$ , SE = 313 kPa, and N = 21.

Using the 14-day cured Atterberg Limits to predict the 14-day cured strengths did not result in significantly better predictions. When compared to Equations [6.42] and [6.43] from the uncured Atterberg Limits analysis, Equations [6.45] and [6.46] for the fly ash and lime stabilization models were only marginally more accurate. The SE terms decreased by approximately 50 kPa, but the errors were still very large compared to the strengths of many of the treated samples. In the case of the samples treated with CKD, using the cured Atterberg Limits as predictive parameters actually reduced the accuracy of the model.

#### 6.5.4 Combined Atterberg Limits Model

In this section, uncured and cured Atterberg Limits were combined to create a new model in an attempt to better predict the strength gains. In keeping with the same pattern of analysis, Figure 6.18 is the plot created by using the statistical models for each of the three additive types in Equations [6.47], [6.48], and [6.49].

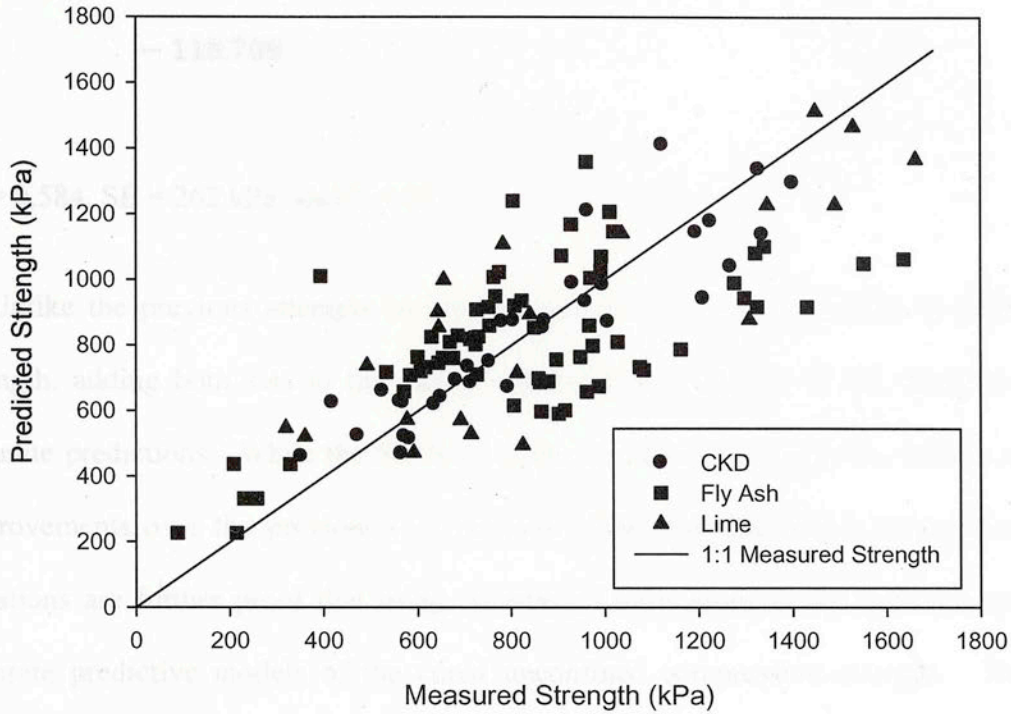


Figure 6.18 - Combined Atterberg Limits Model for All Soils

$$\begin{aligned}
 UCS_{CKD} = & 84.707(\%) - 22.086(LL_o) - 7.348(PL_o) + 15.96(LL_{14}) + 14.7(PL_{14}) \\
 & + 194.003
 \end{aligned}$$

[6.47]

Adjusted  $R^2 = 0.794$ , SE = 133 kPa, and N = 33.

$$\begin{aligned}
 UCS_{FA} = & 35.066(\%) - 10.604(LL_o) + 24.466(PL_o) + 5.208(LL_{14}) + 13.833(PL_{14}) \\
 & - 88.707
 \end{aligned}$$

[6.48]

Adjusted  $R^2 = 0.498$ , SE = 254 kPa, and N = 71.



$$UCS_{Lime} = -35.92(\%) - 80.24(LL_o) + 30.74(PL_o) + 50.012(LL_{14}) + 62.88(PL_{14}) - 118.708$$

[6.49]

$R^2 = 0.584$ ,  $SE = 262$  kPa, and  $N = 21$ .

Unlike the previous attempts to use just one set of Atterberg Limits to predict the strength, adding both sets to the model improved the capacity of the model to make accurate predictions. While the SE error terms are still rather high, the models are still improvements over the previous two versions. The poor predictions from these three equations are further proof that using Atterberg Limits alone is not sufficient to make accurate predictive models of the cured unconfined compression strength. The next model will use many more parameters to attempt to further improve the model predictions.

### 6.5.5 Full Analysis Model

Using the full suite of tested parameters resulted in the three statistical “full” models Equations [6.50], [6.51], and [6.52]. Solving each of those equations using the actual tested data resulted in different predicted strength values which are plotted against the corresponding measured strength values in Figure 6.19.

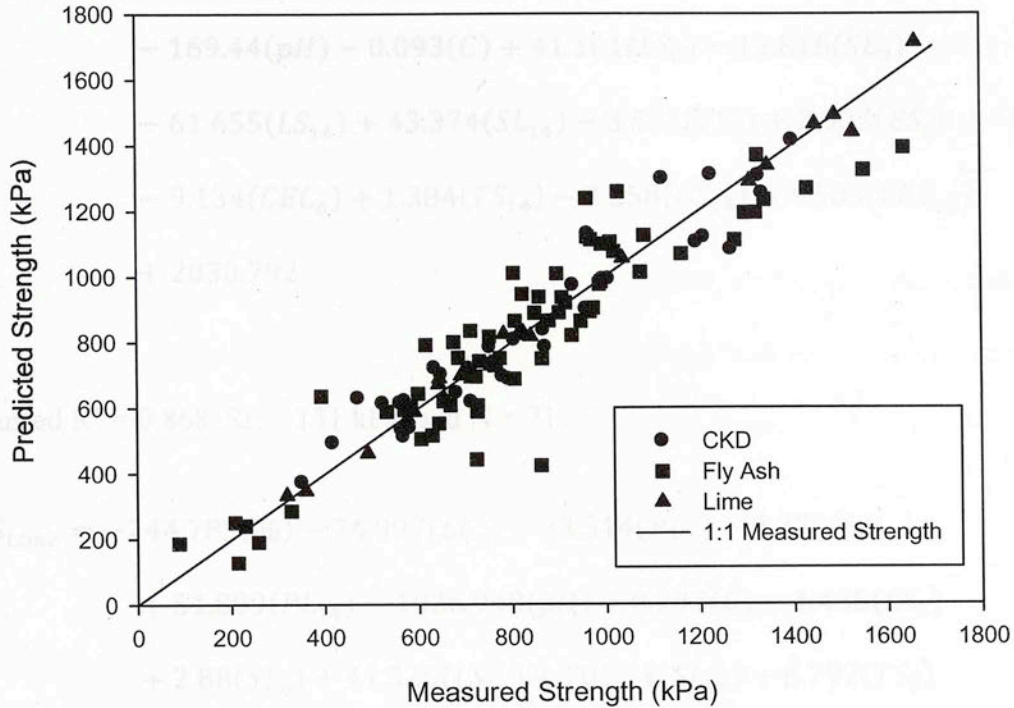


Figure 6.19 - Full Analysis Model for All Soils

$$\begin{aligned}
 UCS_{CKD} = & 139.062(\%) + 6.833(LL_0) - 0.158(PL_0) - 9.313(LL_{14}) + 1.196(PL_{14}) \\
 & + 182.803(pH) - 0.181(C) - 106.132(LS_0) + 14.635(SL_0) \\
 & + 55.3(LS_{14}) - 13.171(SL_{14}) - 0.767(TS_0) + 4.642(ES_0) \\
 & - 1.196(CEC_0) + 1.191(TS_{14}) - 0.394(ES_{14}) - 2.304(CEC_{14}) \\
 & - 1477.208
 \end{aligned}$$

[6.50]

Adjusted  $R^2 = 0.822$ ,  $SE = 124$  kPa, and  $N = 33$ .

$$\begin{aligned}
 UCS_{FA} = & 40.24(\%) - 8.063(LL_o) + 26.081(PL_o) + 8.222(LL_{14}) - 0.918(PL_{14}) \\
 & - 169.44(pH) - 0.093(C) + 41.101(LS_o) - 12.816(SL_o) \\
 & - 61.655(LS_{14}) + 43.374(SL_{14}) - 3.531(TS_o) + 2.905(ES_o) \\
 & - 9.134(CEC_o) + 1.384(TS_{14}) - 3.258(ES_{14}) + 4.505(CEC_{14}) \\
 & + 2030.792
 \end{aligned}$$

[6.51]

Adjusted  $R^2 = 0.868$ , SE = 131 kPa, and N = 71.

$$\begin{aligned}
 UCS_{Lime} = & -244.785(\%) - 74.997(LL_o) - 33.314(PL_o) - 0.279(LL_{14}) \\
 & + 51.899(PL_{14}) - 1026.948(pH) + 0.293(C) - 1.435(LS_o) \\
 & + 2.88(SL_o) + 41.325(LS_{14}) + 70.324(SL_{14}) + 6.792(TS_o) \\
 & + 10.62(ES_o) + 0.082(CEC_o) + 3.627(TS_{14}) - 37.722(ES_{14}) \\
 & - 9.851(CEC_{14}) + 13603.472
 \end{aligned}$$

[6.52]

$R^2 = 0.960$ , SE = 82 kPa, and N = 21.

As seen by the drastically reduced scatter in Figure 6.19 as compared to the other most accurate model, Figure 6.18, the full models provide much better predictions of the 14-day cured strengths. The SE error for the CKD model was approximately 10 kPa lower than the SE from the combined Atterberg Limits analysis, and in the cases of the fly ash and lime stabilization models, the error terms were decreased by approximately 50% between the combined Atterberg Limits model and the full model. Despite these improvements, the error terms are still relatively large in comparison to some of the measured strength values. This could pose a problem if these equations were adopted for



use in the construction industry where under-predicting the strength of a treated soil could have severe consequences. However, the fact that the models did improve lends support to the concept that equations could be created that are not soil group specific.

### 6.5.6 Practical Analysis Model

After running the full analyses on the three chemical stabilizer groups, the same analyses were repeated using only the relatively simple tests that can be done over a short period of time. The results of this “practical” analysis are shown in Figure 6.20 and the plot was created using Equations [6.53], [6.54], and [6.55].

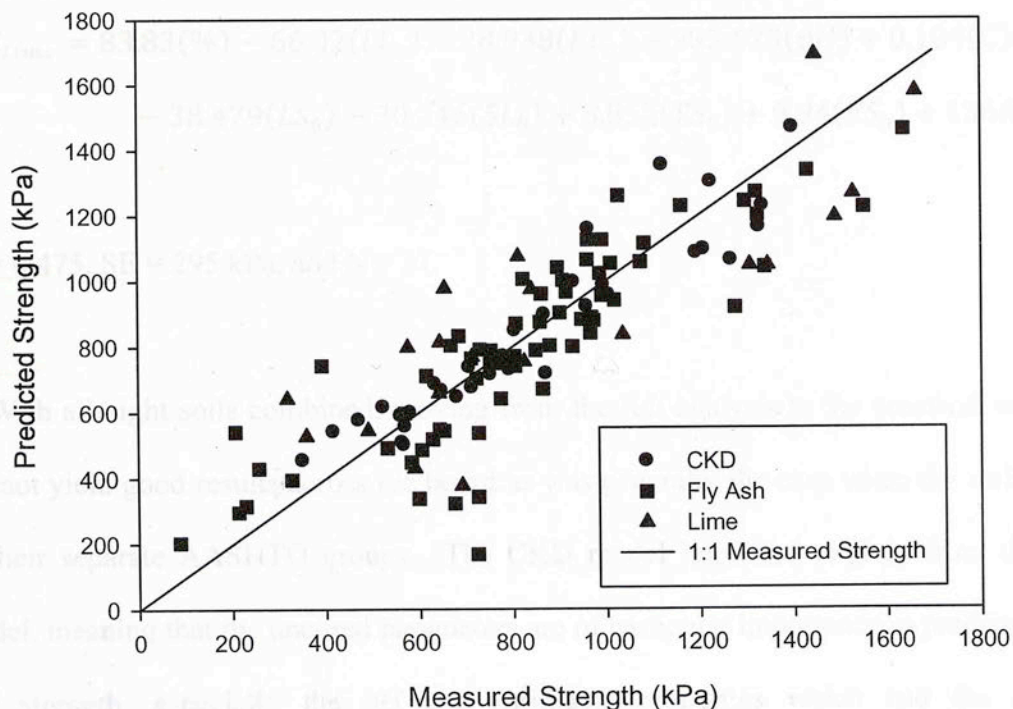


Figure 6.20 - Practical Analysis Model for All Soils

$$UCS_{CKD} = 127.885(\%) - 3.631(LL_o) - 1.874(PL_o) - 46.804(pH) - 0.148(C) \\ - 56.391(LS_o) - 0.972(SL_o) + 1.239(TS_o) + 9.945(ES_o) + 1043.109$$

[6.53]

Adjusted  $R^2 = 0.843$ , SE = 116 kPa, and N = 33.

$$UCS_{FA} = 45.453(\%) - 28.181(LL_o) + 53.289(PL_o) - 249.622(pH) - 0.089(C) \\ + 46.885(LS_o) + 9.899(SL_o) - 5.16(TS_o) + 6.39(ES_o) + 2847.74$$

[6.54]

Adjusted  $R^2 = 0.650$ , SE = 212 kPa, and N = 71.

$$UCS_{Lime} = 83.83(\%) - 66.02(LL_o) + 28.938(PL_o) - 993.679(pH) + 0.104(C) \\ - 38.479(LS_o) - 30.746(SL_o) + 8.855(TS_o) + 9.94(ES_o) + 13665.294$$

[6.55]

$R^2 = 0.475$ , SE = 295 kPa, and N = 21.

With all eight soils combined, moving from the full analysis to the practical analysis did not yield good results across the board as was generally the case when the soils were in their separate AASHTO groups. The CKD model improved slightly from the full model, meaning that the uncured parameters are of particular importance in predicting the soil strength, especially the pH and shrinkage properties which had the largest coefficients. Both the fly ash and lime models became markedly less accurate in the practical model than they were in their respective full models. This likely indicates that the cured parameters are more important for these two chemical stabilizers, or that the cation exchange capacity may be more important in these instances than with CKD

stabilization because the fly ash and lime models became less accurate when the cured parameters and the CEC values were removed from the model.

### 6.5.7 Summary of Combined Soil Models

Table 6-4 contains the coefficients of the best models from the statistical analyses of the data from the eight soils combined and the related statistical values of those models.

**Table 6-4 - Coefficients of Best Combined Soil Models**

	CKD	Fly Ash	Lime
Model Type	Practical	Full	Full
Adjusted R <sup>2</sup>	0.843	0.868	0.960
Standard Estimate Error	116 kPa	131 kPa	82 kPa
Number of Terms in Model	33	71	21
Constant	1043.109	2030.792	13603.472
Additive Percentage	127.885	40.240	-244.785
Liquid Limit (0-day)	-3.631	-8.063	-74.997
Plastic Limit (0-day)	-1.874	26.081	-33.314
Liquid Limit (14-day)	0	8.222	-.279
Plastic Limit (14-day)	0	-.918	51.899
pH	-46.804	-169.440	-1026.948
Conductivity	-.148	-.093	.293
Linear Shrinkage (0-day)	-56.391	41.101	-1.435
Shrinkage Limit (0-day)	-.972	-12.816	2.880
Linear Shrinkage (14-day)	0	-61.655	41.325
Shrinkage Limit (14-day)	0	43.374	70.324
Total SSA (0-day)	1.239	-3.531	6.792
External SSA (0-day)	9.945	2.905	10.620
CEC (0-day)	0	-9.134	.082
Total SSA (14-day)	0	1.384	3.627
External SSA (14-day)	0	-3.258	-37.722
CEC (14-day)	0	4.505	-9.851

As expected, the full and practical analysis models produced the best predictor equations when the eight soils were analyzed together. For CKD stabilization, the practical analysis model actually provided a slightly lower estimate error than the full model. The full model was the most accurate for fly ash and lime stabilization. As noted earlier, a few parameters seem to reappear in each of the best models, in the different



AASHTO group analyses and in the combined analysis. The most notable of these parameters are the pH, the shrinkage properties, and the surface area properties. The cation exchange capacity also seems to be important, but it has an involved testing procedure that may limit its effectiveness for strength predictions. These four soil properties, combined with the Atterberg Limits, are important properties to include in future predictions of the stabilized soil strength.

## **6.6 Optimum Additive Percentage Prediction Using Raw Soils**

### **6.6.1 Introduction**

After performing the different analyses to try to predict the strength of chemically stabilized soils, new models were created in an attempt to predict the optimum additive percentage, the first additive percentage at which a particular soil reaches the 345 kPa strength gain over the raw soil strength, using only various properties of the different raw soils. Multiple scenarios were tested involving different combinations of parameters to find the best predictions. However, only three different models will be presented in this subsection: a model using only the Atterberg Limits, a model using all available tested properties of the raw soils, and a model using the Atterberg Limits, average pH, and the clay size fraction of each soil. These models were chosen because they provided the most accurate optimum additive percentage predictions and contained easy-to-test parameters, especially in the case of the Atterberg Limits model and the Atterberg Limits, average pH, and clay fraction model.

### **6.6.2 Atterberg Limits Model**

The first attempt at predicting the optimum additive percentage of a treated soil was done using only the raw soil Atterberg Limits. Figure 6.21 shows the predicted optimum

percentage points plotted against the measured optimum percentages. The plots were created by substituting actual values into the predictions made by Equations [6.56], [6.57], and [6.58].

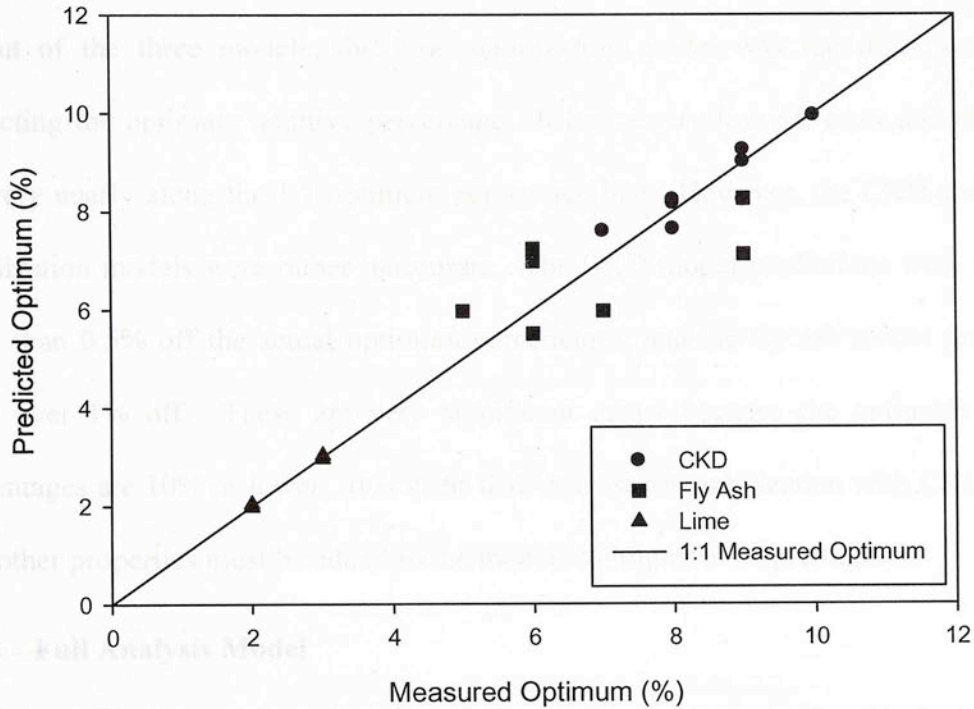


Figure 6.21 - Atterberg Limits Model for Raw Soils

$$Op\%_{CKD} = 0.007(UCS^+) + 0.061(LL_0) - 0.205(PL_0) + 5.137 \quad [6.56]$$

Adjusted  $R^2 = 0.639$ , SE = 0.556 %, and N = 8.

$$Op\%_{FA} = 0.021(UCS^+) + 0.037(LL_0) - 0.512(PL_0) + 1.424 \quad [6.57]$$

Adjusted  $R^2 = 0.199$ , SE = 1.317 %, and N = 13.

$$Op\%_{Lime} = 0.013(UCS^+) - 0.084(LL_0) + 0.227(PL_0) - 6.471$$

[6.58]

Adjusted  $R^2 = 0.985$ , SE = 0.068 %, and N = 5.

Out of the three models, the lime stabilization model was the most accurate at predicting the optimum additive percentage. It had a very low SE error and the points fell very nearly along the 1:1 optimum percentage line. However, the CKD and fly ash stabilization models were rather inaccurate. The CKD model predictions were typically more than 0.5% off the actual optimum percentages, and the fly ash model predictions were over 1% off. These are very significant errors because the optimum additive percentages are 10% or lower. It is clear that, at least for stabilization with CKD and fly ash, other properties must be added to the models to improve the predictions.

### 6.6.3 Full Analysis Model

Figure 6.22 shows the results of the full analysis on the raw soils with the individual points determined by solving Equations [6.59], [6.60], and [6.61] with the actual data values.



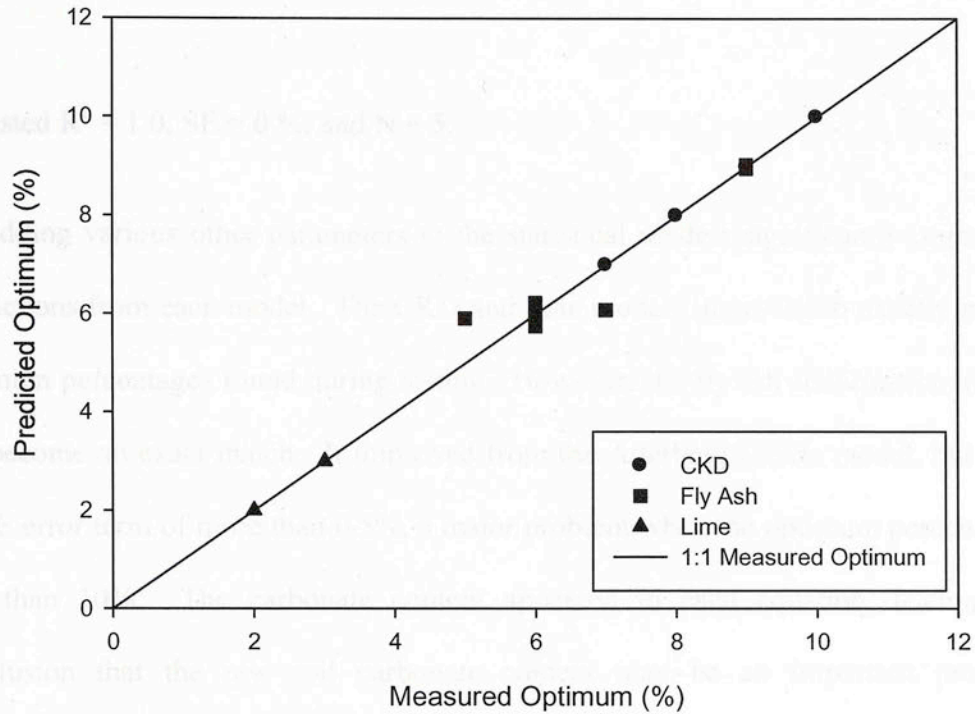


Figure 6.22 - Full Analysis Model for Raw Soils

$$Op\%_{CKD} = 0.11(LL_0) - 0.139(PL_0) - 0.846(pH) + 0.648(pH_{avg}) + 0.00019(Sulf) - 0.03(Clay) - 0.085(Carb) + 7.818$$

[6.59]

Adjusted  $R^2 = 1.0$ , SE = 0 %, and N = 8.

$$Op\%_{FA} = -0.003(UCS^+) - 1.9(pH) + 0.965(pH_{avg}) + 0.001(C) - 0.00039(Sulf) - 0.092(Carb) + 15.96$$

[6.60]

Adjusted  $R^2 = 0.789$ , SE = 0.676 %, and N = 13.

$$Op\%_{Lime} = 0.00017(UCS^+) - 0.001(C) + 0.039(CEC_0) - 0.018(Carb) + 2.682 \quad [6.61]$$

Adjusted  $R^2 = 1.0$ , SE = 0 %, and N = 5.

Adding various other parameters to the statistical models significantly improved the predictions from each model. The CKD and lime models improved to exactly match the optimum percentages found during testing. However, the fly ash stabilization model did not become an exact match. It improved from the Atterberg Limits model, but still had an SE error term of more than 0.5%, a major problem when the optimum percentages are less than 10%. The carbonate content appeared in each equation, leading to the conclusion that the raw soil carbonate content may be an important property to investigate when predicting the optimum additive percentage.

#### 6.6.4 Atterberg Limits, Average pH, and Clay Fraction Model

The results of the statistical analyses performed using the Atterberg Limits, the average pH, and the clay fraction are shown in Equations [6.62], [6.63], and [6.64], which were used to calculate the points shown in Figure 6.23

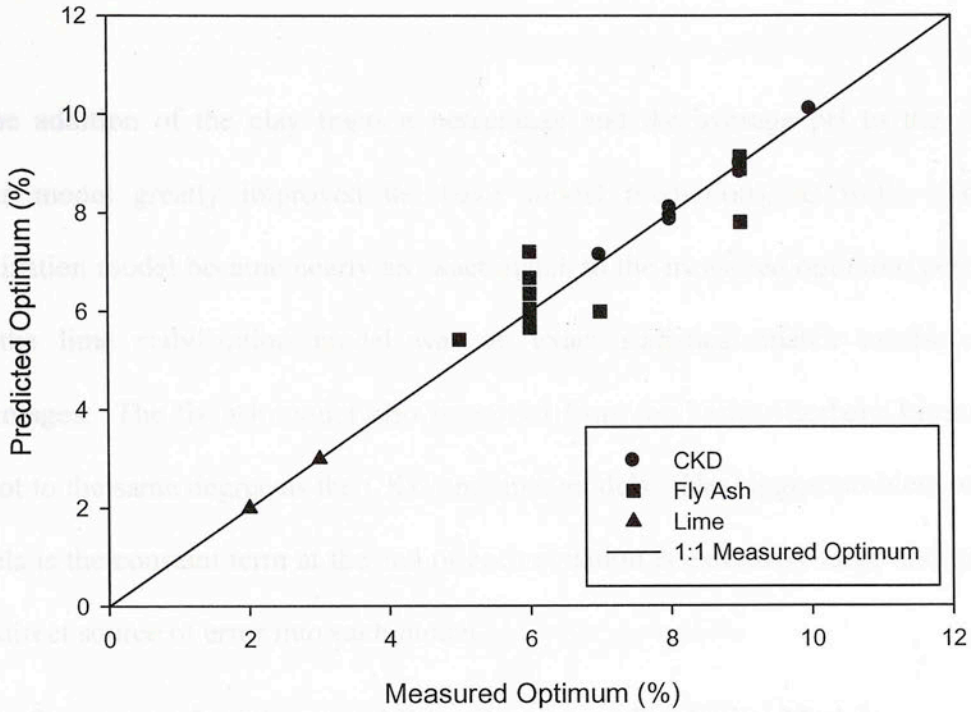


Figure 6.23 - Atterberg Limits, Average pH, and Clay Fraction Model for Raw Soils

$$Op\%_{CKD} = 0.03(UCS^+) - 0.057(Clay) + 0.02(LL_0) - 0.198(PL_0) + 1.132(pH_{avg}) - 17.538$$

[6.62]

Adjusted  $R^2 = 0.944$ ,  $SE = 0.220$  %, and  $N = 8$ .

$$Op\%_{FA} = 0.066(UCS^+) - 0.211(LL_0) + 0.301(PL_0) - 0.106(Clay) + 3.165(pH_{avg}) - 57.43$$

[6.63]

Adjusted  $R^2 = 0.549$ ,  $SE = 0.988$  %, and  $N = 13$ .

$$Op\%_{Lime} = 0.00047(UCS^+) + 0.02(Clay) + 1.419(pH_{avg}) + 0.01(PI_0) - 15.403$$

[6.64]



Adjusted  $R^2 = 1.0$ , SE = 0 %, and N = 5.

The addition of the clay fraction percentage and the average pH to the Atterberg Limits model greatly improved the basic model predictions, as well. The CKD stabilization model became nearly an exact match to the measured optimum percentages, and the lime stabilization model was an exact statistical match to the optimum percentages. The fly ash model also improved from the basic Atterberg Limits model, but not to the same degree as the CKD and lime models. The biggest problem with these models is the constant term at the end of each equation is extremely large and introduces an indirect source of error into each model.

### 6.6.5 Summary of Optimum Additive Percentage Prediction Models

Table 6.5 presents a summary of the most accurate raw soil models and the coefficients of each term in those models.

**Table 6-5 - Coefficients of Best Raw Soil Models**

Model Type	CKD Full	Fly Ash Full	Lime Atterberg, Average pH, and Clay Fraction
Adjusted $R^2$	1.0	0.789	1.0
Standard Estimate Error	0 %	0.676%	0 %
Number of Terms in Model	8	13	5
Constant	7.818	15.960	-15.403
UCS <sup>+</sup>	0	-.003	.00047
Liquid Limit (0-day)	.110	0	0
Plastic Limit (0-day)	-.139	0	0
Plasticity Index (0-day)	0	0	.010
Conductivity	0	.001	0
pH	-.846	-1.900	0
Average pH	.648	.965	1.419
Sulfate Content	.00019	-0.00039	0
Clay Fraction	-.030	0	.020
Carbonate Content	-.085	-.092	0

The best models for stabilization with CKD and fly ash were the full models and the best model for lime stabilization was the Atterberg Limit, average pH, and clay fraction model. For CKD and lime, the models were able to exactly predict the optimum additive percentage with the given data using only a few different parameters, most notably the average pH and the clay fraction of the soil. The fly ash stabilization full model was the most accurate of the three different fly ash models, but was not very accurate overall. The SE error was over 0.65% and the constant term was also very large. This model still put significant emphasis on the average pH term as the other two did. This repetition may perhaps indicate that the average pH may be a parameter of interest when trying to predict the optimum additive percentage using raw soils alone. The only problem with using the average pH is that one needs to know the average pH at the percentage of interest, which happens to be the parameter that the model is trying to predict.

## **CHAPTER 7: CONCLUSIONS AND RECOMMENDATIONS**

### **7.1 Introduction**

This chapter presents conclusions gathered during the evaluation of this study on the effects of chemical additives on soil parameters and the prediction of stabilized soil strengths. Additionally, recommendations are presented for future research and interpretation of the analytical models.

The overall objective of this research was to determine soil parameters that would predict adequate strength gain for stabilized subgrade soils more accurately than the current classification system based on Atterberg Limits. To accomplish this objective, eight common fine-grained soils (classified as either A-4, A-6, or A-7-6 soils by the

AASHTO classification system) were sampled from across the state of Oklahoma, tested with four different chemical additives, and then subjected to various soil property tests to determine the effects of these different properties on predictions of the stabilized soil strength.

## 7.2 Conclusions

Based on the results of the research work conducted, the following conclusions may be made:

1. In general, the use of the Atterberg Limits alone does not provide an accurate prediction of the stabilized strength.
2. Model predictions were considerably more accurate when the soils were divided according to the AASHTO classification.
3. The more parameters, whether from cured or uncured tests, which can be added to a predictive model for the soil strength, the more accurate that model will become. In each instance, adding the 14 days cured Atterberg Limits to the uncured Atterberg Limits model improved it, and adding the full set of tested parameters to the cured/uncured Atterberg Limits model significantly improved that model also.
4. The pH response of soils treated with CKD and fly ash is similar to that of the lime response, but the pH curves with fly ash never reached a constant value. However, additional research is needed to see if a standard pH threshold can be established for these stabilizers.



5. The pH is a significant factor in predicting the stabilized strength of fine-grained soils. The pH term was never removed by the analysis algorithms and routinely carried the largest leading coefficient in each model equation.

The bar linear shrinkage test also provides valuable data for predicting stabilized soil strengths. As with the pH parameter, the shrinkage properties appeared in each full analysis model and generally carried the next-highest leading coefficients after the pH. Since the shrinkage test is a direct measure of the capacity of a soil to undergo drying-induced shrinkage, it is a good test to include when dealing with problematic shrinking/expanding soils. As noted earlier in Table 5.1 - Table of Linear Shrinkage Decreases over 345 kPa Strength Gain, a specific decrease in the value of the linear shrinkage could be used to determine the optimum additive percentage to achieve adequate stabilization. For example, if an A-6 soil treated with 8% CKD shows a linear shrinkage decrease of 3% from the raw soil linear shrinkage, then that soil should be adequately stabilized.

6. The specific surface area test should be included in any prediction of the stabilized strengths of fine-grained soils. While the terms never had the highest coefficients, specific surface area terms appeared in each of the full parameter models. Even in the practical variations of the full models, the uncured total specific surface area parameter was never excluded from the final model equation.

7. For fine-grained soils, the cation exchange capacity is a significant strength predictor. The terms usually did not have large coefficients, but they continually showed up in the full models. Also, when the cation exchange capacity terms

were left out of the practical models and some accuracy was lost, leading to the conclusion that the CEC is an effective parameter at predicting strengths.

8. Attempts at combining all fine-grained soils together into additive-specific groups can provide general predictions of stabilized soil strengths. However, these models have higher estimate errors than the models separated by soil classification.
9. It is possible to use only parameters from raw soils to predict the optimum additive percentages. The full models were typically the most accurate, but the models using only the Atterberg Limits, clay fraction, and average pH were also effective at making predictions. These models are promising because being able to predict the optimum additive percentage while only testing a raw soil would save considerable time and effort during testing.
10. Based on the results of this study, improvements, shown in Table 7-1, can be made to the OHD L – 50 Design Table.

**Table 7-1 - OHD L-50 Soil Stabilization Table (ODOT, 2006)**

SOIL STABILIZATION TABLE												
ADDITIVE (Expressed as a percentage added on dry over basis)	SOIL GROUP CLASSIFICATION – AASHTO M145											
	A-1		A-2				A-3	A-4	A-5	A-6	A-7	
	A-1-a	A-1-b	A-2-4	A-2-5	A-2-6	A-2-7					A-7-5	A-7-6
<b>PORTLAND CEMENT</b>	4	4	4	4	4	4	5	√	√	√		
<b>FLY ASH</b>					10	10	11	12	12	6+		9+
<b>CEMENT KILN DUST (Pre-Calciner Plants)</b>	4	4	4	4	4	4	5	√	√			
<b>CEMENT KILN DUST (Other Type Plants)</b>	8	8	8	9	9	9	10	10	10	9+		9+
<b>HYDRATED LIME*</b>										3+	5**	3+

A blank in the table indicates the additive is not recommended for that soil group. Recommended amounts include a safety factor for loss due to wind, grading, and/or mixing. Pre-calciner plants are identified on the Materials Division approved list for cement kiln dust.

√ = Mix Design Required

\* = Reduce quantity by 20% when quick lime is used, i.e. 4% x 0.8 = 3.2%, 5% x 0.8 = 4.0%, 6% x 0.8 = 4.8%

\*\* = Use 6% when liquid limit is greater than 50.

+ = Addition or modification to the design chart based on results from this study

### 7.3 Recommendations

Based on the outcomes of the current research, several recommendations can be made with respect to future research plans and the interpretation of the models.

1. Compare the laboratory results from this study to the actual stabilized soil properties from the same soils treated in the field.
2. Investigate the bonding between the different additives and the individual soil particles using an advanced microscopy technique.
3. Investigate the CEC response of soil-additive mixtures to determine if the CEC is a time-dependent property.
4. Link the current study results to resilient modulus test data to provide a larger picture of stabilized soil properties to the road construction industry.
5. Verify the model equations through additional lab testing and correlate the results to field test results before adopting the analytical models.
6. Test additional soils to determine if a standard can be established for strength gain based upon changes in the linear shrinkage.
7. Modify existing mix design procedures to include the bar linear shrinkage test as a parameter to determine the optimum additive content and stabilized soil strength.



## REFERENCES

- AASHTO (2002). "Standard Method of Test for Determining Water-Soluble Sulfate Ion Content in Soil," Test Designation T 290-95, *Standard Specifications for Transportation Materials and Methods of Sampling and Testing*, Part 2B Tests.
- Akbulut, S., Arasan, S., and Kalkan, E. (2007). "Modification of Clayey Soils Using Scrap Tire Rubber and Synthetic Fibers." *Applied Clay Science*. Vol. 38. pp 23 – 32.
- A1-Amoudi, O.S.B. (1994). "Chemical Stabilization of Sabkha Soils at High Moisture Contents." *Engineering Geology*. Volume 36. pp. 279-291.
- Arabi, M., Delpak, R., and Wild, S. (1988). "Assessment of the Unconfined Compressive Strength of a Lime Stabilized Soil by an Abrasion Test." *Geotechnical Testing Journal*. GTJODJ. Vol. 11, No. 1. pp 56 – 59.
- ASTM. (2005). *American Society for Testing and Materials Annual Book of ASTM Standards*, Volume 04.08, Soil and Rock (I): D 420 – D 5611. West Conshohocken, Pennsylvania.
- Bozbey, I., and Garaisayev, S. (2009) "Effects of Soil Pulverization Quality on Lime Stabilization of an Expansive Clay." *Environmental Earth Sciences*.
- Brooks, R., Udoeyo, F., and Takkalapelli, K. (2009). "Compaction Delay Characteristics of Clay with Cement Kiln Dust." *Proceedings of the Institution of Civil Engineers, Geotechnical Engineering* 162. pp 283 – 286.
- Brunauer, S., Emmett, P. H., and Teller, E. (1938). "Adsorption of Gases in Multi Molecular Layers," *Journal of the American Chemical Society*, Vol. 60, pp. 309-319.
- BS 1377 (1990). *British Standard Methods of Testing for Soils for Civil Engineering Purposes*. British Standards Institution, London.
- Buhler, R., and Cerato, A. (2007). "Stabilization of Oklahoma Expansive Soils Using Lime and Class C Fly Ash." *GeoDenver: New Peaks in Geotechnics*. GSP 162: Problematic Soils and Rocks and In Situ Characterization. Denver, CO, Feb. 18-21, 2007.
- Carter, D. L., Mortland, M. M., and Kemper, W. D. (1986). "Specific Surface. Methods of Soil Analysis," Chapter 16, *Agronomy*, No.9, Part 1, 2<sup>nd</sup> Ed., American Society of Agronomy.
- Cerato, A., and Lutenegeger, A. (2002). "Determination of Surface Area of Fine-Grained Soils by the Ethylene Glycol Monoethyl Ether (EGME) Method." *Geotechnical Testing Journal*. Vol. 25, No. 3.

- Çokça, E. (2001). "Use of Class C Fly Ashes for the Stabilization of an Expansive Soil." *Journal of Geotechnical and Geoenvironmental Engineering*. pp 568 – 573.
- Das, Braja M. (2007). *Principles of Foundation Engineering*. 6<sup>th</sup> ed. Cengage Learning, Stamford, CT.
- Dreimanis, A. (1962) "Quantitative Gasometric Determination of Calcite and Dolomite by Using Chittick Apparatus," *Journal of Sedimentary Petrology*, Vol. 32, p. 520-529.
- Heidema, P.B. (1957). The Bar-Shrinkage Test and the Practical Importance of Bar-Linear Shrinkage as an Identifier of Soils. *Proceedings of the 4<sup>th</sup> International Conference on Soil Mechanics and Foundation Engineering*, Vol. 1, pp. 44-48.
- Hossain, K., Lachemi, M., and Easa, S. (2007). "Stabilized Soils for Construction Applications Incorporating Natural Resources of Papua New Guinea." *Resources, Conservation, & Recycling*. Vol. 51. pp. 711 – 731.
- IDOT. (2005). "Pavement Technology Advisory – Subgrade Modification and Stabilization – PTA-D7." Illinois DOT (IDOT) Bureau of Materials and Physical Research.
- Khoury, N., and Khoury, C. (2005). "New Laboratory Methods for Characterization of Compaction in Fine-Grained Soils." Internal Report, School of Civil Engineering and Environmental Science, The University of Oklahoma.
- Lionjanga, A.V., Toole, T., and Greening, P.A.K.. (1987). "The Use of Calcrete in Paved Roads in Botswana." 9<sup>th</sup> Regional Conference for Africa on Soil Mechanics and Foundation Engineering. Lagos, Nigeria. September, 1987.
- Little, D., Males, E., Prusinski, J., and Stewart, B. (2000). "Cementitious Stabilization." *A2J01: Committee on Cementitious Stabilization*. Transportation Research Board of the National Academies. Accessed 17 Feb, 2010.
- Mackiewicz, S., and Ferguson, E. (2005). "Stabilization of Soil with Self-Cementing Coal Ashes." Center for Applied Energy Research, University of Kentucky, Lexington. [www.flyash.info/2005/108mac.pdf](http://www.flyash.info/2005/108mac.pdf).
- Miller, G., and Azad, S. (2000), "Influence of Soil Type on Stabilization with Cement Kiln Dust." *Construction and Building Materials*. Vol. 14, No. 2, pp. 89-97.
- Miller, G., Azad, S., and Dhar, B. (1997). "The Effect of Cement Kiln Dust on the Collapse Potential of Compacted Shale." *Testing Soil Mixed with Waste or Recycled Materials, ASTM STP 1275*. Wasemiller, M. and Hoddinott, K., Eds. American Society for Testing of Materials.



- Miller, G.A., and Zaman, M. (2000). "Field and Laboratory Evaluation of Cement Kiln Dust as a Soil Stabilizer." *Transportation Research Record*. No. 1714. pp 25 – 32.
- Mohamed, A. (2002). "Hydro-Mechanical Evaluation of Soil Stabilized with Cement-Kiln Dust in Arid Lands." *Environmental Geology*. Vol. 42. pp 910 – 921.
- ODOT. (2005). "OHD L – 49: Method of Test for Determining Soluble Sulfate Content in Soil," *Oklahoma DOT (OKDOT) Department Test Methods (OHDL)*.
- ODOT. (2006). "OHD L – 50: Soil Stabilization Mix Design Procedure," *Oklahoma DOT (OKDOT) Department Test Methods (OHDL)*.
- Olive, W., Chleborad, A., Frahme, C., Shlocker, J., Schneider, R., and Schuster, R. (1989). "Map I-1940 – Swelling Clays Map of the Conterminous United States." USGS Miscellaneous Investigations Series. United States Geologic Survey (USGS).
- Rhoades, J.D. (1982). "Cation Exchange Capacity," In A.L. Page, et al, Eds. *Methods of Soil Analysis*. Agronomy 9, 2<sup>nd</sup> ed. American Society of Agronomy, Madison, WI, pp. 159-165.
- Roy, L. (1988). "Comparative Study of Tensile and Compressive Strength of Lime and Rice Husk Ash Stabilized Soils." *Indian Geotechnical Conference, December 15-17, 1988, on Evaluation and Applications in Geotechnical Engineering, Proceedings*. Vol 1.
- Si, Z., and Herrera, C. (2007). "Laboratory and Field Evaluation of Base Stabilization Using Cement Kiln Dust." *Transportation Research Record: Journal of the Transportation Research Board, No. 1989*, Vol. 2. pp 42 – 49.
- Singh, S., Tripathy, D., and Ranjith, P. (2008). "Performance Evaluation of Cement Stabilizer Fly Ash – GBFS Mixes as a Highway Construction Material." *Waste Management*. Vol. 28. pp 1331 – 1337.
- Turner, J. (1997). "Evaluation of Western Coal Fly Ashes for Stabilization of Low-Volume Roads." *Testing Soil Mixed with Waste or Recycled Materials, ASTM STP 1275*. Wasemiller, M. and Hoddinott, K., Eds. American Society for Testing of Materials.
- U.S. Army, U.S. Air Force and U.S. Navy (2005). *Soil Stabilization for Pavements*. University Press of the Pacific, Honolulu, Hawaii.
- Yukselen, Y., and Kaya, A. (2006). "Prediction of Cation Exchange Capacity from Soil Index Properties." *Clay Minerals*. Vol. 41. pp 827 – 837.



## LIST OF FIGURES

Figure A.1: Deval (A-4) OMC Curves with C&D	153
Figure A.2: Deval (A-4) OMC Curves with Red Rock Fly Ash	154
Figure A.3: Ashport-Granite (A-6) OMC Curves with C&D	155
Figure A.4: Ashport-Granite (A-6) OMC Curves with L&S	156
Figure A.5: Ashport-Granite (A-6) OMC Curves with Red Rock Fly Ash	157
Figure A.6: Ashport-Granite (A-6) OMC Curves with New England Fly Ash	158
Figure A.7: Kirkland-Pawnee (A-8) OMC Curves with C&D	159
Figure A.8: Kirkland-Pawnee (A-8) OMC Curves with L&S	160
Figure A.9: Kirkland-Pawnee (A-8) OMC Curves with Red Rock Fly Ash	161
Figure A.10: Kirkland-Pawnee (A-8) OMC Curves with New England Fly Ash	162
Figure A.11: Flower Pot (A-9) OMC Curves with C&D	163
Figure A.12: Flower Pot (A-9) OMC Curves with L&S	164
Figure A.13: Flower Pot (A-9) OMC Curves with Red Rock Fly Ash	165
Figure A.14: Flower Pot (A-9) OMC Curves with New England Fly Ash	166
Figure A.15: Hollywood (A-7) OMC Curves with C&D	167
Figure A.16: Hollywood (A-7) OMC Curves with L&S	168
Figure A.17: Hollywood (A-7) OMC Curves with Red Rock Fly Ash	169
Figure A.18: Hollywood (A-7) OMC Curves with New England Fly Ash	170
Figure A.19: Heiden (A-5) OMC Curves with C&D	171
Figure A.20: Heiden (A-5) OMC Curves with L&S	172
Figure A.21: Heiden (A-5) OMC Curves with Red Rock Fly Ash	173
Figure A.22: Heiden (A-5) OMC Curves with New England Fly Ash	174
Figure A.23: UCS Plots for A-1 to A-9 with C&D	175
Figure A.24: UCS Plots for A-1 to A-9 with L&S	176
Figure A.25: UCS Plots for A-1 to A-9 with Red Rock Fly Ash	177
Figure A.26: UCS Plots for A-1 to A-9 with New England Fly Ash	178
Figure A.27: UCS Plots for A-1 to A-9 with Red Rock Fly Ash	179
Figure A.28: UCS Plots for A-1 to A-9 with New England Fly Ash	180
Figure A.29: UCS Plots for A-1 to A-9 with C&D	181
Figure A.30: UCS Plots for A-1 to A-9 with L&S	182
Figure A.31: UCS Plots for A-1 to A-9 with Red Rock Fly Ash	183
Figure A.32: UCS Plots for A-1 to A-9 with New England Fly Ash	184
Figure A.33: Payne (A-4) Admixtures with C&D	185
Figure A.34: Payne (A-4) Admixtures with Red Rock Fly Ash	186
Figure A.35: Deval (A-4) Admixtures with C&D	187
Figure A.36: Ashport-Granite (A-6) Admixtures with C&D	188
Figure A.37: Ashport-Granite (A-6) Admixtures with L&S	189
Figure A.38: Ashport-Granite (A-6) Admixtures with Red Rock Fly Ash	190
Figure A.39: Ashport-Granite (A-6) Admixtures with New England Fly Ash	191
Figure A.40: Kirkland-Pawnee (A-8) Admixtures with C&D	192
Figure A.41: Kirkland-Pawnee (A-8) Admixtures with L&S	193
Figure A.42: Kirkland-Pawnee (A-8) Admixtures with Red Rock Fly Ash	194
Figure A.43: Kirkland-Pawnee (A-8) Admixtures with New England Fly Ash	195
Figure A.44: Flower Pot (A-9) Admixtures with C&D	196
Figure A.45: Flower Pot (A-9) Admixtures with L&S	197
Figure A.46: Flower Pot (A-9) Admixtures with Red Rock Fly Ash	198
Figure A.47: Flower Pot (A-9) Admixtures with New England Fly Ash	199
Figure A.48: Hollywood (A-7) Admixtures with C&D	200
Figure A.49: Hollywood (A-7) Admixtures with L&S	201
Figure A.50: Hollywood (A-7) Admixtures with Red Rock Fly Ash	202
Figure A.51: Hollywood (A-7) Admixtures with New England Fly Ash	203
Figure A.52: Heiden (A-5) Admixtures with C&D	204
Figure A.53: Heiden (A-5) Admixtures with L&S	205
Figure A.54: Heiden (A-5) Admixtures with Red Rock Fly Ash	206
Figure A.55: Heiden (A-5) Admixtures with New England Fly Ash	207

## APPENDIX A

## LIST OF FIGURES

Figure A.1: Devol (A-4) OMC Curves with CKD .....	158
Figure A.2: Devol (A-4) OMC Curves with Red Rock Fly Ash .....	158
Figure A.3: Ashport-Grainola (A-6) OMC Curves with CKD .....	160
Figure A.4: Ashport-Grainola (A-6) OMC Curves with Lime .....	160
Figure A.5: Ashport-Grainola (A-6) OMC Curves with Red Rock FA .....	161
Figure A.6: Ashport-Grainola (A-6) OMC Curves with Muskogee FA.....	161
Figure A.7: Kirkland-Pawhuska (A-6) OMC Curves with CKD .....	163
Figure A.8: Kirkland-Pawhuska (A-6) OMC Curves with Lime .....	163
Figure A.9: Kirkland-Pawhuska (A-6) OMC Curves with Red Rock FA.....	164
Figure A.10: Kirkland-Pawhuska (A-6) OMC Curves with Muskogee FA .....	164
Figure A.11: Flower Pot (A-6) OMC Curves with CKD.....	166
Figure A.12: Flower Pot (A-6) OMC Curves with Lime.....	166
Figure A.13: Flower Pot (A-6) OMC Curves with Red Rock FA.....	167
Figure A.14: Flower Pot (A-6) OMC Curves with Muskogee FA .....	167
Figure A.15: Hollywood (A-7-6) OMC Curves with CKD.....	169
Figure A.16: Hollywood (A-7-6) OMC Curves with Lime.....	169
Figure A.17: Hollywood (A-7-6) OMC Curves with Red Rock FA .....	170
Figure A.18: Hollywood (A-7-6) OMC Curves with Muskogee FA.....	170
Figure A.19: Heiden (A-7-6) OMC Curves with CKD .....	172
Figure A.20: Heiden (A-7-6) OMC Curves with Lime .....	172
Figure A.21: Heiden (A-7-6) OMC Curves with Red Rock FA.....	173
Figure A.22: Heiden (A-7-6) OMC Curves with Muskogee FA.....	173
Figure A.23: UCS Plots for A-4 Soils with CKD.....	175
Figure A.24: UCS Plots for A-4 Soils with Red Rock FA .....	175
Figure A.25: UCS Plots for A-6 Soils with CKD.....	176
Figure A.26: UCS Plots for A-6 Soils with Lime.....	176
Figure A.27: UCS Plots for A-6 Soils with Red Rock FA .....	177
Figure A.28: UCS Plots for A-6 Soils with Muskogee FA.....	177
Figure A.29: UCS Plots for A-7-6 Soils with CKD.....	178
Figure A.30: UCS Plots for A-7-6 Soils with Lime.....	178
Figure A.31: UCS Plots for A-7-6 Soils with Red Rock FA .....	179
Figure A.32: UCS Plots for A-7-6 Soils with Muskogee FA .....	179
Figure A.33: Payne (A-4) Atterberg Limits with CKD .....	181
Figure A.34: Payne (A-4) Atterberg Limits with Red Rock FA.....	181
Figure A.35: Devol (A-4) Atterberg Limits with CKD .....	183
Figure A.36: Ashport-Grainola (A-6) Atterberg Limits with CKD.....	184
Figure A.37: Ashport-Grainola (A-6) Atterberg Limits with Lime.....	184
Figure A.38: Ashport-Grainola (A-6) Atterberg Limits with Red Rock FA .....	185
Figure A.39: Ashport-Grainola (A-6) Atterberg Limits with Muskogee FA .....	185
Figure A.40: Kirkland-Pawhuska (A-6) Atterberg Limits with CKD .....	187
Figure A.41: Kirkland-Pawhuska (A-6) Atterberg Limits with Lime .....	187
Figure A.42: Kirkland-Pawhuska (A-6) Atterberg Limits with Red Rock FA.....	188
Figure A.43: Kirkland-Pawhuska (A-6) Atterberg Limits with Muskogee FA.....	188
Figure A.44: Flower Pot (A-6) Atterberg Limits with CKD .....	190
Figure A.45: Flower Pot (A-6) Atterberg Limits with Lime .....	190



Figure A.46: Flower Pot (A-6) Atterberg Limits with Red Rock FA.....	191
Figure A.47: Flower Pot (A-6) Atterberg Limits with Muskogee FA.....	191
Figure A.48: Hollywood (A-7-6) Atterberg Limits with CKD.....	193
Figure A.49: Hollywood (A-7-6) Atterberg Limits with Lime.....	193
Figure A.50: Hollywood (A-7-6) Atterberg Limits with Red Rock FA.....	194
Figure A.51: Hollywood (A-7-6) Atterberg Limits with Muskogee FA.....	194
Figure A.52: Heiden (A-7-6) Atterberg Limits with CKD.....	196
Figure A.53: Heiden (A-7-6) Atterberg Limits with Lime.....	196
Figure A.54: Heiden (A-7-6) Atterberg Limits with Red Rock FA.....	197
Figure A.55: Heiden (A-7-6) Atterberg Limits with Muskogee FA.....	197
Figure A.56: Devol (A-4) Shrinkage Curves with CKD.....	199
Figure A.57: Devol (A-4) Shrinkage Curves with Red Rock FA.....	199
Figure A.58: Ashport-Grainola (A-6) Shrinkage Curves with CKD.....	201
Figure A.59: Ashport-Grainola (A-6) Shrinkage Curves with Lime.....	201
Figure A.60: Ashport-Grainola (A-6) Shrinkage Curves with Red Rock FA.....	202
Figure A.61: Ashport-Grainola (A-6) Shrinkage Curves with Muskogee FA.....	202
Figure A.62: Kirkland-Pawhuska (A-6) Shrinkage Curves with CKD.....	204
Figure A.63: Kirkland-Pawhuska (A-6) Shrinkage Curves with Lime.....	204
Figure A.64: Kirkland-Pawhuska (A-6) Shrinkage Curves with Red Rock FA.....	205
Figure A.65: Kirkland-Pawhuska (A-6) Shrinkage Curves with Muskogee FA.....	205
Figure A.66: Flower Pot (A-6) Shrinkage Curves with CKD.....	207
Figure A.67: Flower Pot (A-6) Shrinkage Curves with Lime.....	207
Figure A.68: Flower Pot (A-6) Shrinkage Curves with Red Rock FA.....	208
Figure A.69: Flower Pot (A-6) Shrinkage Curves with Muskogee FA.....	208
Figure A.70: Hollywood (A-7-6) Shrinkage Curves with CKD.....	210
Figure A.71: Hollywood (A-7-6) Shrinkage Curves with Lime.....	210
Figure A.72: Hollywood (A-7-6) Shrinkage Curves with Red Rock FA.....	211
Figure A.73: Hollywood (A-7-6) Shrinkage Curves with Muskogee FA.....	211
Figure A.74: Heiden (A-7-6) Shrinkage Curves with CKD.....	213
Figure A.75: Heiden (A-7-6) Shrinkage Curves with Lime.....	213
Figure A.76: Heiden (A-7-6) Shrinkage Curves with Red Rock FA.....	214
Figure A.77: Heiden (A-7-6) Shrinkage Curves with Muskogee FA.....	214
Figure A.78: pH Curves for A-4 Soils with CKD.....	216
Figure A.79: pH Curves for A-4 Soils with Red Rock FA.....	216
Figure A.80: Conductivity Curves for A-4 Soils with CKD.....	217
Figure A.81: Conductivity Curves for A-4 Soils with Red Rock FA.....	217
Figure A.82: pH Curves for A-6 Soils with CKD.....	219
Figure A.83: pH Curves for A-6 Soils with Lime.....	219
Figure A.84: pH Curves for A-6 Soils with Red Rock FA.....	220
Figure A.85: pH Curves for A-6 Soils with Muskogee FA.....	220
Figure A.86: Conductivity Curves for A-6 Soils with CKD.....	221
Figure A.87: Conductivity Curves for A-6 Soils with Lime.....	221
Figure A.88: Conductivity Curves for A-6 Soils with Red Rock FA.....	222
Figure A.89: Conductivity Curves for A-6 Soils with Muskogee FA.....	222
Figure A.90: pH Curves for A-7-6 Soils with CKD.....	224
Figure A.91: pH Curves for A-7-6 Soils with Lime.....	224



Figure A.92: pH Curves for A-7-6 Soils with Red Rock FA.....	225
Figure A.93: pH Curves for A-7-6 Soils with Muskogee FA.....	225
Figure A.94: Conductivity Curves for A-7-6 Soils with CKD .....	226
Figure A.95: Conductivity Curves for A-7-6 Soils with Lime .....	226
Figure A.96: Conductivity Curves for A-7-6 Soils with Red Rock FA.....	227
Figure A.97: Conductivity Curves for A-7-6 Soils with Muskogee FA.....	227
Figure A.98: Cation Exchange Capacity Curves for A-4 Soils with CKD.....	229
Figure A.99: Cation Exchange Capacity Curves for A-4 Soils with Red Rock FA .....	229
Figure A.100: Cation Exchange Capacity Curves for A-6 Soils with CKD.....	231
Figure A.101: Cation Exchange Capacity Curves for A-6 Soils with Lime.....	231
Figure A.102: Cation Exchange Capacity Curves for A-6 Soils with Red Rock FA .....	232
Figure A.103: Cation Exchange Capacity Curves for A-6 Soils with Muskogee FA ....	232
Figure A.104: Cation Exchange Capacity Curves for A-7-6 Soils with CKD .....	234
Figure A.105: Cation Exchange Capacity Curves for A-7-6 Soils with Lime .....	234
Figure A.106: Cation Exchange Capacity Curves for A-7-6 Soils with Red Rock FA..	235
Figure A.107: Cation Exchange Capacity Curves for A-7-6 Soils with Muskogee FA.	235
Figure A.108: Total SSA Curves for A-4 Soils with CKD .....	237
Figure A.109: External SSA Curves for A-4 Soils with CKD .....	237
Figure A.110: Internal SSA Curves for A-4 Soils with CKD .....	238
Figure A.111: Total SSA Curves for A-4 Soils with Red Rock FA .....	238
Figure A.112: External SSA Curves for A-4 Soils with Red Rock FA.....	239
Figure A.113: Internal SSA Curves for A-4 Soils with Red Rock FA.....	239
Figure A.114: Total SSA Curves for A-6 Soils with CKD .....	241
Figure A.115: External SSA Curves for A-6 Soils with CKD .....	241
Figure A.116: Internal SSA Curves for A-6 Soils with CKD .....	242
Figure A.117: Total SSA Curves for A-6 Soils with Lime .....	242
Figure A.118: External SSA Curves for A-6 Soils with Lime .....	243
Figure A.119: Ashport-Grainola (A-6) Internal SSA Curves with Lime .....	243
Figure A.120: Total SSA Curves for A-6 Soils with Red Rock FA .....	244
Figure A.121: External SSA Curves for A-6 Soils with Red Rock FA.....	244
Figure A.122: Internal SSA Curves for A-6 Soils with Red Rock FA.....	245
Figure A.123: Total SSA Curves for A-6 Soils with Muskogee FA .....	245
Figure A.124: External SSA Curves for A-6 Soils with Muskogee FA .....	246
Figure A.125: Internal SSA Curves for A-6 Soils with Muskogee FA .....	246
Figure A.126: Total SSA Curves for A-7-6 Soils with CKD .....	250
Figure A.127: External SSA Curves for A-7-6 Soils with CKD .....	250
Figure A.128: Internal SSA Curves for A-7-6 Soils with CKD .....	251
Figure A.129: Total SSA Curves for A-7-6 Soils with Lime .....	251
Figure A.130: External SSA Curves for A-7-6 Soils with Lime .....	252
Figure A.131: Internal SSA Curves for A-7-6 Soils with Lime .....	252
Figure A.132: Total SSA Curves for A-7-6 Soils with Red Rock FA.....	253
Figure A.133: External SSA Curves for A-7-6 Soils with Red Rock FA.....	253
Figure A.134: Internal SSA Curves for A-7-6 Soils with Red Rock FA.....	254
Figure A.135: Total SSA Curves for A-7-6 Soils with Muskogee FA.....	254
Figure A.136: External SSA Curves for A-7-6 Soils with Muskogee FA.....	255
Figure A.137: Internal SSA Curves for A-7-6 Soils with Muskogee FA.....	255



## LIST OF TABLES

Table A-1: Devol (A-4) OMC and Dry Unit Weight Values .....	159
Table A-2: Anadarko (A-4) OMC and Dry Unit Weight Values .....	159
Table A-3: Payne (A-4) OMC and Dry Unit Weight Values .....	159
Table A-4: Ashport-Grainola (A-6) OMC and Dry Unit Weight Values.....	162
Table A-5: Kirkland-Pawhuska (A-6) OMC and Dry Unit Weight Values .....	165
Table A-6: Flower Pot (A-6) OMC and Dry Unit Weight Values .....	168
Table A-7: Hollywood (A-7-6) OMC and Dry Unit Weight Values.....	171
Table A-8: Heiden (A-7-6) OMC and Dry Unit Weight Values .....	174
Table A-9: UCS Values for All Soils .....	180
Table A-10: Anadarko (A-4) Atterberg Limits.....	182
Table A-11: Payne (A-4) Atterberg Limits.....	182
Table A-12: Devol (A-4) Atterberg Limits.....	183
Table A-13: Ashport-Grainola (A-6) Atterberg Limits .....	186
Table A-14: Kirkland-Pawhuska (A-6) Atterberg Limits.....	189
Table A-15: Flower Pot (A-6) Atterberg Limits.....	192
Table A-16: Hollywood (A-7-6) Atterberg Limits .....	195
Table A-17: Heiden (A-7-6) Atterberg Limits.....	198
Table A-18: Devol (A-4) Shrinkage Values .....	200
Table A-19: Anadarko (A-4) Shrinkage Values .....	200
Table A-20: Payne (A-4) Shrinkage Values .....	200
Table A-21: Ashport-Grainola (A-6) Shrinkage Values.....	203
Table A-22: Kirkland-Pawhuska (A-6) Shrinkage Values .....	206
Table A-23: Flower Pot (A-6) Shrinkage Values .....	209
Table A-24: Hollywood (A-7-6) Shrinkage Values.....	212
Table A-25: Heiden (A-7-6) Shrinkage Values.....	215
Table A-26: Measured pH and Conductivity Values for A-4 Soils.....	218
Table A-27: Measured pH and Conductivity Values for A-6 Soils.....	223
Table A-28: Measured pH and Conductivity Values for A-7-6 Soils .....	228
Table A-29: Cation Exchange Capacity Values for A-4 Soils .....	230
Table A-30: Cation Exchange Capacity Values for A-6 Soils .....	233
Table A-31: Cation Exchange Capacity Values for A-7-6 Soils .....	236
Table A-32: Devol (A-4) Specific Surface Area Values .....	240
Table A-33: Anadarko (A-4) Specific Surface Area Values .....	240
Table A-34: Payne (A-4) Specific Surface Area Values .....	240
Table A-35: Ashport-Grainola (A-6) Specific Surface Area Values.....	247
Table A-36: Kirkland-Pawhuska (A-6) Specific Surface Area Values .....	248
Table A-37: Flower Pot (A-6) Specific Surface Area Values .....	249
Table A-38: Hollywood (A-7-6) Specific Surface Area Values.....	256
Table A-39: Heiden (A-7-6) Specific Surface Area Values .....	257

Table A-1: Devol (A-4) OMC and Dry Unit Weight Values

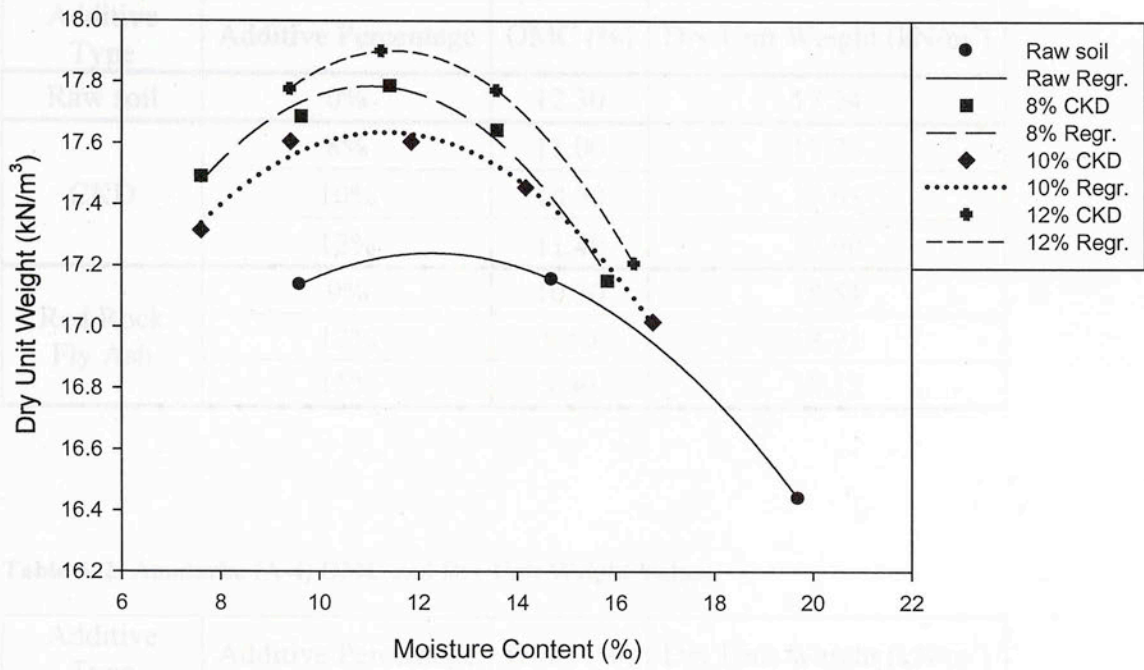


Figure A.1: Devol (A-4) OMC Curves with CKD

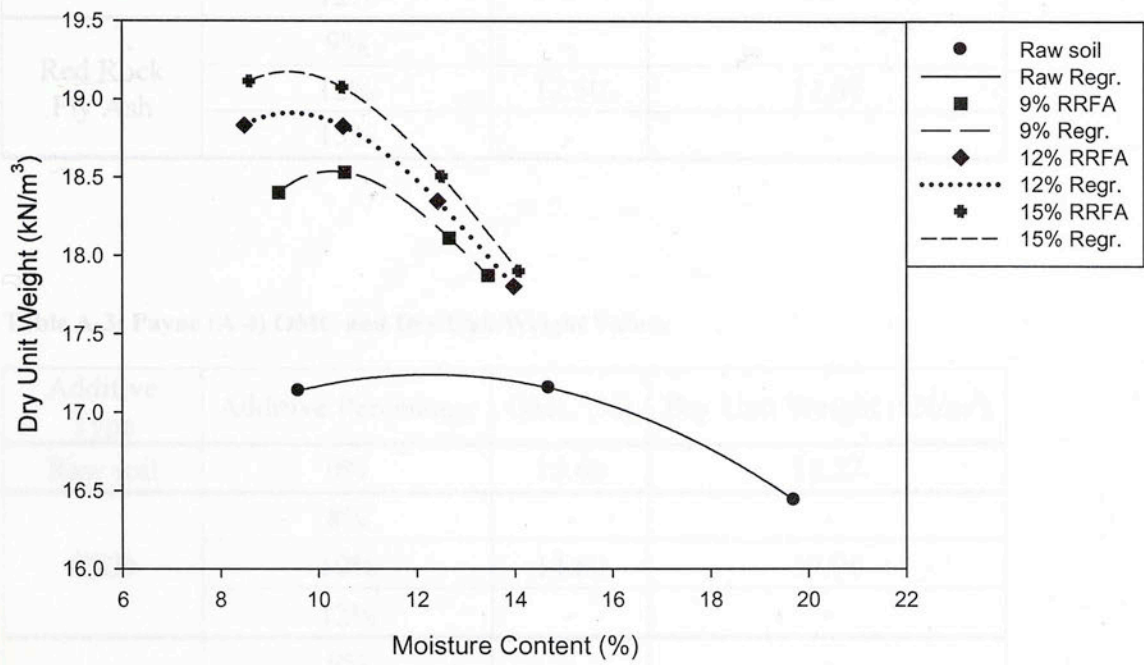


Figure A.2: Devol (A-4) OMC Curves with Red Rock Fly Ash



**Table A-1: Devol (A-4) OMC and Dry Unit Weight Values**

Additive Type	Additive Percentage	OMC (%)	Dry Unit Weight (kN/m <sup>3</sup> )
Raw soil	0%	12.30	17.24
CKD	8%	11.00	17.79
	10%	10.50	17.65
	12%	11.40	17.90
Red Rock Fly Ash	9%	10.30	18.54
	12%	9.50	18.91
	15%	9.40	19.17

**Table A-2: Anadarko (A-4) OMC and Dry Unit Weight Values**

Additive Type	Additive Percentage	OMC (%)	Dry Unit Weight (kN/m <sup>3</sup> )
Raw soil	0%	13.30	17.65
CKD	8%	-	-
	10%	15.10	16.96
	12%	-	-
Red Rock Fly Ash	9%	-	-
	12%	12.50	17.87
	15%	-	-

**Table A-3: Payne (A-4) OMC and Dry Unit Weight Values**

Additive Type	Additive Percentage	OMC (%)	Dry Unit Weight (kN/m <sup>3</sup> )
Raw soil	0%	13.60	18.27
CKD	8%	-	-
	10%	14.60	17.96
	12%	-	-
Red Rock Fly Ash	9%	-	-
	12%	12.40	18.57
	15%	-	-

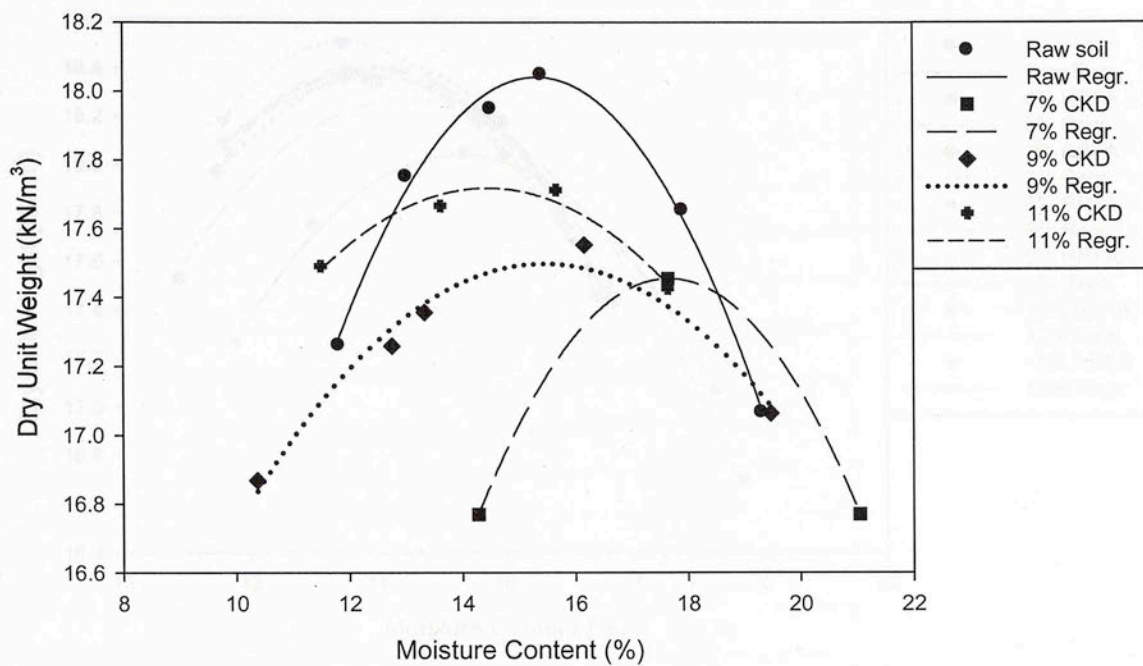


Figure A.3: Ashport-Grainola (A-6) OMC Curves with CKD

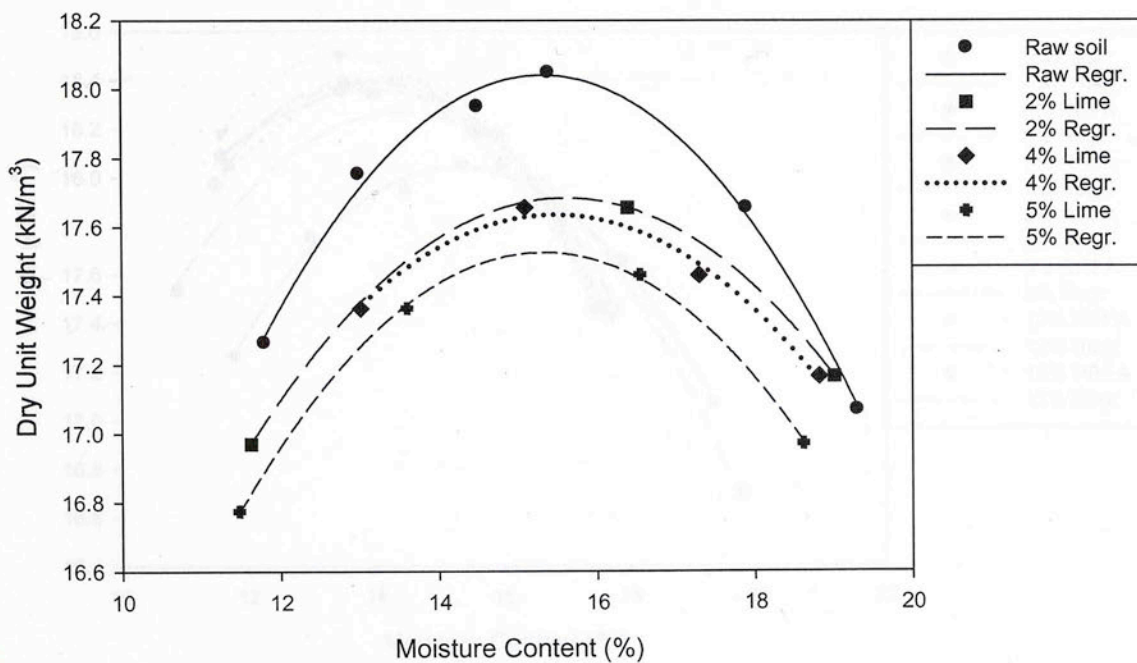


Figure A.4: Ashport-Grainola (A-6) OMC Curves with Lime

Table A-4: Ashport-Grainola (A-6) OMC and Dry Unit Weight Values

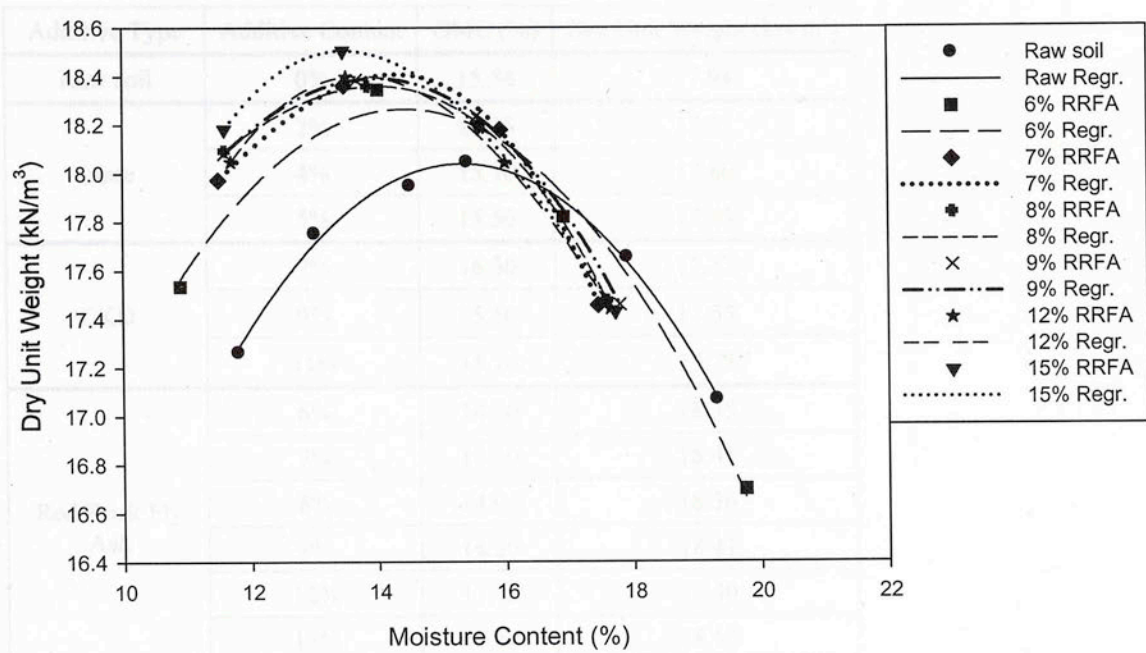


Figure A.5: Ashport-Grainola (A-6) OMC Curves with Red Rock FA

Muskogee FA

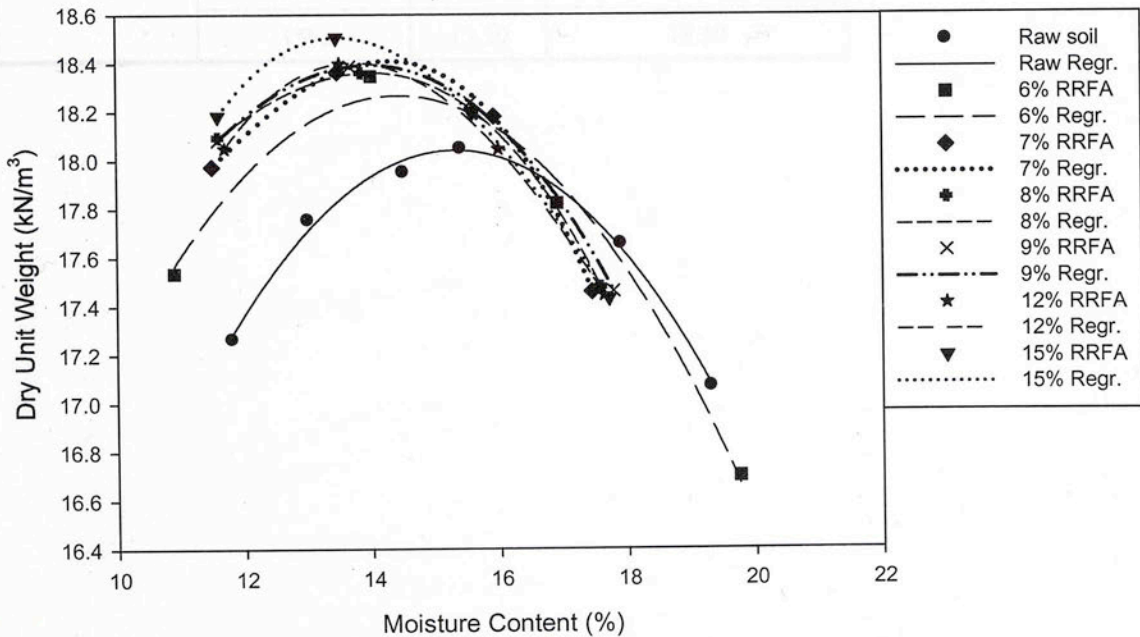


Figure A.6: Ashport-Grainola (A-6) OMC Curves with Muskogee FA



**Table A-4: Ashport-Grainola (A-6) OMC and Dry Unit Weight Values**

Additive Type	Additive Content	OMC (%)	Dry Unit Weight (kN/m <sup>3</sup> )
Raw soil	0%	15.54	17.98
Lime	2%	15.25	17.71
	4%	15.10	17.60
	5%	15.50	17.43
CKD	7%	16.30	17.32
	9%	15.50	17.55
	11%	15.10	17.73
Red Rock Fly Ash	6%	14.00	18.35
	7%	14.30	18.41
	8%	14.00	18.36
	9%	14.30	18.41
	12%	13.70	18.40
	15%	13.50	18.50
Muskogee Fly Ash	6%	14.00	18.35
	7%	14.30	18.41
	8%	14.00	18.36
	9%	14.30	18.41
	12%	13.70	18.40
	15%	13.50	18.50

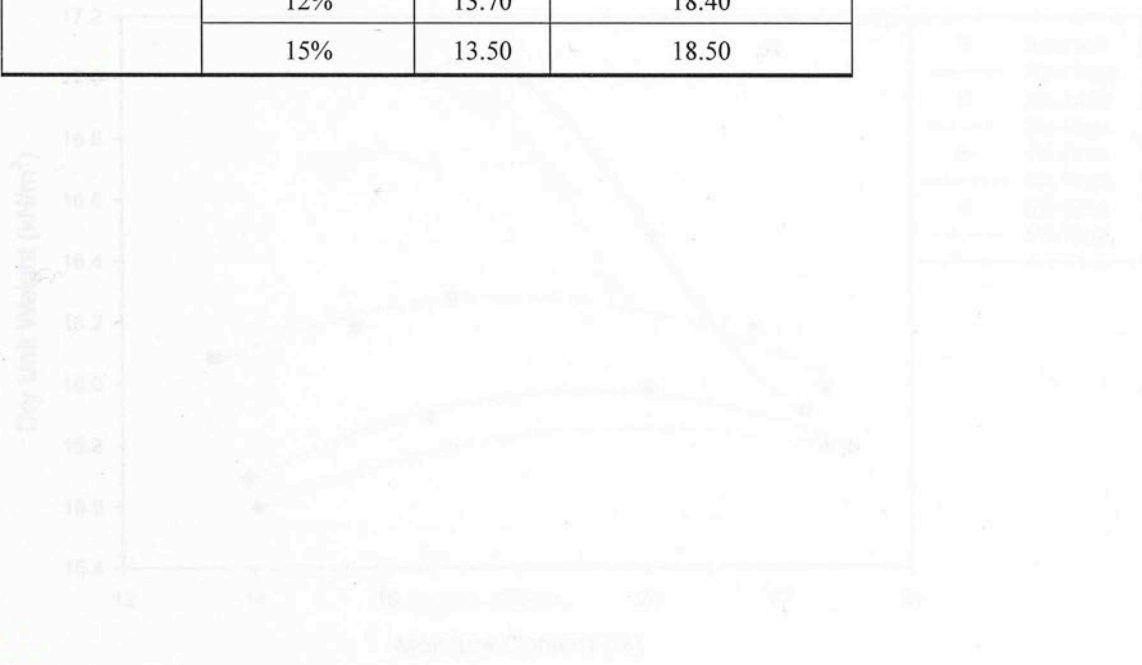


Figure A.7. Kirkland Potentials (A-6) OMC-Curve with Lime

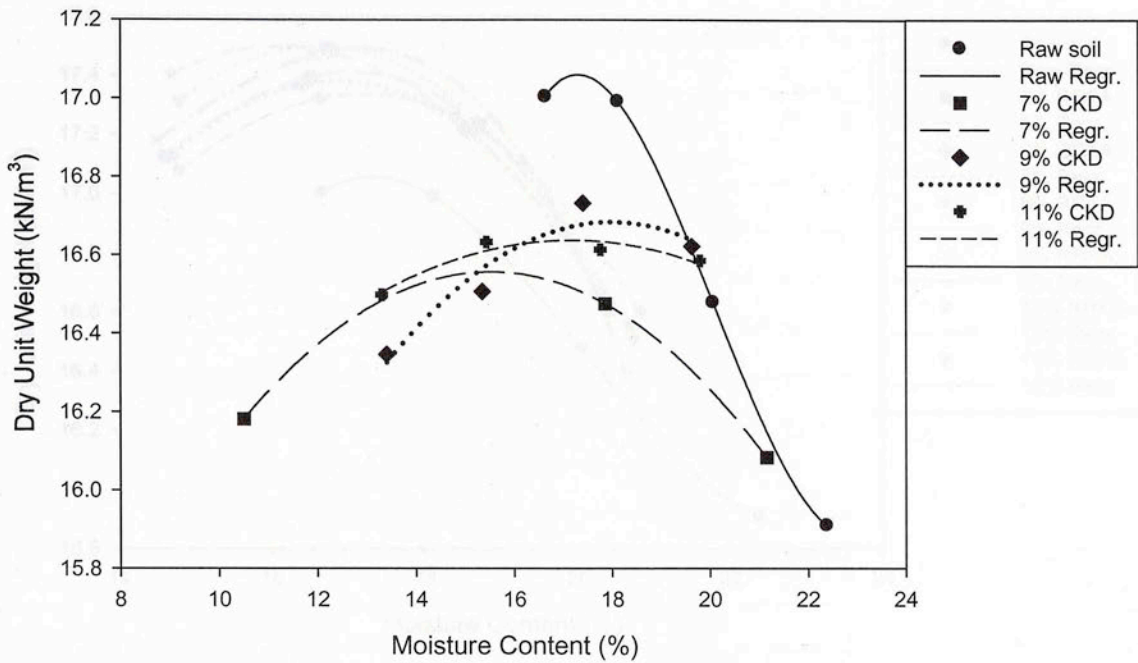


Figure A.7: Kirkland-Pawhuska (A-6) OMC Curves with CKD

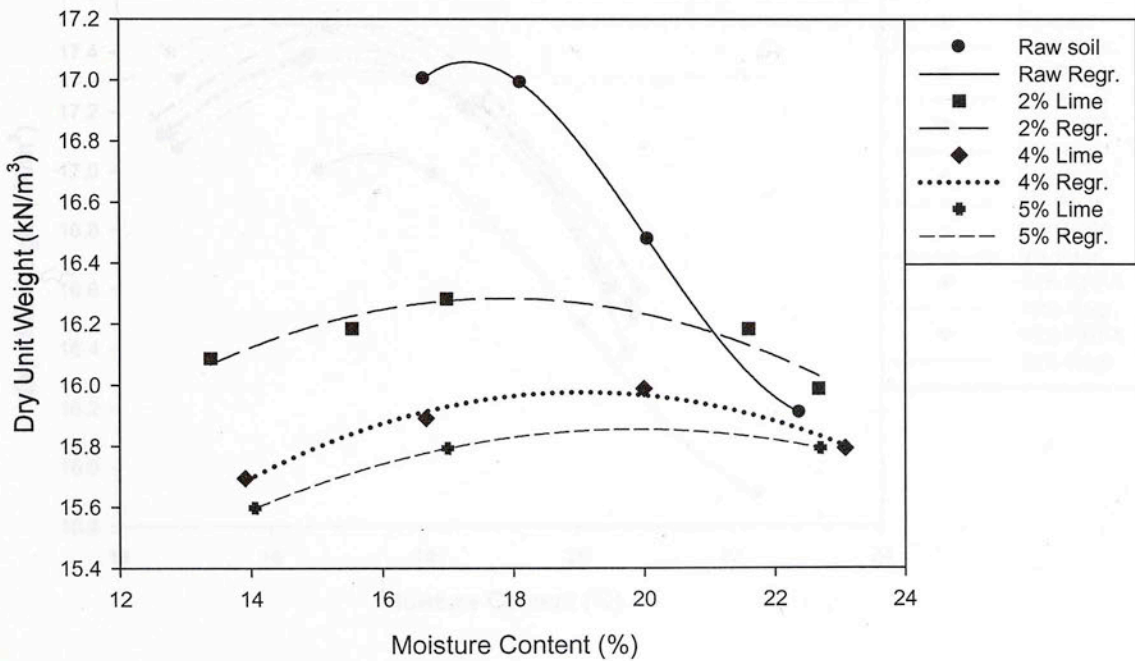


Figure A.8: Kirkland-Pawhuska (A-6) OMC Curves with Lime

Table A-9: Kirkland-Pawhuska (A-6) OMC and Dry Unit Weight Values

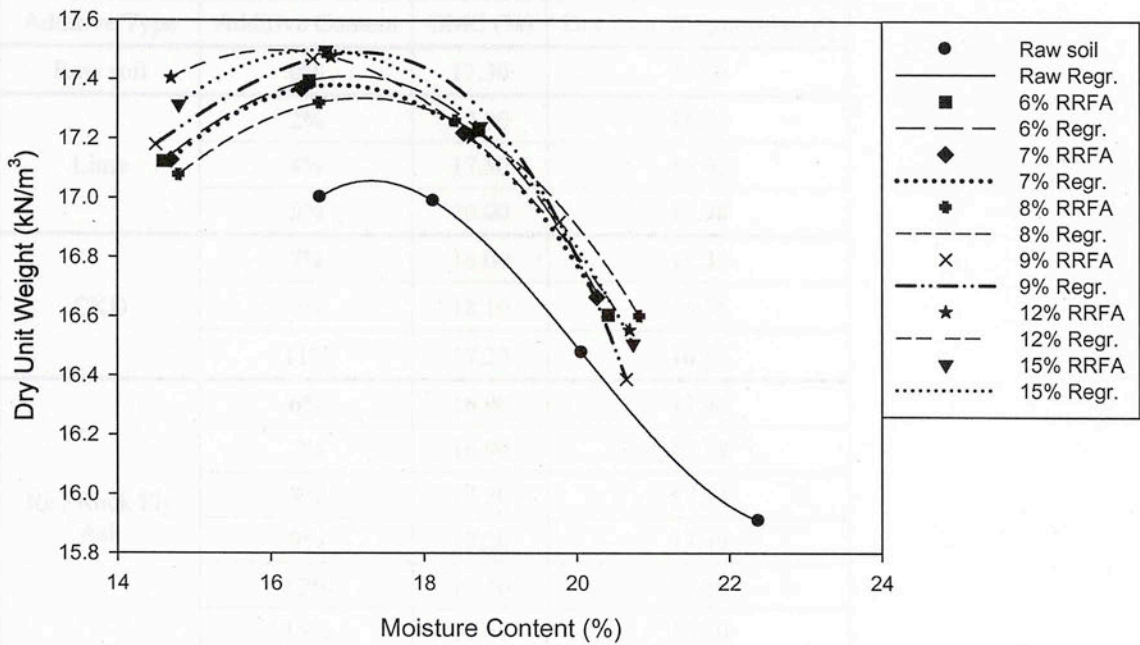


Figure A.9: Kirkland-Pawhuska (A-6) OMC Curves with Red Rock FA

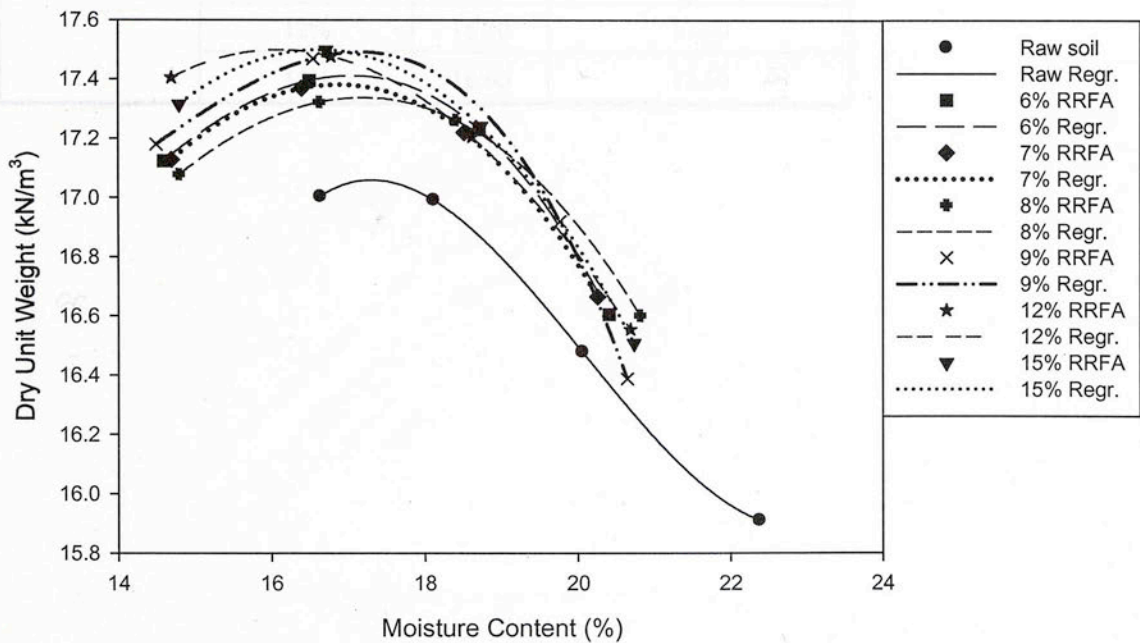


Figure A.10: Kirkland-Pawhuska (A-6) OMC Curves with Muskogee FA



**Table A-5: Kirkland-Pawhuska (A-6) OMC and Dry Unit Weight Values**

Additive Type	Additive Content	OMC (%)	Dry Unit Weight (kN/m <sup>3</sup> )
Raw soil	0%	17.30	17.06
Lime	2%	17.90	16.32
	4%	17.50	16.02
	5%	20.00	15.98
CKD	7%	16.00	16.33
	9%	18.10	16.76
	11%	17.20	16.64
Red Rock Fly Ash	6%	16.90	17.40
	7%	16.90	17.38
	8%	17.20	17.34
	9%	17.20	17.49
	12%	16.10	17.50
	15%	16.60	17.50
Muskogee Fly Ash	6%	16.90	17.40
	7%	16.90	17.38
	8%	17.20	17.34
	9%	17.20	17.49
	12%	16.10	17.50
	15%	16.60	17.50

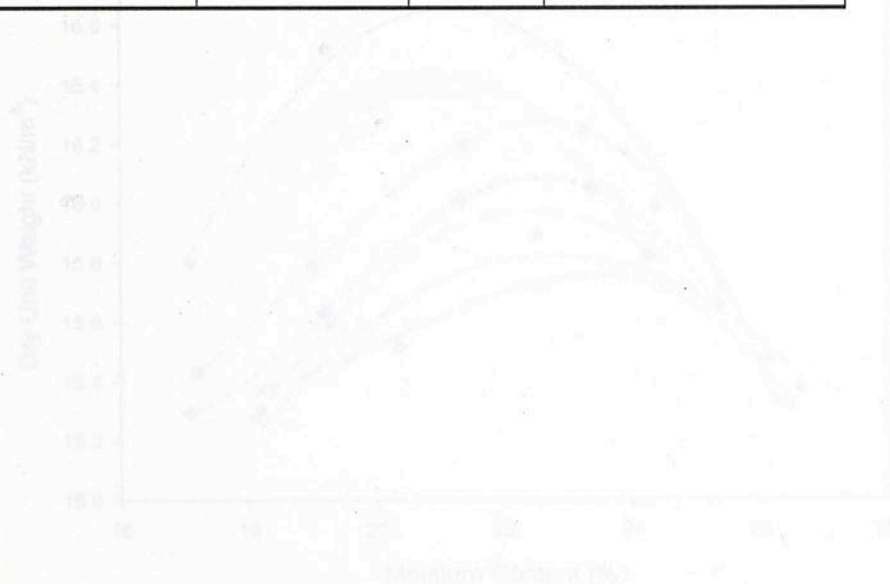


Figure A-12: Flowchart (A-6) OMC Curve weights

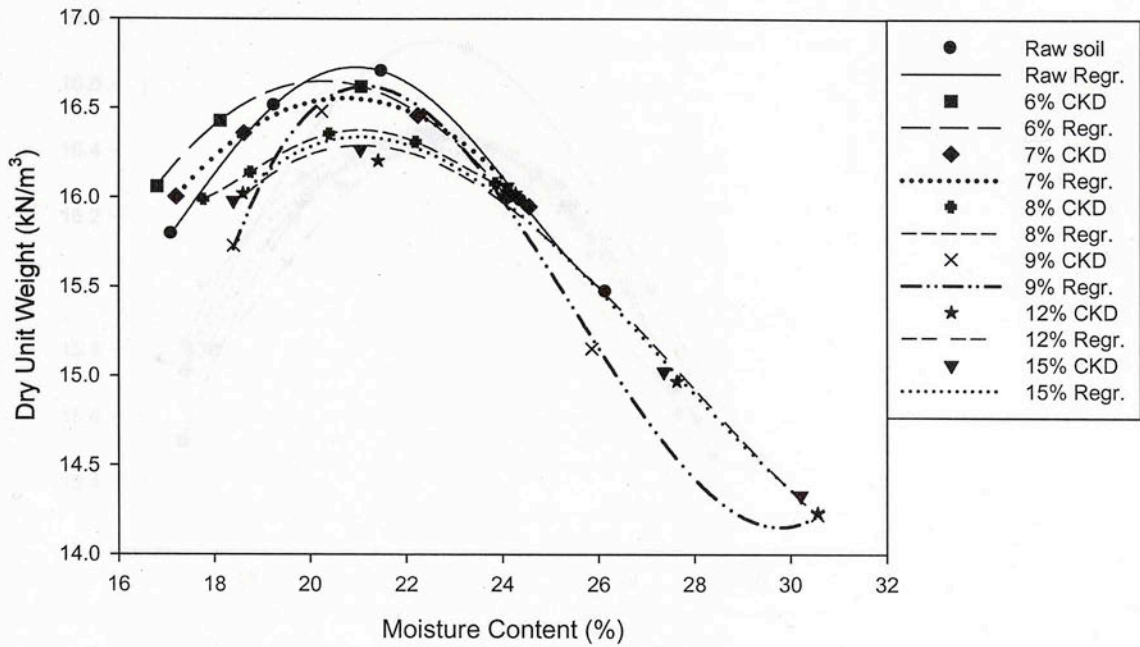


Figure A.11: Flower Pot (A-6) OMC Curves with CKD

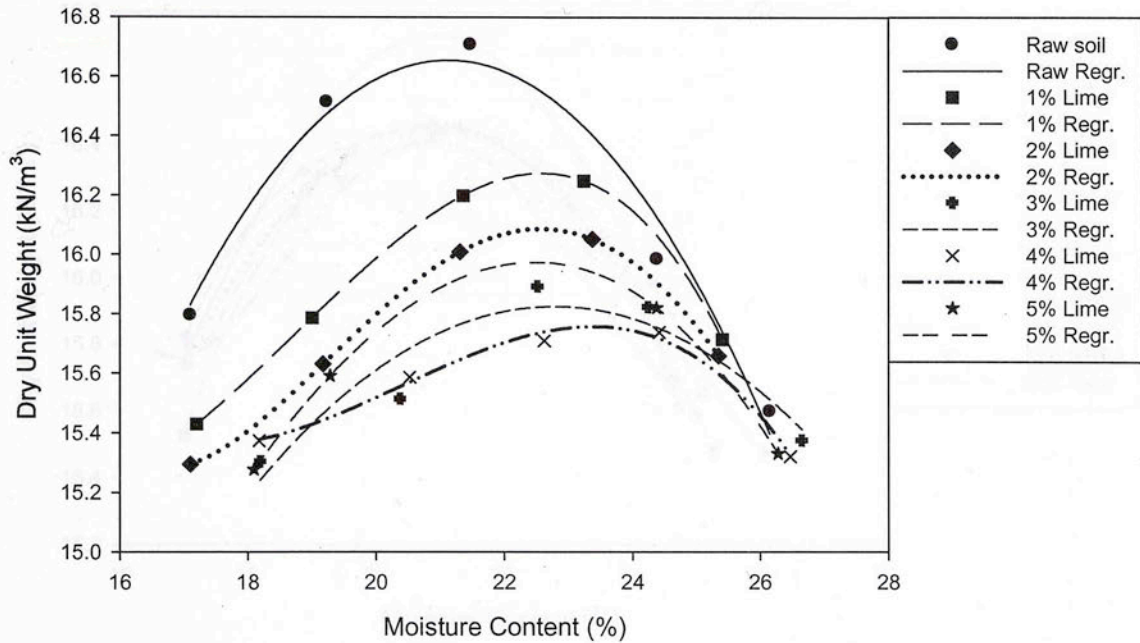


Figure A.12: Flower Pot (A-6) OMC Curves with Lime

Table A-6: Flower Pot (A-6) OMC and Dry Unit Weight Values

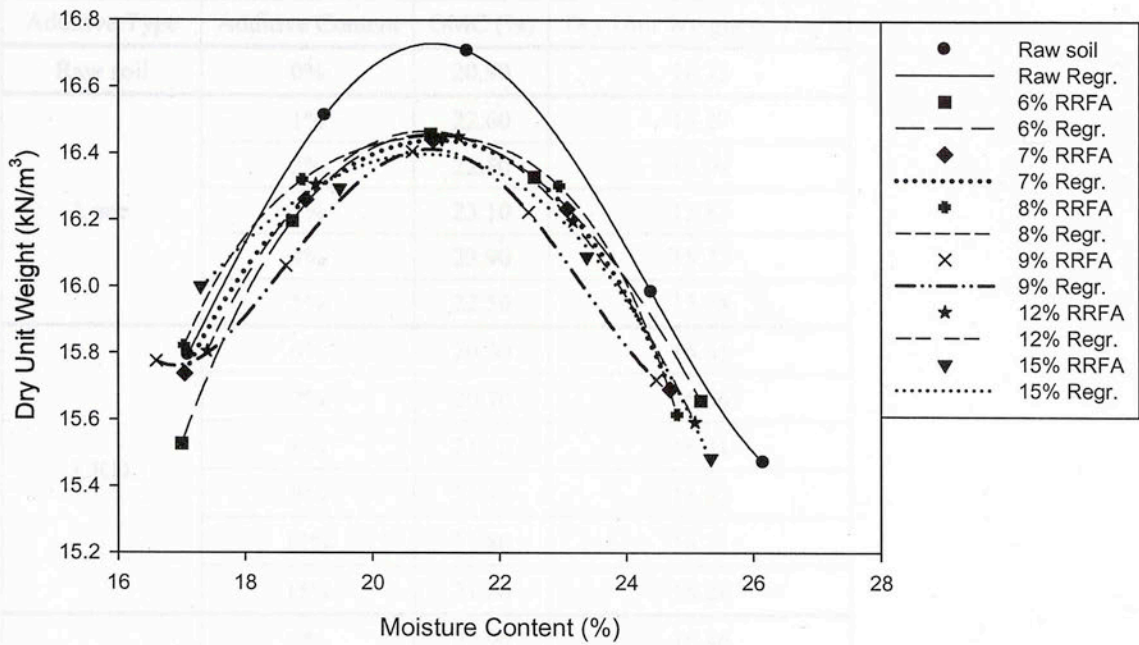


Figure A.13: Flower Pot (A-6) OMC Curves with Red Rock FA

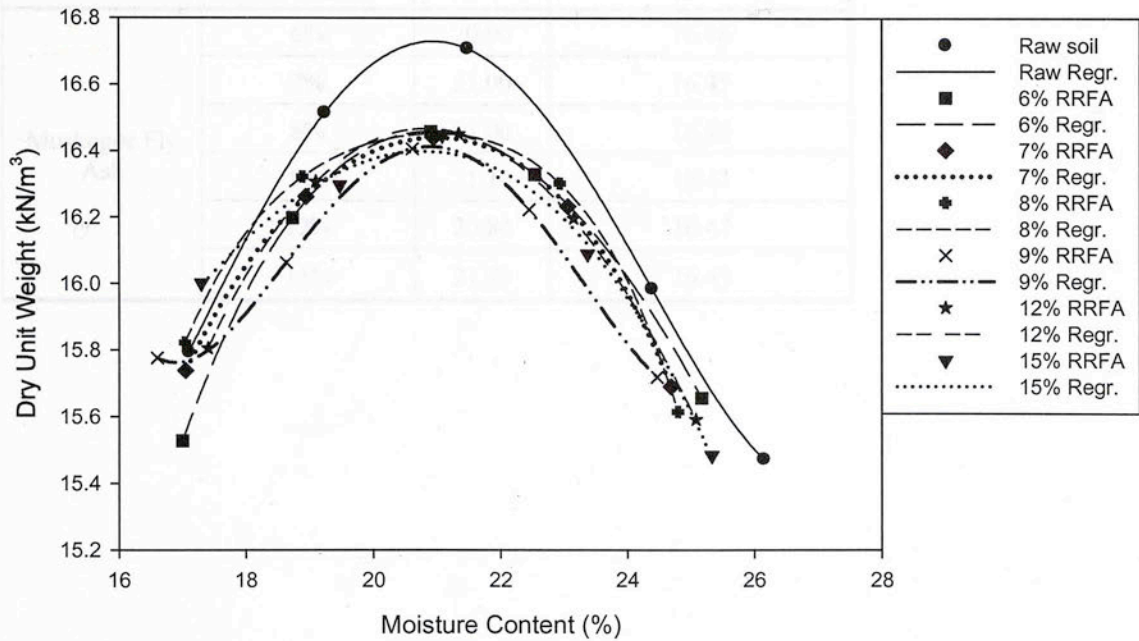


Figure A.14: Flower Pot (A-6) OMC Curves with Muskogee FA



**Table A-6: Flower Pot (A-6) OMC and Dry Unit Weight Values**

Additive Type	Additive Content	OMC (%)	Dry Unit Weight (kN/m <sup>3</sup> )
Raw soil	0%	20.90	16.73
Lime	1%	22.60	16.27
	2%	22.60	16.09
	3%	23.10	15.83
	4%	23.90	15.73
	5%	22.50	15.98
CKD	6%	20.30	16.65
	7%	20.70	16.56
	8%	21.10	16.41
	9%	21.40	16.62
	12%	21.80	16.21
	15%	21.60	16.28
Red Rock Fly Ash	6%	20.90	16.46
	7%	21.00	16.45
	8%	21.00	16.46
	9%	21.10	16.43
	12%	20.80	16.47
	15%	21.30	16.45
Muskogee Fly Ash	6%	20.90	16.46
	7%	21.00	16.45
	8%	21.00	16.46
	9%	21.10	16.43
	12%	20.80	16.47
	15%	21.30	16.45

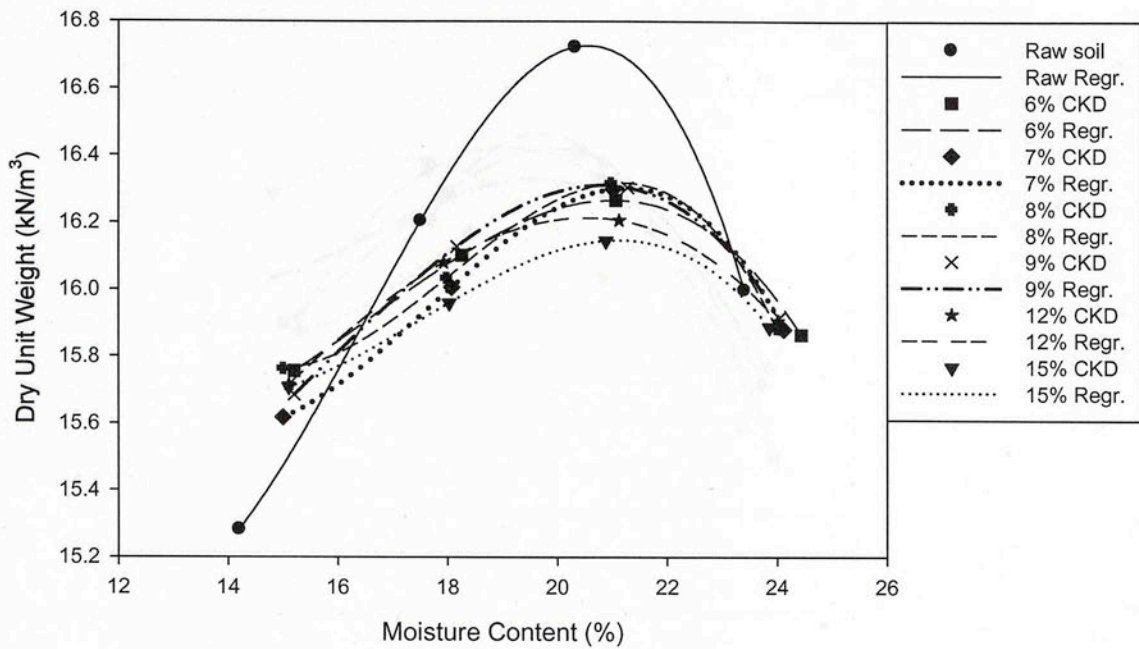


Figure A.15: Hollywood (A-7-6) OMC Curves with CKD

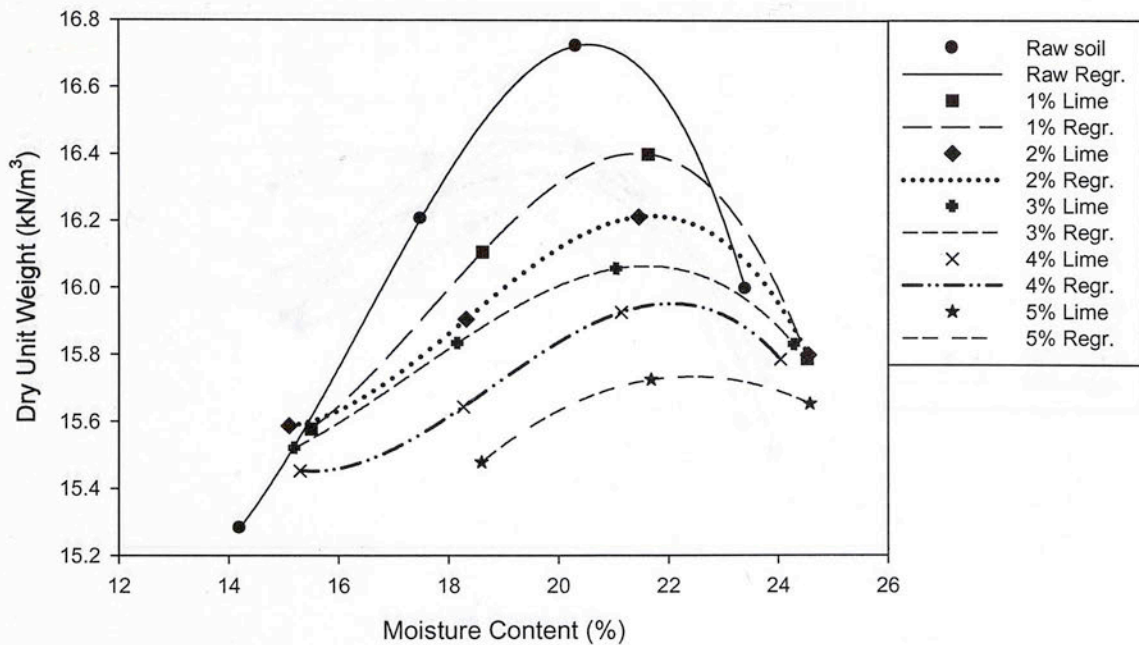


Figure A.16: Hollywood (A-7-6) OMC Curves with Lime

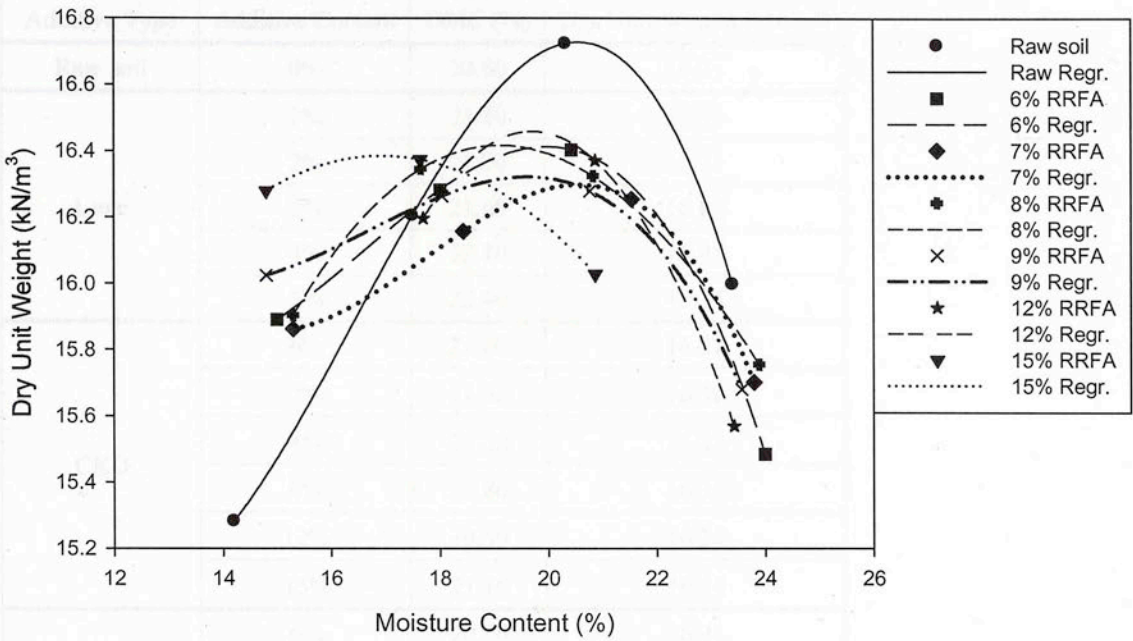


Figure A.17: Hollywood (A-7-6) OMC Curves with Red Rock FA

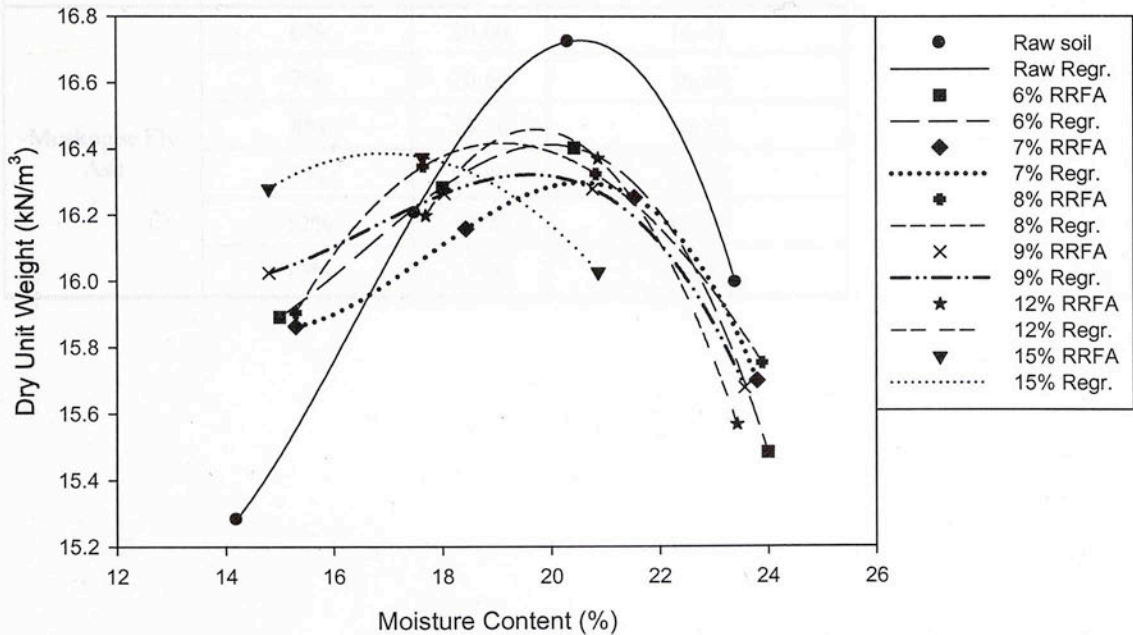


Figure A.18: Hollywood (A-7-6) OMC Curves with Muskogee FA



**Table A-7: Hollywood (A-7-6) OMC and Dry Unit Weight Values**

Additive Type	Additive Content	OMC (%)	Dry Unit Weight (kN/m <sup>3</sup> )
Raw soil	0%	20.60	16.73
Lime	1%	21.40	16.40
	2%	21.70	16.21
	3%	21.60	16.06
	4%	22.10	15.95
	5%	22.40	15.74
CKD	6%	21.00	16.27
	7%	21.30	16.30
	8%	21.20	16.32
	9%	20.80	16.31
	12%	20.50	16.21
	15%	21.10	16.14
Red Rock Fly Ash	6%	20.00	16.41
	7%	20.60	16.30
	8%	19.10	16.42
	9%	19.60	16.32
	12%	19.70	16.46
	15%	17.00	16.39
Muskogee Fly Ash	6%	20.00	16.41
	7%	20.60	16.30
	8%	19.10	16.42
	9%	19.60	16.32
	12%	19.70	16.46
	15%	17.00	16.39

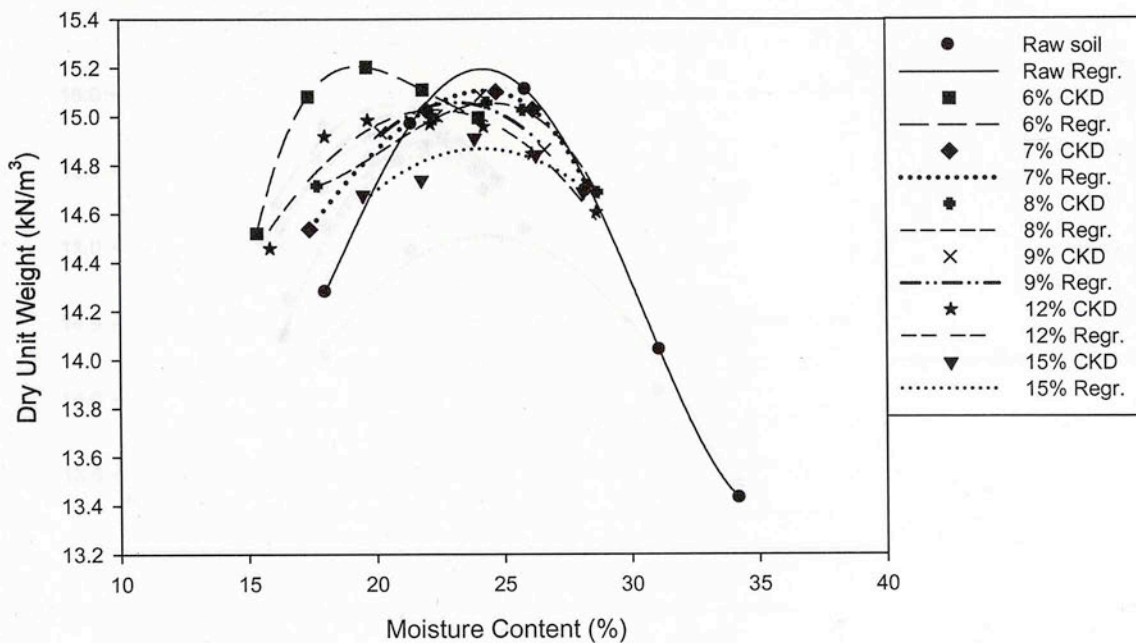


Figure A.19: Heiden (A-7-6) OMC Curves with CKD

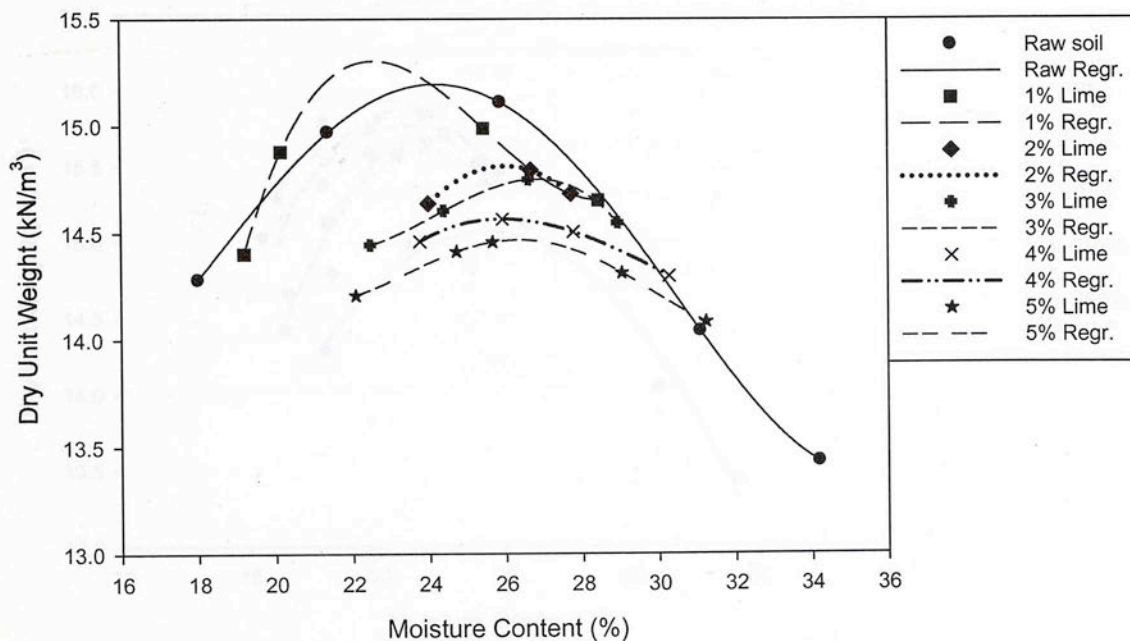


Figure A.20: Heiden (A-7-6) OMC Curves with Lime

Table A-8: Heiden (A-7-6) OMC and Dry Unit Weight Values

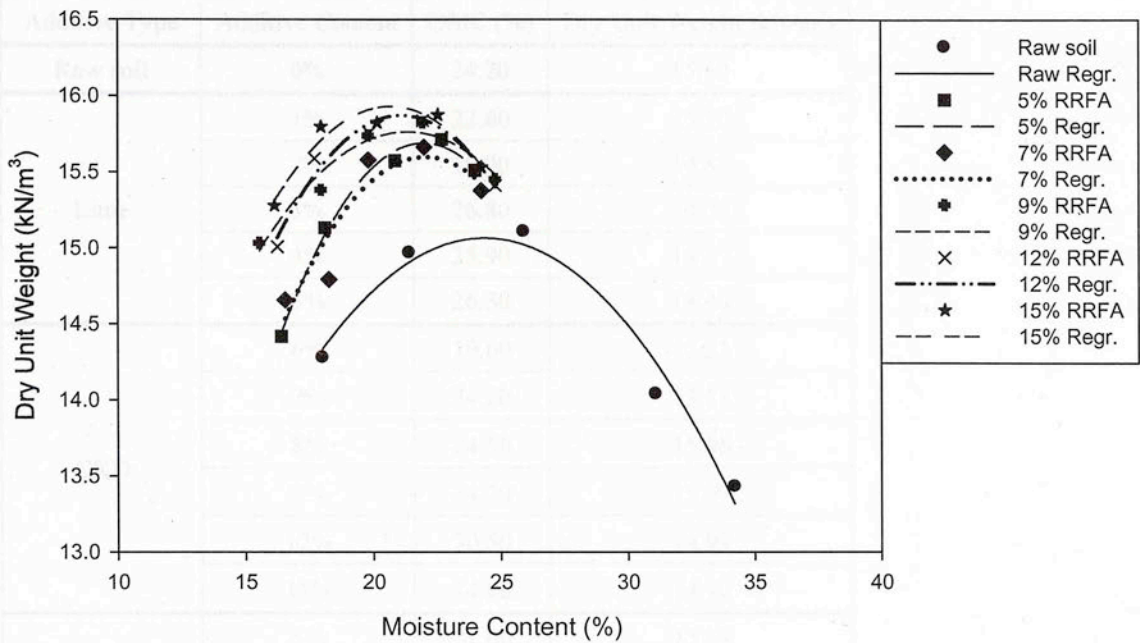


Figure A.21: Heiden (A-7-6) OMC Curves with Red Rock FA

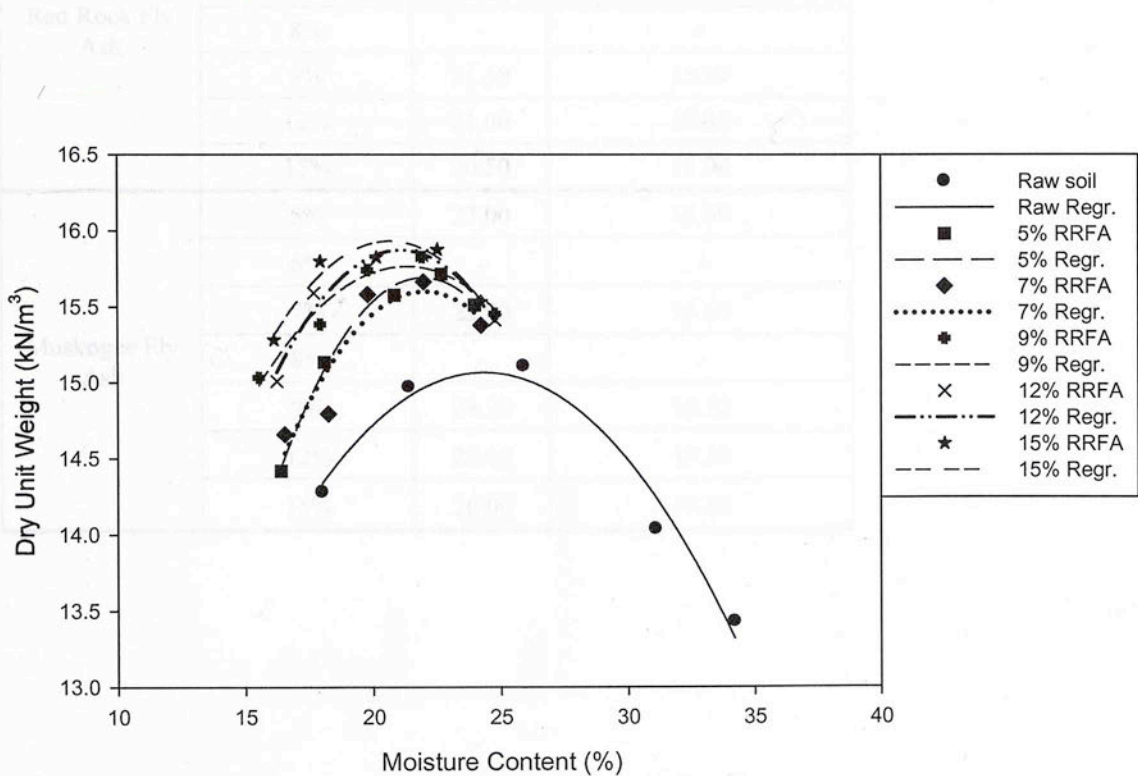


Figure A.22: Heiden (A-7-6) OMC Curves with Muskogee FA



**Table A-8: Heiden (A-7-6) OMC and Dry Unit Weight Values**

Additive Type	Additive Content	OMC (%)	Dry Unit Weight (kN/m <sup>3</sup> )
Raw soil	0%	24.20	15.50
Lime	1%	22.60	15.30
	2%	26.00	14.81
	3%	26.80	14.75
	4%	25.90	14.57
	5%	26.30	14.46
CKD	6%	19.60	15.21
	7%	24.20	15.11
	8%	24.50	15.06
	9%	24.20	15.09
	12%	20.50	14.99
	15%	24.00	14.92
Red Rock Fly Ash	5%	22.00	15.69
	6%	-	-
	7%	22.00	15.60
	8%	-	-
	9%	21.50	15.77
	12%	21.00	15.88
	15%	20.50	15.94
Muskogee Fly Ash	5%	22.00	15.69
	6%	-	-
	7%	22.00	15.60
	8%	-	-
	9%	24.20	15.50
	12%	22.60	15.30
	15%	26.00	14.81

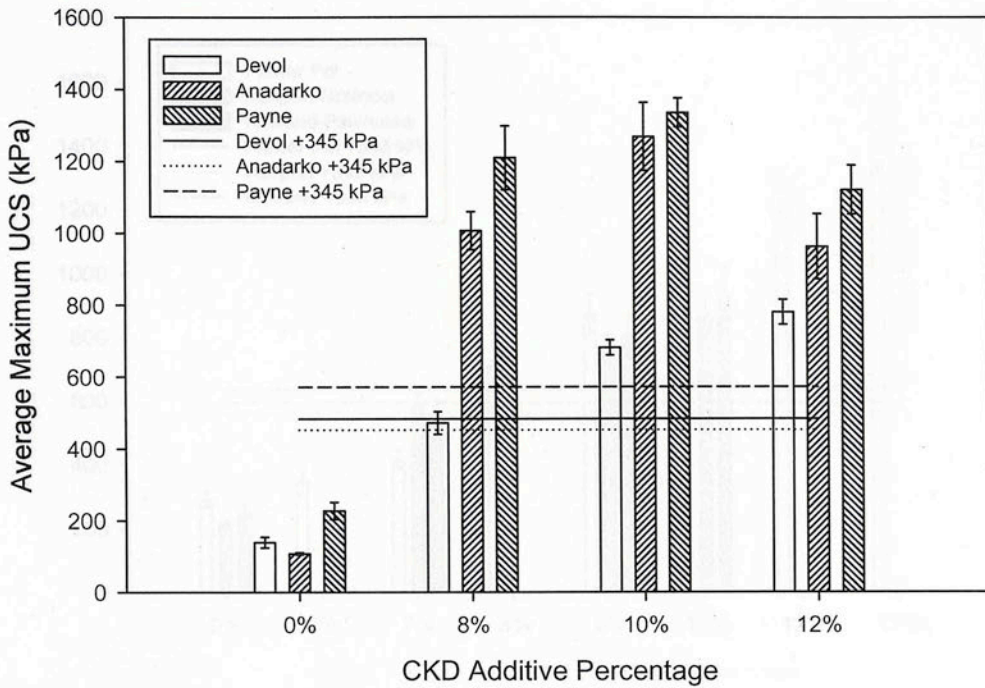


Figure A.23: UCS Plots for A-4 Soils with CKD

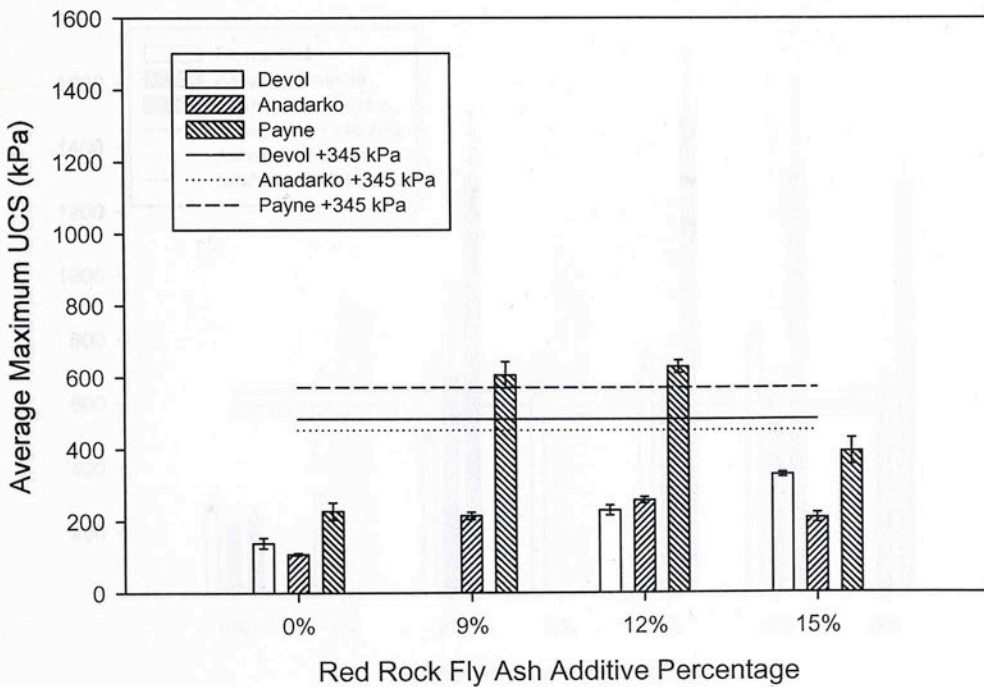


Figure A.24: UCS Plots for A-4 Soils with Red Rock FA

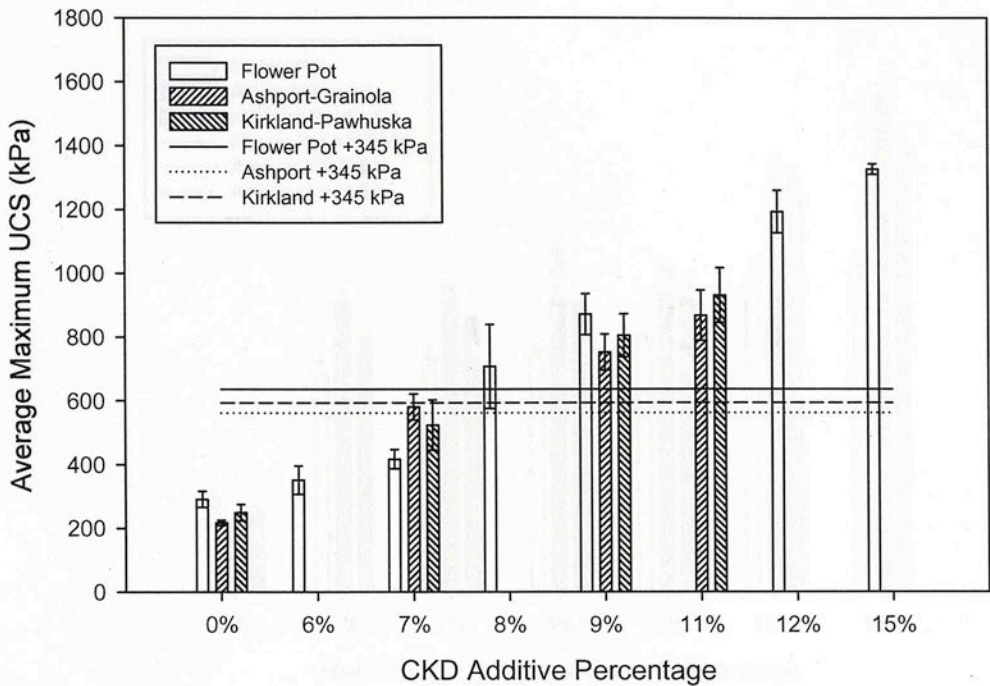


Figure A.25: UCS Plots for A-6 Soils with CKD

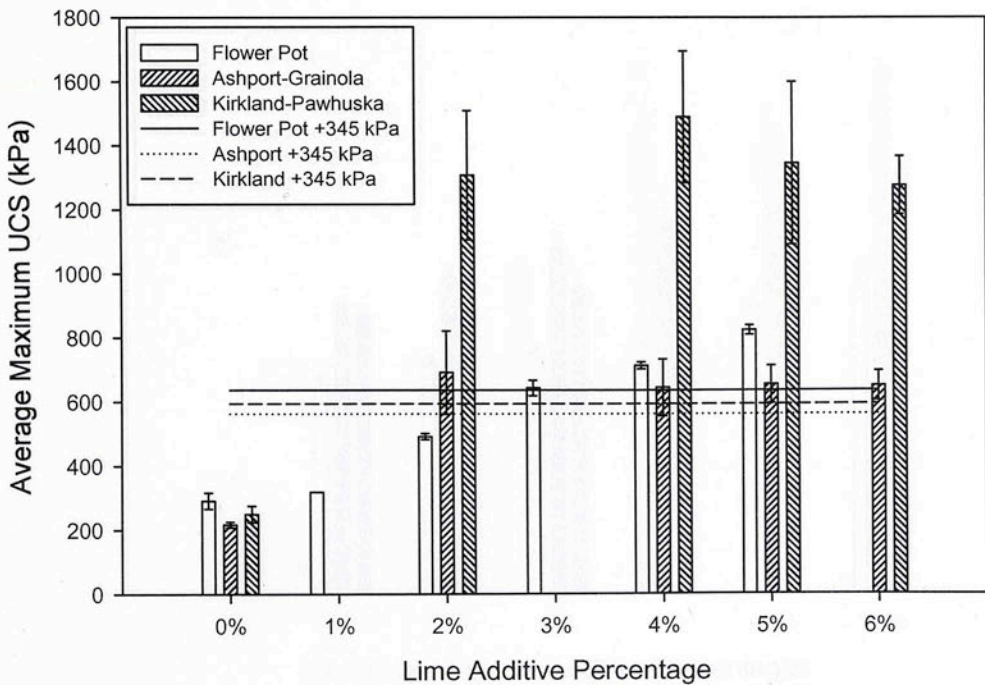


Figure A.26: UCS Plots for A-6 Soils with Lime



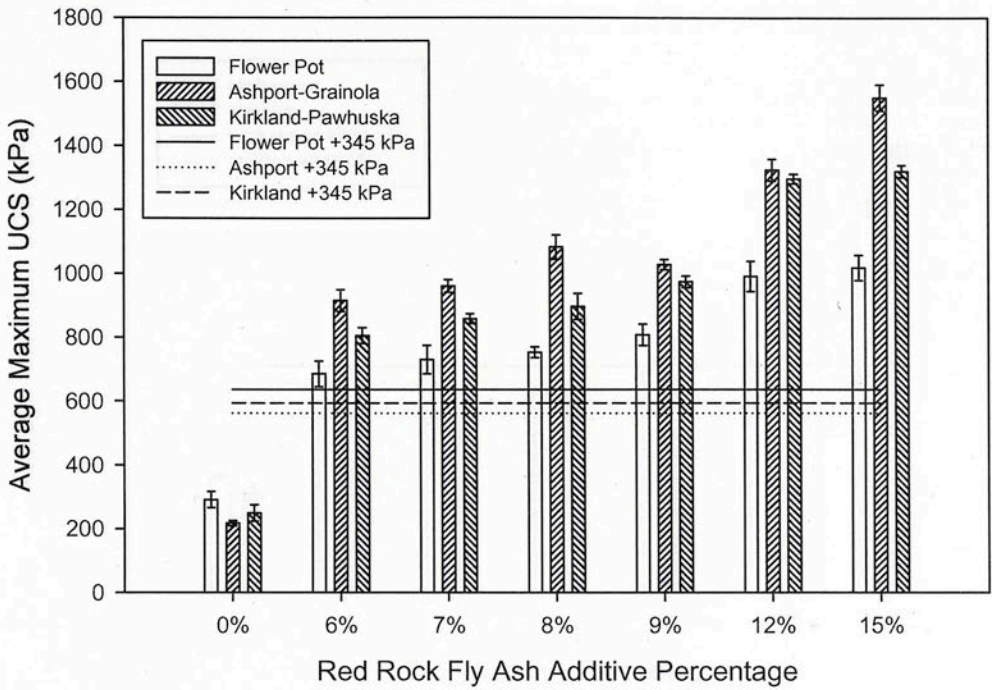


Figure A.27: UCS Plots for A-6 Soils with Red Rock FA

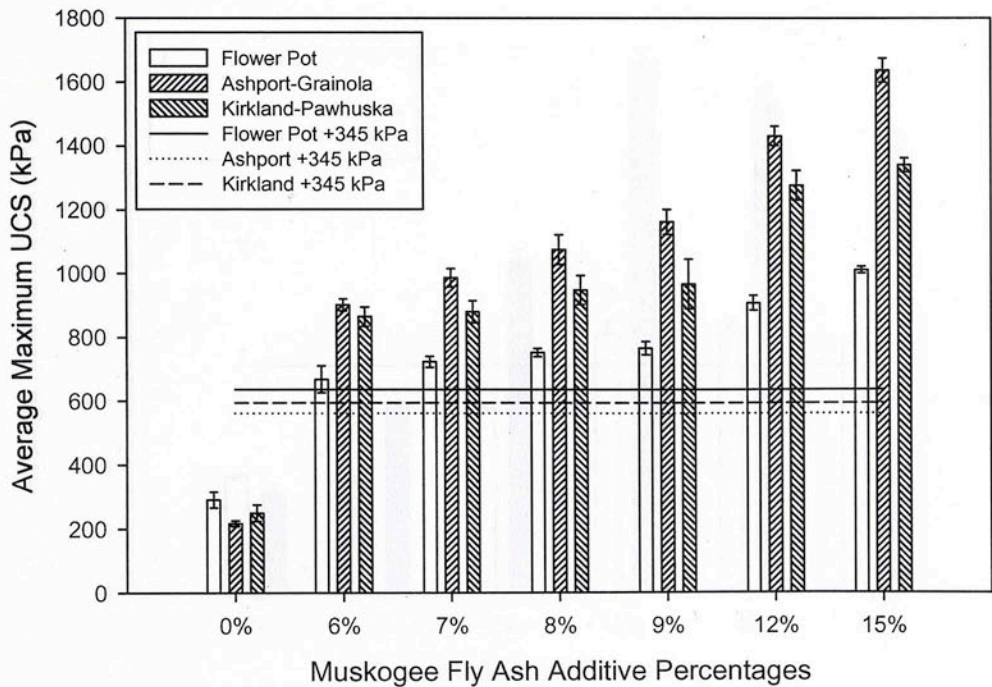


Figure A.28: UCS Plots for A-6 Soils with Muskogee FA

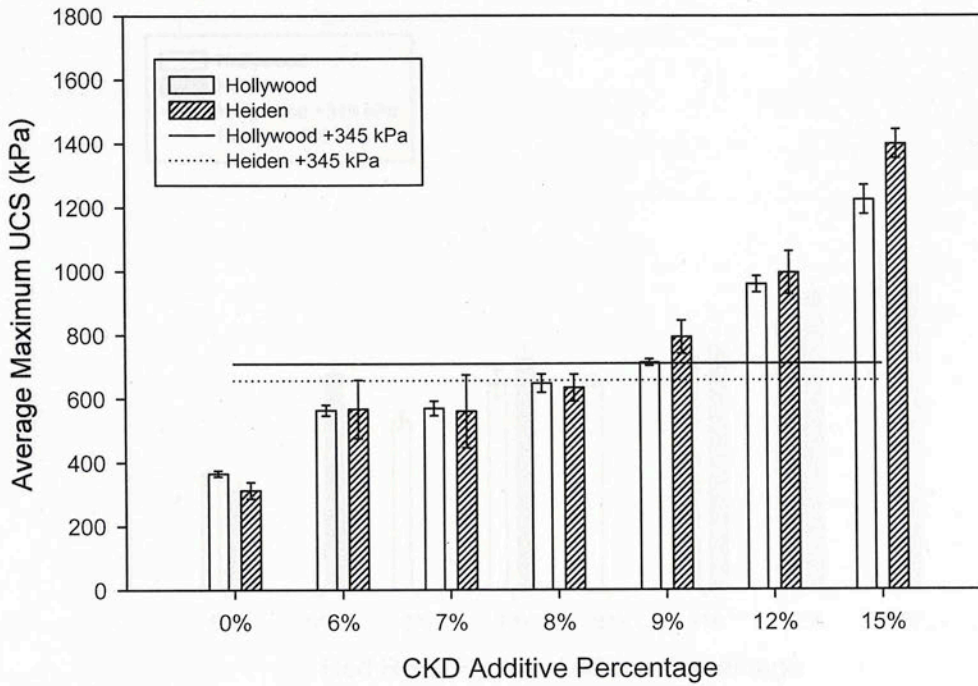


Figure A.29: UCS Plots for A-7-6 Soils with CKD

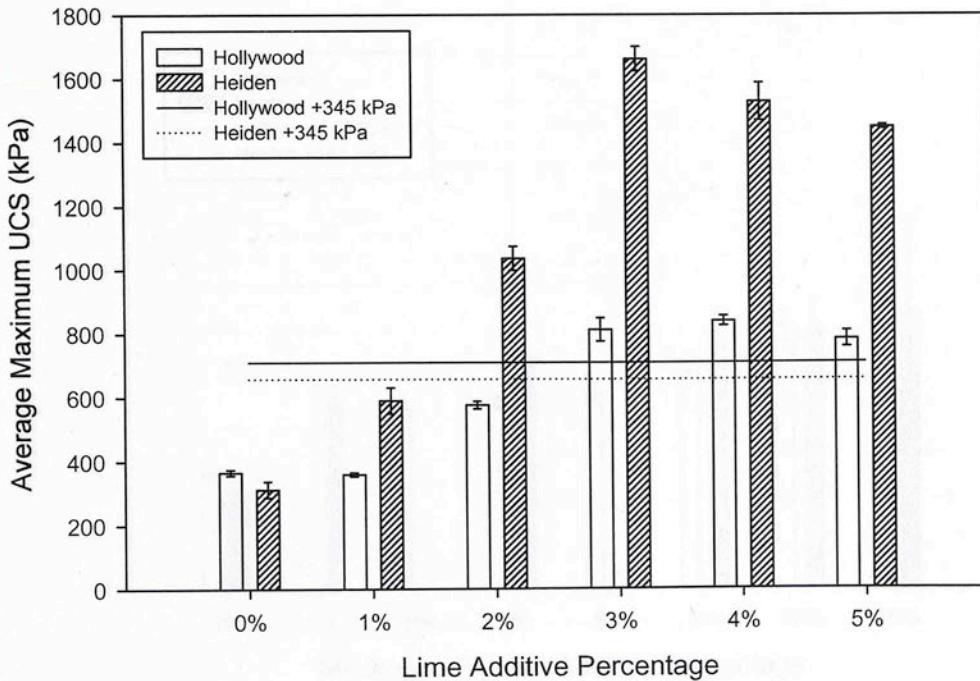


Figure A.30: UCS Plots for A-7-6 Soils with Lime

Table A-9: UCS Values for All Soils

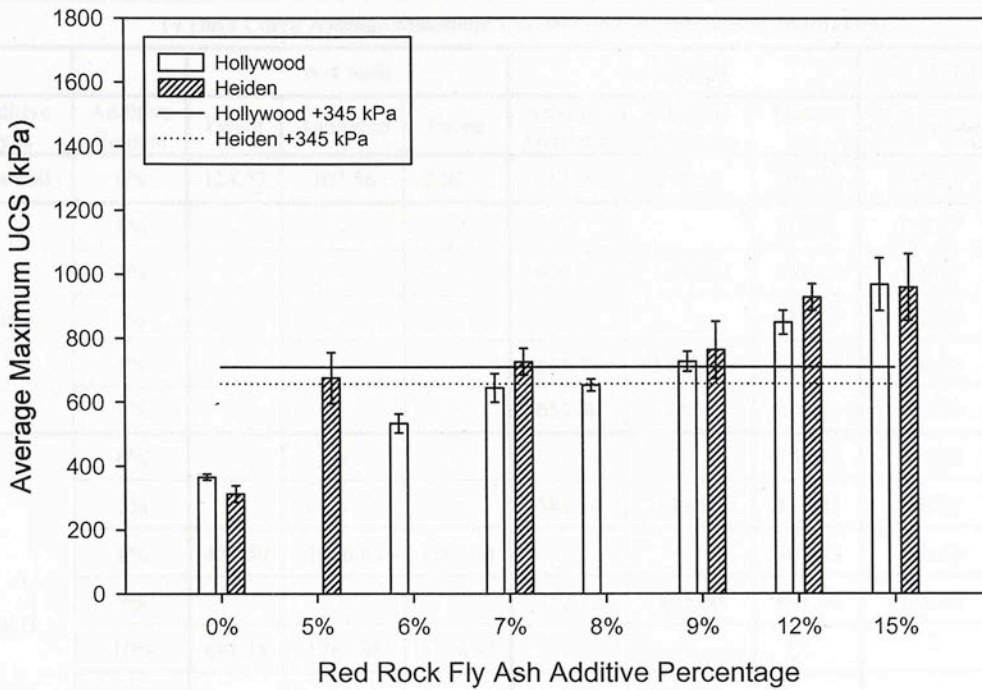


Figure A.31: UCS Plots for A-7-6 Soils with Red Rock FA

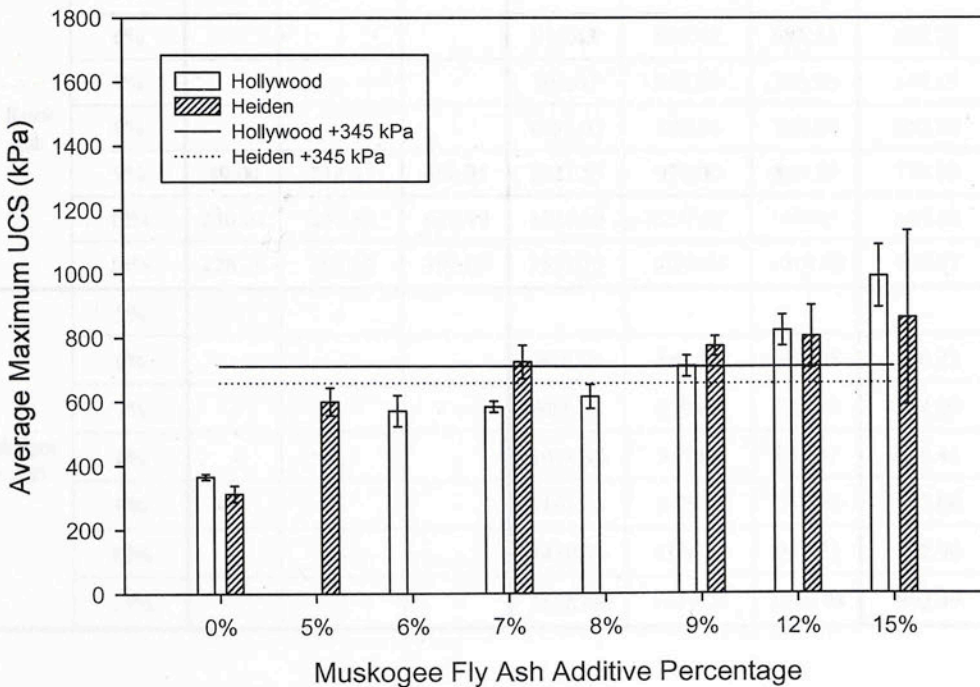


Figure A.32: UCS Plots for A-7-6 Soils with Muskogee FA



**Table A-9: UCS Values for All Soils**

14 Days Cured Average Maximum Unconfined Compression Strength (kPa)									
		A-4 Soils			A-6 Soils			A-7-6 Soils	
Additive Type	Additive Content	Devol	Anadarko	Payne	Ashport-Grainola	Kirkland-Pawhuska	Flower Pot	Hollywood	Heiden
Raw soil	0%	128.72	107.56	226.84	217.00	249.36	291.00	365.25	312.52
Lime	1%	-	-	-	-	-	319.01	359.47	590.65
	2%	-	-	-	690.94	1307.70	491.62	576.77	1036.51
	3%	-	-	-	-	-	642.65	812.56	1661.64
	4%	-	-	-	644.47	1489.77	713.54	840.30	1528.34
	5%	-	-	-	654.80	1345.66	824.51	782.90	1447.90
CKD	6%	-	-	-	-	-	351.38	564.05	567.67
	7%	-	-	-	581.14	524.18	417.03	570.22	560.77
	8%	471.59	1006.63	1209.34	-	-	707.83	648.43	634.32
	9%	-	-	-	752.72	805.20	871.36	713.16	792.90
	10%	681.18	1267.95	1334.82	-	-	-	-	-
	11%	-	-	-	867.76	931.00	-	-	-
	12%	780.20	963.20	1121.78	-	-	1193.36	958.58	995.14
	15%	-	-	-	-	-	1327.23	1225.20	1399.64
Red Rock Fly Ash	5%	-	-	-	-	-	-	-	675.69
	6%	-	-	-	915.43	805.63	685.54	533.23	-
	7%	-	-	-	961.67	858.80	730.50	644.19	726.25
	8%	-	-	-	1083.03	896.94	753.61	653.44	-
	9%	89.00	214.43	606.05	1027.55	974.00	807.55	727.03	763.02
	12%	230.01	257.86	629.49	1324.60	1297.63	990.95	849.16	928.49
	15%	328.26	208.22	393.00	1551.15	1321.14	1018.69	969.37	960.67
Muskogee Fly Ash	5%	-	-	-	-	-	-	-	599.84
	6%	-	-	-	901.56	864.58	668.08	570.22	-
	7%	-	-	-	987.10	879.60	722.79	584.09	723.95
	8%	-	-	-	1074.94	947.80	752.07	616.45	-
	9%	-	-	-	1161.63	967.45	765.94	712.00	312.52
	12%	-	-	-	1430.94	1276.06	907.73	822.96	590.65
	15%	-	-	-	1636.68	1339.24	1010.98	992.49	1036.51

Table A-10: Analytical (A-4) Atterberg Limit

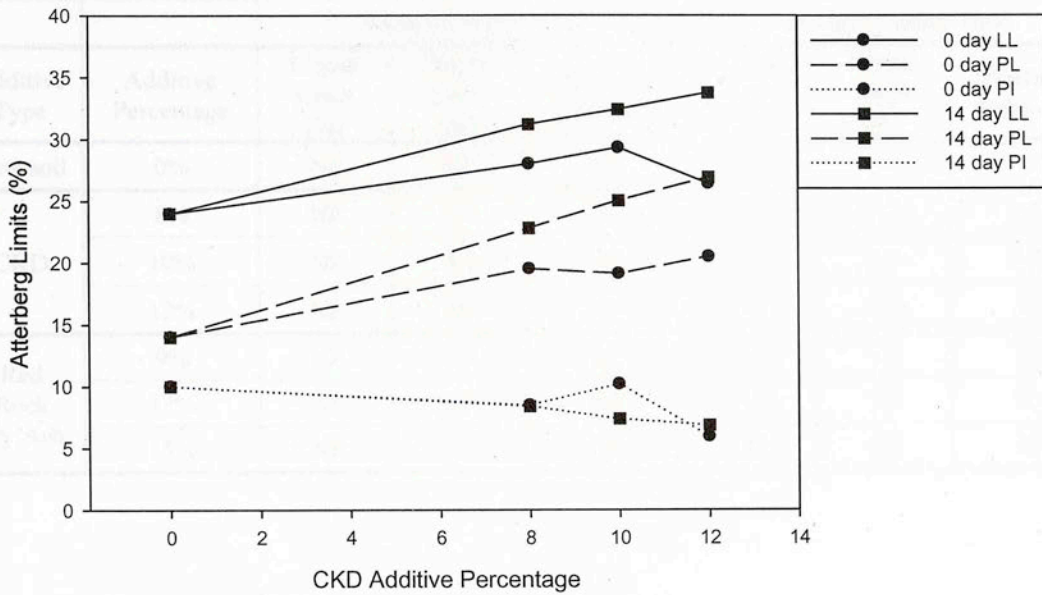


Figure A.33: Payne (A-4) Atterberg Limits with CKD

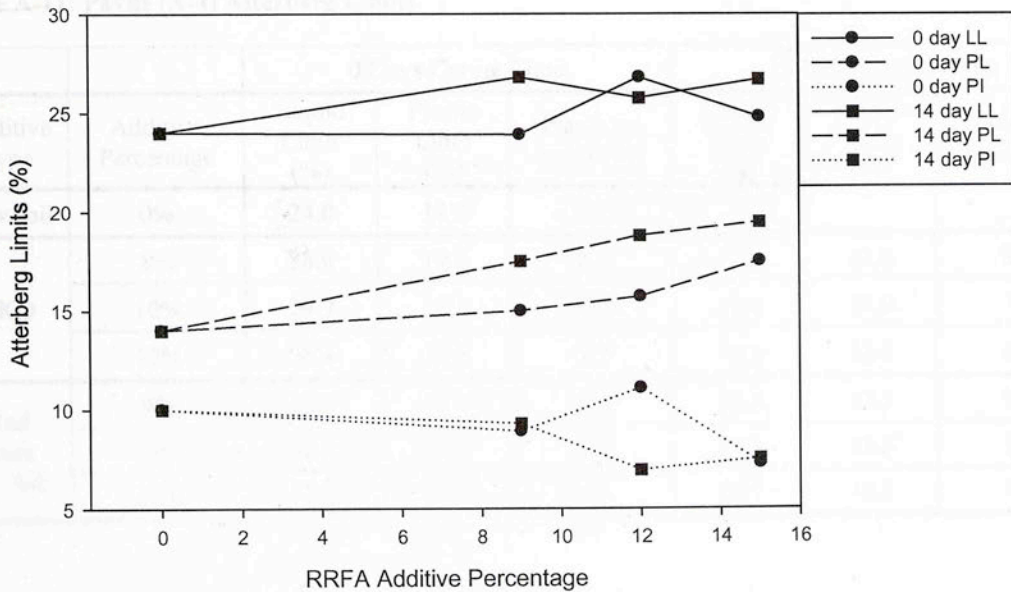


Figure A.34: Payne (A-4) Atterberg Limits with Red Rock FA

**Table A-10: Anadarko (A-4) Atterberg Limits**

Additive Type	Additive Percentage	0 Days Curing Time			14 Days Curing Time		
		Liquid Limit (%)	Plastic Limit (%)	Plasticity Index (%)	Liquid Limit (%)	Plastic Limit (%)	Plasticity Index (%)
Raw soil	0%	NP	NP	NP			
CKD	8%	NP	NP	NP	NP	NP	NP
	10%	NP	NP	NP	NP	NP	NP
	12%	NP	NP	NP	NP	NP	NP
Red Rock Fly Ash	9%	NP	NP	NP	NP	NP	NP
	12%	NP	NP	NP	NP	NP	NP
	15%	NP	NP	NP	NP	NP	NP

**Table A-11: Payne (A-4) Atterberg Limits**

Additive Type	Additive Percentage	0 Days Curing Time			14 Days Curing Time		
		Liquid Limit (%)	Plastic Limit (%)	Plasticity Index (%)	Liquid Limit (%)	Plastic Limit (%)	Plasticity Index (%)
Raw soil	0%	24.0	14.0	10.0			
CKD	8%	28.0	19.5	8.5	31.2	22.8	8.4
	10%	29.3	19.1	10.2	32.4	25.0	7.4
	12%	26.4	20.5	5.9	33.8	26.8	6.8
Red Rock Fly Ash	9%	23.9	15.0	8.9	26.8	17.5	9.3
	12%	26.8	15.7	11.1	25.8	18.8	7.0
	15%	24.8	17.5	7.3	26.7	19.5	7.5



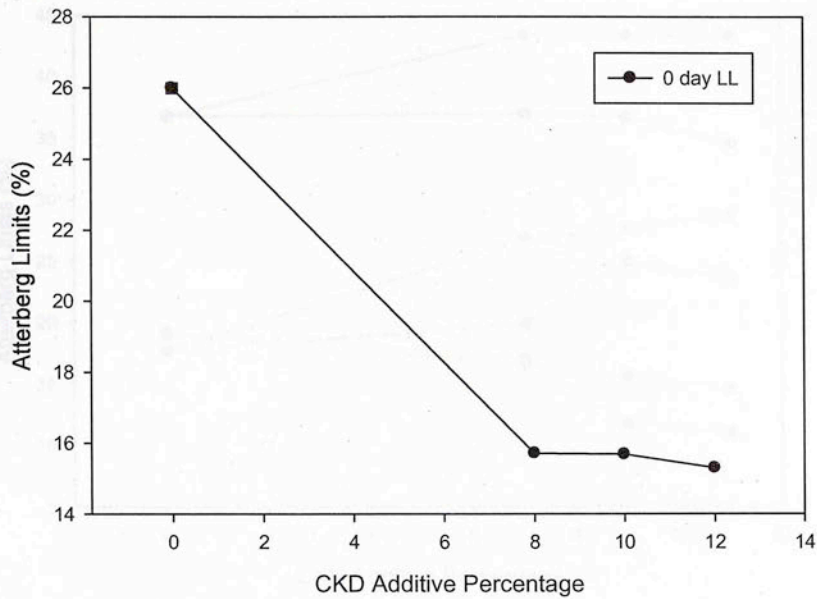


Figure A.35: Devol (A-4) Atterberg Limits with CKD

Table A-12: Devol (A-4) Atterberg Limits

Additive Type	Additive Percentage	0 Days Curing Time			14 Days Curing Time		
		Liquid Limit (%)	Plastic Limit (%)	Plasticity Index (%)	Liquid Limit (%)	Plastic Limit (%)	Plasticity Index (%)
Raw soil	0%	26.0	NP	NP			
CKD	8%	15.7	NP	NP	NP	NP	NP
	10%	15.7	NP	NP	NP	NP	NP
	12%	15.3	NP	NP	NP	NP	NP
Red Rock Fly Ash	9%	NP	NP	NP	NP	NP	NP
	12%	NP	NP	NP	NP	NP	NP
	15%	NP	NP	NP	NP	NP	NP

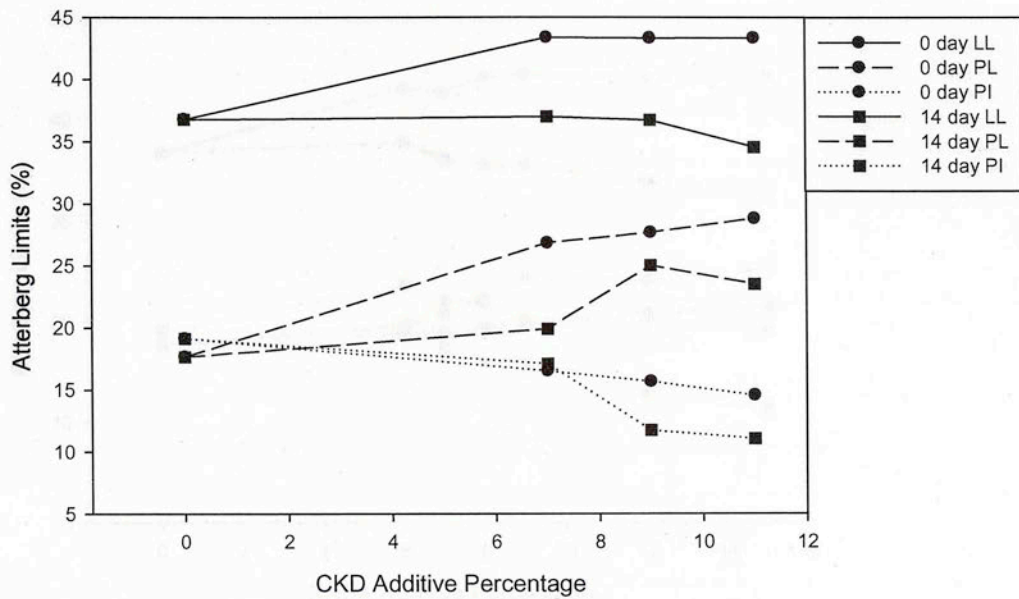


Figure A.36: Ashport-Grainola (A-6) Atterberg Limits with CKD

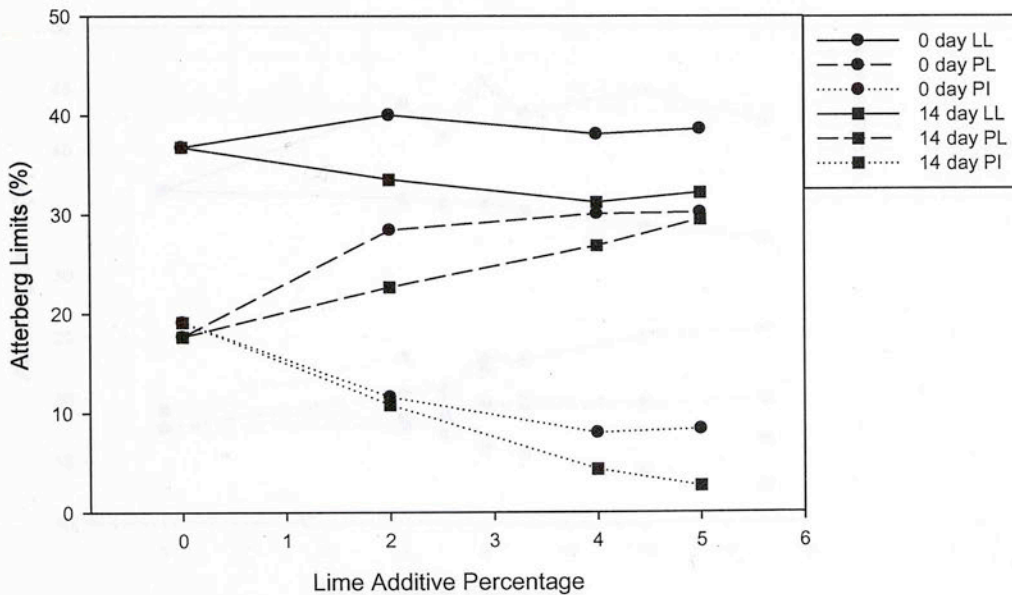


Figure A.37: Ashport-Grainola (A-6) Atterberg Limits with Lime

Table A-13: Ashport-Grainola (A-6) Atterberg Limits

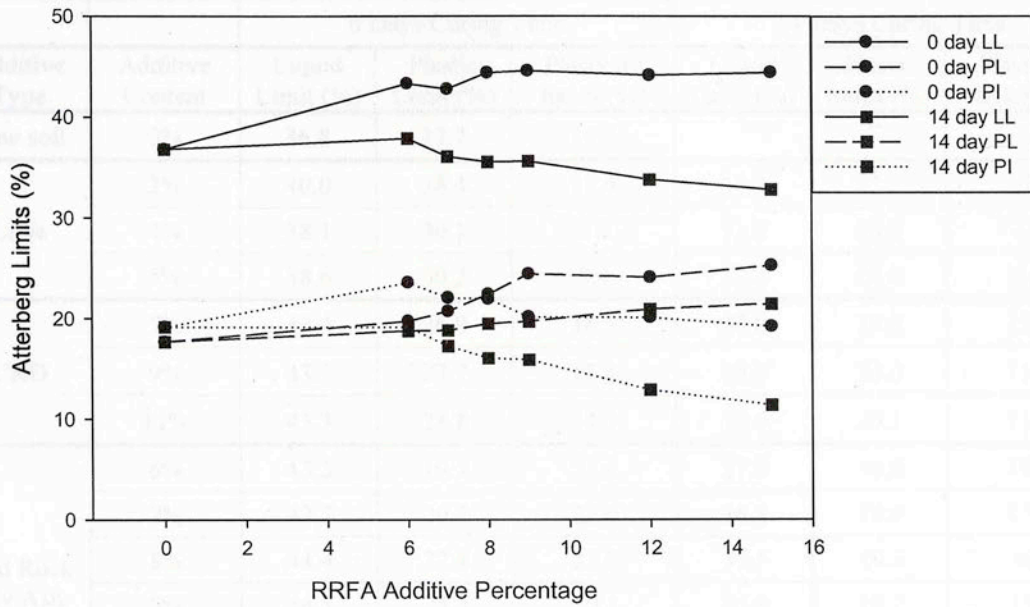


Figure A.38: Ashport-Grainola (A-6) Atterberg Limits with Red Rock FA

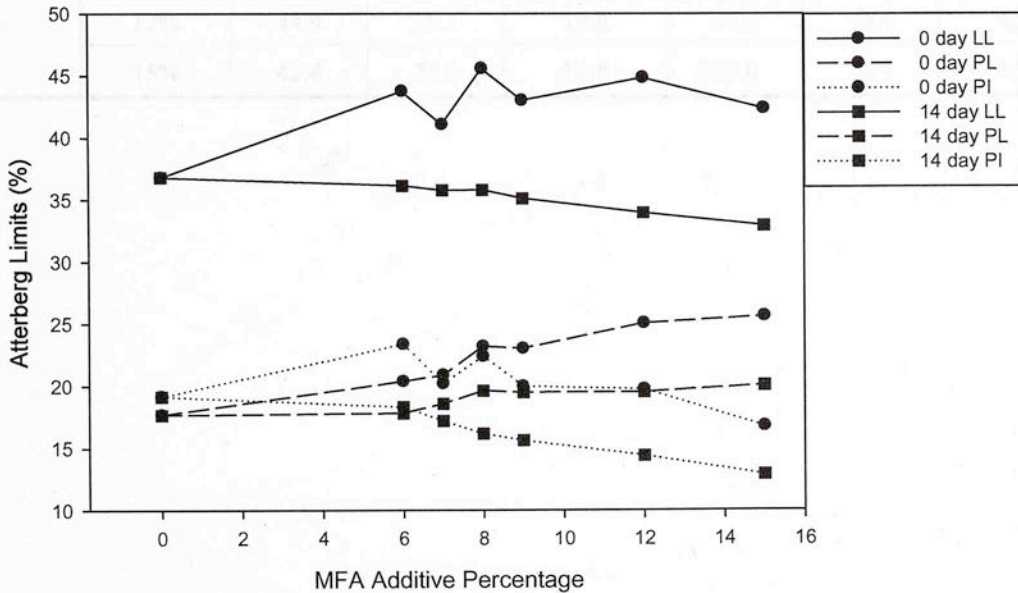


Figure A.39: Ashport-Grainola (A-6) Atterberg Limits with Muskogee FA



**Table A-13: Ashport-Grainola (A-6) Atterberg Limits**

Additive Type	Additive Content	0 Days Curing Time			14 Days Curing Time		
		Liquid Limit (%)	Plastic Limit (%)	Plasticity Index (%)	Liquid Limit (%)	Plastic Index (%)	Plasticity Index (%)
Raw soil	0%	36.8	17.7	19.1			
Lime	2%	40.0	28.4	11.6	33.5	22.7	10.8
	4%	38.1	30.1	8.0	31.2	26.9	4.3
	5%	38.6	30.2	8.4	32.2	29.6	2.6
CKD	7%	43.4	26.9	16.5	37.0	19.9	17.1
	9%	43.3	27.7	15.6	36.7	25.0	11.7
	11%	43.3	28.8	14.5	34.6	23.5	11.1
Red Rock Fly Ash	6%	43.3	19.7	23.6	37.9	18.8	19.1
	7%	42.7	20.7	22.0	36.1	18.8	17.3
	8%	44.4	22.4	22.0	35.5	19.5	16.0
	9%	44.5	24.4	20.1	35.6	19.7	15.9
	12%	44.1	24.1	20.0	33.8	20.9	12.9
	15%	44.4	25.2	19.2	32.8	21.4	11.4
Muskogee Fly Ash	6%	43.8	20.4	23.4	36.1	17.8	18.3
	7%	41.1	20.9	20.2	35.8	18.6	17.2
	8%	45.6	23.2	22.4	35.8	19.6	16.2
	9%	43.0	23.0	20.0	35.1	19.5	15.6
	12%	44.9	25.1	19.8	34.0	19.6	14.4
	15%	42.4	25.6	16.8	33.0	20.1	12.9

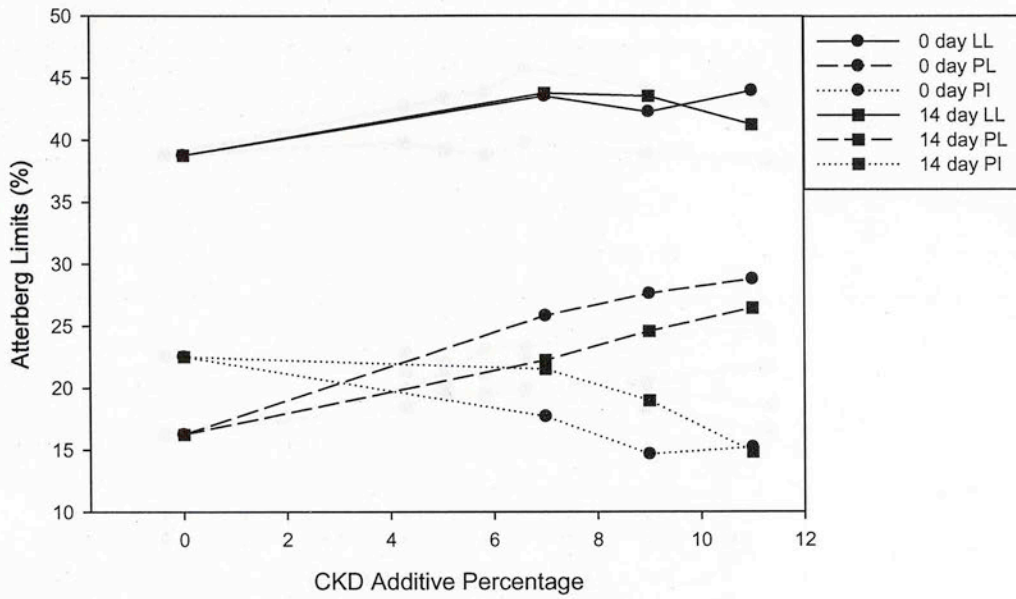


Figure A.40: Kirkland-Pawhuska (A-6) Atterberg Limits with CKD

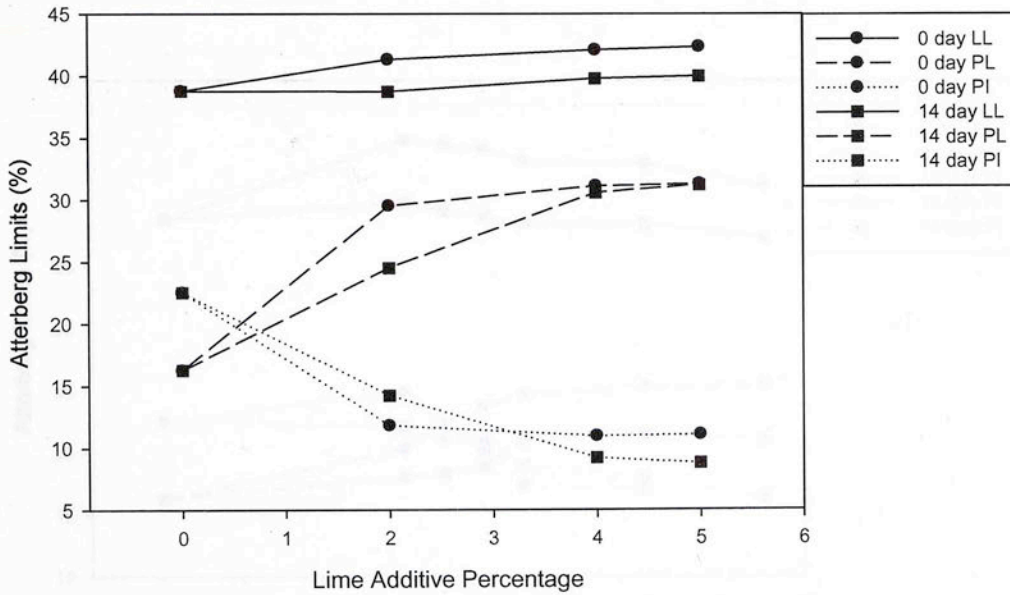


Figure A.41: Kirkland-Pawhuska (A-6) Atterberg Limits with Lime

Table A-14: Kirkland-Pawhuska (A-6) Atterberg Limits

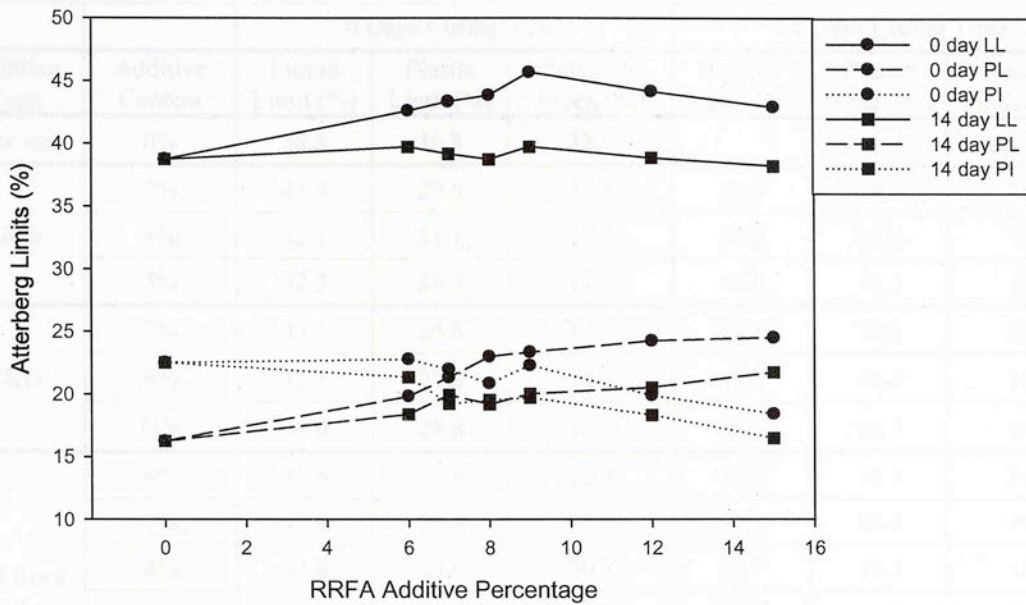


Figure A.42: Kirkland-Pawhuska (A-6) Atterberg Limits with Red Rock FA

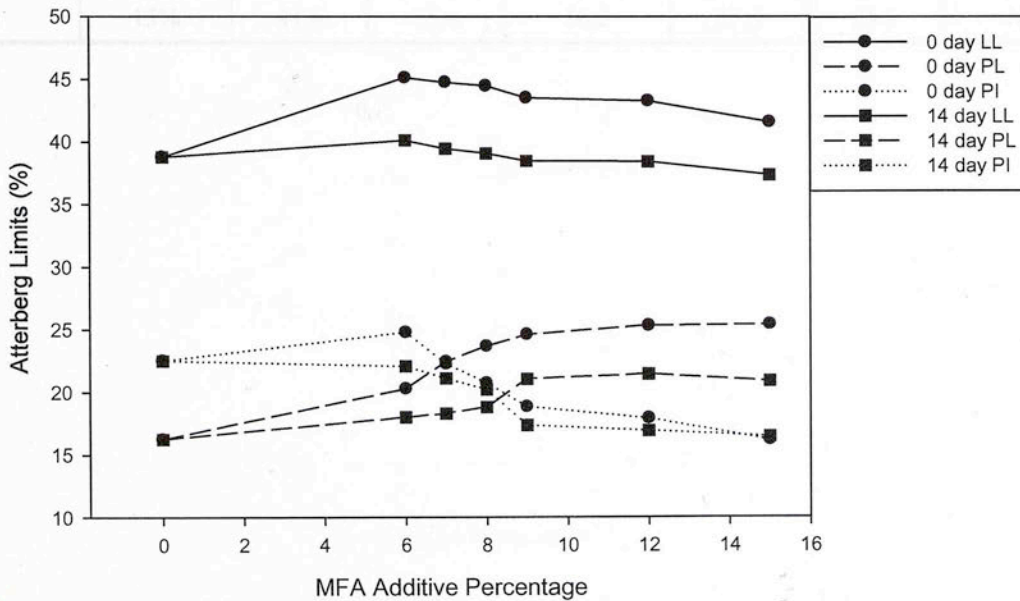


Figure A.43: Kirkland-Pawhuska (A-6) Atterberg Limits with Muskogee FA



**Table A-14: Kirkland-Pawhuska (A-6) Atterberg Limits**

Additive Type	Additive Content	0 Days Curing Time			14 Days Curing Time		
		Liquid Limit (%)	Plastic Limit (%)	Plasticity Index (%)	Liquid Limit (%)	Plastic Index (%)	Plasticity Index (%)
Raw soil	0%	38.8	16.3	22.5			
Lime	2%	41.3	29.5	11.8	38.7	24.5	14.2
	4%	42.1	31.1	11.0	39.8	30.6	9.2
	5%	42.3	31.3	11.0	40.0	31.2	8.8
CKD	7%	43.5	25.8	17.7	43.8	22.2	21.5
	9%	42.3	27.6	14.7	43.5	24.6	18.9
	11%	44.0	28.8	15.2	41.3	26.5	14.8
Red Rock Fly Ash	6%	42.6	19.8	22.8	39.8	18.4	21.4
	7%	43.4	21.4	22.0	39.2	20.0	19.2
	8%	43.8	23.0	20.8	38.7	19.2	19.5
	9%	45.7	23.4	22.3	39.8	20.0	19.7
	12%	44.2	24.3	19.9	38.9	20.5	18.3
	15%	42.9	24.5	18.4	38.2	21.7	16.5
Muskogee Fly Ash	6%	45.1	20.3	24.8	40.1	18.0	22.1
	7%	44.8	22.5	22.3	39.5	18.3	21.1
	8%	44.5	23.7	20.8	39.1	18.8	20.2
	9%	43.5	24.6	18.9	38.5	21.1	17.4
	12%	43.3	25.4	17.9	38.4	21.5	16.9
	15%	41.6	25.4	16.2	37.4	20.9	16.5

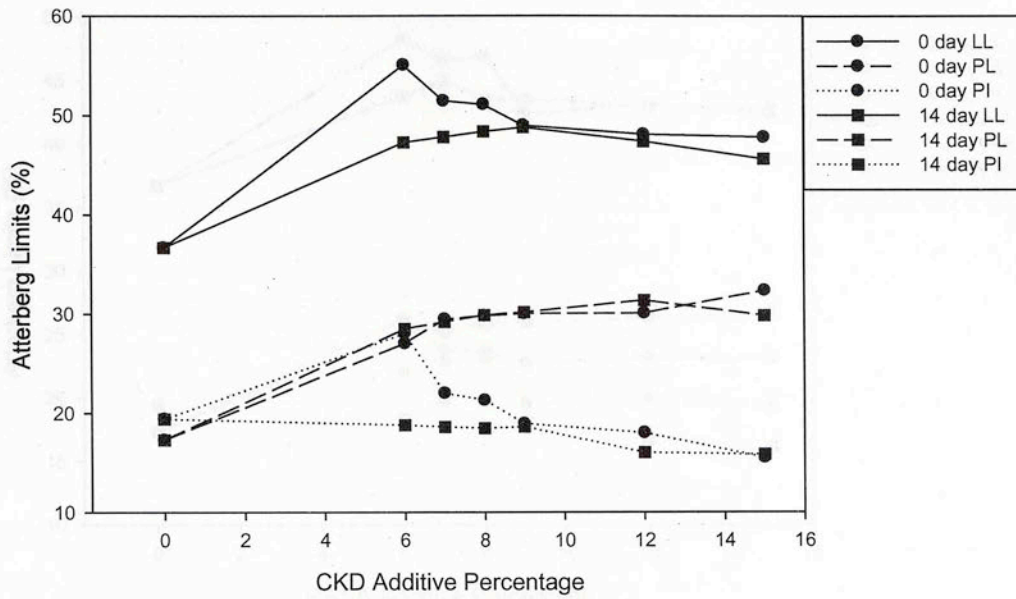


Figure A.44: Flower Pot (A-6) Atterberg Limits with CKD

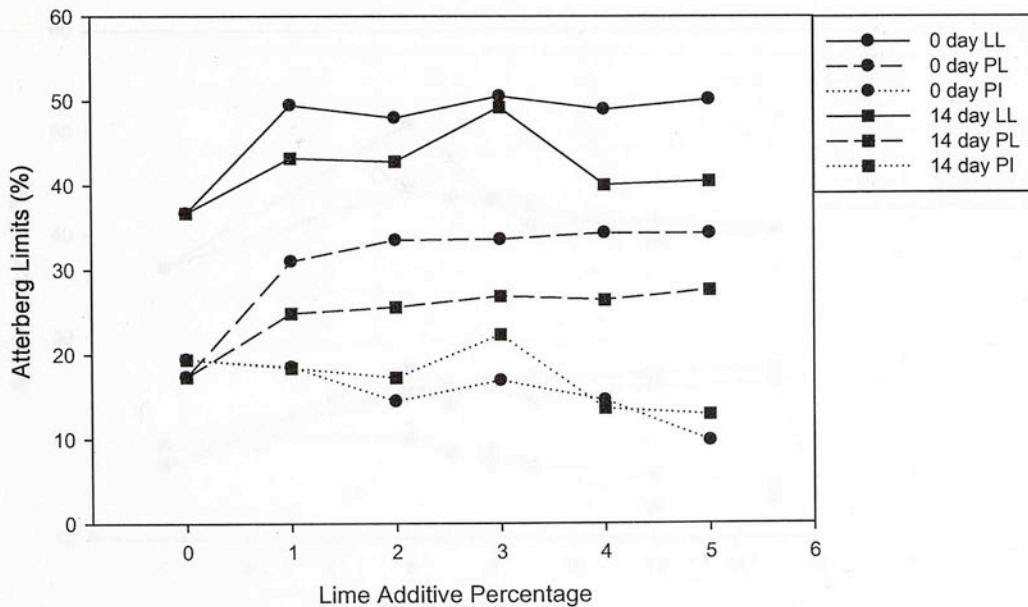


Figure A.45: Flower Pot (A-6) Atterberg Limits with Lime

Table A-15: Flower Pot (A-6) Atterberg Limits

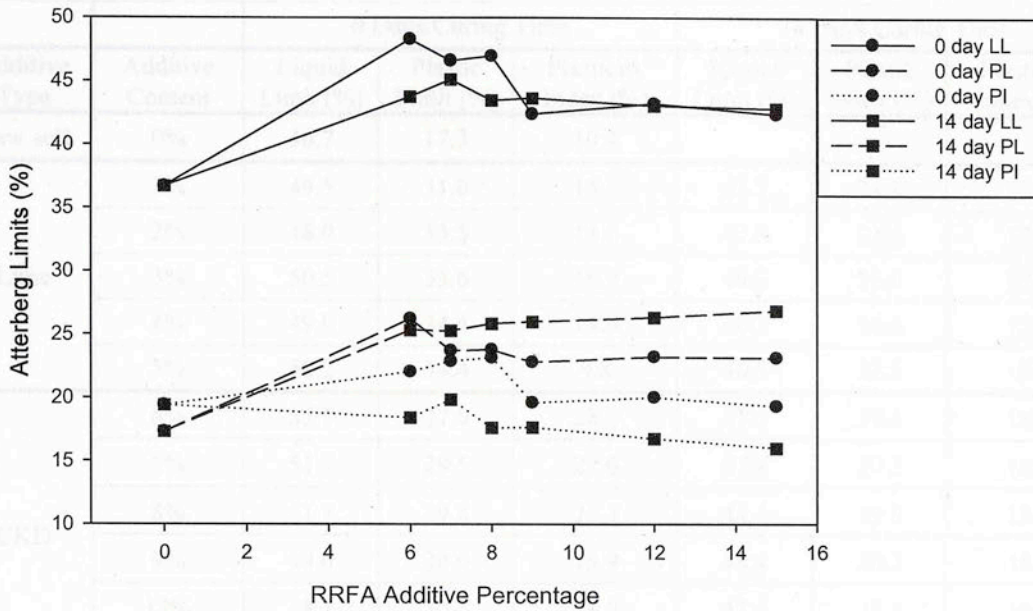


Figure A.46: Flower Pot (A-6) Atterberg Limits with Red Rock FA

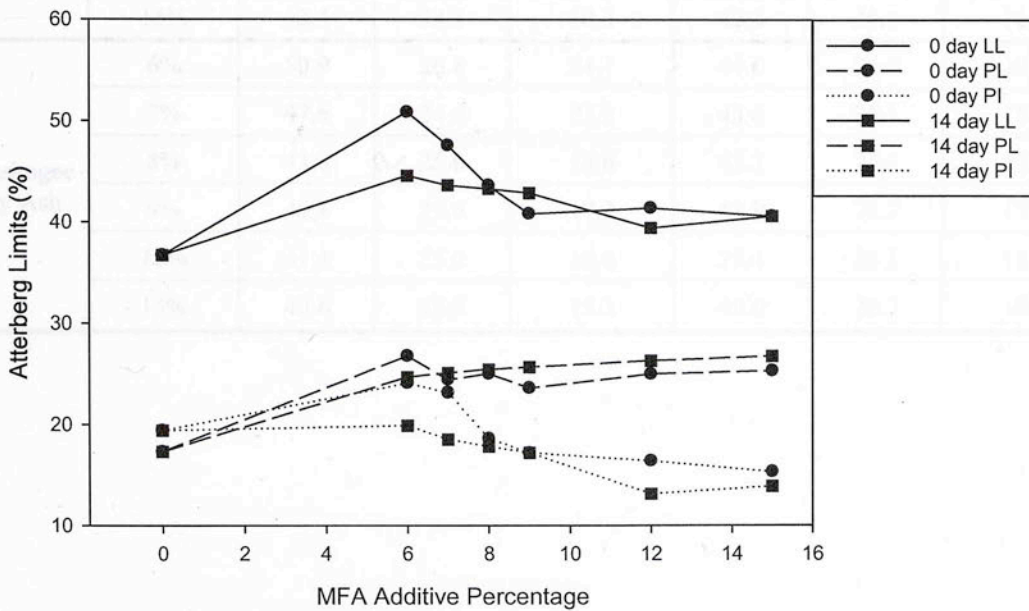


Figure A.47: Flower Pot (A-6) Atterberg Limits with Muskogee FA



**Table A-15: Flower Pot (A-6) Atterberg Limits**

Additive Type	Additive Content	0 Days Curing Time			14 Days Curing Time		
		Liquid Limit (%)	Plastic Limit (%)	Plasticity Index (%)	Liquid Limit (%)	Plastic Index (%)	Plasticity Index (%)
Raw soil	0%	36.7	17.3	19.4			
Lime	1%	49.5	31.0	18.5	43.2	24.8	18.4
	2%	48.0	33.5	14.5	42.8	25.6	17.2
	3%	50.5	33.6	16.9	49.2	26.9	22.3
	4%	49.0	34.4	14.6	40.1	26.4	13.6
	5%	50.2	34.4	9.8	40.5	27.6	12.9
CKD	6%	55.1	27.0	28.0	47.3	28.5	18.8
	7%	51.5	29.5	22.0	47.8	29.2	18.6
	8%	51.1	29.8	21.3	48.4	29.9	18.5
	9%	49.0	30.0	18.9	48.8	30.2	18.6
	12%	48.1	30.1	18.0	47.4	31.4	16.0
	15%	47.8	32.3	15.5	45.6	29.8	15.8
Red Rock Fly Ash	6%	48.3	26.2	22.1	43.8	25.3	18.4
	7%	46.6	23.7	22.9	45.1	25.3	19.8
	8%	47.0	23.8	23.2	43.5	25.9	17.6
	9%	42.4	22.8	19.6	43.6	26.0	17.6
	12%	43.2	23.2	20.0	43.1	26.3	16.7
	15%	42.4	23.1	19.3	42.8	26.8	16.0
Muskogee Fly Ash	6%	50.9	26.8	24.1	44.6	24.7	19.9
	7%	47.6	24.4	23.2	43.6	25.1	18.5
	8%	43.6	25.0	18.6	43.3	25.4	17.8
	9%	40.8	23.6	17.2	42.9	25.7	17.2
	12%	41.4	25.0	16.4	39.4	26.3	13.1
	15%	40.6	25.3	15.3	40.6	26.7	13.9

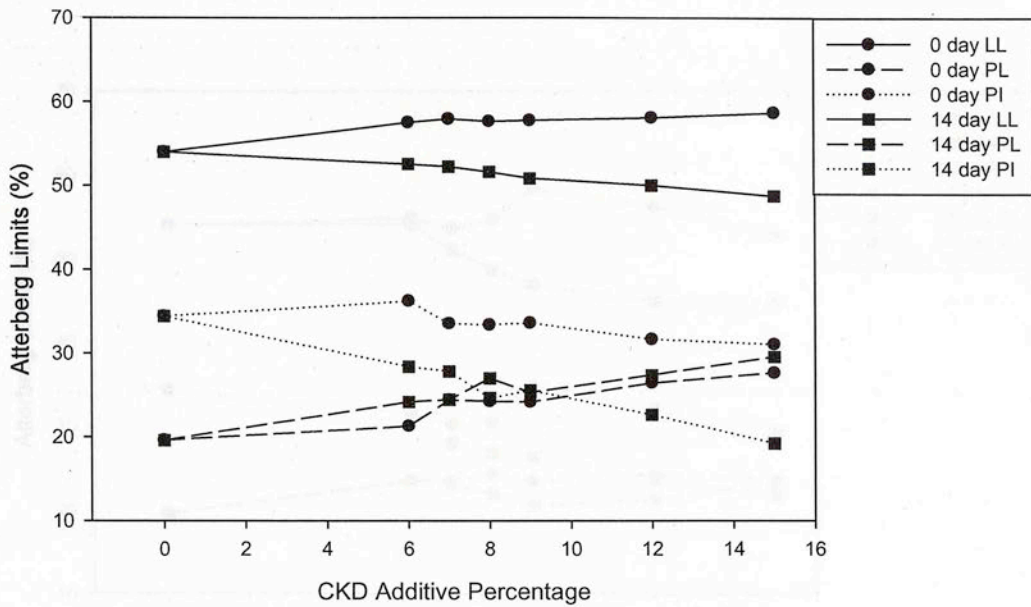


Figure A.48: Hollywood (A-7-6) Atterberg Limits with CKD

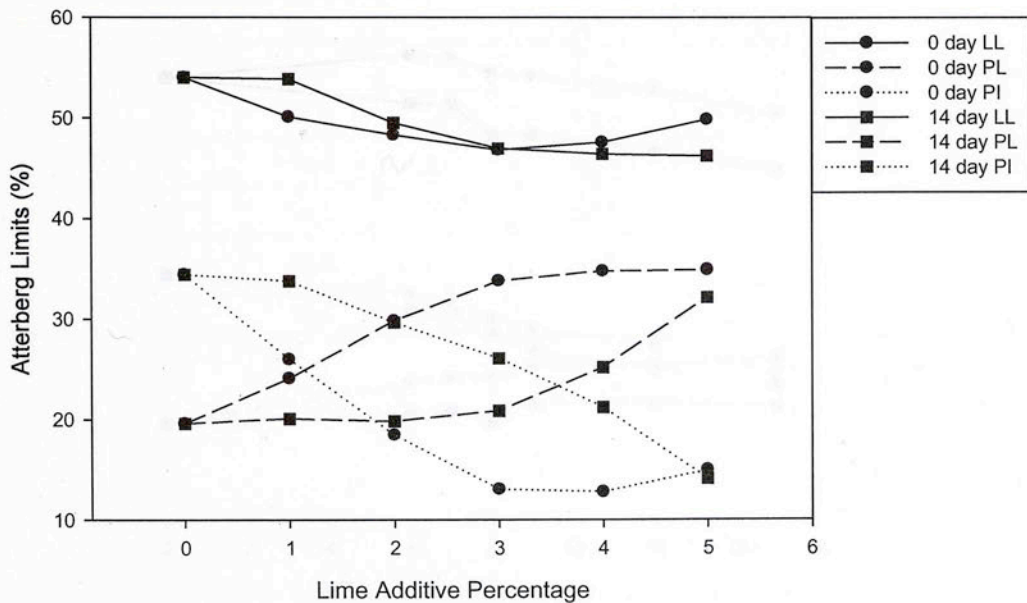


Figure A.49: Hollywood (A-7-6) Atterberg Limits with Lime

Table A-16: Hollywood (A-7-6) Atterberg Limits

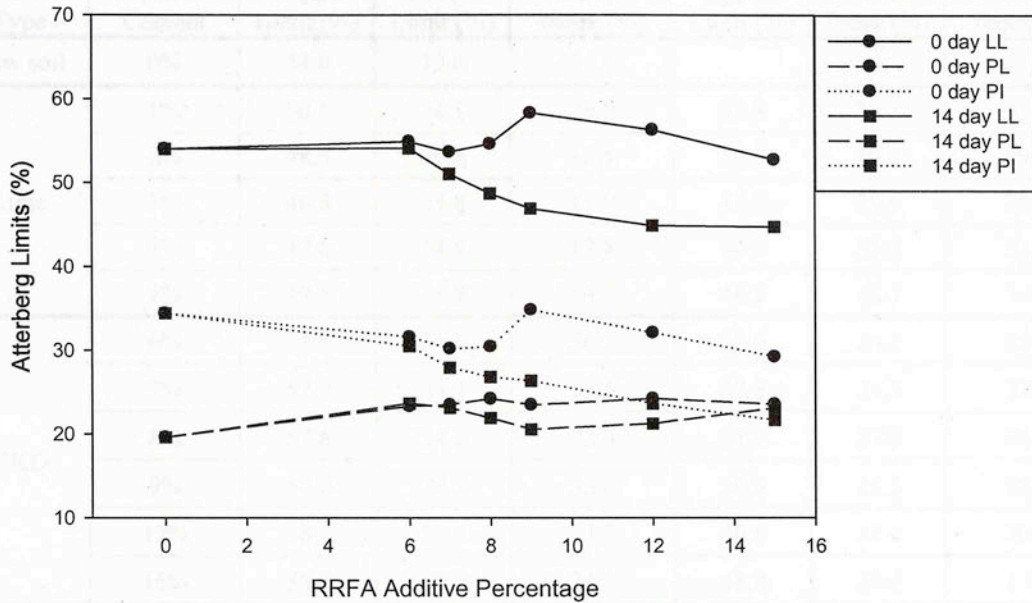


Figure A.50: Hollywood (A-7-6) Atterberg Limits with Red Rock FA

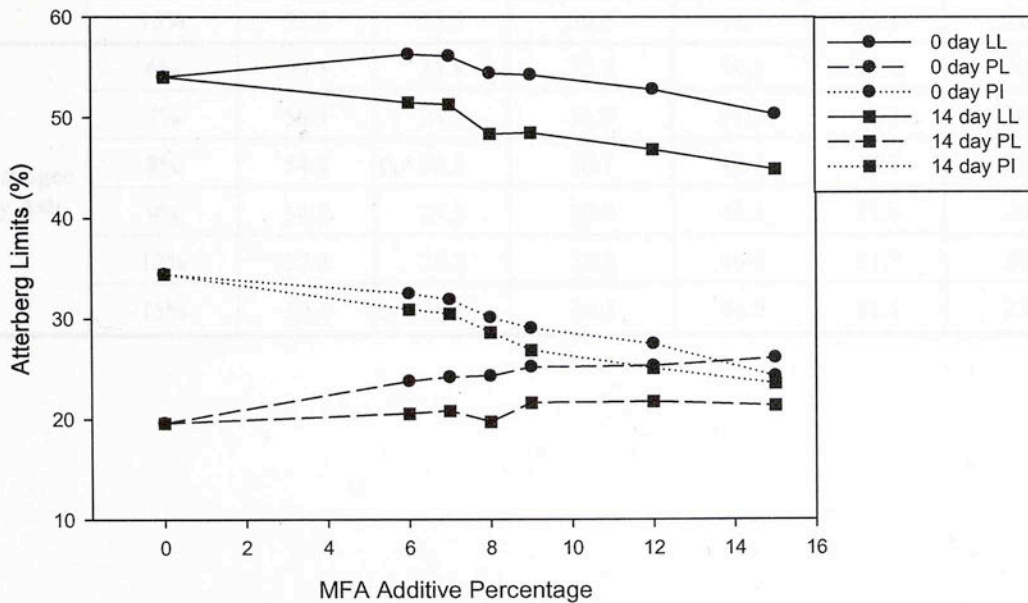


Figure A.51: Hollywood (A-7-6) Atterberg Limits with Muskogee FA



**Table A-16: Hollywood (A-7-6) Atterberg Limits**

Additive Type	Additive Content	0 Days Curing Time			14 Days Curing Time		
		Liquid Limit (%)	Plastic Limit (%)	Plasticity Index (%)	Liquid Limit (%)	Plastic Index (%)	Plasticity Index (%)
Raw soil	0%	54.0	19.6	34.4			
Lime	1%	50.1	24.1	26.0	53.8	20.1	33.7
	2%	48.3	29.8	18.5	49.5	19.8	29.7
	3%	46.8	33.8	13.0	47.0	20.9	26.1
	4%	47.6	34.8	12.8	46.4	25.2	21.2
	5%	49.8	34.9	14.9	46.2	32.1	14.1
CKD	6%	57.5	21.3	36.2	52.6	24.2	28.4
	7%	57.9	24.4	33.5	52.3	24.5	27.8
	8%	57.6	24.2	33.4	51.7	27.0	24.7
	9%	57.8	24.2	33.6	50.9	25.3	25.6
	12%	58.1	26.4	31.7	50.0	27.4	22.6
	15%	58.7	27.6	31.1	48.8	29.6	19.2
Red Rock Fly Ash	6%	54.9	23.3	31.6	54.1	23.6	30.5
	7%	53.7	23.5	30.2	51.1	23.1	27.9
	8%	54.6	24.2	30.4	48.7	21.9	26.8
	9%	58.3	23.5	34.8	46.9	20.6	26.3
	12%	56.3	24.2	32.1	44.9	21.2	23.6
	15%	52.8	23.5	29.3	44.7	23.1	21.6
Muskogee Fly Ash	6%	56.3	23.8	32.5	51.5	20.6	30.9
	7%	56.1	24.2	31.9	51.3	20.8	30.5
	8%	54.4	24.3	30.1	48.4	19.7	28.6
	9%	54.2	25.2	29.0	48.5	21.6	26.9
	12%	52.8	25.3	27.5	46.8	21.7	25.1
	15%	50.4	26.1	24.3	44.9	21.4	23.5

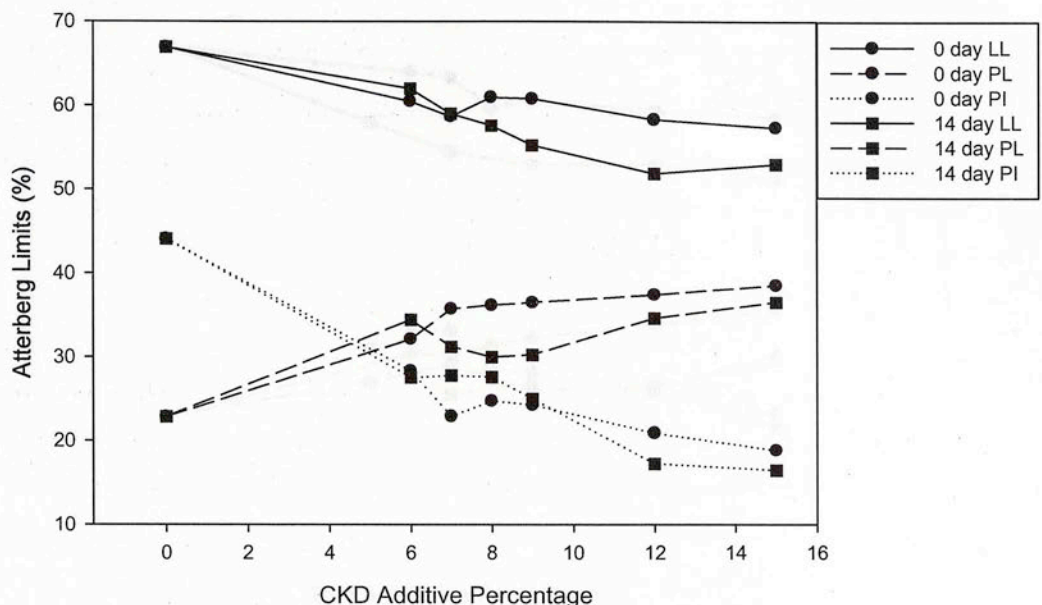


Figure A.52: Heiden (A-7-6) Atterberg Limits with CKD

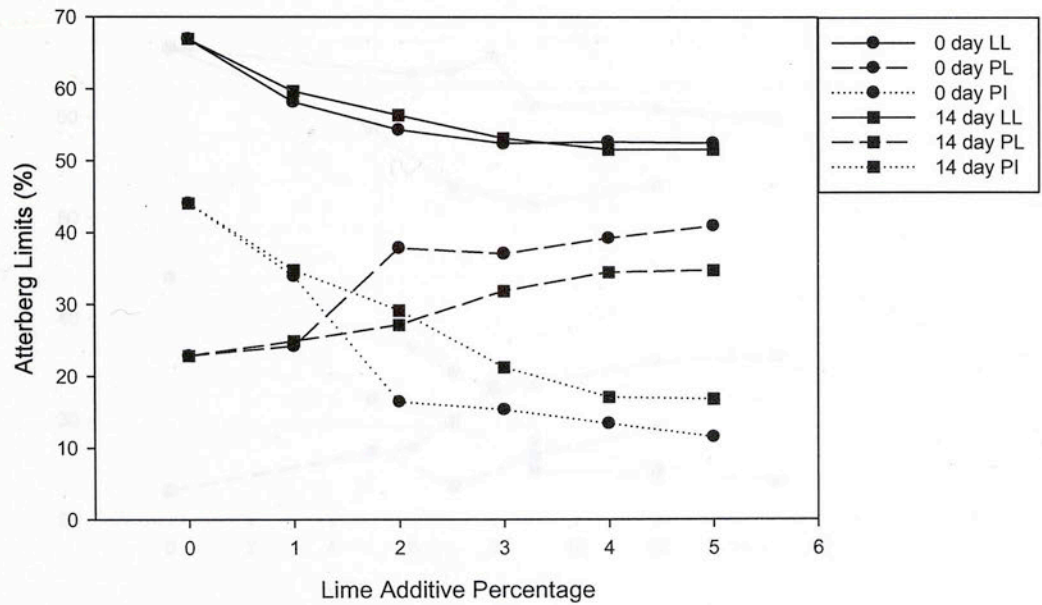


Figure A.53: Heiden (A-7-6) Atterberg Limits with Lime

Table A-17: Heiden (A-7-6) Atterberg Limits

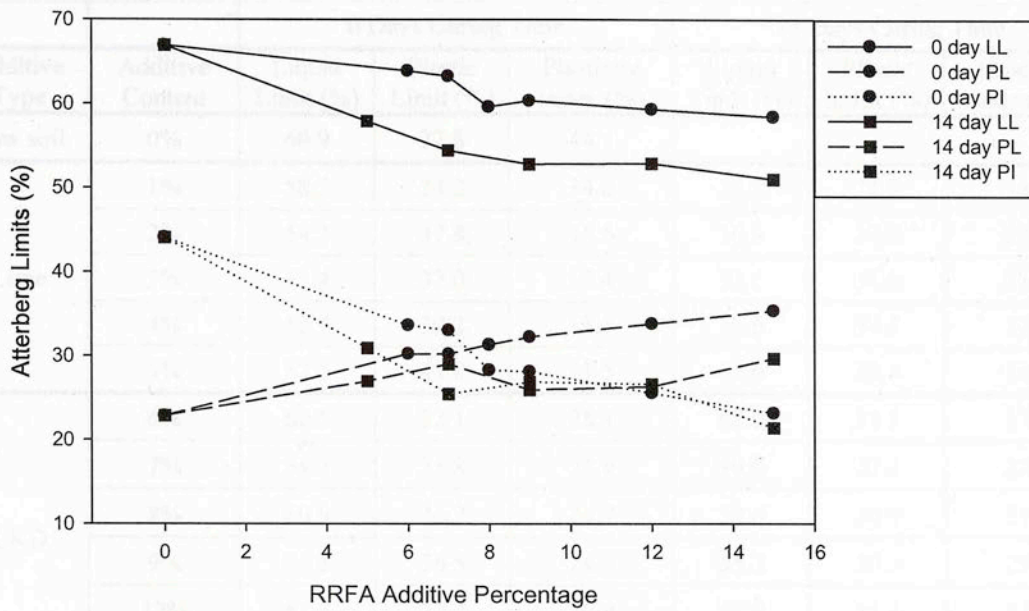


Figure A.54: Heiden (A-7-6) Atterberg Limits with Red Rock FA

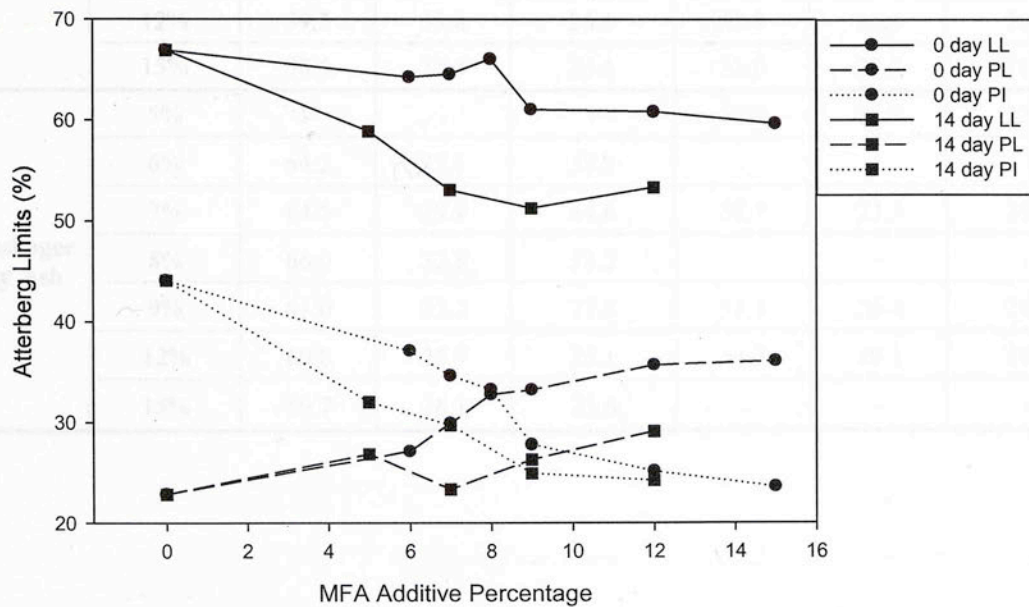


Figure A.55: Heiden (A-7-6) Atterberg Limits with Muskogee FA



**Table A-17: Heiden (A-7-6) Atterberg Limits**

Additive Type	Additive Content	0 Days Curing Time			14 Days Curing Time		
		Liquid Limit (%)	Plastic Limit (%)	Plasticity Index (%)	Liquid Limit (%)	Plastic Index (%)	Plasticity Index (%)
Raw soil	0%	66.9	22.8	44.1			
Lime	1%	58.2	24.2	34.0	59.7	24.9	34.8
	2%	54.3	37.8	16.5	56.3	27.2	29.1
	3%	52.4	37.0	15.4	53.1	31.9	21.2
	4%	52.7	39.2	13.5	51.6	34.5	17.1
	5%	52.5	41.0	11.5	51.6	34.8	16.8
CKD	6%	60.5	32.1	28.4	62.0	34.5	27.5
	7%	58.7	35.8	22.9	59.0	31.2	27.8
	8%	60.9	36.2	24.7	57.6	30.0	27.6
	9%	60.8	36.5	24.3	55.3	30.3	25.0
	12%	58.3	37.4	20.9	51.9	34.6	17.3
	15%	57.4	38.5	18.9	53.0	36.5	16.5
Red Rock Fly Ash	5%	-	-	-	57.9	27.0	30.9
	6%	63.9	30.2	33.7	-	-	-
	7%	63.2	30.2	33.0	54.4	29.0	25.4
	8%	59.6	31.3	28.3	-	-	-
	9%	60.3	32.2	28.1	52.8	25.9	26.9
	12%	59.3	33.8	25.5	52.9	26.3	26.6
	15%	58.5	35.4	23.1	51.0	29.7	21.3
Muskogee Fly Ash	5%	-	-	-	58.9	26.9	32.0
	6%	64.2	27.1	37.1	-	-	-
	7%	64.5	29.9	34.6	53.1	23.3	29.8
	8%	66.0	32.8	33.2	-	-	-
	9%	61.0	33.2	27.8	51.3	26.4	24.9
	12%	60.8	35.7	25.1	53.3	29.1	24.2
	15%	59.7	36.1	23.6	-	-	-

Table A-18: Devol (A-4) Shrinkage Values

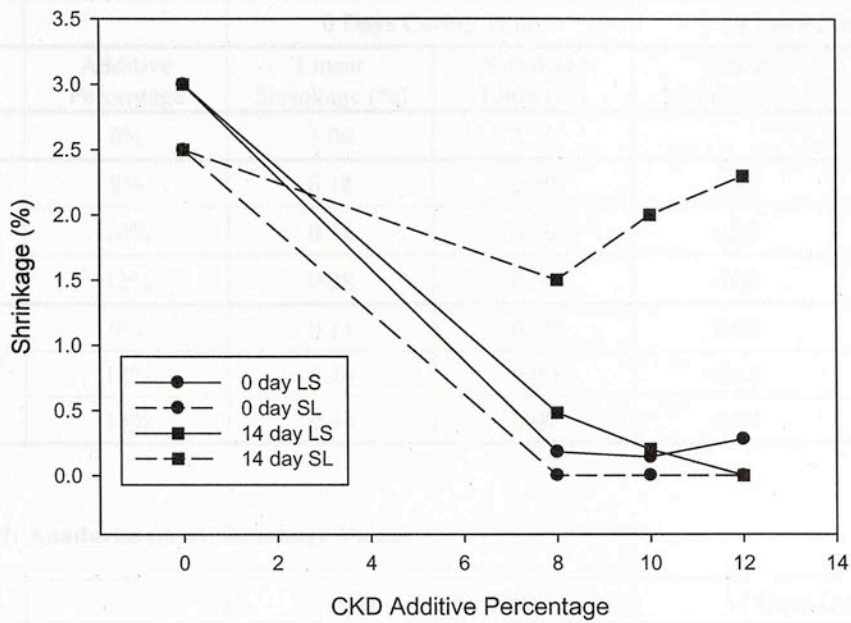


Figure A.56: Devol (A-4) Shrinkage Curves with CKD

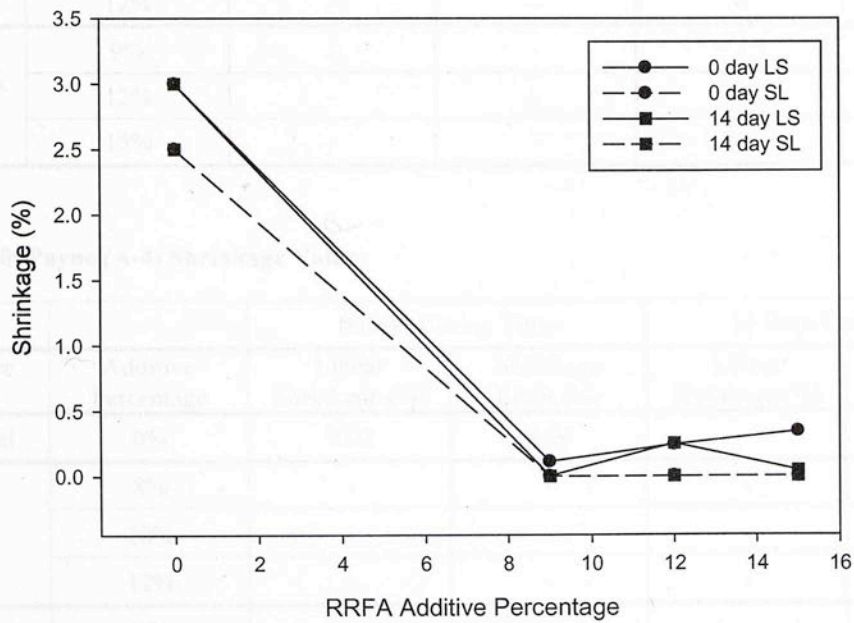


Figure A.57: Devol (A-4) Shrinkage Curves with Red Rock FA

**Table A-18: Devol (A-4) Shrinkage Values**

Additive Type	Additive Percentage	0 Days Curing Time		14 Days Curing Time	
		Linear Shrinkage (%)	Shrinkage Limit (%)	Linear Shrinkage (%)	Shrinkage Limit (%)
Raw soil	0%	3.00	2.50		
CKD	8%	0.18	0.00	0.48	1.50
	10%	0.14	0.00	0.20	2.00
	12%	0.28	0.00	0.00	2.30
Red Rock Fly Ash	9%	0.11	0.00	0.00	0.00
	12%	0.24	0.00	0.25	0.00
	15%	0.34	0.00	0.04	0.00

**Table A-19: Anadarko (A-4) Shrinkage Values**

Additive Type	Additive Percentage	0 Days Curing Time		14 Days Curing Time	
		Linear Shrinkage (%)	Shrinkage Limit (%)	Linear Shrinkage (%)	Shrinkage Limit (%)
Raw soil	0%	2.04	4.50		
CKD	8%	-	-	-	-
	10%	-	-	-	-
	12%	-	-	-	-
Red Rock Fly Ash	9%	-	-	-	-
	12%	-	-	-	-
	15%	-	-	-	-

**Table A-20: Payne (A-4) Shrinkage Values**

Additive Type	Additive Percentage	0 Days Curing Time		14 Days Curing Time	
		Linear Shrinkage (%)	Shrinkage Limit (%)	Linear Shrinkage (%)	Shrinkage Limit (%)
Raw soil	0%	9.02	9.50		
CKD	8%	-	-	-	-
	10%	-	-	-	-
	12%	-	-	-	-
Red Rock Fly Ash	9%	-	-	-	-
	12%	-	-	-	-
	15%	-	-	-	-



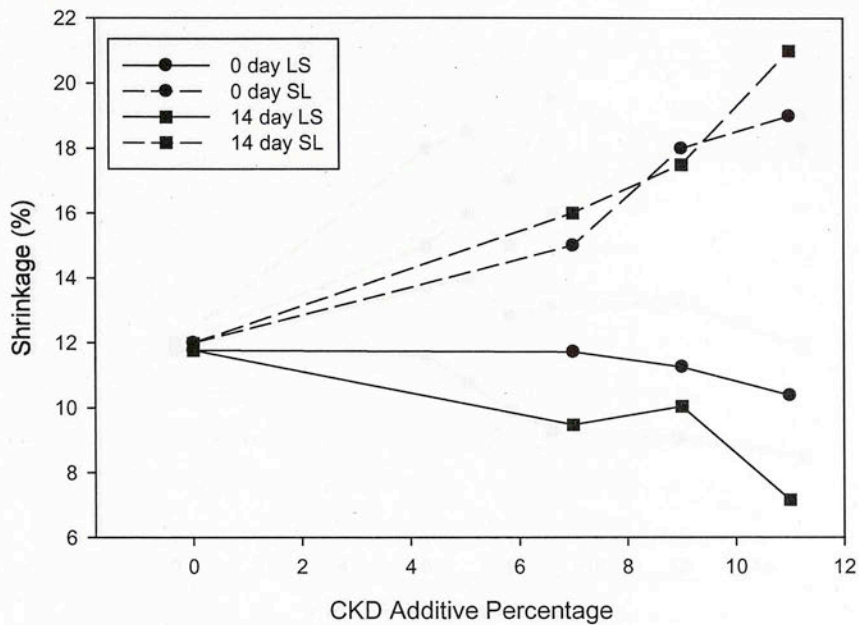


Figure A.58: Ashport-Grainola (A-6) Shrinkage Curves with CKD

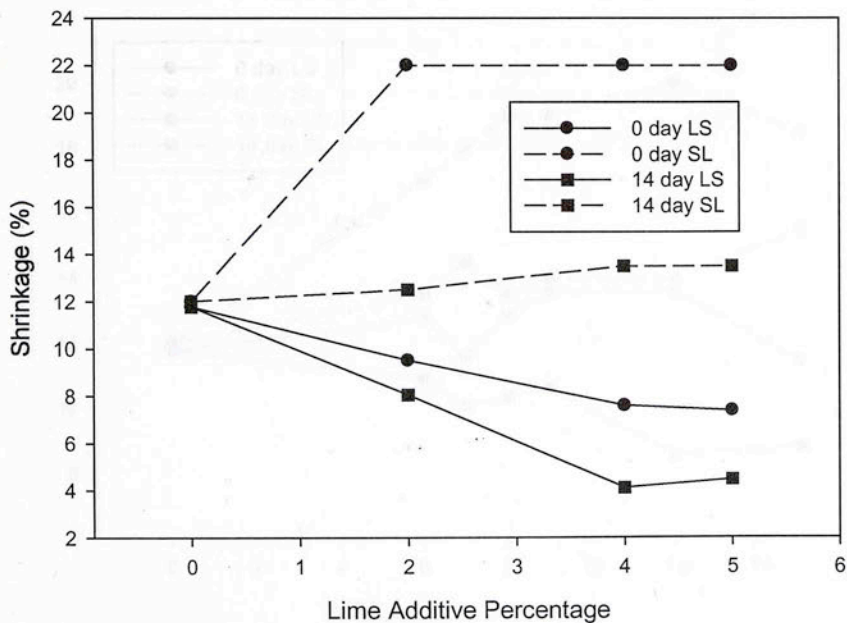


Figure A.59: Ashport-Grainola (A-6) Shrinkage Curves with Lime

Table A-21: Ashport-Grainola (A-6) Shrinkage Curves

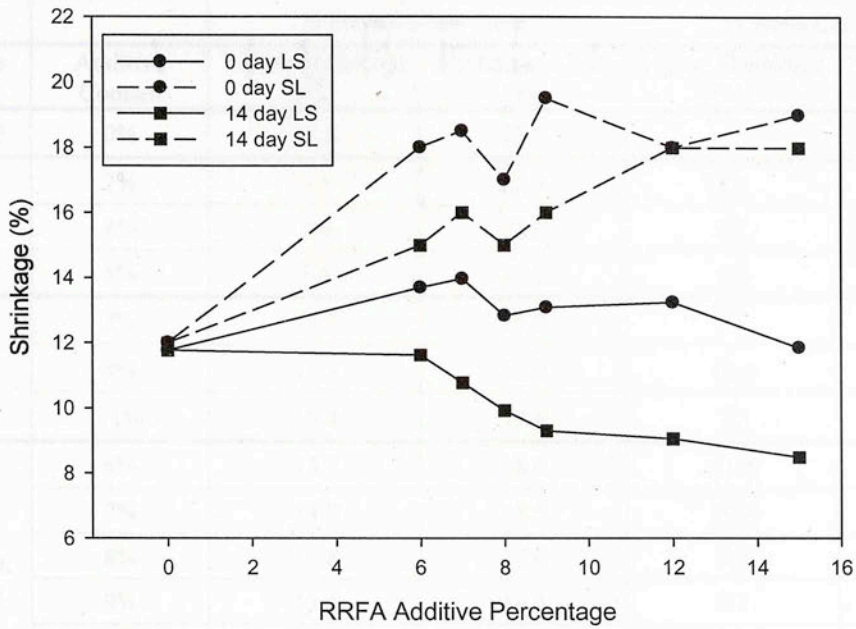


Figure A.60: Ashport-Grainola (A-6) Shrinkage Curves with Red Rock FA

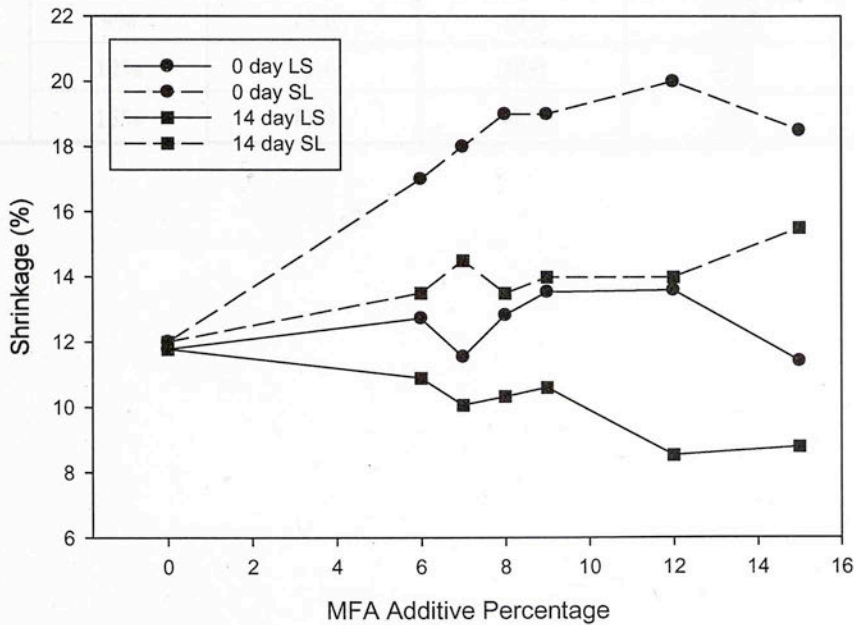


Figure A.61: Ashport-Grainola (A-6) Shrinkage Curves with Muskogee FA

**Table A-21: Ashport-Grainola (A-6) Shrinkage Values**

Additive Type	Additive Content	0 Days Curing Time		14 Days Curing Time	
		Linear Shrinkage (%)	Shrinkage Limit (%)	Linear Shrinkage (%)	Shrinkage Limit (%)
Raw soil	0%	11.8	12.0		
Lime	2%	9.5	22.0	8.1	12.5
	4%	7.6	22.0	4.1	13.5
	5%	7.4	22.0	4.5	13.5
CKD	7%	11.7	15.0	9.5	16.0
	9%	11.3	18.0	10.0	17.5
	11%	10.4	19.0	7.2	21.0
Red Rock Fly Ash	6%	13.7	18.0	11.6	15.0
	7%	14.0	18.5	10.8	16.0
	8%	12.8	17.0	9.9	15.0
	9%	13.1	19.5	9.3	16.0
	12%	13.2	18.0	9.1	18.0
	15%	11.9	19.0	8.5	18.0
Muskogee Fly Ash	6%	12.7	17.0	10.9	13.5
	7%	11.6	18.0	10.1	14.5
	8%	12.8	19.0	10.3	13.5
	9%	13.6	19.0	10.6	14.0
	12%	13.6	20.0	8.5	14.0
	15%	11.4	18.5	8.8	15.5



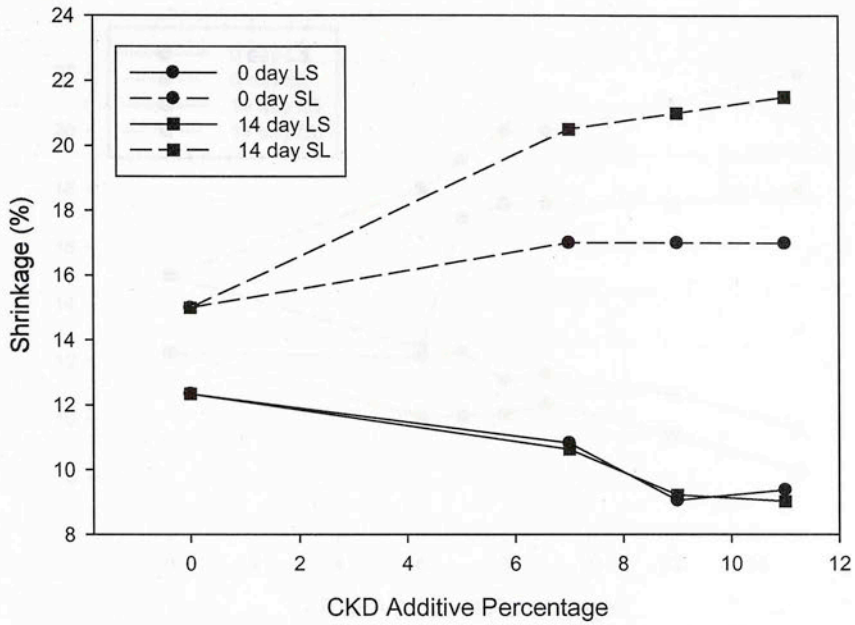


Figure A.62: Kirkland-Pawhuska (A-6) Shrinkage Curves with CKD

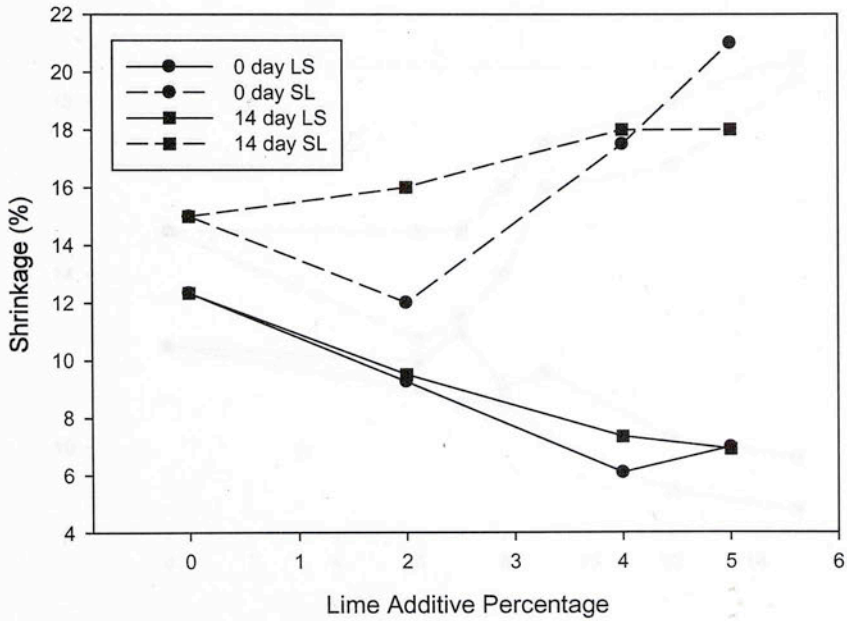


Figure A.63: Kirkland-Pawhuska (A-6) Shrinkage Curves with Lime

Table A-22: Kirkland-Pawhuska (A-6) Shrinkage Values

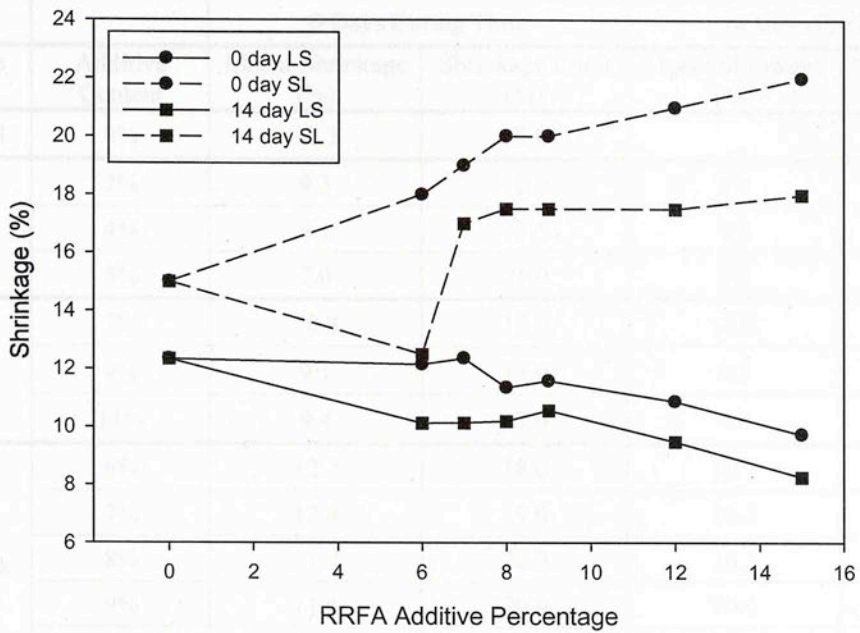


Figure A.64: Kirkland-Pawhuska (A-6) Shrinkage Curves with Red Rock FA

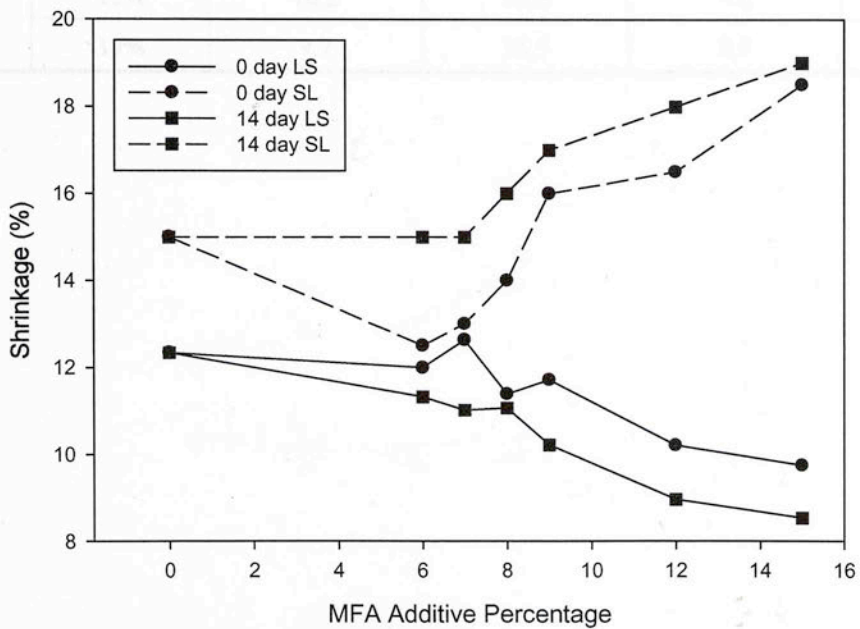


Figure A.65: Kirkland-Pawhuska (A-6) Shrinkage Curves with Muskogee FA

**Table A-22: Kirkland-Pawhuska (A-6) Shrinkage Values**

Additive Type	Additive Content	0 Days Curing Time		14 Days Curing Time	
		Linear Shrinkage (%)	Shrinkage Limit (%)	Linear Shrinkage (%)	Shrinkage Limit (%)
Raw soil	0%	12.3	15.0		
Lime	2%	9.3	12.0	9.5	16.0
	4%	6.1	17.5	7.3	18.0
	5%	7.0	21.0	6.9	18.0
CKD	7%	10.8	17.0	10.6	20.5
	9%	9.1	17.0	9.2	21.0
	11%	9.4	17.0	9.0	21.5
Red Rock Fly Ash	6%	12.2	18.0	10.1	12.5
	7%	12.4	19.0	10.1	17.0
	8%	11.4	20.0	10.2	17.5
	9%	11.6	20.0	10.6	17.5
	12%	10.9	21.0	9.5	17.5
	15%	9.7	22.0	8.3	18.0
Muskogee Fly Ash	6%	12.0	12.5	11.3	15.0
	7%	12.6	13.0	11.0	15.0
	8%	11.4	14.0	11.1	16.0
	9%	11.7	16.0	10.2	17.0
	12%	10.2	16.5	9.0	18.0
	15%	9.7	18.5	8.5	19.0



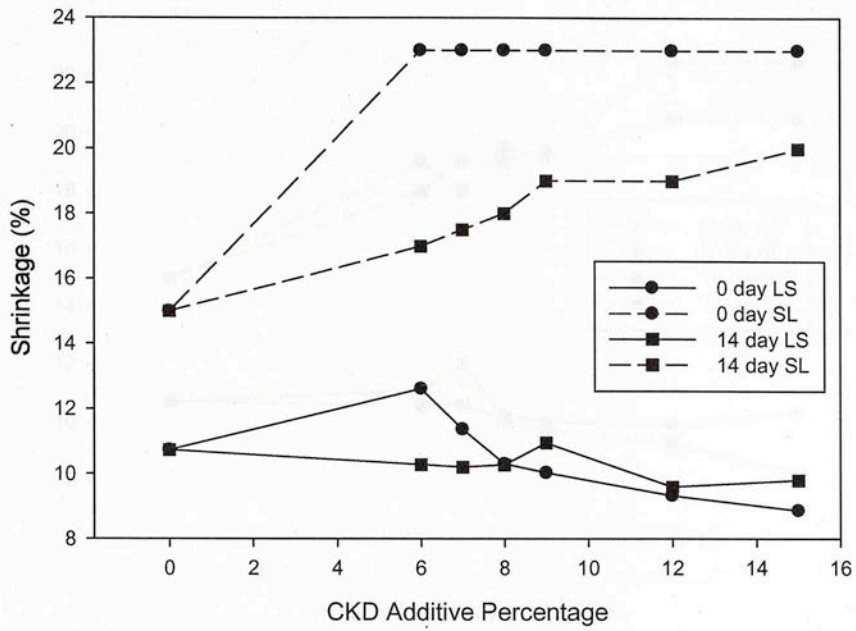


Figure A.66: Flower Pot (A-6) Shrinkage Curves with CKD

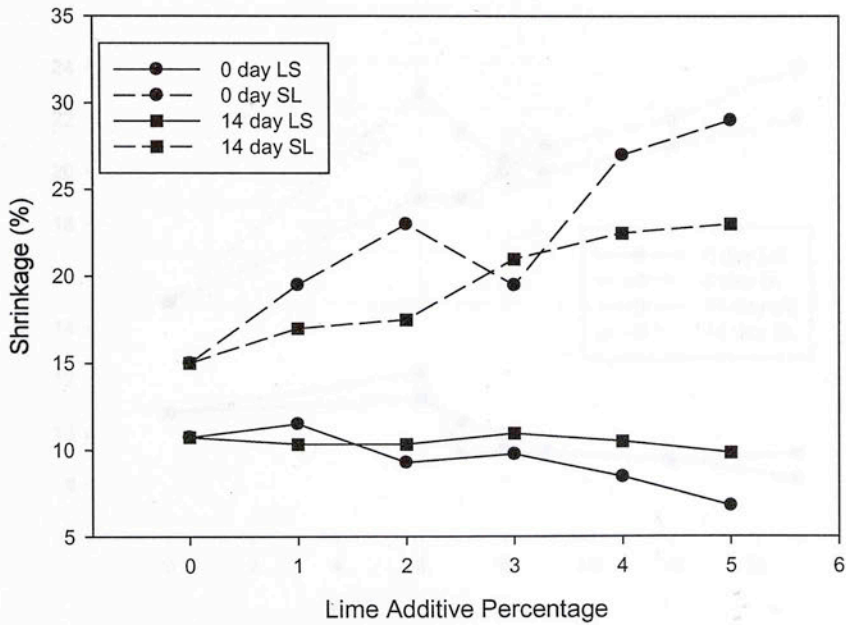


Figure A.67: Flower Pot (A-6) Shrinkage Curves with Lime

Table A-23: Flower Pot (A-6) Shrinkage Values

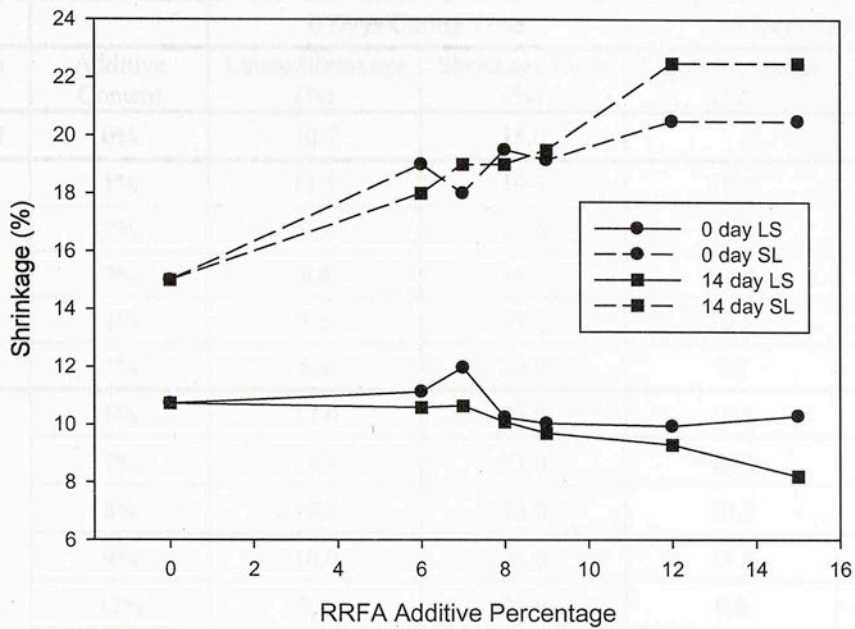


Figure A.68: Flower Pot (A-6) Shrinkage Curves with Red Rock FA

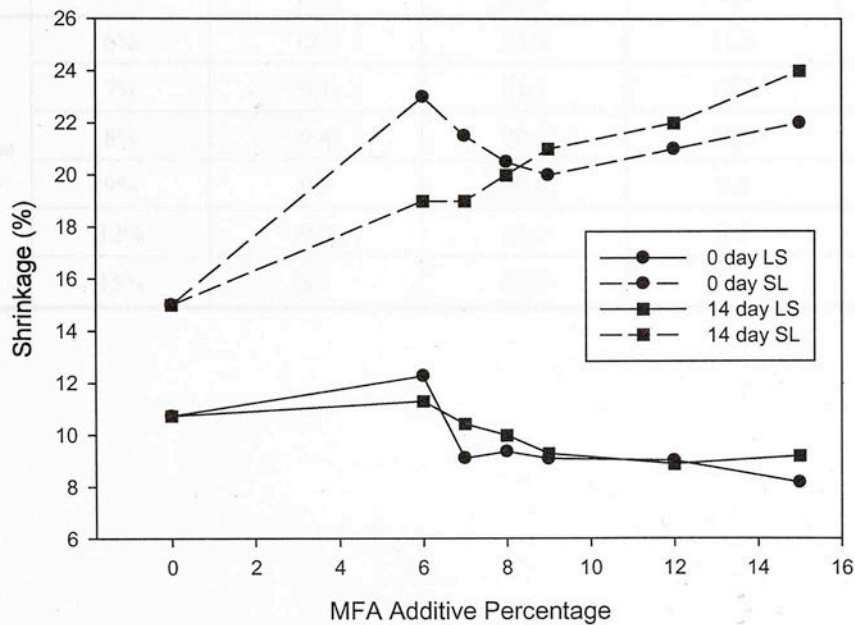


Figure A.69: Flower Pot (A-6) Shrinkage Curves with Muskogee FA

**Table A-23: Flower Pot (A-6) Shrinkage Values**

Additive Type	Additive Content	0 Days Curing Time		14 Days Curing Time	
		Linear Shrinkage (%)	Shrinkage Limit (%)	Linear Shrinkage (%)	Shrinkage Limit (%)
Raw soil	0%	10.7	15.0		
Lime	1%	11.5	19.5	10.3	17.0
	2%	9.3	23.0	10.3	17.5
	3%	9.8	19.5	11.0	21.0
	4%	8.5	27.0	10.5	22.5
	5%	6.8	29.0	9.8	23.0
CKD	6%	12.6	23.0	10.3	17.0
	7%	11.4	23.0	10.2	17.5
	8%	10.3	23.0	10.3	18.0
	9%	10.0	23.0	11.0	19.0
	12%	9.3	23.0	9.6	19.0
	15%	8.9	23.0	9.8	20.0
Red Rock Fly Ash	6%	11.1	19.0	10.6	18.0
	7%	12.0	18.0	10.6	19.0
	8%	10.2	19.5	10.1	19.0
	9%	10.0	19.5	9.7	19.5
	12%	9.9	20.5	9.3	22.5
	15%	10.3	20.5	8.2	22.5
Muskogee Fly Ash	6%	12.3	23.0	11.3	19.0
	7%	9.1	21.5	10.4	19.0
	8%	9.4	20.5	10.0	20.0
	9%	9.1	20.0	9.3	21.0
	12%	9.0	21.0	8.9	22.0
	15%	8.2	22.0	9.2	24.0



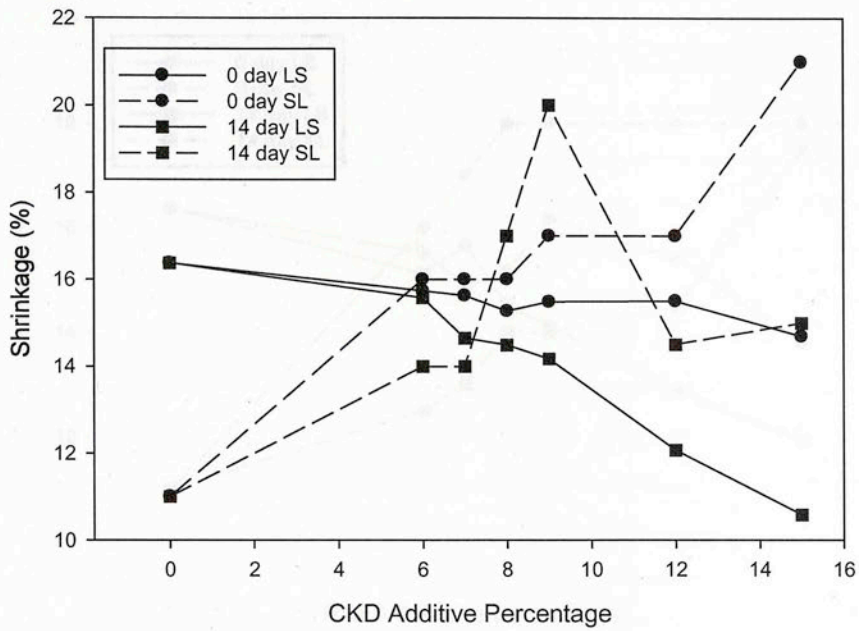


Figure A.70: Hollywood (A-7-6) Shrinkage Curves with CKD

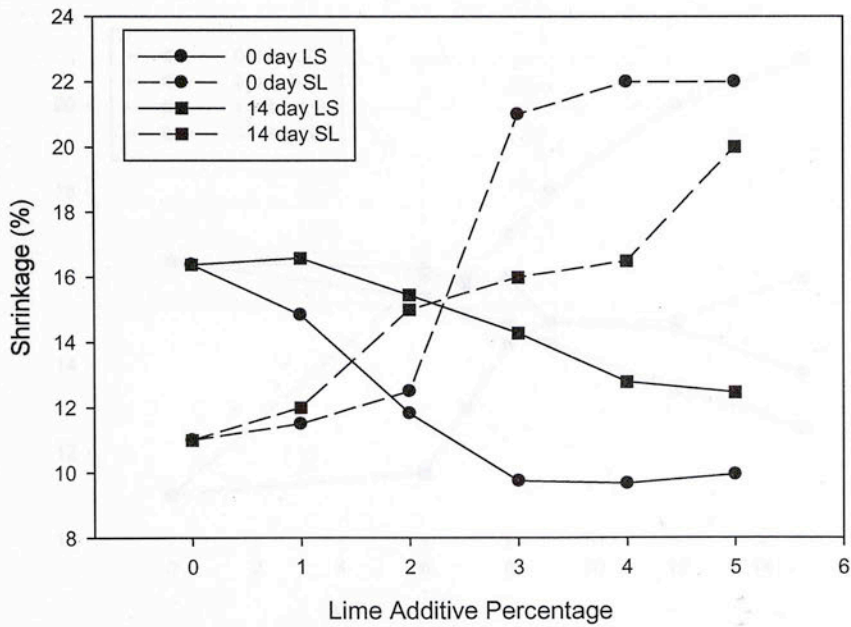


Figure A.71: Hollywood (A-7-6) Shrinkage Curves with Lime

Table A-24: Hollywood (A-7-6) Shrinkage Values

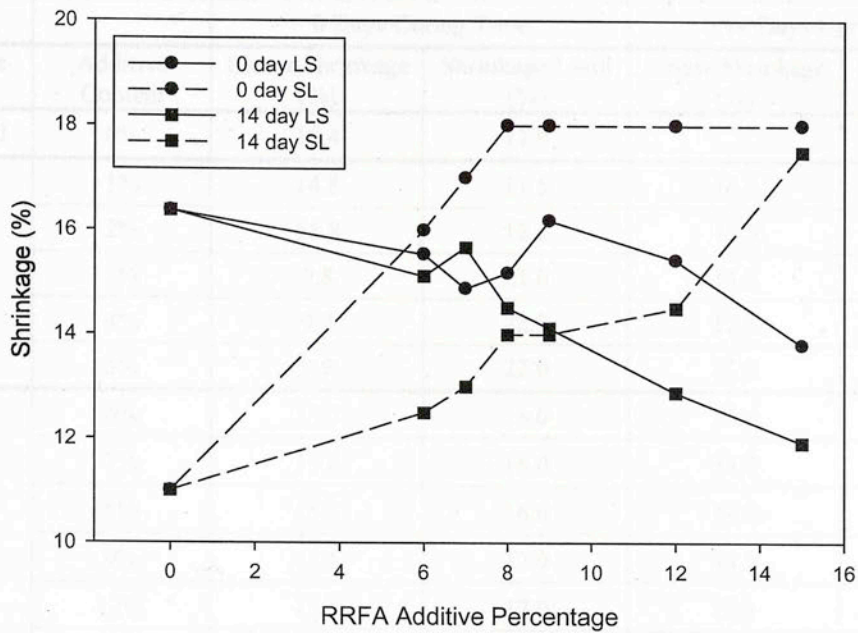


Figure A.72: Hollywood (A-7-6) Shrinkage Curves with Red Rock FA

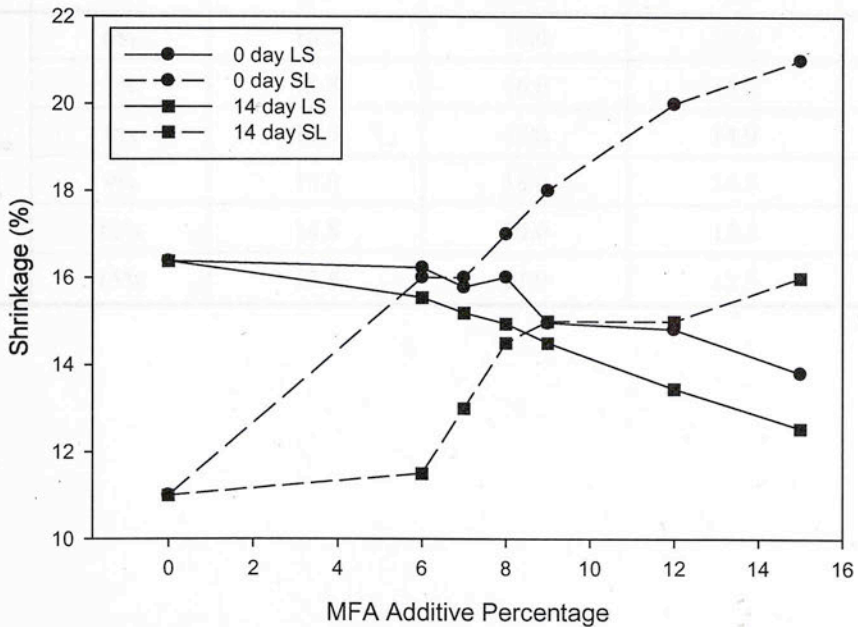


Figure A.73: Hollywood (A-7-6) Shrinkage Curves with Muskogee FA

**Table A-24: Hollywood (A-7-6) Shrinkage Values**

Additive Type	Additive Content	0 Days Curing Time		14 Days Curing Time	
		Linear Shrinkage (%)	Shrinkage Limit (%)	Linear Shrinkage (%)	Shrinkage Limit (%)
Raw soil	0%	16.4	11.0		
Lime	1%	14.8	11.5	16.6	12.0
	2%	11.8	12.5	15.5	15.0
	3%	9.8	21.0	14.3	16.0
	4%	9.7	22.0	12.8	16.5
	5%	9.9	22.0	12.5	20.0
CKD	6%	15.7	16.0	15.6	14.0
	7%	15.6	16.0	14.7	14.0
	8%	15.3	16.0	14.5	17.0
	9%	15.5	17.0	14.2	20.0
	12%	15.5	17.0	12.1	14.5
	15%	14.7	21.0	10.6	15.0
Red Rock Fly Ash	6%	15.5	16.0	15.1	12.5
	7%	14.9	17.0	15.7	13.0
	8%	15.2	18.0	14.5	14.0
	9%	16.2	18.0	14.1	14.0
	12%	15.4	18.0	12.9	14.5
	15%	13.8	18.0	11.9	17.5
Muskogee Fly Ash	6%	16.2	16.0	15.5	11.5
	7%	15.8	16.0	15.2	13.0
	8%	16.0	17.0	14.9	14.5
	9%	15.0	18.0	14.5	15.0
	12%	14.8	20.0	13.5	15.0
	15%	13.8	21.0	12.5	16.0



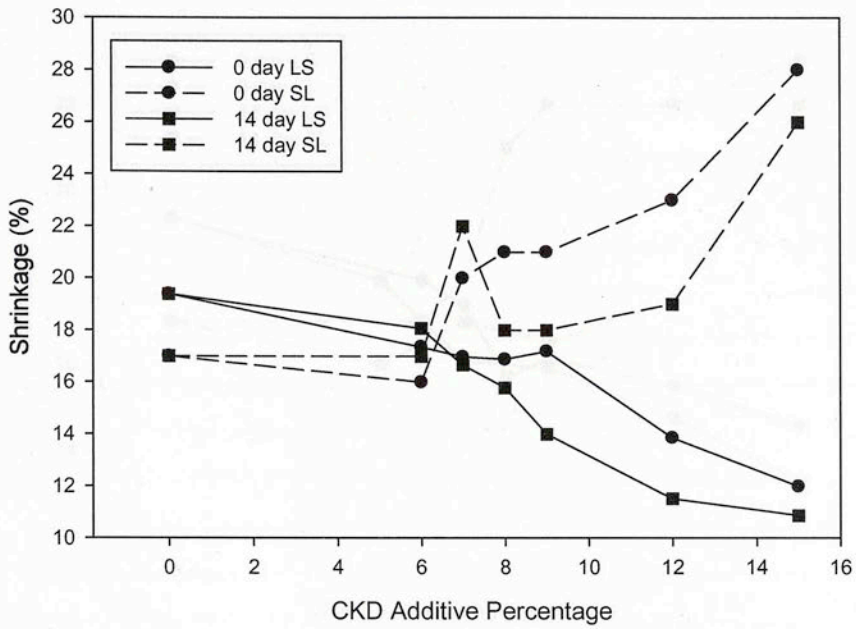


Figure A.74: Heiden (A-7-6) Shrinkage Curves with CKD

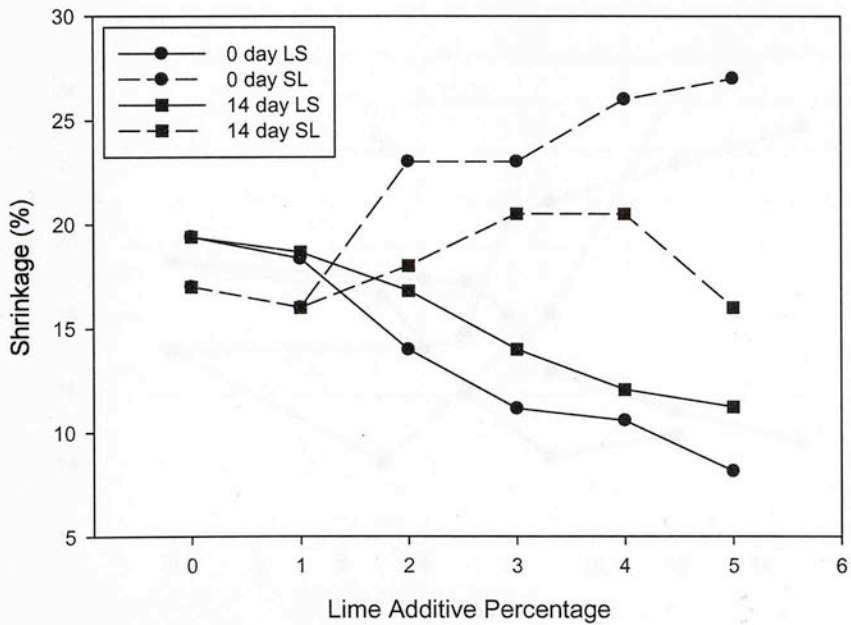


Figure A.75: Heiden (A-7-6) Shrinkage Curves with Lime

Table A-25: Heiden (A-7-6) Shrinkage Values

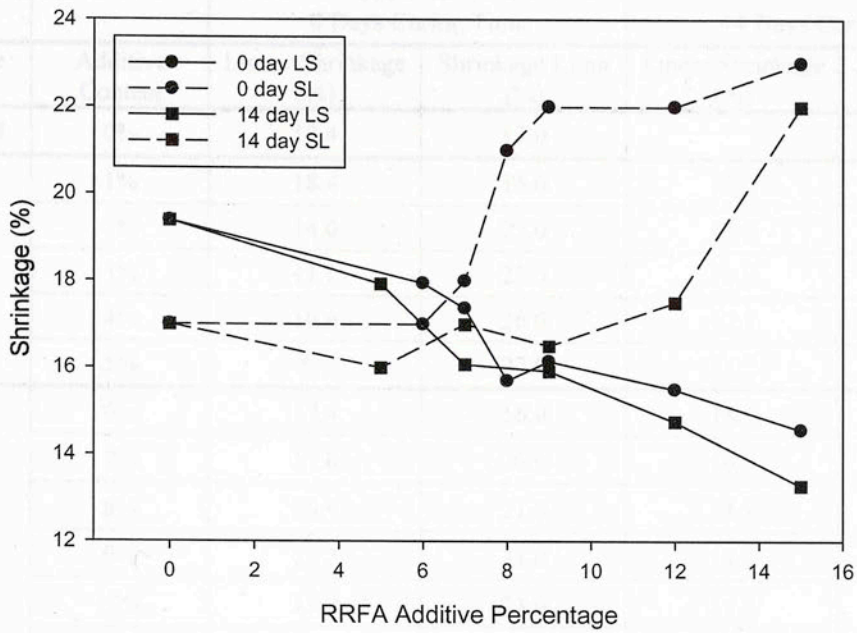


Figure A.76: Heiden (A-7-6) Shrinkage Curves with Red Rock FA

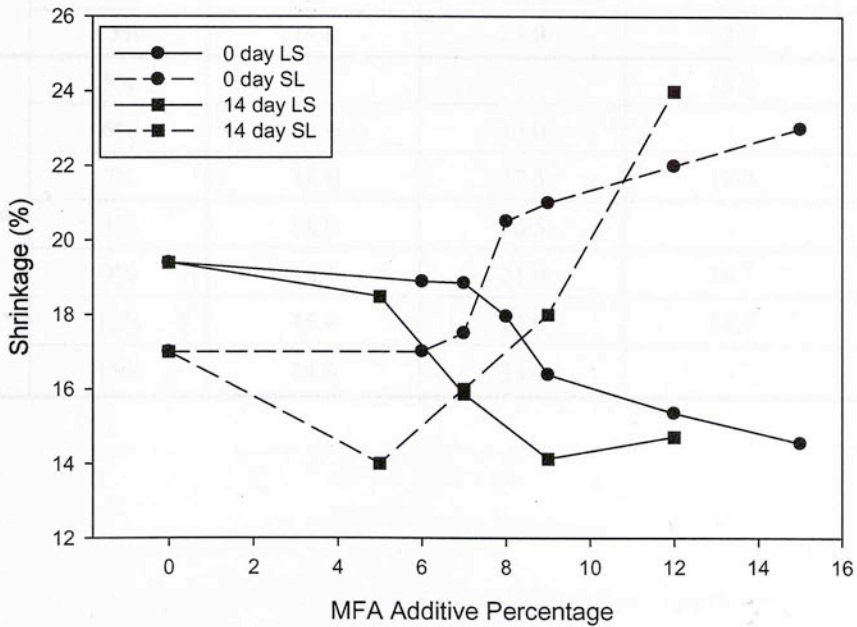


Figure A.77: Heiden (A-7-6) Shrinkage Curves with Muskogee FA

**Table A-25: Heiden (A-7-6) Shrinkage Values**

Additive Type	Additive Content	0 Days Curing Time		14 Days Curing Time	
		Linear Shrinkage (%)	Shrinkage Limit (%)	Linear Shrinkage (%)	Shrinkage Limit (%)
Raw soil	0%	19.4	17.0		
Lime	1%	18.4	16.0	18.7	16.0
	2%	14.0	23.0	16.8	18.0
	3%	11.2	23.0	14.0	20.5
	4%	10.6	26.0	12.1	20.5
	5%	8.1	27.0	11.2	16.0
CKD	6%	17.4	16.0	18.1	17.0
	7%	17.0	20.0	16.7	22.0
	8%	16.9	21.0	15.8	18.0
	9%	17.2	21.0	14.0	18.0
	12%	13.9	23.0	11.5	19.0
	15%	12.0	28.0	10.9	26.0
Red Rock Fly Ash	5%	-	-	17.9	16.0
	6%	18.0	17.0	-	-
	7%	17.4	18.0	16.1	17.0
	8%	15.7	21.0	-	-
	9%	16.2	22.0	15.9	16.5
	12%	15.5	22.0	14.7	17.5
	15%	14.6	23.0	13.3	22.0
Muskogee Fly Ash	5%	-	-	18.5	14.0
	6%	18.9	17.0	-	-
	7%	18.8	17.5	15.9	16.0
	8%	18.0	20.5	-	-
	9%	16.4	21.0	14.1	18.0
	12%	15.4	22.0	14.7	24.0
	15%	14.6	23.0	-	-



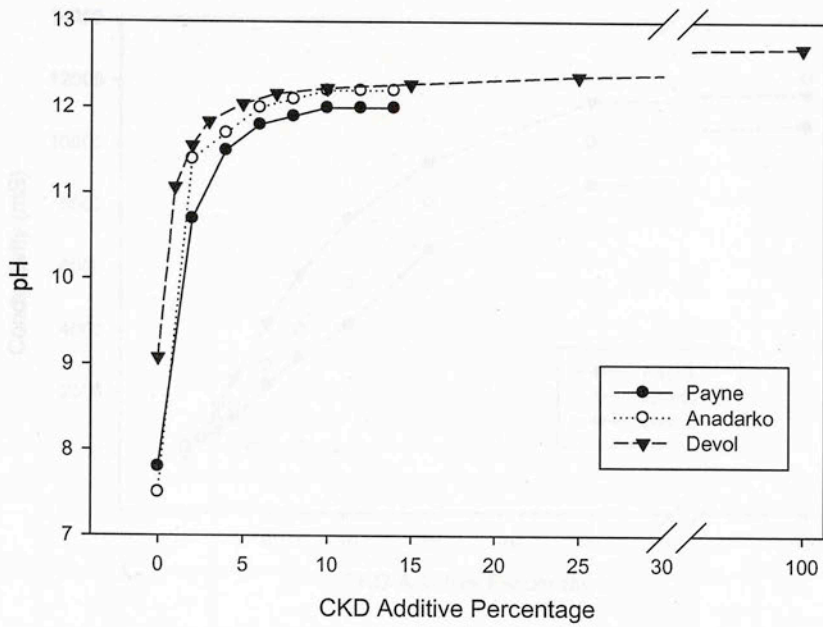


Figure A.78: pH Curves for A-4 Soils with CKD

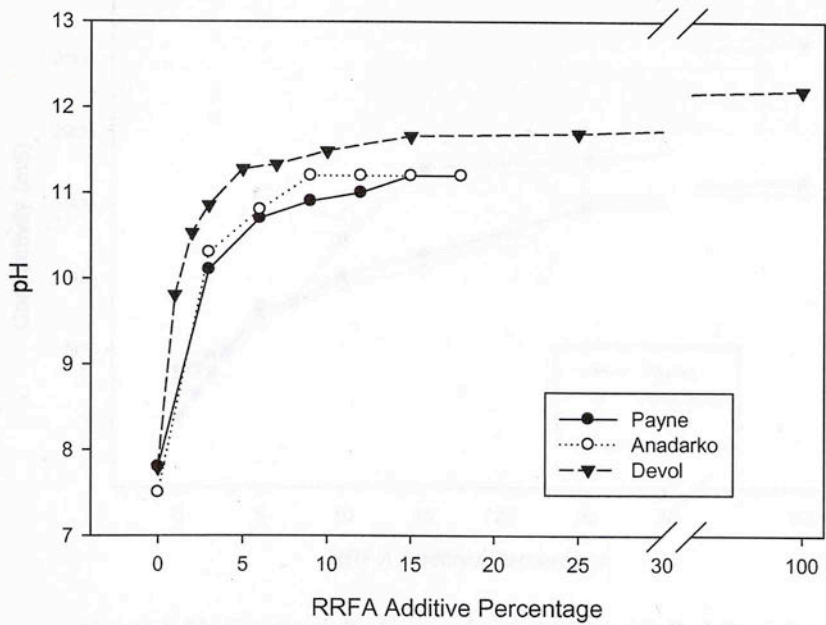


Figure A.79: pH Curves for A-4 Soils with Red Rock FA

Table A-24: Measured pH and Conductivity Values for A-4 Soils

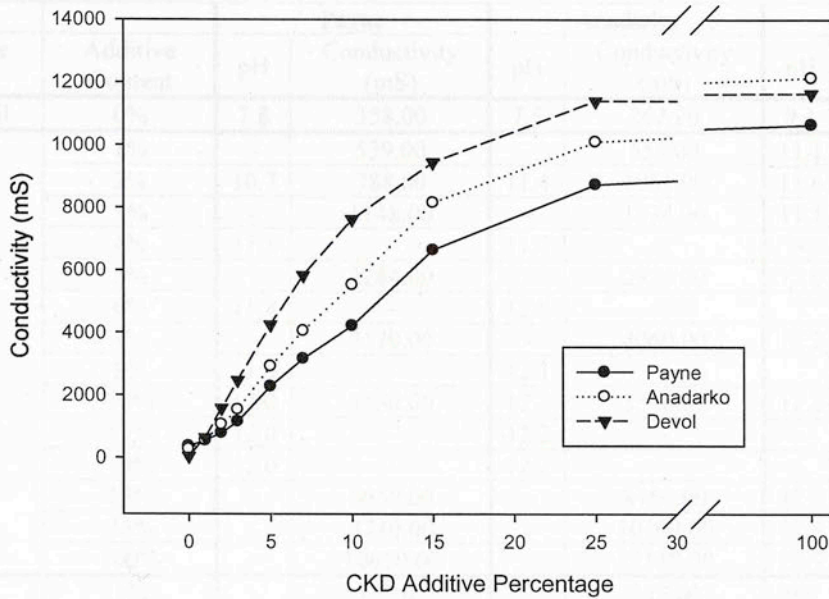


Figure A.80: Conductivity Curves for A-4 Soils with CKD

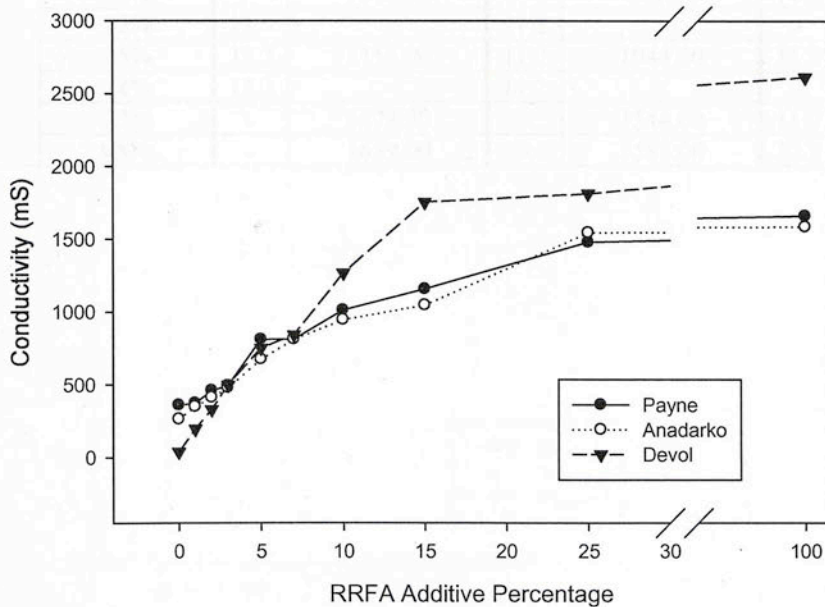


Figure A.81: Conductivity Curves for A-4 Soils with Red Rock FA

**Table A-26: Measured pH and Conductivity Values for A-4 Soils**

Additive Type	Additive Content	Payne		Anadarko		Devol	
		pH	Conductivity (mS)	pH	Conductivity (mS)	pH	Conductivity (mS)
Raw soil	0%	7.8	358.00	7.5	262.20	9.1	37.81
CKD	1%	-	539.00	-	551.00	11.1	637.33
	2%	10.7	788.00	11.4	1061.00	11.6	1576.67
	3%	-	1148.00	-	1534.00	11.8	2474.67
	4%	11.5	-	11.7	-	-	-
	5%	-	2284.00	-	2924.00	12.0	4253.33
	6%	11.8	-	12.0	-	-	-
	7%	-	3170.00	-	4060.00	12.2	5836.67
	8%	11.9	-	12.1	-	-	-
	10%	12.0	4230.00	12.2	5540.00	12.2	7626.67
	12%	12.0	-	12.2	-	-	-
	14%	12.0	-	12.2	-	-	-
	15%	-	6650.00	-	8160.00	12.3	9446.67
25%	-	8740.00	-	10100.00	12.4	11400.00	
100%	-	10650.00	-	12140.00	12.7	11646.67	
Red Rock Fly Ash	1%	-	372.00	-	347.00	9.8	194.77
	2%	-	458.00	-	410.00	10.5	329.67
	3%	10.1	492.00	10.3	477.00	10.9	495.67
	5%	-	808.00	-	672.00	11.3	749.67
	6%	10.7	-	10.8	-	-	-
	7%	-	811.00	-	809.00	11.3	839.33
	9%	10.9	-	11.2	-	-	-
	10%	-	1010.00	-	943.00	11.5	1265.67
	12%	11.0	-	11.2	-	-	-
	15%	11.2	1155.00	11.2	1044.00	11.7	1752.67
	18%	11.2	-	11.2	-	-	-
	25%	-	1479.00	-	1544.00	11.7	1811.67
100%	-	1659.00	-	1585.00	12.2	2613.33	



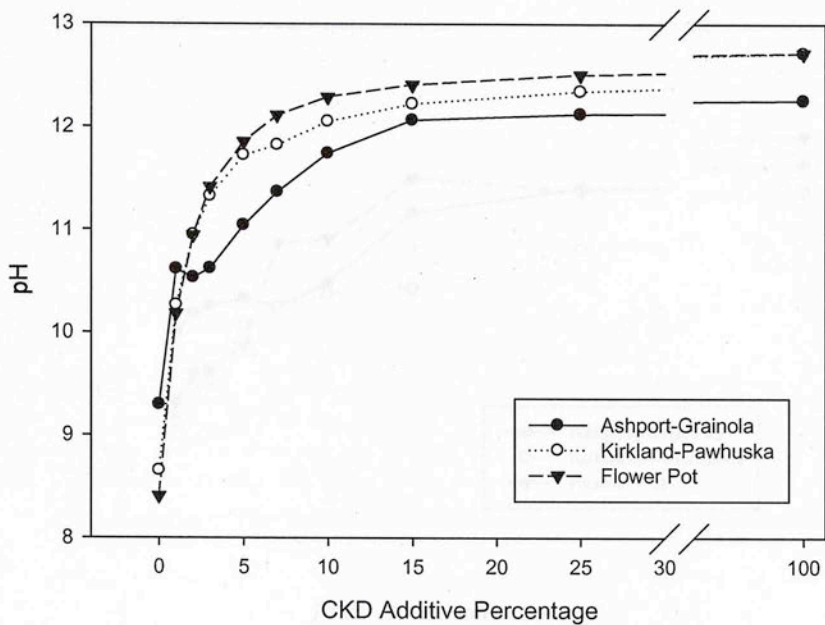


Figure A.82: pH Curves for A-6 Soils with CKD

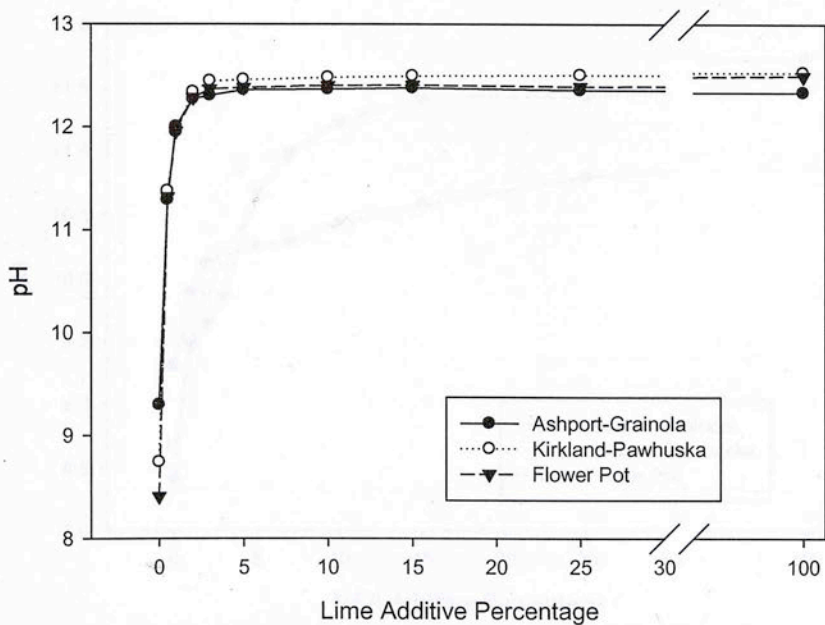


Figure A.83: pH Curves for A-6 Soils with Lime

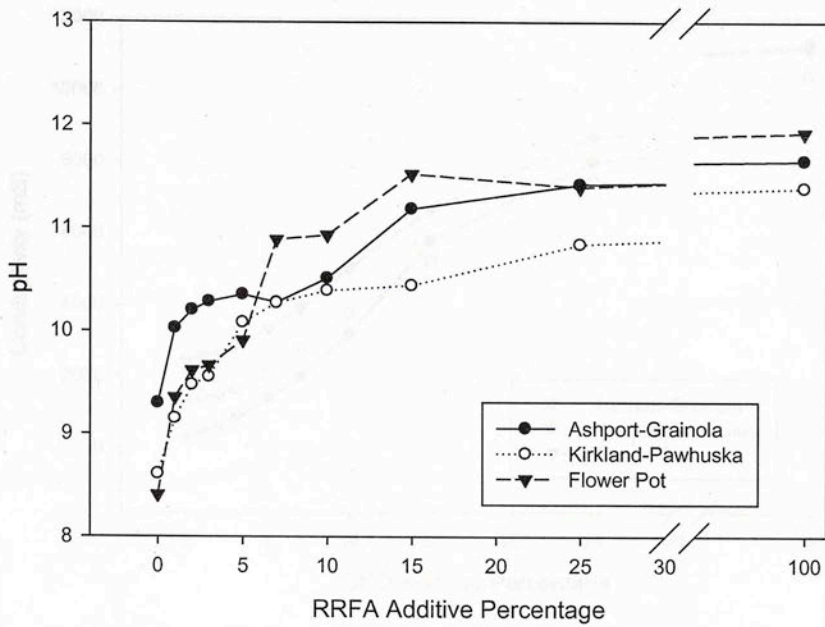


Figure A.84: pH Curves for A-6 Soils with Red Rock FA

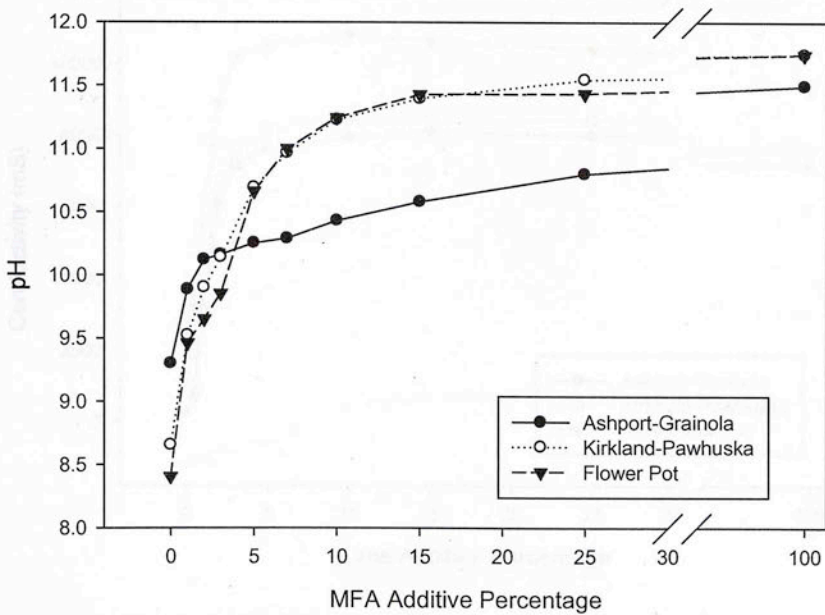


Figure A.85: pH Curves for A-6 Soils with Muskogee FA

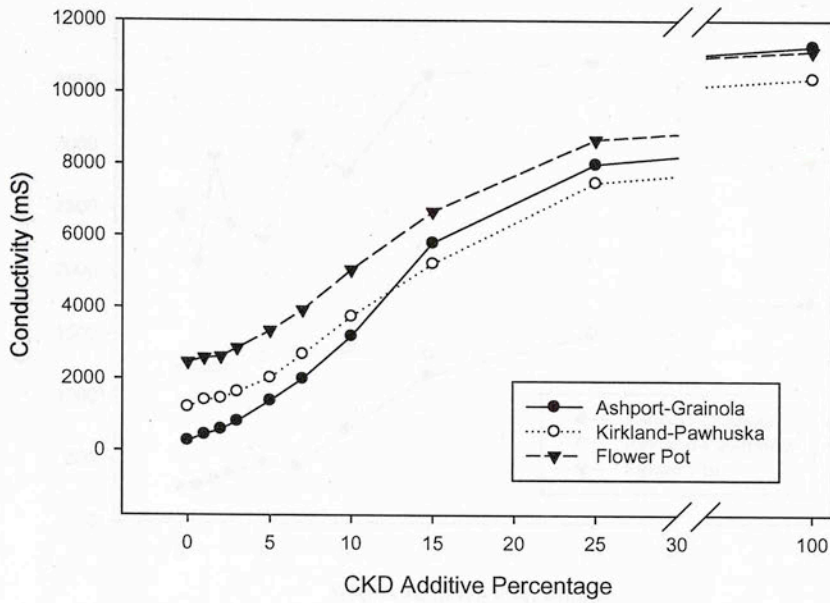


Figure A.86: Conductivity Curves for A-6 Soils with CKD

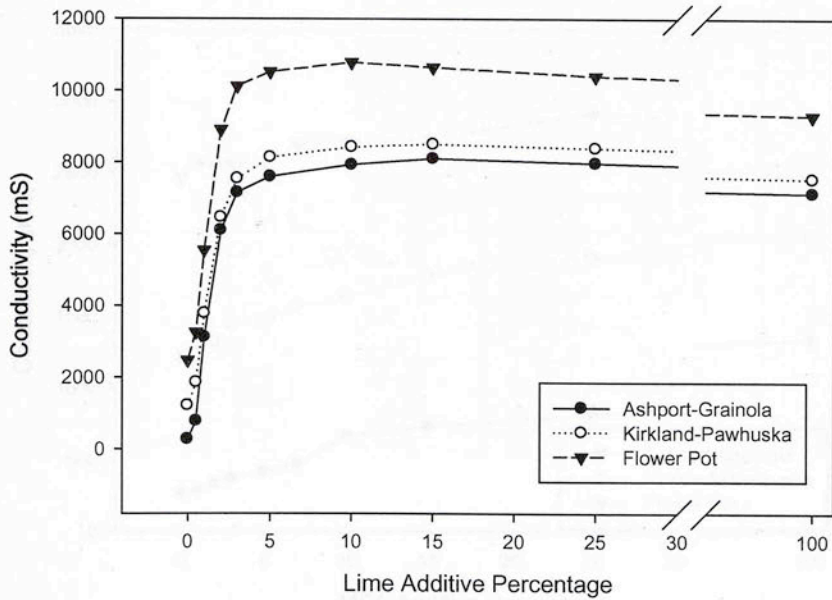


Figure A.87: Conductivity Curves for A-6 Soils with Lime



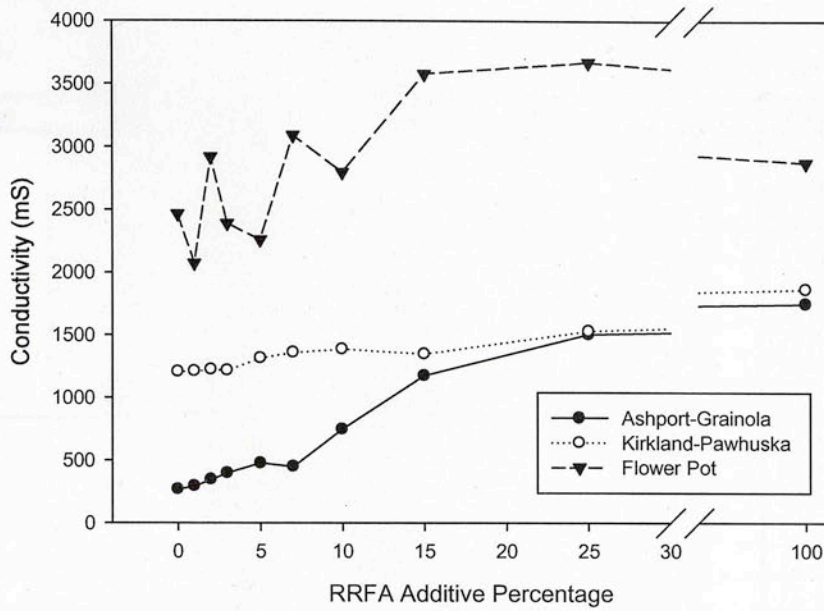


Figure A.88: Conductivity Curves for A-6 Soils with Red Rock FA

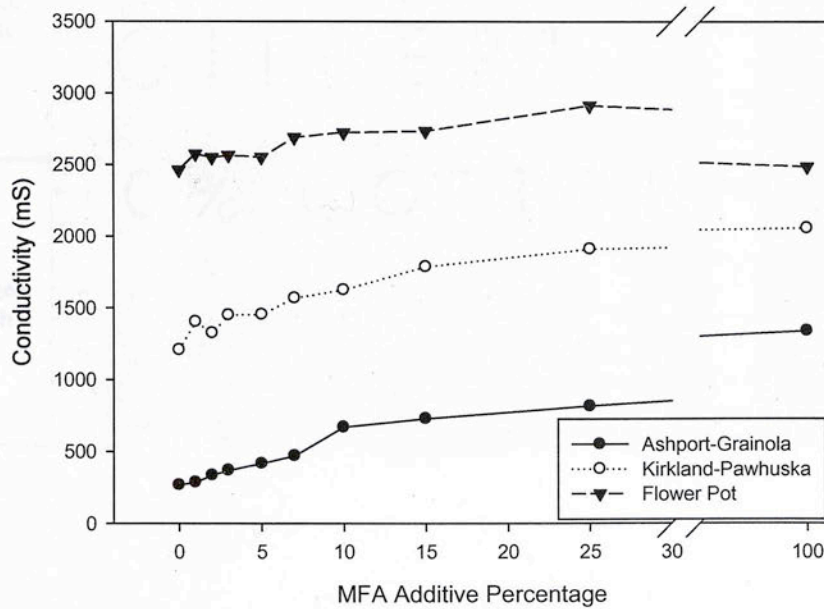


Figure A.89: Conductivity Curves for A-6 Soils with Muskogee FA

**Table A-27: Measured pH and Conductivity Values for A-6 Soils**

Additive Type	Additive Content	Ashport-Grainola		Kirkland-Pawhuska		Flower Pot	
		pH	Conductivity (mS)	pH	Conductivity (mS)	pH	Conductivity (mS)
Raw soil	0%	9.30	265.67	8.61	1205.33	8.41	2463.00
CKD	1%	10.62	439.67	10.27	1404.67	10.18	2587.33
	2%	10.53	587.67	10.95	1455.00	10.95	2623.00
	3%	10.62	811.67	11.33	1635.33	11.42	2862.33
	5%	11.05	1386.00	11.73	2030.00	11.86	3350.00
	7%	11.37	2003.33	11.83	2691.67	12.11	3930.00
	10%	11.74	3201.00	12.05	3750.00	12.29	5053.33
	15%	12.07	5806.67	12.23	5226.67	12.41	6683.33
	25%	12.12	8000.00	12.35	7486.67	12.51	8686.67
	100%	12.26	11280.00	12.72	10386.67	12.72	11153.33
Lime	0.5%	11.29	767.00	11.38	1848.33	11.32	3250.00
	1%	12.00	3116.67	11.95	3773.33	11.96	5540.00
	2%	12.27	6096.67	12.34	6453.33	12.28	8903.33
	3%	12.30	7150.00	12.45	7533.33	12.37	10113.33
	5%	12.36	7590.00	12.46	8130.00	12.38	10516.67
	10%	12.37	7926.67	12.48	8416.67	12.40	10780.00
	15%	12.38	8093.33	12.49	8496.67	12.41	10640.00
	25%	12.36	7966.67	12.50	8386.67	12.39	10396.67
	100%	12.33	7136.67	12.53	7536.67	12.50	9296.67
Red Rock Fly Ash	1%	10.03	292.33	9.15	1210.00	9.35	2071.00
	2%	10.20	345.00	9.47	1222.67	9.62	2916.67
	3%	10.29	395.67	9.55	1216.67	9.66	2388.33
	5%	10.36	475.00	10.08	1313.67	9.91	2257.67
	7%	10.28	448.00	10.28	1358.33	10.89	3086.67
	10%	10.52	745.33	10.40	1384.67	10.94	2793.67
	15%	11.19	1172.67	10.45	1345.33	11.53	3576.67
	25%	11.43	1502.33	10.84	1529.33	11.40	3670.00
	100%	11.66	1750.33	11.39	1865.33	11.93	2877.33
Muskogee Fly Ash	1%	9.88	284.43	9.52	1403.00	9.46	2574.00
	2%	10.12	334.00	9.90	1324.00	9.65	2549.67
	3%	10.16	367.33	10.14	1448.67	9.85	2564.33
	5%	10.25	414.33	10.69	1453.67	10.66	2551.67
	7%	10.29	468.33	10.96	1567.33	11.00	2689.33
	10%	10.43	668.33	11.23	1625.67	11.24	2724.67
	15%	10.58	729.00	11.39	1788.00	11.43	2734.33
	25%	10.80	818.00	11.54	1913.67	11.43	2913.67
	100%	11.49	1340.67	11.74	2057.33	11.74	2486.67

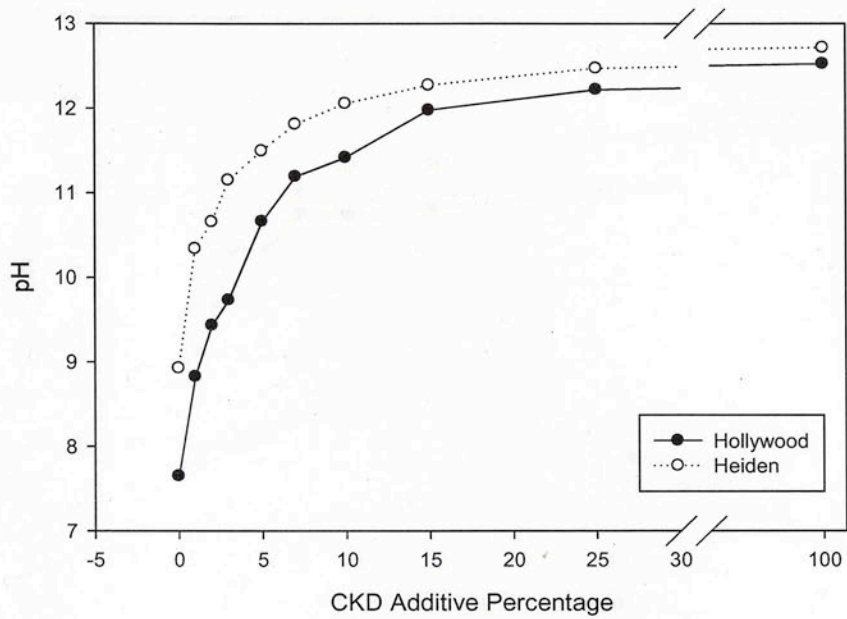


Figure A.90: pH Curves for A-7-6 Soils with CKD

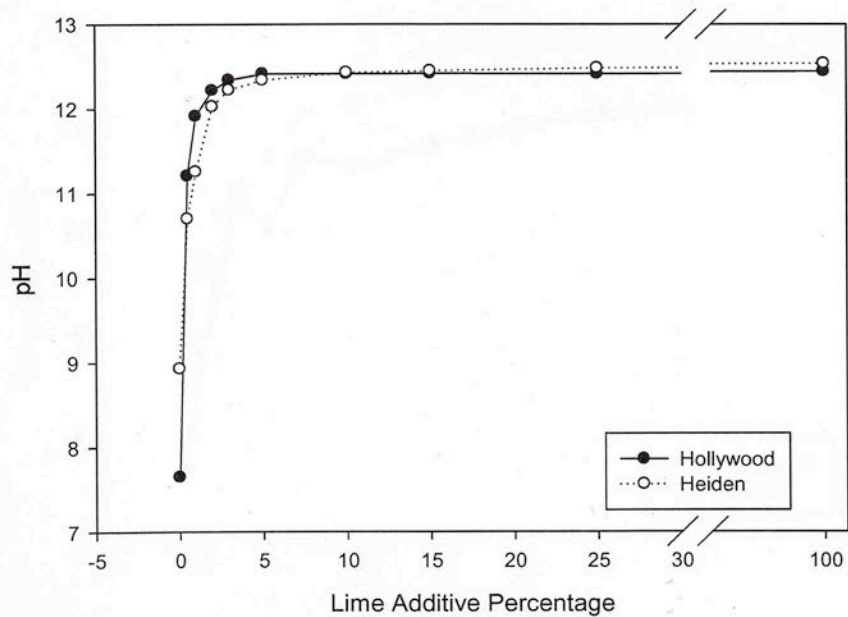


Figure A.91: pH Curves for A-7-6 Soils with Lime



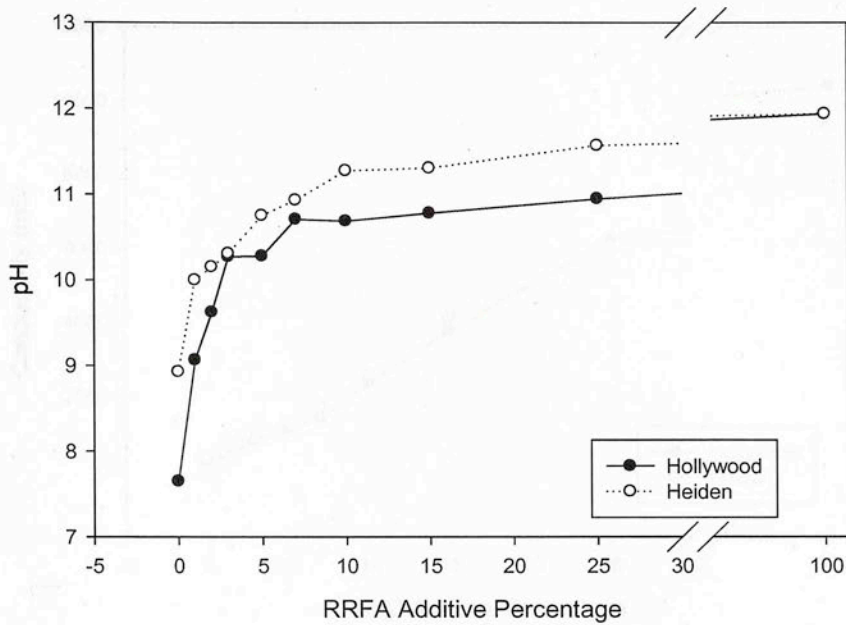


Figure A.92: pH Curves for A-7-6 Soils with Red Rock FA

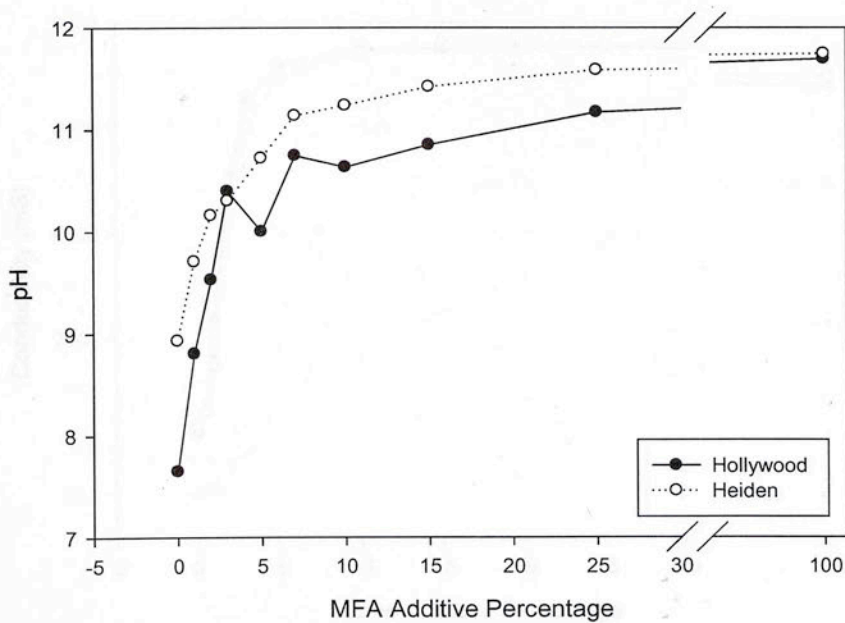


Figure A.93: pH Curves for A-7-6 Soils with Muskogee FA

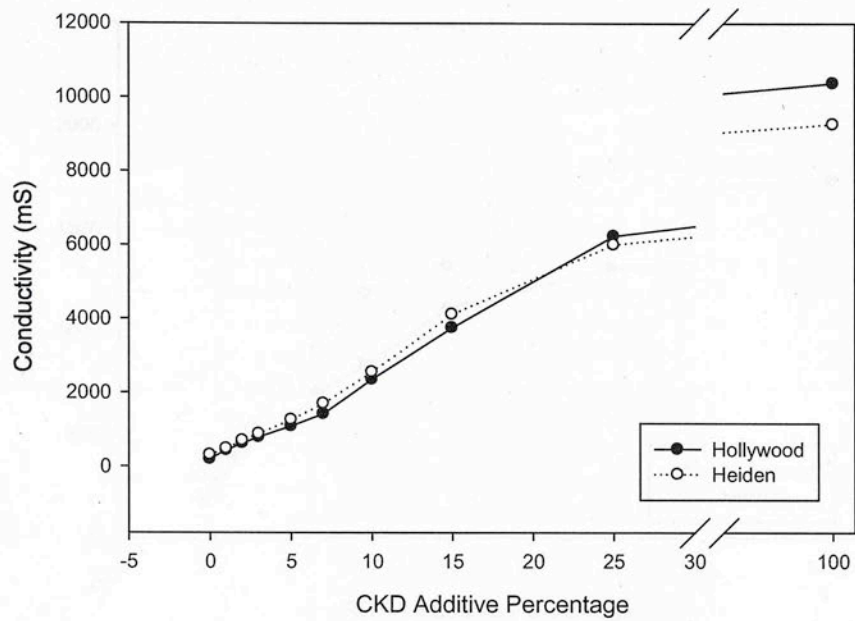


Figure A.94: Conductivity Curves for A-7-6 Soils with CKD

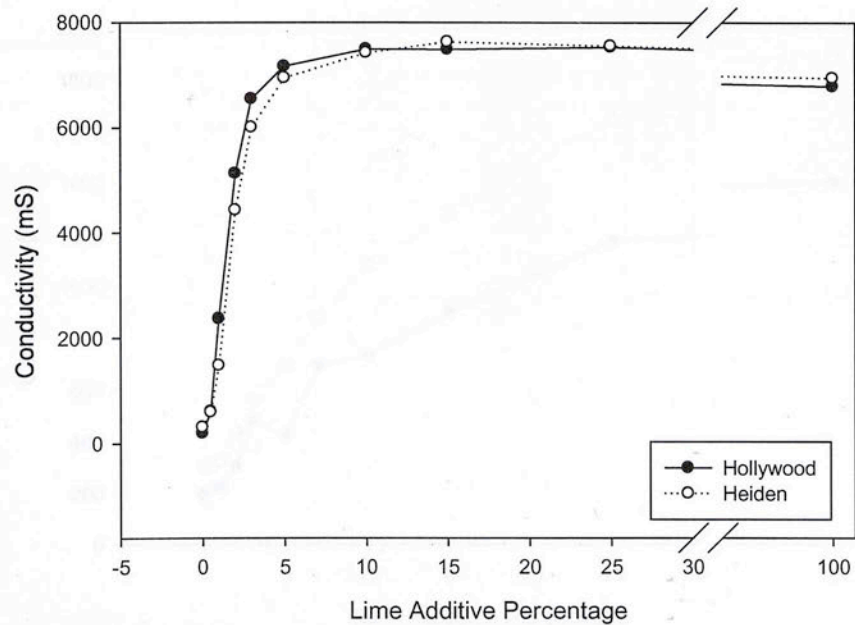


Figure A.95: Conductivity Curves for A-7-6 Soils with Lime

Table A-28: Measured pH and Conductivity Values for A-7-6 Soils

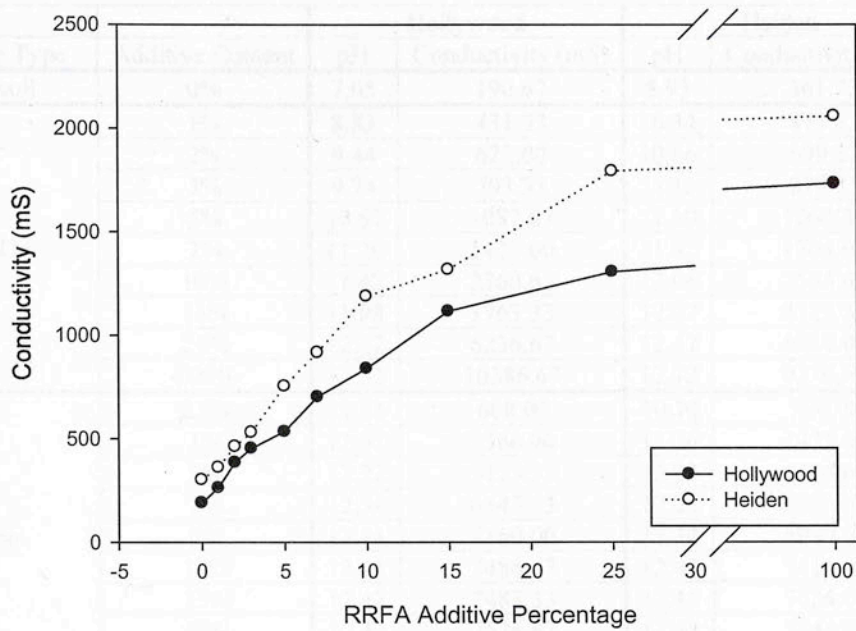


Figure A.96: Conductivity Curves for A-7-6 Soils with Red Rock FA

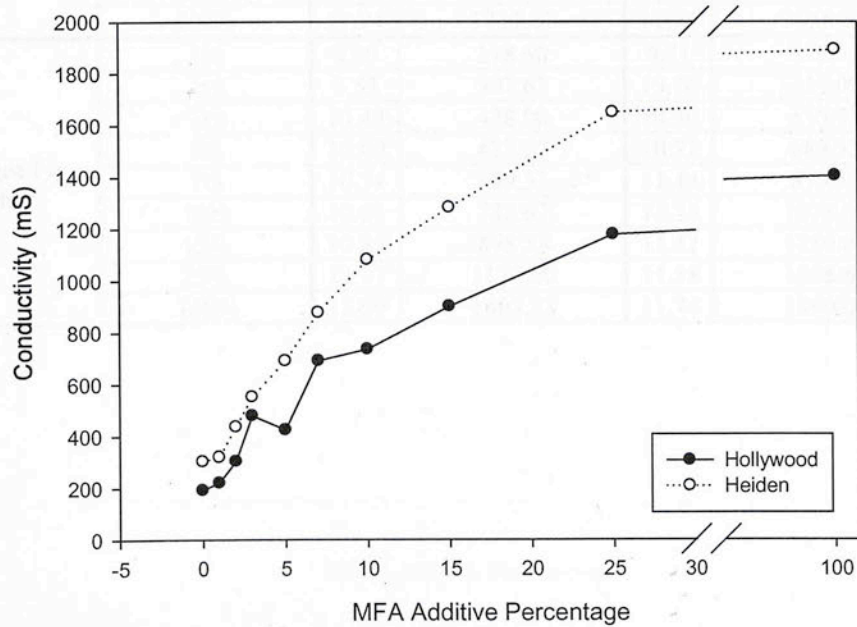


Figure A.97: Conductivity Curves for A-7-6 Soils with Muskogee FA



**Table A-28: Measured pH and Conductivity Values for A-7-6 Soils**

Additive Type	Additive Content	Hollywood		Heiden	
		pH	Conductivity (mS)	pH	Conductivity (mS)
Raw soil	0%	7.65	190.67	8.93	301.73
CKD	1%	8.83	431.33	10.34	475.33
	2%	9.44	622.00	10.66	699.33
	3%	9.74	793.33	11.16	879.33
	5%	10.67	1087.67	11.50	1260.33
	7%	11.20	1425.00	11.82	1704.00
	10%	11.42	2360.67	12.06	2555.67
	15%	11.98	3763.33	12.27	4123.33
	25%	12.22	6236.67	12.47	6010.00
	100%	12.53	10386.67	12.72	9276.67
Lime	0.5%	11.21	608.00	10.70	590.00
	1%	11.91	2366.00	11.26	1475.67
	2%	12.22	5123.33	12.03	4426.67
	3%	12.34	6543.33	12.22	6000.00
	5%	12.41	7160.00	12.34	6940.00
	10%	12.41	7486.67	12.43	7416.67
	15%	12.42	7483.33	12.45	7626.67
	25%	12.41	7526.67	12.48	7546.67
	100%	12.44	6780.00	12.53	6936.67
Red Rock Fly Ash	1%	9.07	261.43	10.00	361.00
	2%	9.63	385.67	10.16	462.33
	3%	10.28	453.33	10.31	531.33
	5%	10.28	534.33	10.76	754.67
	7%	10.71	703.00	10.94	917.33
	10%	10.69	840.67	11.28	1190.00
	15%	10.78	1116.67	11.31	1318.67
	25%	10.95	1306.67	11.57	1793.33
	100%	11.94	1734.67	11.94	2058.67
Muskogee Fly Ash	1%	8.80	218.60	9.71	318.57
	2%	9.53	302.67	10.16	435.00
	3%	10.40	478.00	10.30	550.33
	5%	10.00	423.27	10.72	689.33
	7%	10.74	689.33	11.14	875.33
	10%	10.63	733.67	11.24	1078.67
	15%	10.85	898.33	11.42	1280.67
	25%	11.17	1177.00	11.58	1648.67
	100%	11.69	1403.33	11.74	1890.00

Table A-29: Cation Exchange Capacity Values for A-4 Soils

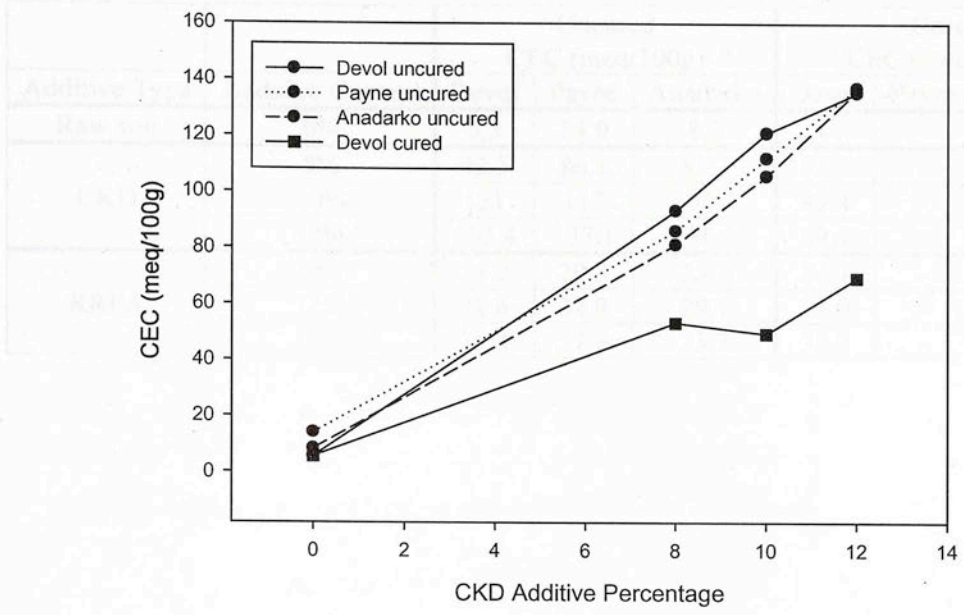


Figure A.98: Cation Exchange Capacity Curves for A-4 Soils with CKD

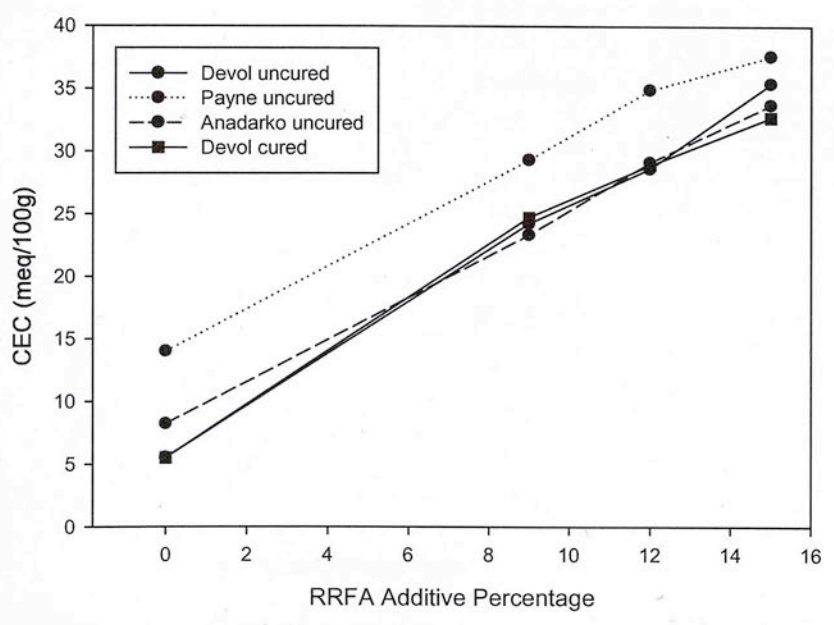


Figure A.99: Cation Exchange Capacity Curves for A-4 Soils with Red Rock FA

**Table A-29: Cation Exchange Capacity Values for A-4 Soils**

Additive Type	Additive Content	Uncured CEC (meq/100g)			Cured CEC (meq/100g)		
		Devol	Payne	Anadarko	Devol	Payne	Anadarko
Raw soil	0%	5.5	14.0	8.2			
CKD	8%	93.3	86.1	81.2	53.3	-	-
	10%	121	112	105.7	49.4	-	-
	12%	135.4	137.1	136.1	69.4	-	-
RRFA	9%	24.2	29.3	23.3	24.7	-	-
	12%	28.6	34.9	29.1	28.9	-	-
	15%	35.4	37.6	33.7	32.7	-	-





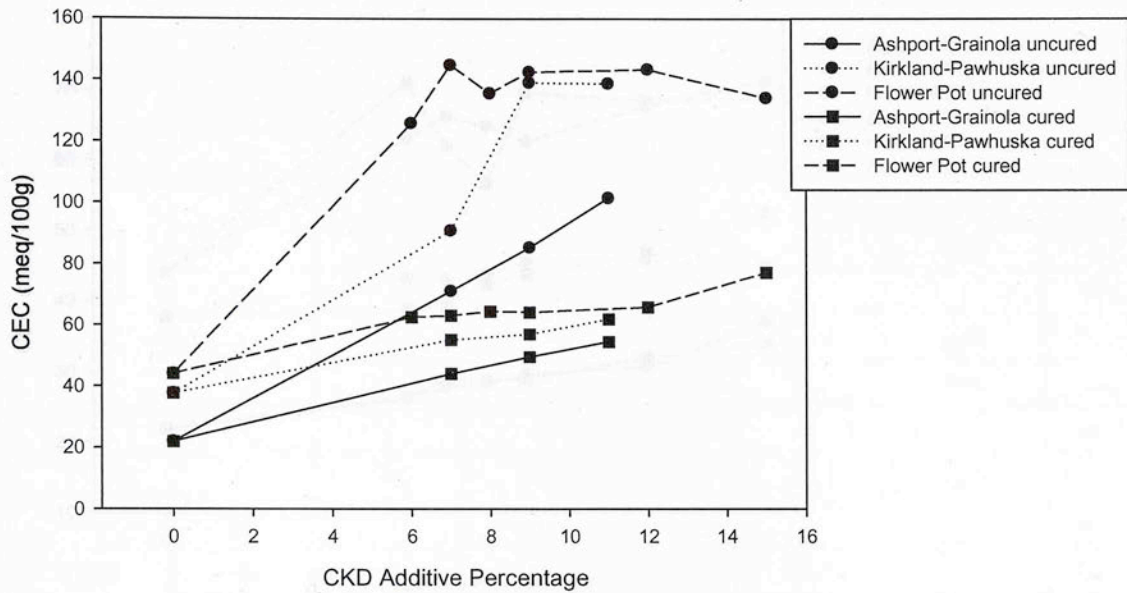


Figure A.100: Cation Exchange Capacity Curves for A-6 Soils with CKD

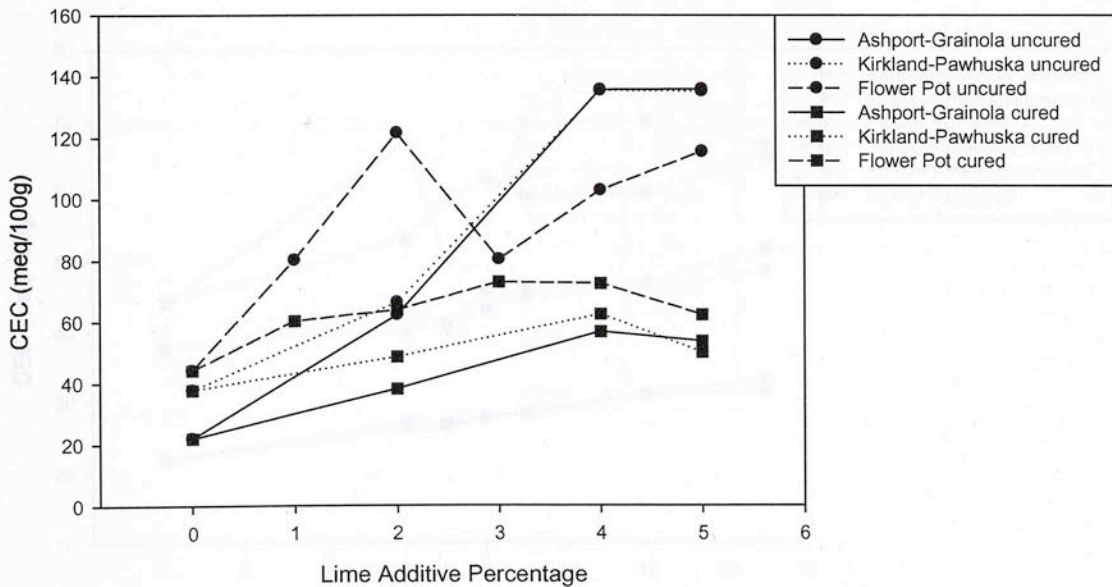


Figure A.101: Cation Exchange Capacity Curves for A-6 Soils with Lime

Table A-30: Cation Exchange Capacity Values for A-6 Soils

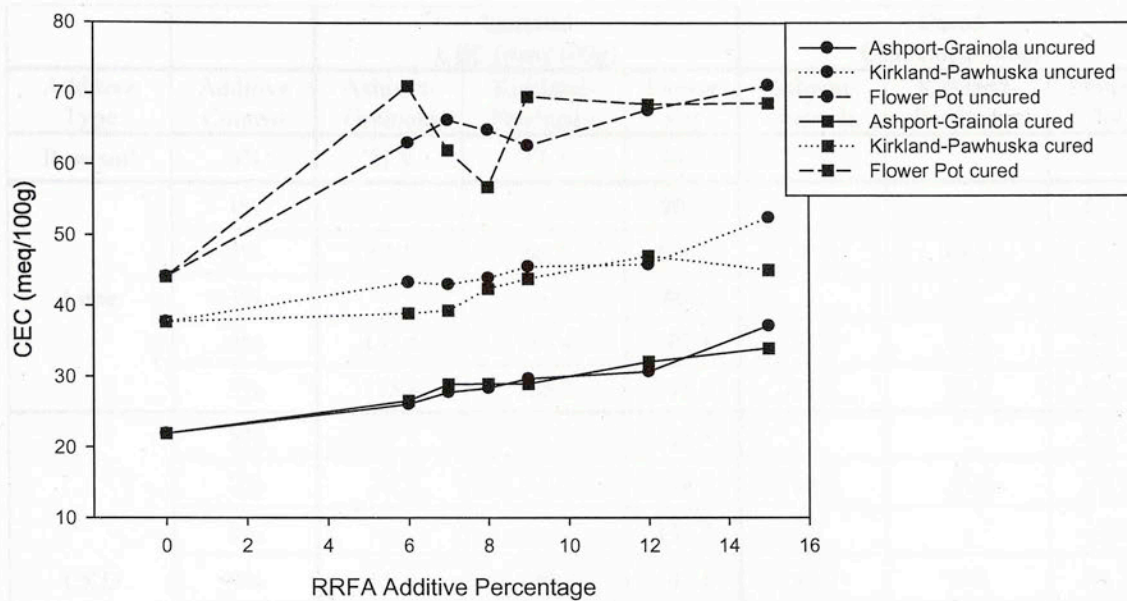


Figure A.102: Cation Exchange Capacity Curves for A-6 Soils with Red Rock FA

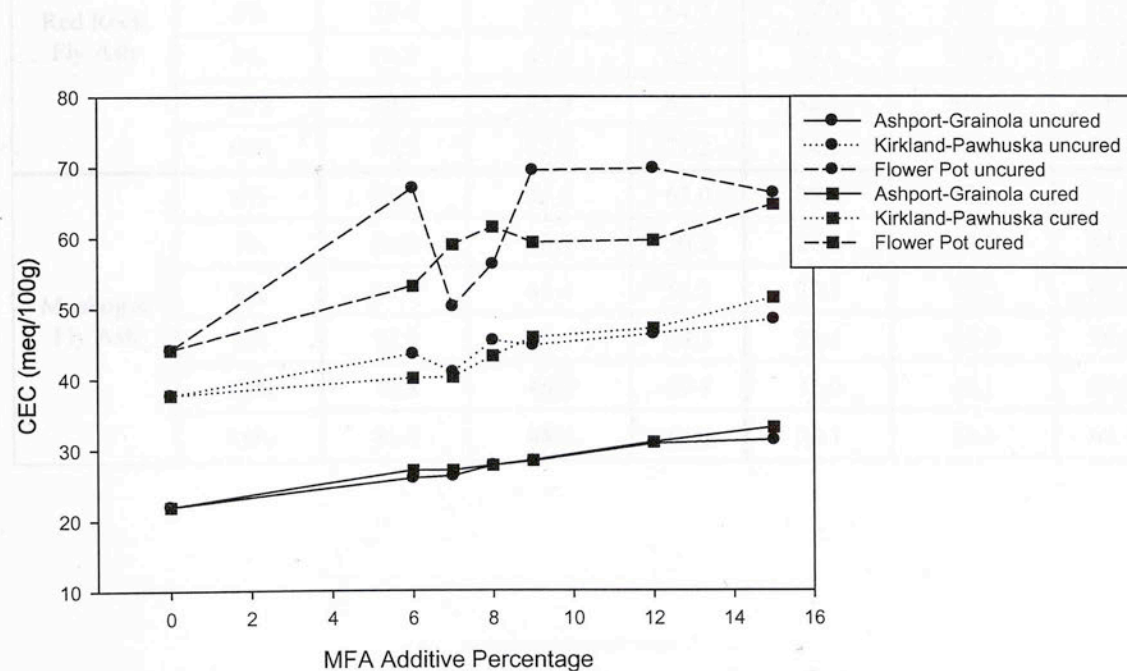


Figure A.103: Cation Exchange Capacity Curves for A-6 Soils with Muskogee FA

**Table A-30: Cation Exchange Capacity Values for A-6 Soils**

Additive Type	Additive Content	Uncured CEC (meq/100g)			Cured CEC (meq/100g)		
		Ashport-Grainola	Kirkland-Pawhuska	Flower Pot	Ashport-Grainola	Kirkland-Pawhuska	Flower Pot
Raw soil	0%	21.9	37.7	44.1			
Lime	1%	-	-	80.1	-	-	60.2
	2%	62.1	66.2	121.5	38.0	48.5	63.7
	3%	-	-	80.2	-	-	72.8
	4%	135.6	135.4	102.8	56.6	62.3	72.3
	5%	135.8	135.2	115.4	53.5	49.9	62.1
CKD	6%	-	-	125.9	-	-	62.7
	7%	71.2	91.0	144.9	44.2	55.3	63.2
	8%	-	-	135.7	-	-	64.6
	9%	85.4	139.2	142.6	49.7	57.1	64.3
	11%	101.5	138.8	-	54.6	62.0	
	12%	-	-	143.4	-	-	65.9
	15%	-	-	134.2	-	-	77.2
Red Rock Fly Ash	6%	26.1	43.4	63.1	26.6	39.0	71.1
	7%	27.8	43.1	66.3	28.9	39.4	62.1
	8%	28.4	44.0	64.9	29.0	42.5	56.9
	9%	29.7	45.6	62.7	29.0	43.9	69.6
	12%	30.7	45.9	67.7	32.1	47.1	68.5
	15%	37.2	52.5	71.2	34.0	45.1	68.7
Muskogee Fly Ash	6%	25.9	43.5	67.0	27.0	40.1	53.1
	7%	26.2	40.9	50.2	27.0	40.2	59.0
	8%	27.7	45.4	56.2	27.7	43.2	61.5
	9%	28.3	44.7	69.5	28.4	45.8	59.3
	12%	30.8	46.3	69.8	31.0	47.1	59.6
	15%	31.3	48.4	66.3	33.1	51.5	64.7



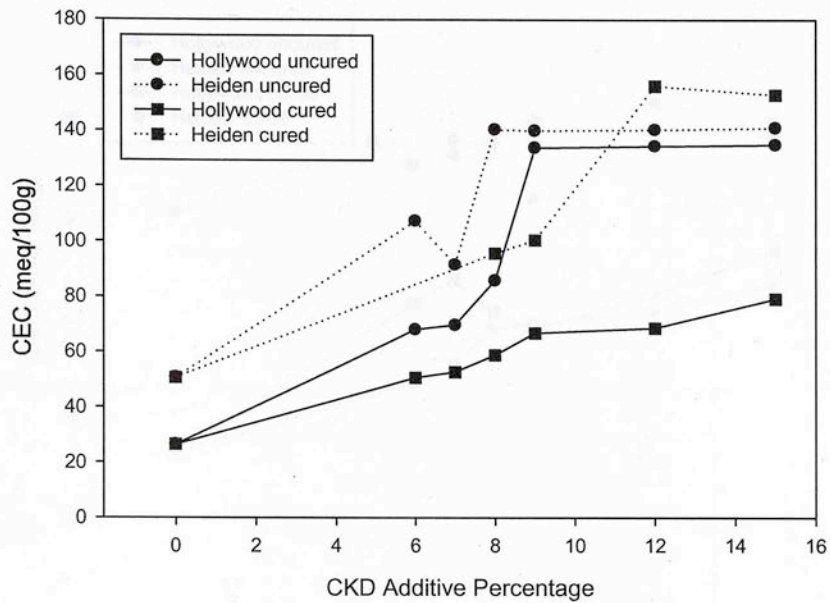


Figure A.104: Cation Exchange Capacity Curves for A-7-6 Soils with CKD

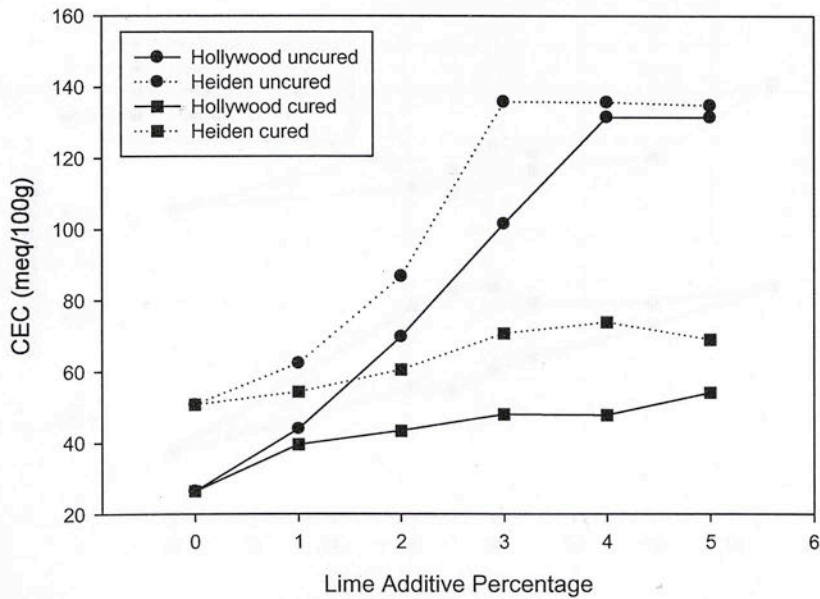


Figure A.105: Cation Exchange Capacity Curves for A-7-6 Soils with Lime

Table A-31: Cation Exchange Capacity Values for A-7-6 Soils

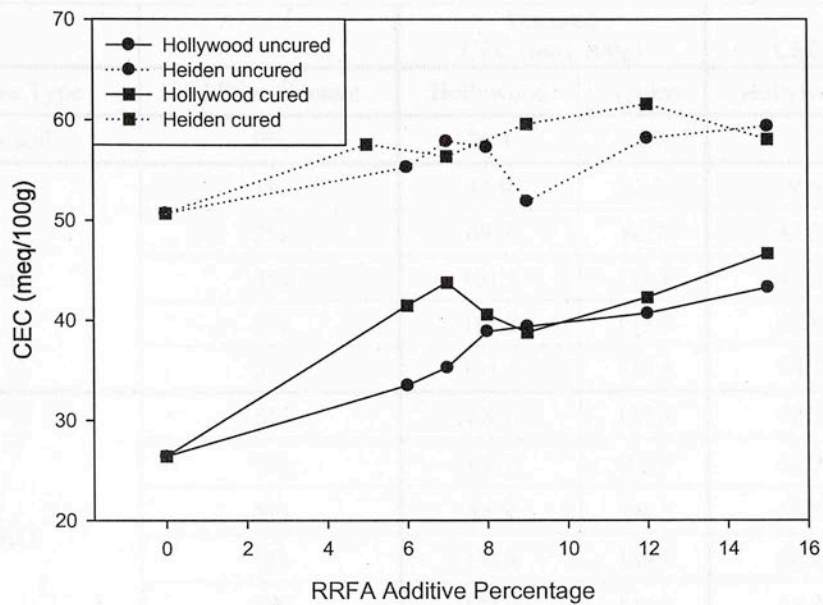


Figure A.106: Cation Exchange Capacity Curves for A-7-6 Soils with Red Rock FA

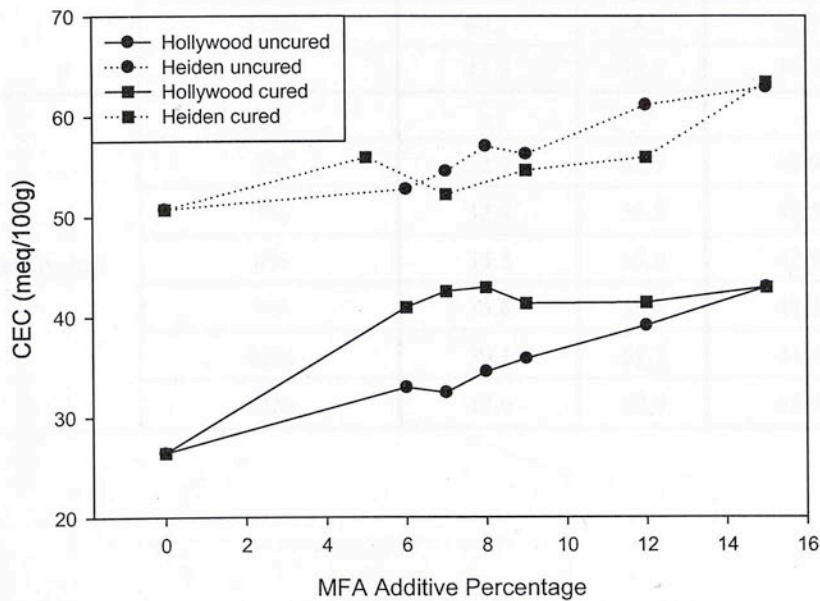


Figure A.107: Cation Exchange Capacity Curves for A-7-6 Soils with Muskogee FA

**Table A-31: Cation Exchange Capacity Values for A-7-6 Soils**

Additive Type	Additive Content	Uncured CEC (meq/100g)		Cured CEC (meq/100g)	
		Hollywood	Heiden	Hollywood	Heiden
Raw soil	0%	26.4	50.7		
Lime	1%	43.9	62.3	39.5	54.3
	2%	69.7	86.7	43.3	60.5
	3%	101.5	135.8	48.0	70.7
	4%	131.5	135.7	47.8	73.9
	5%	131.5	134.8	54.1	69.0
CKD	6%	68.1	107.4	50.7	-
	7%	69.7	91.5	52.7	-
	8%	85.8	140.3	58.8	95.7
	9%	133.8	139.9	66.8	100.4
	12%	134.4	140.3	68.6	156.1
	15%	135.0	141.1	79.3	153.0
Red Rock Fly Ash	5%	-	-	-	57.6
	6%	33.5	55.3	41.5	-
	7%	35.3	57.9	43.8	56.4
	8%	38.9	57.3	40.6	-
	9%	39.4	51.9	38.8	59.6
	12%	40.7	58.2	42.3	61.6
	15%	43.3	59.4	46.7	58.1
Muskogee Fly Ash	5%	-	-	-	55.9
	6%	32.9	52.7	40.9	-
	7%	32.4	54.5	42.5	52.2
	8%	34.5	57.0	42.9	-
	9%	35.8	56.2	41.3	54.6
	12%	39.1	61.1	41.4	55.9
	15%	42.9	62.9	42.9	63.4



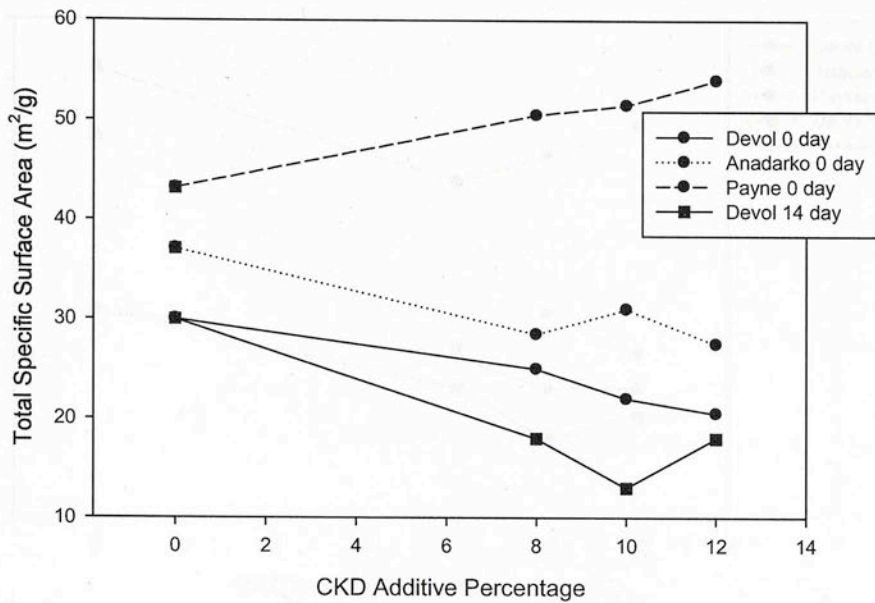


Figure A.108: Total SSA Curves for A-4 Soils with CKD

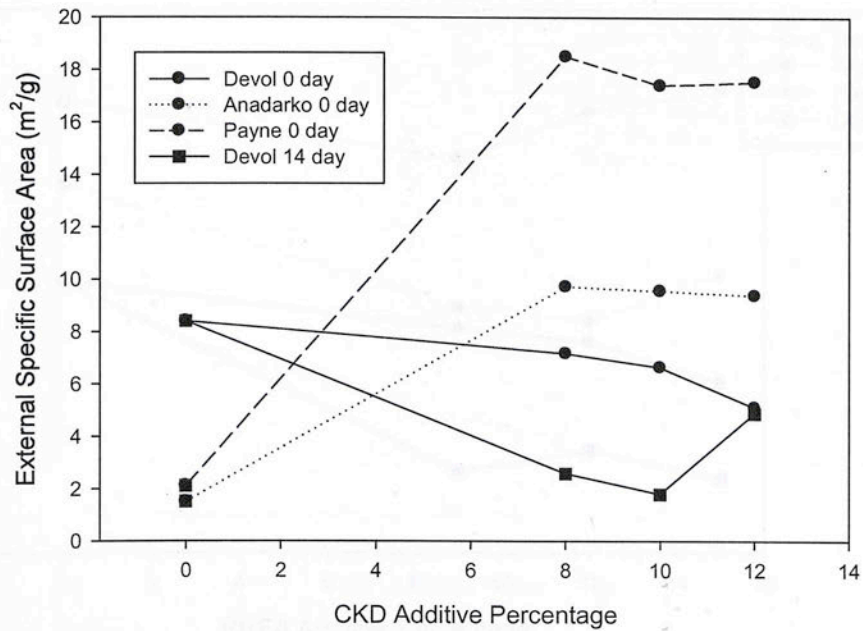


Figure A.109: External SSA Curves for A-4 Soils with CKD

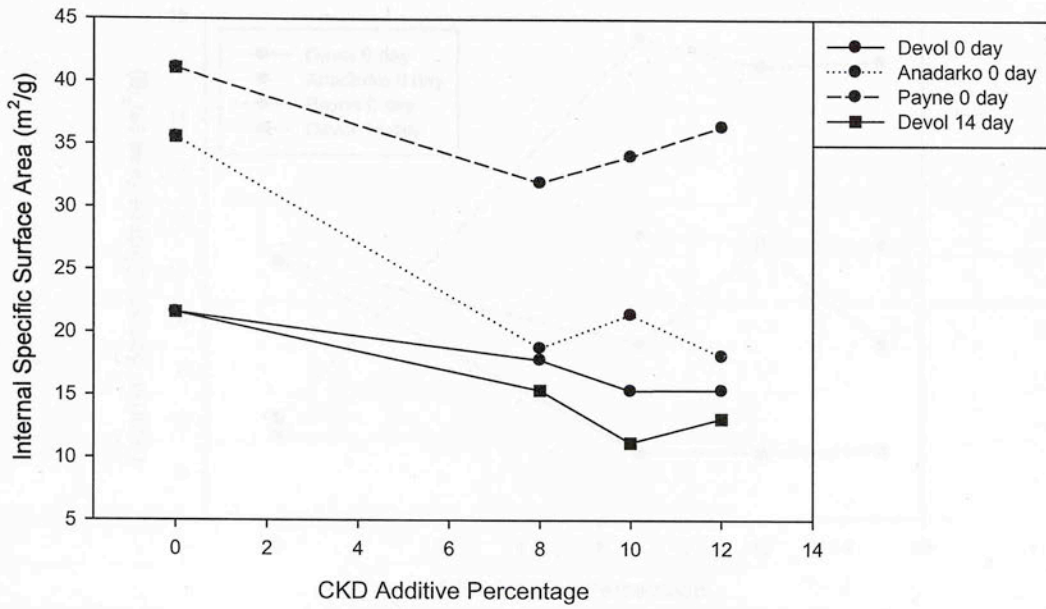


Figure A.110: Internal SSA Curves for A-4 Soils with CKD

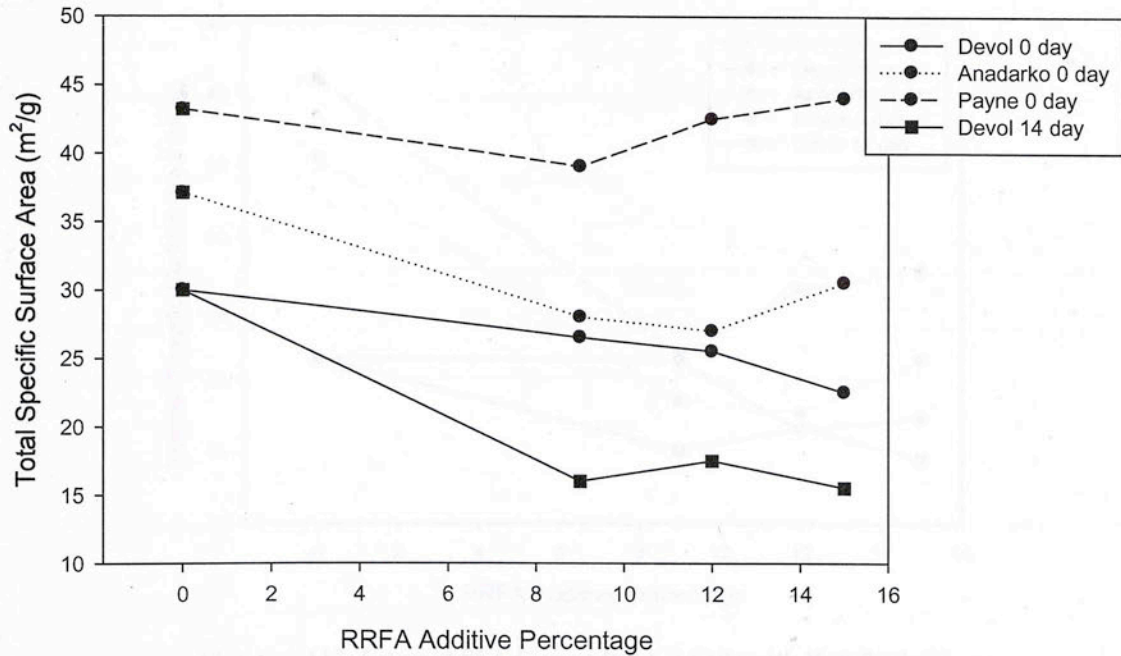


Figure A.111: Total SSA Curves for A-4 Soils with Red Rock FA

Table A-32: Devol (A-4) specific Surface Area Values

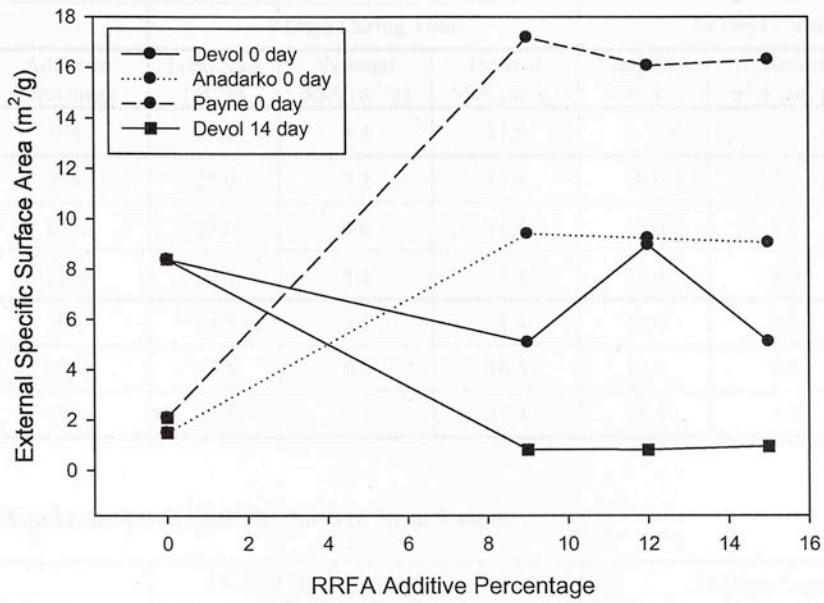


Figure A.112: External SSA Curves for A-4 Soils with Red Rock FA

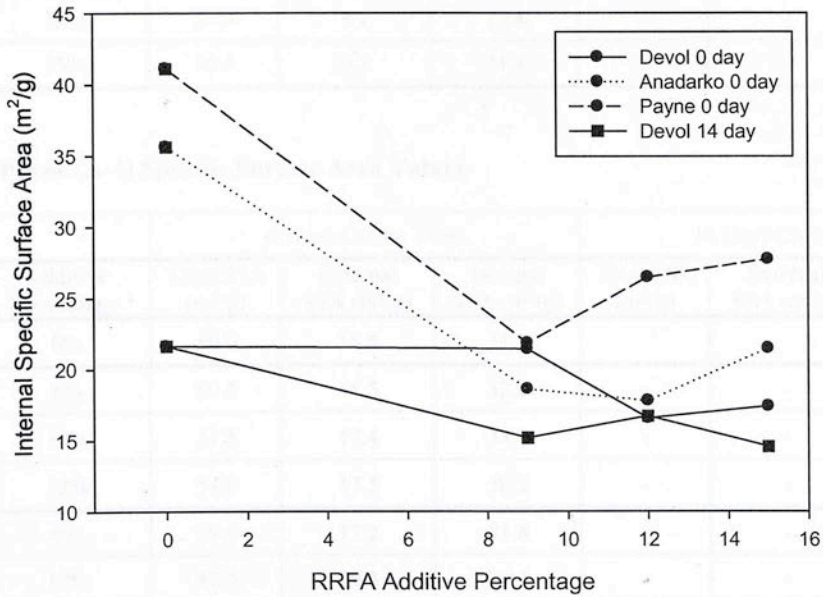


Figure A.113: Internal SSA Curves for A-4 Soils with Red Rock FA



**Table A-32: Devol (A-4) Specific Surface Area Values**

Additive Type	Additive Percentage	0 Days Curing Time			14 Days Curing Time		
		Total SSA (m <sup>2</sup> /g)	External SSA (m <sup>2</sup> /g)	Internal SSA (m <sup>2</sup> /g)	Total SSA (m <sup>2</sup> /g)	External SSA (m <sup>2</sup> /g)	Internal SSA (m <sup>2</sup> /g)
Raw soil	0%	30.0	8.4	21.6			
CKD	8%	25.0	7.2	17.8	18.0	2.6	15.4
	10%	22.0	6.6	15.4	13.0	1.8	11.2
	12%	20.5	5.1	15.4	18.0	4.9	13.1
RRFA	9%	26.5	5.1	21.4	16.0	0.8	15.2
	12%	25.5	9.0	16.5	17.5	0.8	16.7
	15%	22.5	5.1	17.4	15.5	1.0	14.5

**Table A-33: Anadarko (A-4) Specific Surface Area Values**

Additive Type	Additive Percentage	0 Days Curing Time			14 Days Curing Time		
		Total SSA (m <sup>2</sup> /g)	External SSA (m <sup>2</sup> /g)	Internal SSA (m <sup>2</sup> /g)	Total SSA (m <sup>2</sup> /g)	External SSA (m <sup>2</sup> /g)	Internal SSA (m <sup>2</sup> /g)
Raw soil	0%	40.5	1.5	39.0			
CKD	8%	28.5	9.7	18.8	-	-	-
	10%	31.0	9.6	21.4	-	-	-
	12%	27.5	9.4	18.1	-	-	-
RRFA	9%	28.0	9.4	18.6	-	-	-
	12%	27.0	9.2	17.8	-	-	-
	15%	30.5	9.1	21.4	-	-	-

**Table A-34: Payne (A-4) Specific Surface Area Values**

Additive Type	Additive Percentage	0 Days Curing Time			14 Days Curing Time		
		Total SSA (m <sup>2</sup> /g)	External SSA (m <sup>2</sup> /g)	Internal SSA (m <sup>2</sup> /g)	Total SSA (m <sup>2</sup> /g)	External SSA (m <sup>2</sup> /g)	Internal SSA (m <sup>2</sup> /g)
Raw soil	0%	50.0	18.8	31.2			
CKD	8%	50.5	18.5	32.0	-	-	-
	10%	51.5	17.4	34.1	-	-	-
	12%	54.0	17.5	36.5	-	-	-
RRFA	9%	39.0	17.2	21.8	-	-	-
	12%	42.5	16.1	26.4	-	-	-
	15%	44.0	16.3	27.7	-	-	-

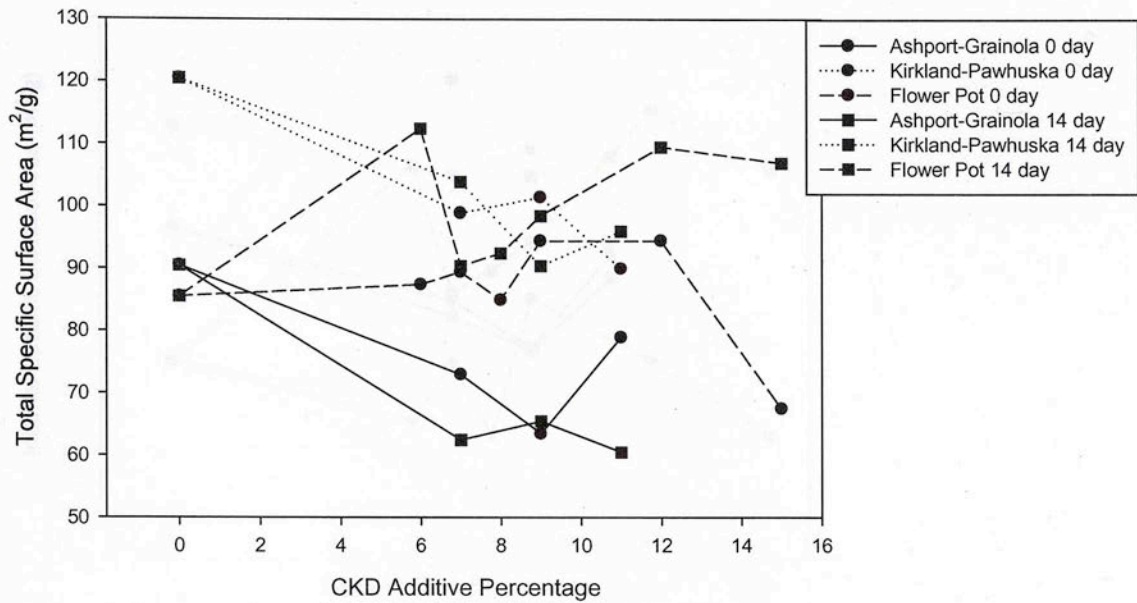


Figure A.114: Total SSA Curves for A-6 Soils with CKD

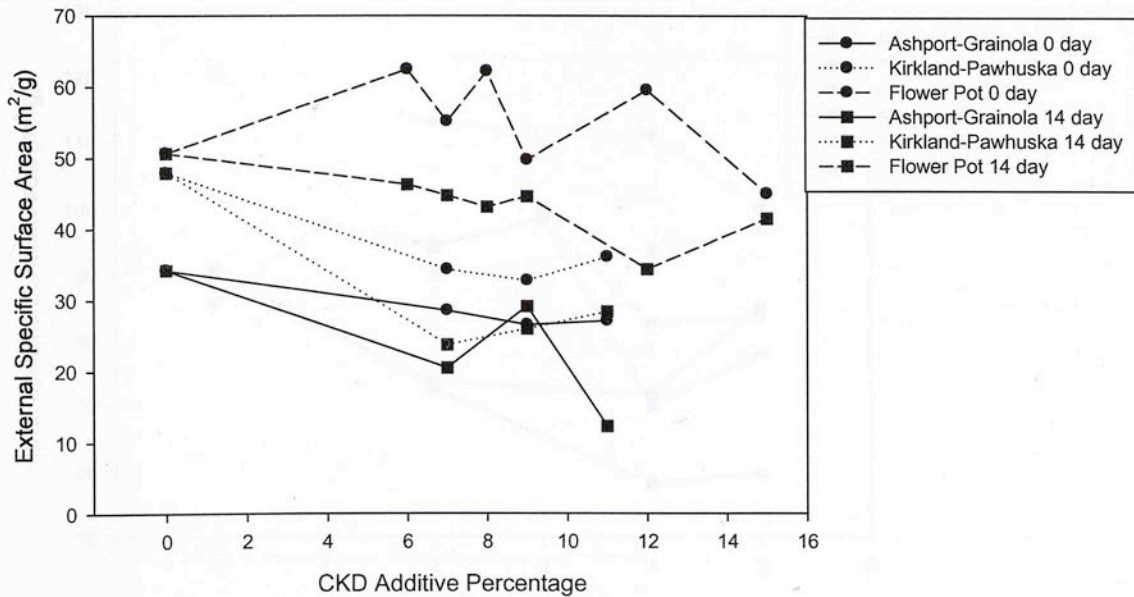


Figure A.115: External SSA Curves for A-6 Soils with CKD

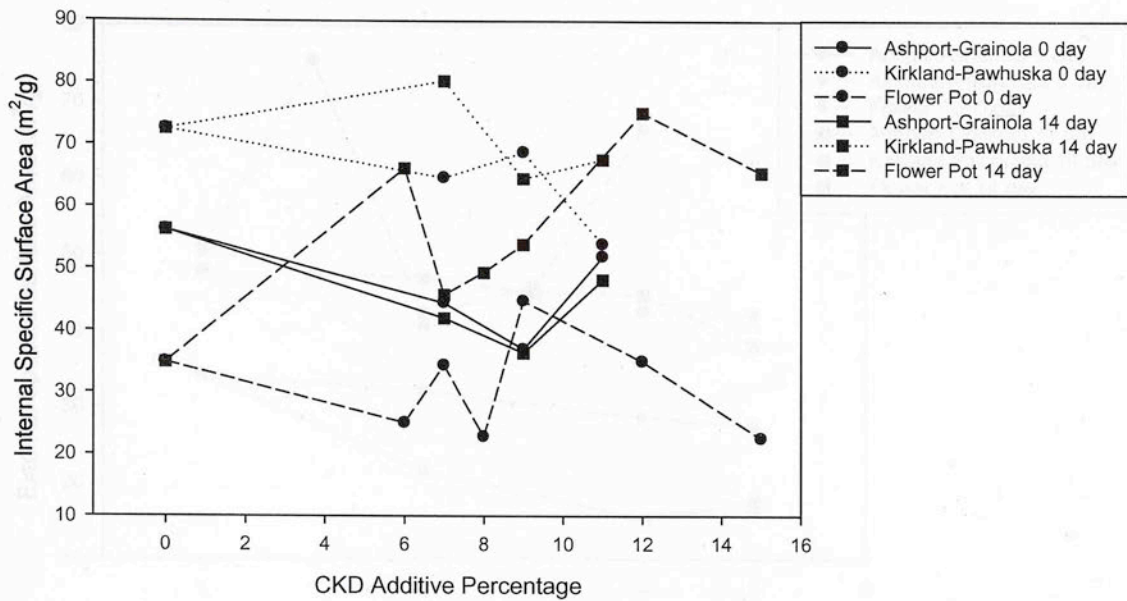


Figure A.116: Internal SSA Curves for A-6 Soils with CKD

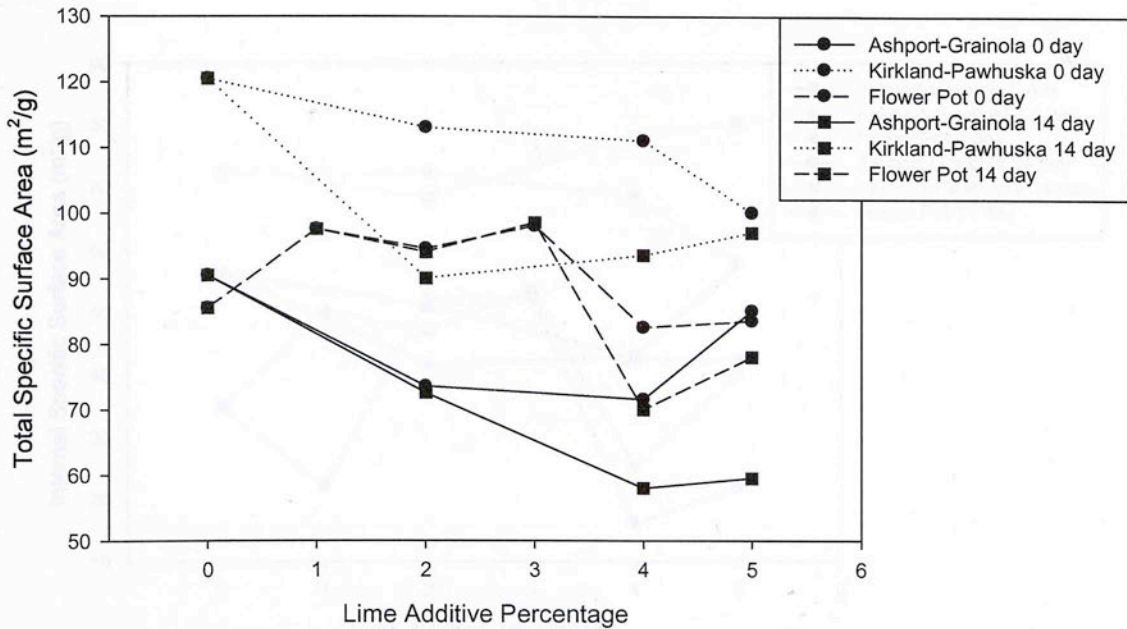


Figure A.117: Total SSA Curves for A-6 Soils with Lime



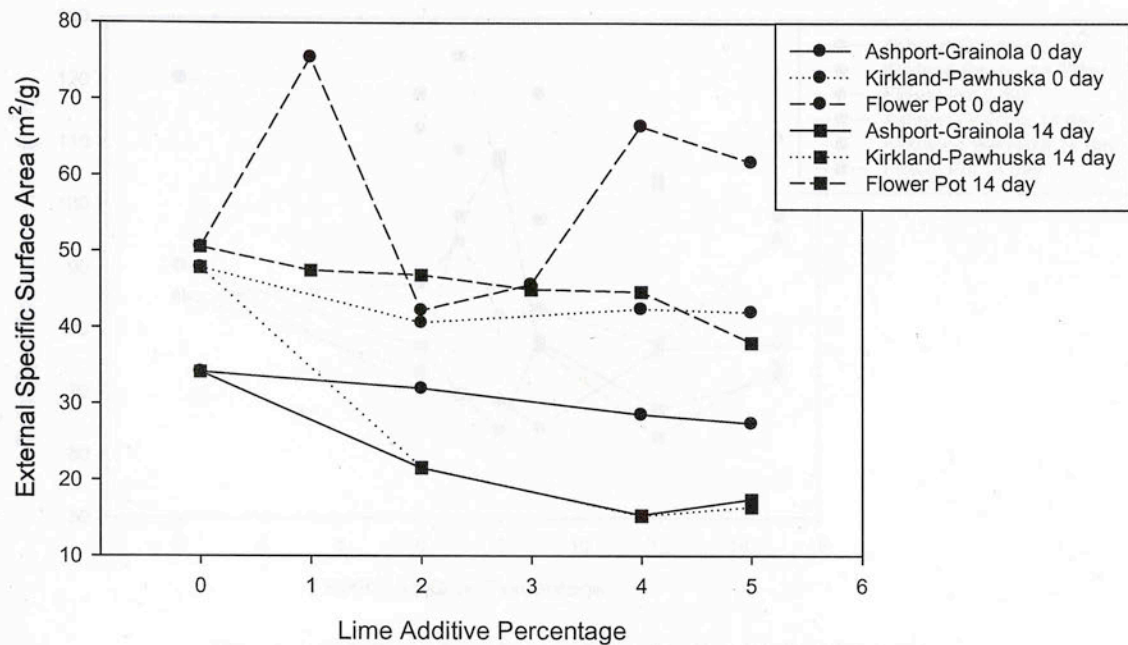


Figure A.118: External SSA Curves for A-6 Soils with Lime

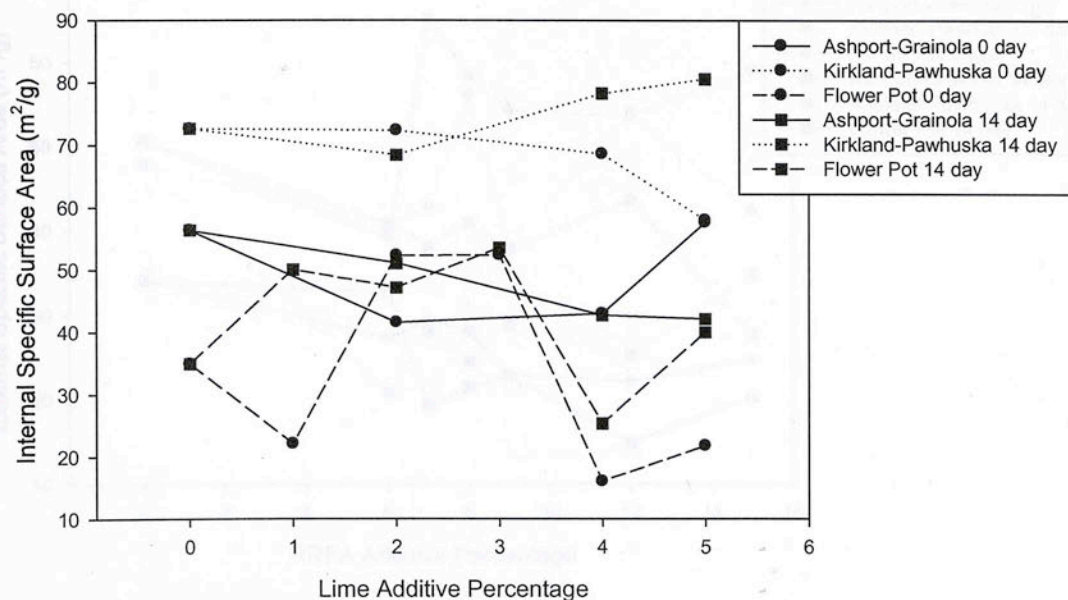


Figure A.119: Internal SSA Curves for A-6 Soils with Lime

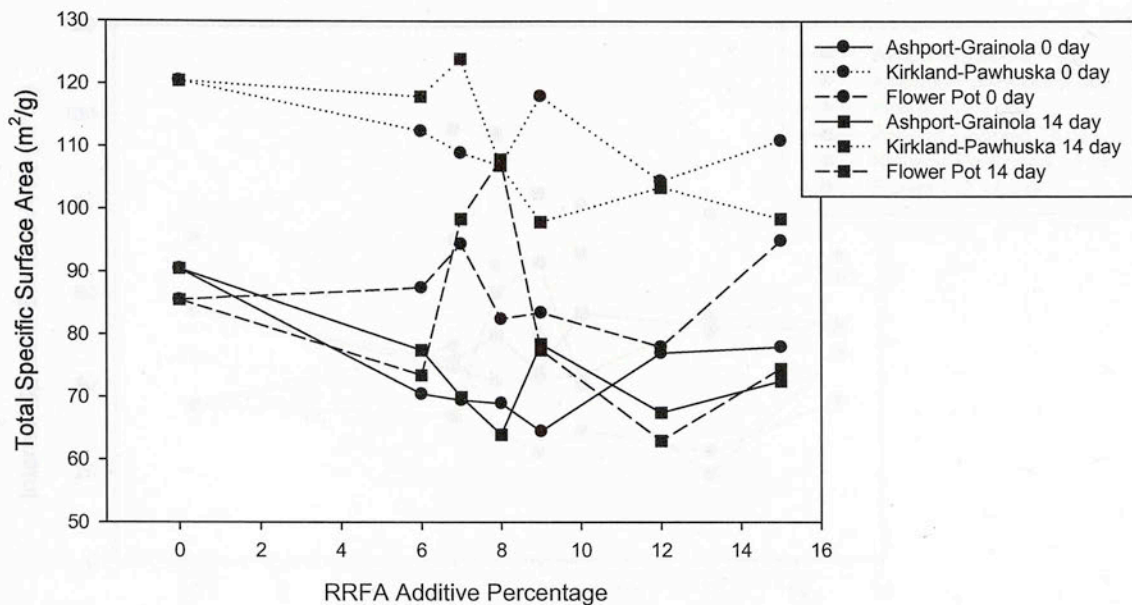


Figure A.120: Total SSA Curves for A-6 Soils with Red Rock FA

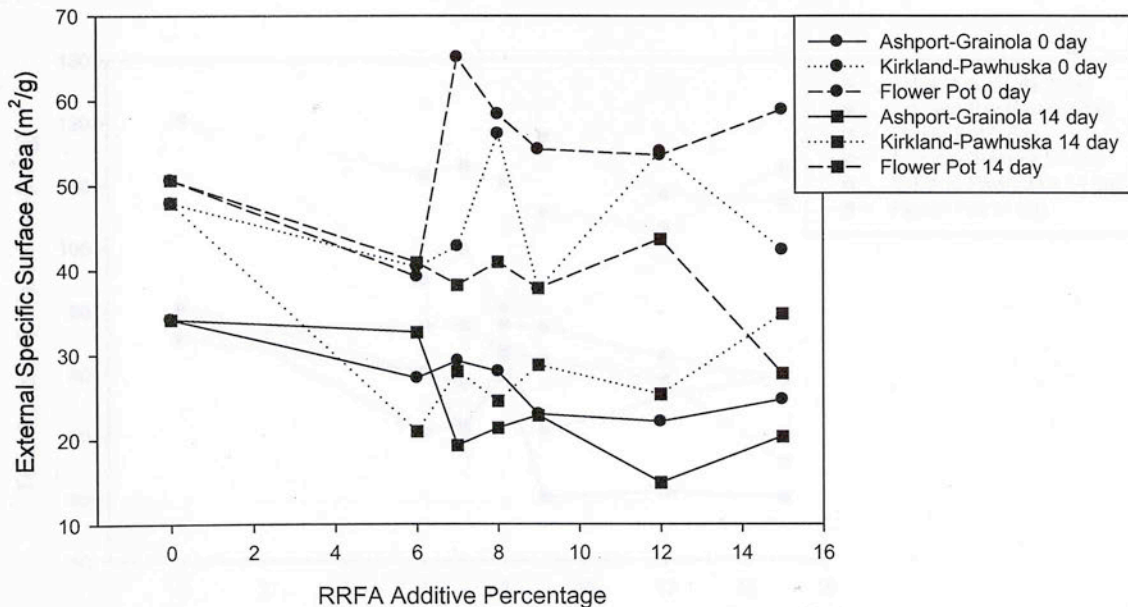


Figure A.121: External SSA Curves for A-6 Soils with Red Rock FA

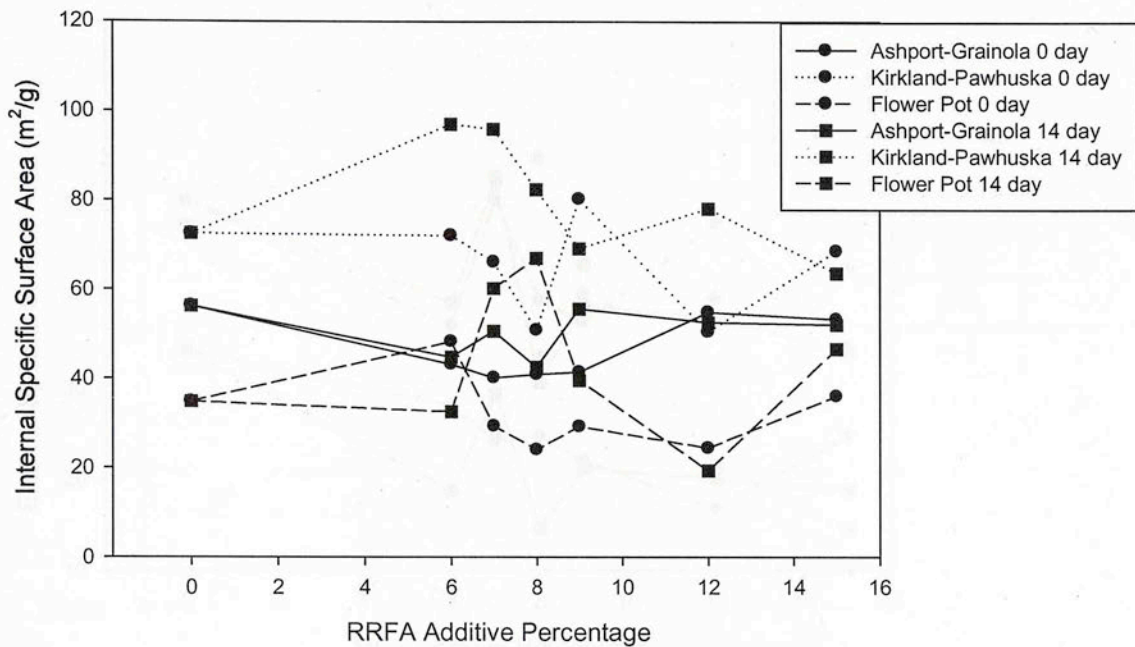


Figure A.122: Internal SSA Curves for A-6 Soils with Red Rock FA

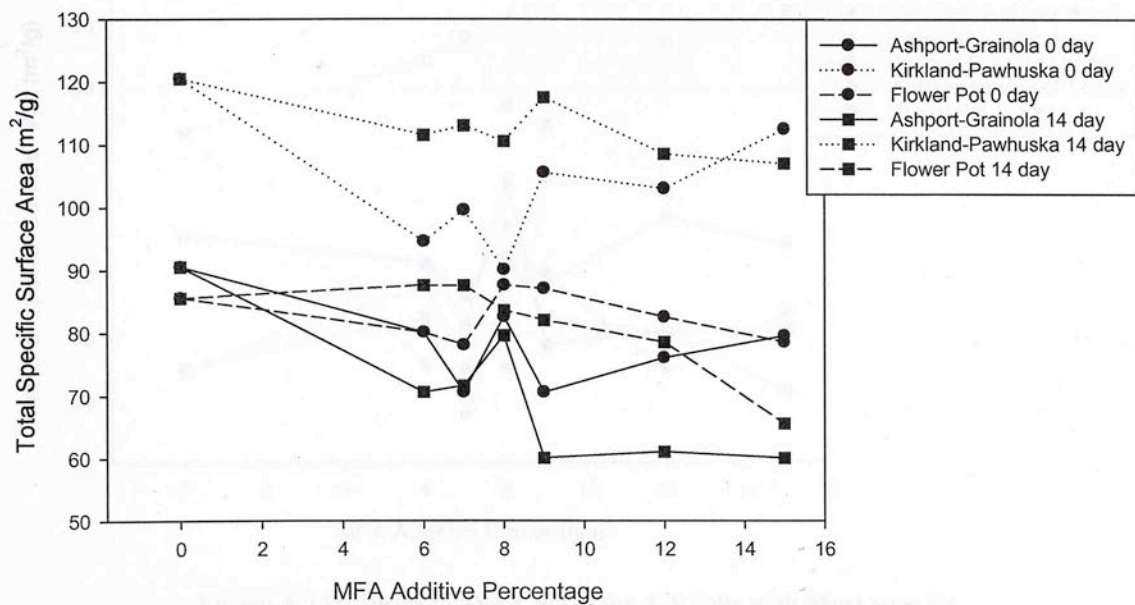


Figure A.123: Total SSA Curves for A-6 Soils with Muskogee FA



Table A-35: Ashport-Grainola (A-6) Specific Surface Area Values

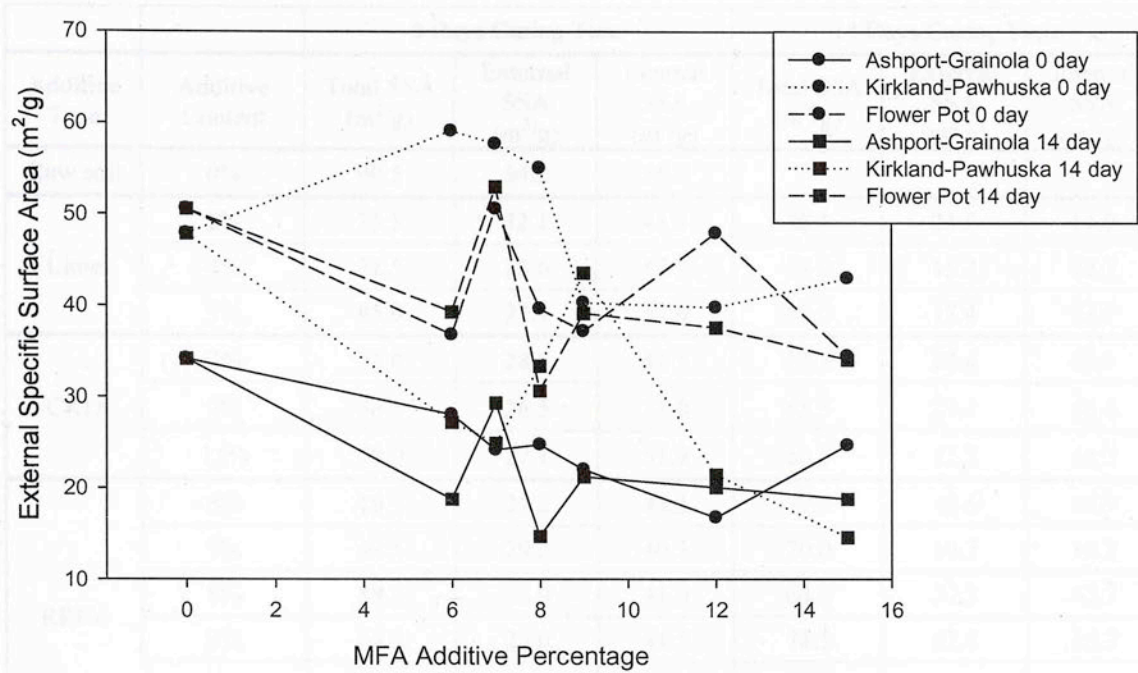


Figure A.124: External SSA Curves for A-6 Soils with Muskogee FA

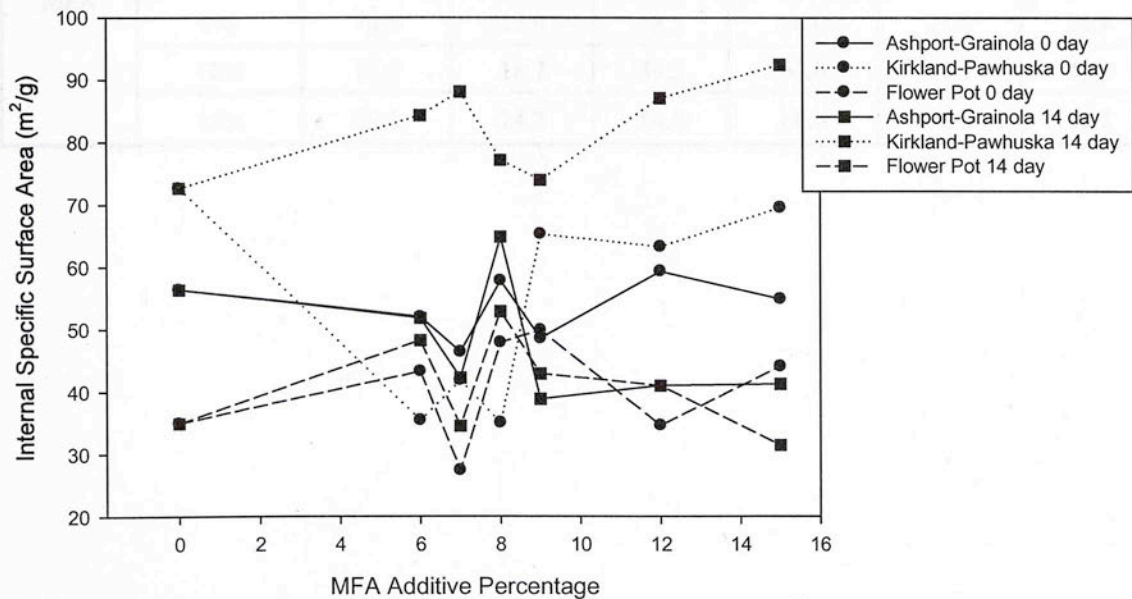


Figure A.125: Internal SSA Curves for A-6 Soils with Muskogee FA

**Table A-35: Ashport-Grainola (A-6) Specific Surface Area Values**

Additive Type	Additive Content	0 Days Curing Time			14 Days Curing Time		
		Total SSA (m <sup>2</sup> /g)	External SSA (m <sup>2</sup> /g)	Internal SSA (m <sup>2</sup> /g)	Total SSA (m <sup>2</sup> /g)	External SSA (m <sup>2</sup> /g)	Internal SSA (m <sup>2</sup> /g)
Raw soil	0%	90.5	34.2	56.3			
Lime	2%	73.5	32.1	41.4	72.5	21.5	51.0
	4%	71.5	28.6	42.9	58.0	15.3	42.7
	5%	85.0	27.4	57.6	59.5	17.4	42.1
CKD	7%	73.0	28.5	44.5	62.5	20.4	42.1
	9%	63.5	26.5	37.0	65.5	29.1	36.4
	11%	79.0	27.1	51.9	60.5	12.3	48.2
RRFA	6%	70.5	27.2	43.3	77.5	32.6	44.9
	7%	69.5	29.2	40.3	70.0	19.3	50.7
	8%	69.0	28.0	41.0	64.0	21.3	42.7
	9%	64.5	23.0	41.5	78.5	22.8	55.7
	12%	77.0	22.1	54.9	67.5	14.9	52.6
	15%	78.0	24.7	53.3	72.5	20.3	52.2
MFA	6%	80.0	28.1	51.9	70.5	18.8	51.7
	7%	70.5	24.2	46.3	71.5	29.4	42.1
	8%	82.5	24.8	57.7	79.5	14.7	64.8
	9%	70.5	22.0	48.5	60.0	21.2	38.8
	12%	76.0	16.7	59.3	61.0	20.1	40.9
	15%	79.5	24.7	54.8	60.0	18.8	41.2

**Table A-36: Kirkland-Pawhuska (A-6) Specific Surface Area Values**

Additive Type	Additive Content	0 Days Curing Time			14 Days Curing Time		
		Total SSA (m <sup>2</sup> /g)	External SSA (m <sup>2</sup> /g)	Internal SSA (m <sup>2</sup> /g)	Total SSA (m <sup>2</sup> /g)	External SSA (m <sup>2</sup> /g)	Internal SSA (m <sup>2</sup> /g)
Raw soil	0%	120.5	47.9	72.6			
Lime	2%	113.0	40.7	72.3	90.0	21.7	68.3
	4%	111.0	42.5	68.5	93.5	15.3	78.2
	5%	100.0	42.1	58.0	97.0	16.4	80.6
CKD	7%	99.0	34.3	64.7	104.0	23.7	80.3
	9%	101.5	32.7	68.8	90.5	25.9	64.6
	11%	90.0	36.0	54.0	96.0	28.4	67.6
RRFA	6%	112.5	40.3	72.2	118.0	20.9	97.1
	7%	109.0	42.7	66.3	124.0	28.0	96.0
	8%	107.0	56.1	50.9	107.0	24.5	82.5
	9%	118.0	37.7	80.3	98.0	28.8	69.2
	12%	104.5	54.0	50.5	103.5	25.3	78.2
	15%	111.0	42.4	68.6	98.5	34.8	63.7
MFA	6%	94.5	59.2	35.3	111.5	27.2	84.3
	7%	99.5	57.7	41.8	113.0	24.9	88.1
	8%	90.0	55.1	34.9	110.5	33.4	77.1
	9%	105.5	40.3	65.2	117.5	43.6	73.9
	12%	103.0	39.8	63.2	108.5	21.5	87.0
	15%	112.5	43.0	69.5	107.0	14.6	92.4



**Table A-37: Flower Pot (A-6) Specific Surface Area Values**

Additive Type	Additive Content	0 Days Curing Time			14 Days Curing Time		
		Total SSA (m <sup>2</sup> /g)	External SSA (m <sup>2</sup> /g)	Internal SSA (m <sup>2</sup> /g)	Total SSA (m <sup>2</sup> /g)	External SSA (m <sup>2</sup> /g)	Internal SSA (m <sup>2</sup> /g)
Raw soil	0%	85.5	50.6	34.9			
Lime	1%	97.5	75.5	22.0	97.5	47.6	49.9
	2%	94.5	42.3	52.2	94.0	47.0	47.0
	3%	98.0	45.7	52.3	98.5	45.1	53.4
	4%	82.5	66.5	16.0	70.0	44.7	25.3
	5%	83.5	61.8	21.7	78.0	38.0	40.0
CKD	6%	87.5	62.4	25.1	112.5	46.2	66.3
	7%	89.5	55.1	34.4	90.5	44.7	45.8
	8%	85.0	62.1	22.9	92.5	43.1	49.4
	9%	94.5	49.7	44.8	98.5	44.5	54.0
	12%	94.5	59.5	35.0	109.5	34.3	75.2
	15%	67.5	44.9	22.6	107.0	41.5	65.5
RRFA	6%	87.5	39.2	48.3	73.5	40.8	32.7
	7%	94.5	65.1	29.4	98.5	38.2	60.3
	8%	82.5	58.4	24.1	108.0	40.9	67.1
	9%	83.5	54.2	29.3	77.5	37.8	39.7
	12%	78.0	53.5	24.5	63.0	43.6	19.4
	15%	95.0	58.9	36.1	74.5	27.8	46.7
MFA	6%	80.0	36.8	43.2	87.5	39.4	48.1
	7%	78.0	50.6	27.4	87.5	53.0	34.5
	8%	87.5	39.7	47.8	83.5	30.7	52.8
	9%	87.0	37.2	49.8	82.0	39.2	42.8
	12%	82.5	47.9	34.6	78.5	37.6	40.9
	15%	78.5	34.5	44.0	65.5	34.1	31.4

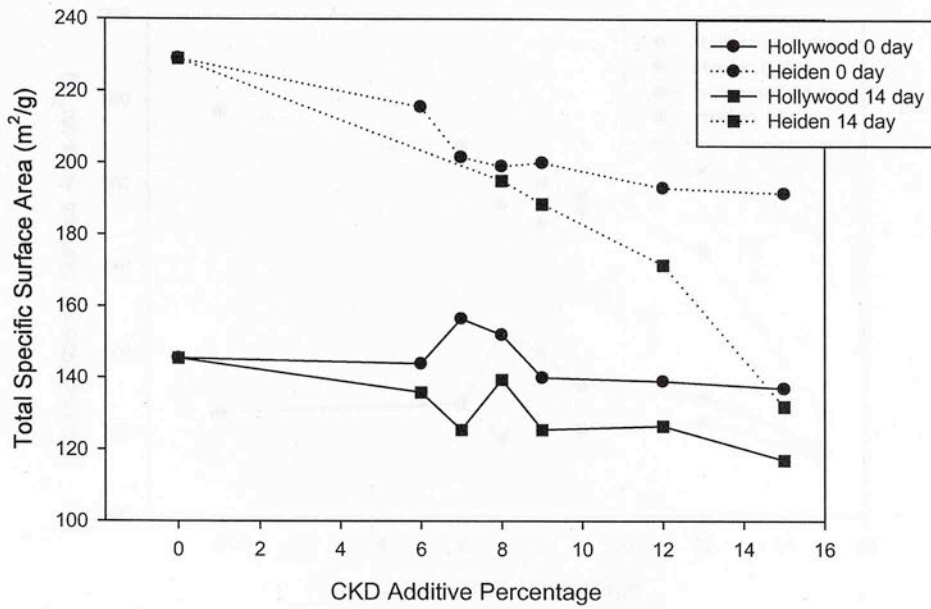


Figure A.126: Total SSA Curves for A-7-6 Soils with CKD

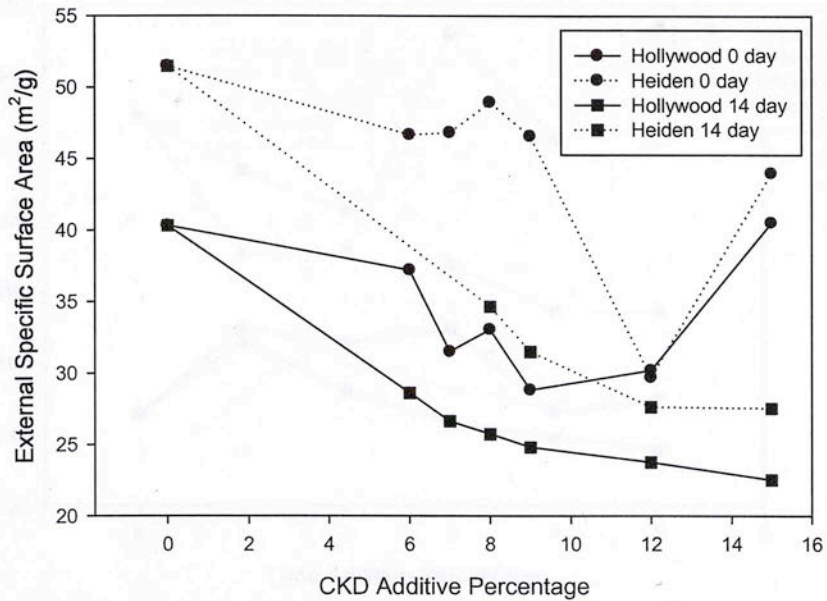


Figure A.127: External SSA Curves for A-7-6 Soils with CKD

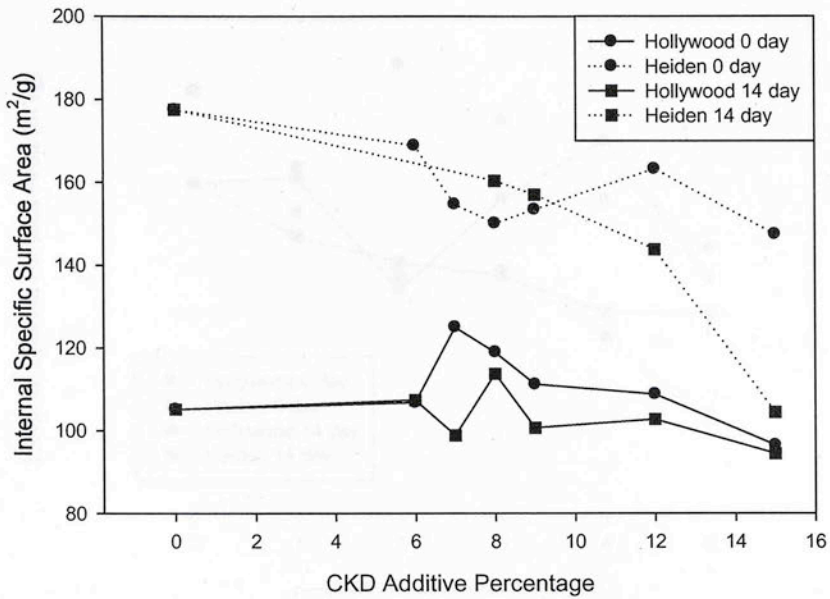


Figure A.128: Internal SSA Curves for A-7-6 Soils with CKD

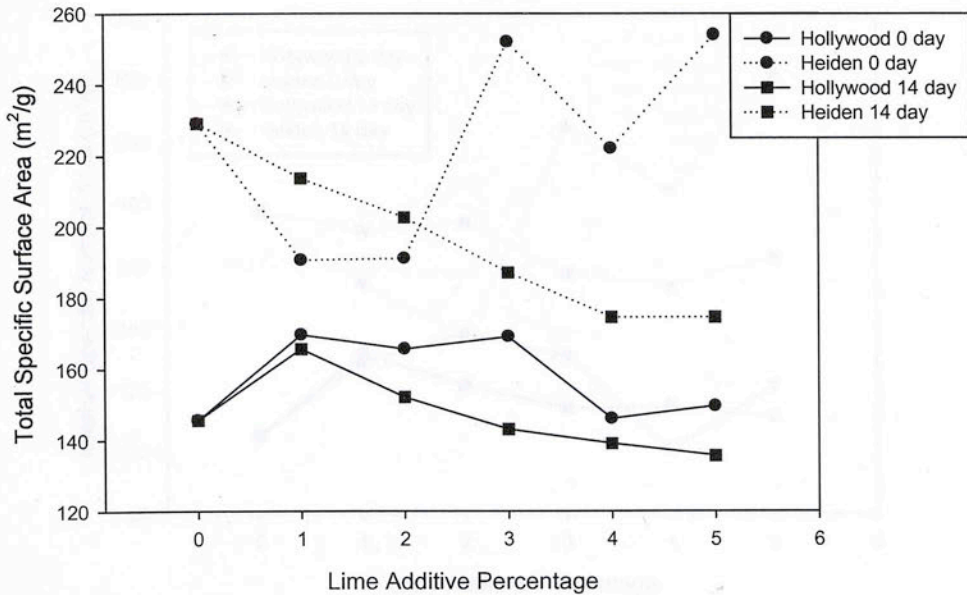


Figure A.129: Total SSA Curves for A-7-6 Soils with Lime



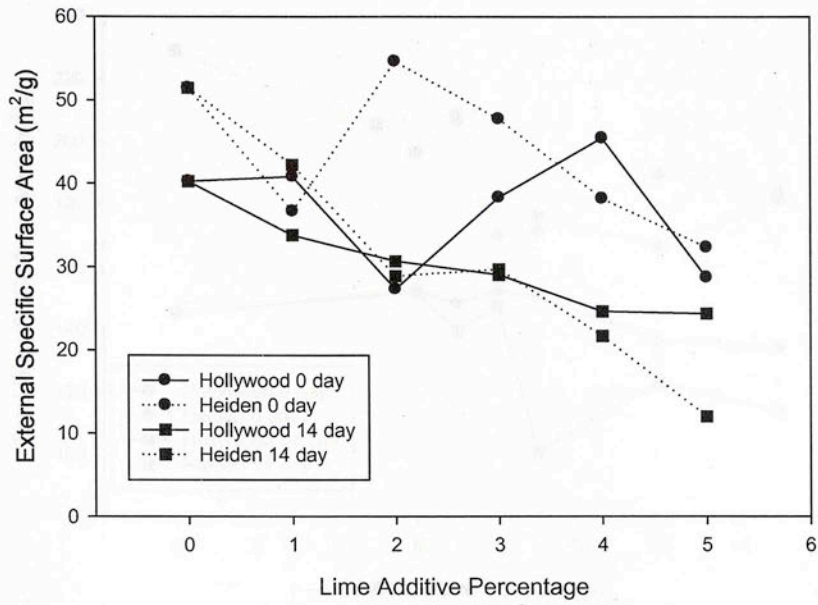


Figure A.130: External SSA Curves for A-7-6 Soils with Lime

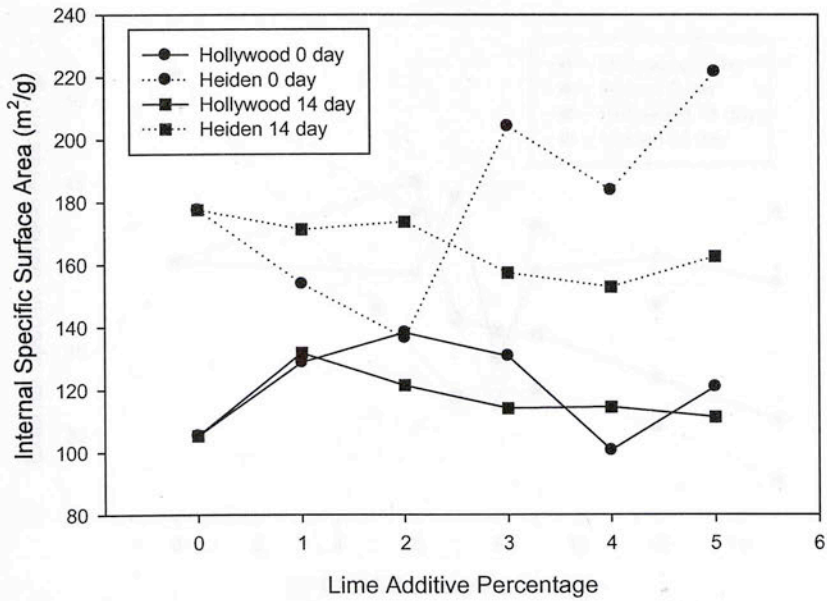


Figure A.131: Internal SSA Curves for A-7-6 Soils with Lime

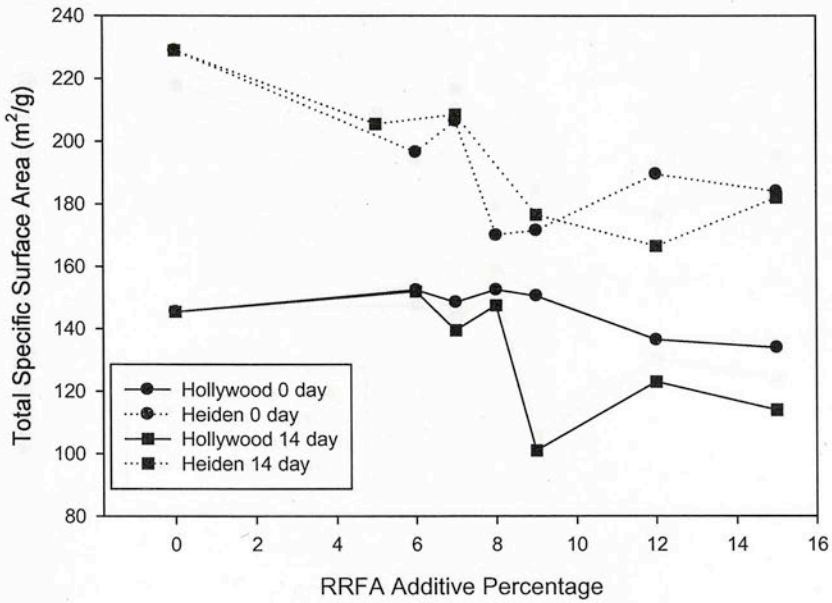


Figure A.132: Total SSA Curves for A-7-6 Soils with Red Rock FA

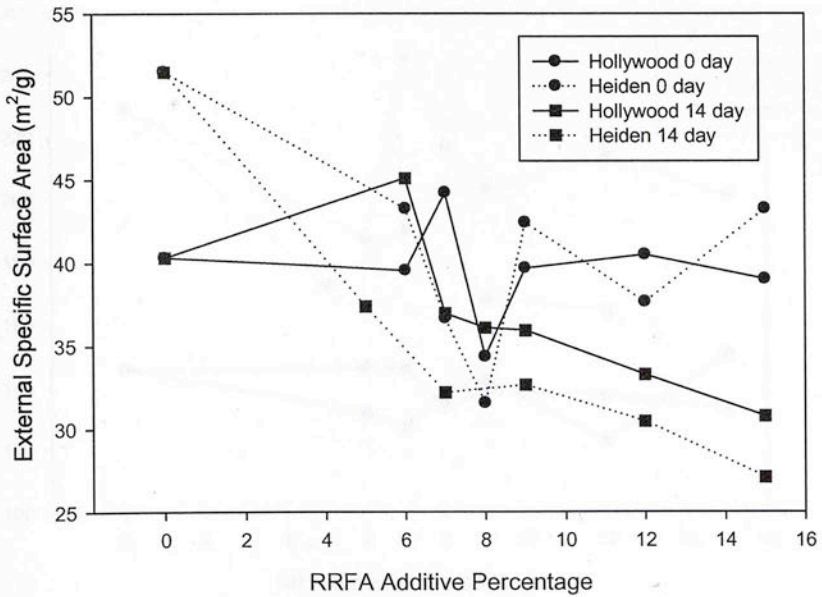


Figure A.133: External SSA Curves for A-7-6 Soils with Red Rock FA

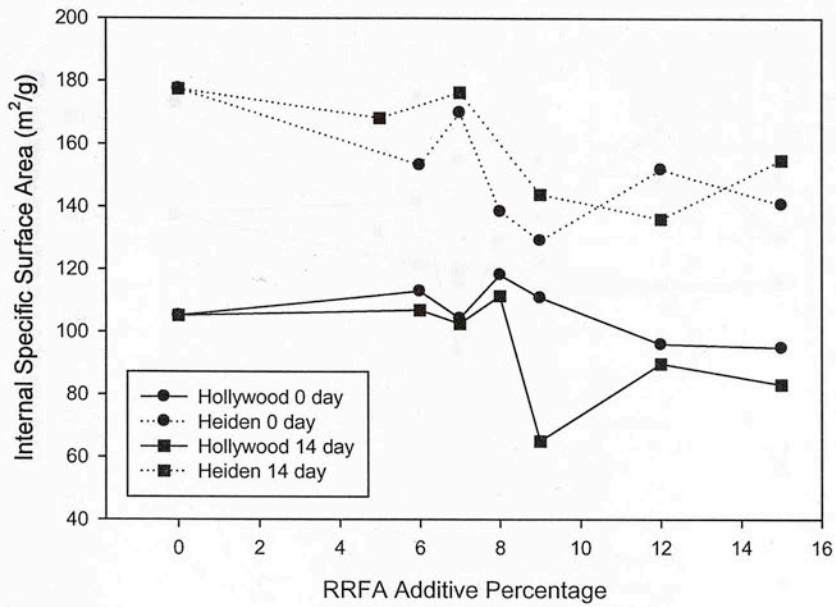


Figure A.134: Internal SSA Curves for A-7-6 Soils with Red Rock FA

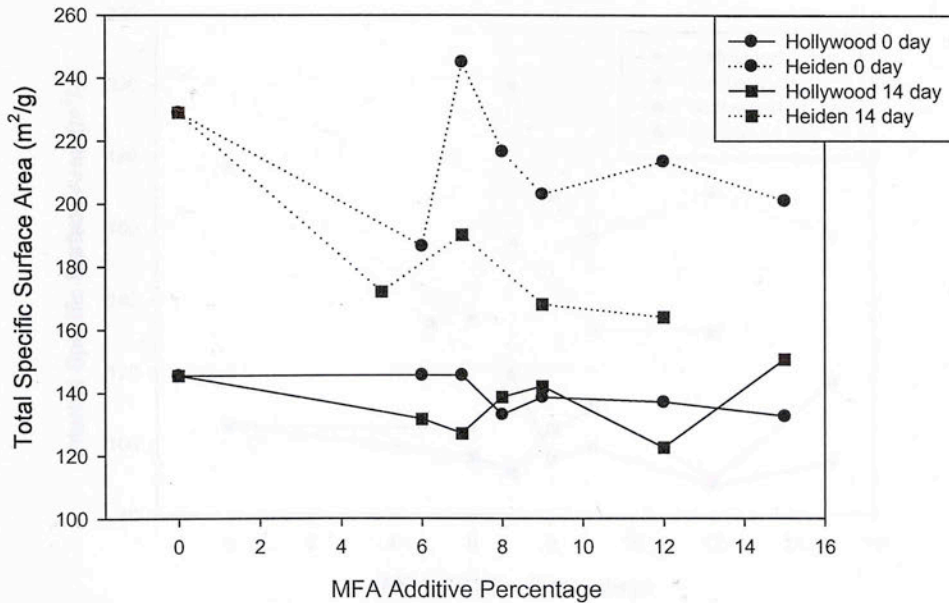


Figure A.135: Total SSA Curves for A-7-6 Soils with Muskogee FA



Table A.136: Hollywood (A-7-6) Specific Surface Area Values

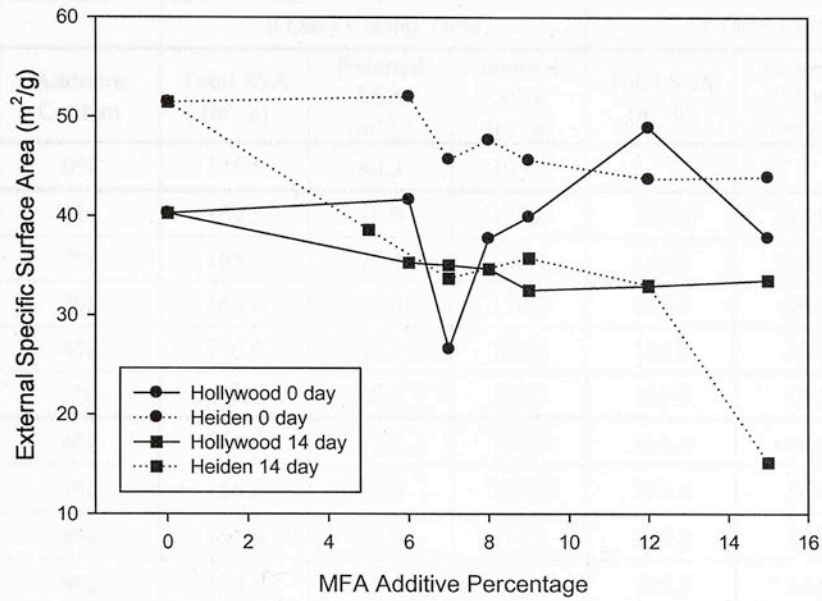


Figure A.136: External SSA Curves for A-7-6 Soils with Muskogee FA

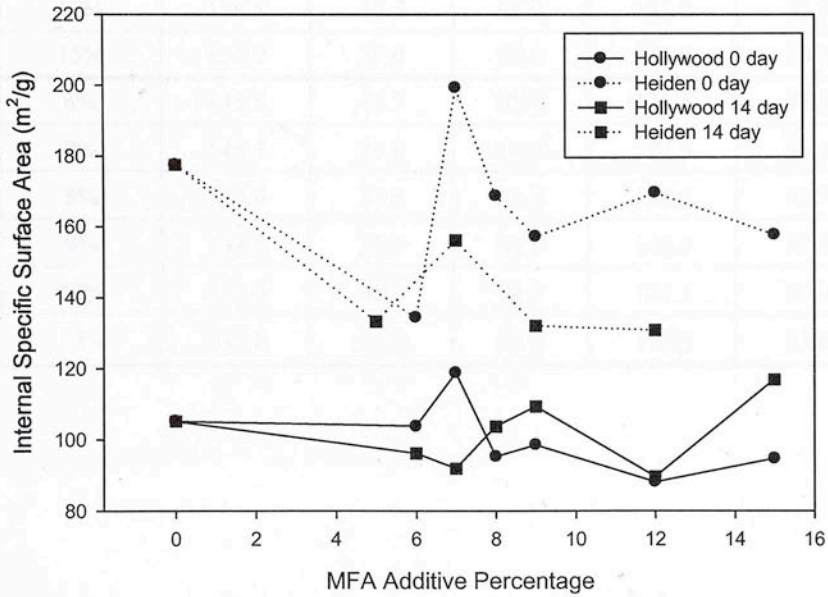


Figure A.137: Internal SSA Curves for A-7-6 Soils with Muskogee FA

**Table A-38: Hollywood (A-7-6) Specific Surface Area Values**

Additive Type	Additive Content	0 Days Curing Time			14 Days Curing Time		
		Total SSA (m <sup>2</sup> /g)	External SSA (m <sup>2</sup> /g)	Internal SSA (m <sup>2</sup> /g)	Total SSA (m <sup>2</sup> /g)	External SSA (m <sup>2</sup> /g)	Internal SSA (m <sup>2</sup> /g)
Raw soil	0%	145.5	40.3	105.2			
Lime	1%	169.5	40.9	128.6	165.5	33.8	131.7
	2%	165.5	27.4	138.1	152.0	30.7	121.3
	3%	169.0	38.3	130.7	143.0	29.0	114.0
	4%	146.0	45.5	100.5	139.0	24.6	114.4
	5%	149.5	28.8	120.7	135.5	24.4	111.1
CKD	6%	144.0	37.2	106.8	136.0	28.6	107.4
	7%	156.5	31.5	125.0	125.5	26.6	98.9
	8%	152.0	33.0	119.0	139.5	25.7	113.8
	9%	140.0	28.8	111.2	125.5	24.8	100.7
	12%	139.0	30.2	108.8	126.5	23.8	102.7
	15%	137.0	40.5	96.5	117.0	22.5	94.5
RRFA	6%	152.5	39.5	113.0	152.0	45.1	106.9
	7%	148.5	44.2	104.3	139.5	36.9	102.6
	8%	152.5	34.3	118.2	147.5	36.1	111.4
	9%	150.5	39.7	110.8	101.0	35.9	65.1
	12%	136.5	40.5	96.0	123.0	33.3	89.7
	15%	134.0	39.0	95.0	114.0	30.8	83.2
MFA	6%	145.5	41.7	103.8	131.5	35.3	96.2
	7%	145.5	26.6	118.9	127.0	35.1	91.9
	8%	133.0	37.8	95.2	138.5	34.7	103.8
	9%	138.5	39.9	98.6	142.0	32.5	109.5
	12%	137.0	48.9	88.1	122.5	33.0	89.5
	15%	132.5	37.9	94.6	150.5	33.6	116.9

**Table A-39: Heiden (A-7-6) Specific Surface Area Values**

Additive Type	Additive Content	0 Days Curing Time			14 Days Curing Time		
		Total SSA (m <sup>2</sup> /g)	External SSA (m <sup>2</sup> /g)	Internal SSA (m <sup>2</sup> /g)	Total SSA (m <sup>2</sup> /g)	External SSA (m <sup>2</sup> /g)	Internal SSA (m <sup>2</sup> /g)
Raw soil	0%	229.0	51.5	177.5			
Lime	1%	190.5	36.7	153.8	213.5	42.3	171.2
	2%	191.0	54.6	136.4	202.5	28.9	173.6
	3%	252.0	47.7	204.3	187.0	29.7	157.3
	4%	222.0	38.2	183.8	174.5	21.7	152.8
	5%	254.0	32.4	221.6	174.5	12.0	162.5
CKD	6%	215.5	46.7	168.8	-	-	-
	7%	201.5	46.8	154.7	-	-	-
	8%	199.0	48.9	150.1	195.0	34.6	160.4
	9%	200.0	46.6	153.4	188.5	31.5	157.0
	12%	193.0	29.7	163.3	171.5	27.6	143.9
	15%	191.5	44.0	147.5	132.0	27.5	104.5
RRFA	5%	-	-	-	205.5	37.4	168.1
	6%	196.5	43.2	153.3	-	-	-
	7%	206.5	36.6	169.9	208.5	32.2	176.3
	8%	170.0	31.5	138.5	-	-	-
	9%	171.5	42.4	129.1	176.5	32.6	143.9
	12%	189.5	37.6	151.9	166.5	30.5	136.0
	15%	184.0	43.2	140.8	182.0	27.1	154.9
MFA	5%	-	-	-	172.0	38.6	133.4
	6%	186.5	52.0	134.5	-	-	-
	7%	245.0	45.7	199.3	190.0	33.7	156.3
	8%	216.5	47.7	168.8	-	-	-
	9%	203.0	45.6	157.4	168.0	35.8	132.2
	12%	213.5	43.8	169.7	164.0	33.1	130.9
	15%	201.0	44.0	157.0	-	15.2	-



This volume is the property of the University of Oklahoma, but the literary rights of the author are a separate property and must be respected. Passages must not be copied or closely paraphrased without the previous written consent of the author. If the reader obtains any assistance from this volume, he must give proper credit in his own work.

I grant the University of Oklahoma Libraries permission to make a copy of my thesis upon the request of individuals or libraries. This permission is granted with the understanding that a copy will be provided for research purposes only, and that requestors will be informed of these restrictions.

NAME \_\_\_\_\_

DATE 5.4.2010

A library which borrows this thesis for use by its patrons is expected to secure the signature of each user.

This thesis by NICHOLAS LAWRENCE HUSSEY has been used by the following persons, whose signatures attest their acceptance of the above restrictions.

---

NAME AND ADDRESS

DATE